Time-resolved characterization of the HGF/Met response and the influence of *L. monocytogenes* InlB on the physiological phosphoproteome

Von der Fakultät für Lebenswissenschaften

der Technischen Universität Carolo-Wilhelmina

zu Braunschweig

zur Erlangung des Grades einer

Doktorin der Naturwissenschaften

(Dr. rer. nat.)

genehmigte

D i s s e r t a t i o n

von Evelin Berger

aus Gehrden

1. Referent: Prof. Dr. Lothar Jänsch

2. Referent: Prof. Dr. Michael Steinert

eingereicht am: 09.01.2013

mündliche Prüfung (Disputation) am: 17.04.2013

Druckjahr 2013

Vorveröffentlichungen der Dissertation

Teilergebnisse aus dieser Arbeit wurden mit Genehmigung der Fakultät für Lebenswissenschaften, vertreten durch den Mentor der Arbeit, in folgenden Beiträgen vorab veröffentlicht:

Publikationen

C. Gernert, **E. Berger**, F. Klawonn, L. Jänsch: Tackling Misleading Peptide Regulation Fold Changes in Quantitative Proteomics. In: M.P. Rocha, N. Luscombe, F. Fdez-Riverola, J.M. Corchadoa Rodriguez (eds.): 6th International Conference on Practical Applications of Computational Biology & Bioinformatics. Springer: 269-276 (2012).

F. Klawonn, N. Abidi, **E. Berger**, L. Jänsch: Curve Fitting for Short Time Series Data from High Throughput Experiments with Correction for Biological Variation. In: J. Hollmén, F. Klawonn, A. Tucker (eds.): Advances in Intelligent Data Analysis XI. Springer: 150-160 (2012).

Tagungsbeiträge

E. Berger, F. Klawonn, L. Jänsch: Time-resolved phosphoproteome analysis of HGF-stimulated DU-145 cells. (Poster) The EMBO Meeting 2011, Wien (2011).

Table of contents

1 Introduction

1.1 The Met receptor and its ligand hepatocyte growth factor

Met (also: c-Met, HGFR) is a transmembrane protein that belongs to the family of receptor tyrosine kinases. It is translated as a 1,390 amino acid polypeptide that is cleaved into a 50 kDa alpha and a 145 kDa beta chain by furin and subsequently forms a disulphide-linked heterodimer (Figure 1-1). The N-terminal alpha chain is exposed extracellularly, while the beta chain forms an ectodomain, a transmembrane helix as well as a cytoplasmatic part. The first 519 extracellular amino acids span the alpha chain and 212 residues of the beta chain and represent the Sema domain. It forms a seven-bladed beta-propeller that is likely to mediate protein-protein interactions. This part is followed by a small cysteine-rich PSI domain and four immunoglobulin-like domains, which are supposed to function as spacers. The intracellular part includes the juxtamembrane and kinase domain as well as binding sites for downstream effector proteins (Niemann et al. 2007; Niemann 2011).

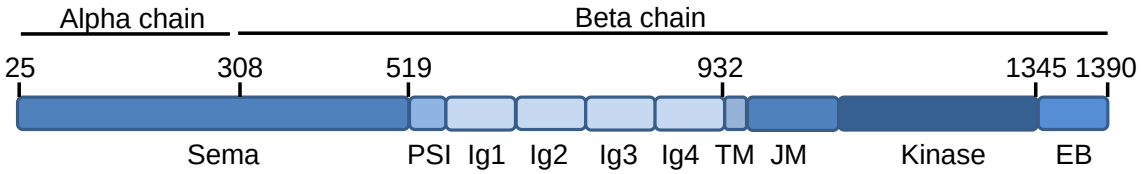

Figure 1-1: Domain structure of Met

The Met receptor is produced as 1,390 amino acid precursor, which is processed at amino acid 308 by furin into an alpha and a beta chain to result in a disulphide-bound heterodimer. Amino acids 25-932 are exposed extracellularly. The Sema domain (for semaphorin) spans alpha and the first amino acids of the beta chain. From residue 519, there follow the PSI (for plexin, semaphorin, integrin) domain and four immunoglobulin-like (Ig1-4) domains. The transmembrane (TM) domain in located in the plasma membrane, while the juxtamembrane (JM), kinase, and effector binding (EB) domains are exposed to the intracellular space. (Figure modified, taken from (Niemann et al. 2007)).

In the late 1980s, a mitotic factor for rat hepatocytes was discovered and named Hepatocyte Growth Factor (HGF). In parallel, Scatter Factor (SF), a protein triggering cellular motility was published. It turned out that both studies concerned

the same protein, which was then called HGF/SF. In the early 1990s, this factor was identified as the physiological ligand for the Met receptor (Birchmeier et al. 2003; Nakamura et al. 2011). While HGF is expressed and secreted from mesenchymal cells, Met is located on the surface of epithelial cells. This paracrine activation of the receptor represents an important layer of regulation.

HGF is expressed as a 728 amino acid single chain and is able to bind to Met, but not capable to stimulate the receptor. It is activated through cleavage into an alpha and a beta chain by the protease Hepatocyte Growth Factor Activator (HGFA). The cleaved and disulphide-linked heterodimer consists of an N-terminal hairpin loop (HL), four kringle domains (K1-4) formed by the alpha chain, and a serine protease-like domain (SPH) representing the beta chain (Figure 1-2). Two shorter splice variants exist, NK1 and NK2, which are agonistic and antagonistic to Met, respectively (Niemann 2011; Nakamura et al. 2011).

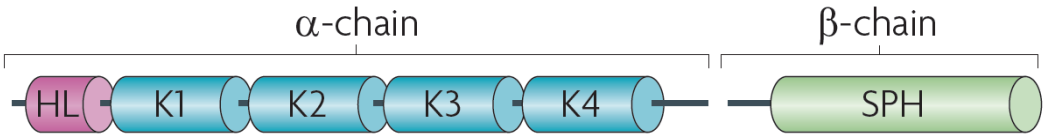

Figure 1-2: Domain structure of HGF

Hepatocyte growth factor is activated through proteolytic cleavage by HGFA. The resulting alpha chain forms an N-terminal hairpin loop (HL) and four subsequent kringle domains (K1-4). The beta chain exhibits a serine protease homology domain (SPH). Both chains are linked through a disulphide-bridge. Figure taken from (Trusolino, Bertotti, and Comoglio 2010).

The Met receptor has developed very late in evolution and therefore, it is only found in vertebrates. Signaling effectors utilized by Met are conserved and can be found downstream of several receptor tyrosine kinases (Birchmeier et al. 2003).

1.2 HGF/Met-induced signaling cascades

During ligand-receptor interaction, HGF is predicted to bind to the extracellular Sema domain of Met with two different sites. A high affinity site is located N-terminal in the HL-K1 fragment of HGF. The second one binds with lower affinity to

Met and is found in the SPH domain. Nevertheless, there is currently no complete crystal structure of the HGF/Met complex available (Niemann 2011).

In response to HGF binding to its receptor, Met dimerizes and autophosphorylates at tyrosines pY^{1234} and pY^{1235} in the activation loop of the kinase domain. This induces further phosphorylations (pY^{1249}, pY^{1256}) in the C-terminal effector binding sequence. Once modified, the latter sites become able to recruit several downstream effectors (Organ and Tsao 2011). Those proteins mostly comprise SH2-domains, which mediate the interaction. For example, the kinase PI3K or the scaffold proteins GRB2 and GAB1 directly bind to Met. Noteworthy, the interaction between Met and multi-adapter GAB1 is special in vertebrates. While other receptors are utilizing GAB1 as part of their downstream network and interact with the adapter through GRB2, GAB1 can also directly bind to Met. Therefore, GAB1 possesses a specific Met binding site (MBS). Due to this relationship, the adapter provides further binding sites for effectors like SHC, SHP2, PI3K, CRK, PLCγ1, and p120-Ras-GAP (Trusolino, Bertotti, and Comoglio 2010).

The signaling downstream of the Met receptor is very complex. Several branches exist that trigger mitogenic, motogenic and morphological cellular responses. These responses involve the transcription of target genes, but also the direct regulation of cytoskeletal or adhesion proteins. It has to be emphasized that the signaling branches leading to these responses also interact with each other to produce directed and consistent outcomes. Furthermore, evoked reactions depend on the cell type and culture conditions (Birchmeier et al. 2003).

According to Trusolino et al., 2010, there are four main pathways induced by the receptor (Figure 1-3). Firstly, Met activates the MAPK cascades through GRB2, SOS, and Ras. This pathway is also activated through SHC-2 dephosphorylating GAB1, which in turn causes p120-Ras-GAP to stimulate Ras, which then activates Raf. Once triggered, the MAP kinase families MEKK1-4, MEK1-7, ERK1-2 (alias MK01, MK03), JNK1-3, and p38α-δ can induce proliferation, migration, invasion, differentiation, or apoptosis. Secondly, the PI3K-AKT pathway can either stimulate protein synthesis and cellular growth through mTOR, or proliferation via inhibition of GSK3β. Furthermore, AKT suppresses apoptosis by inhibiting BAD and activating MDM2. Thirdly, Met phosphorylates STAT3, which dimerizes and translocates into the nucleus to activate the transcription of genes leading to

differentiation and proliferation. Finally, NFκB is released from the complex with IκB by IKK in response to Met activating the PI3K-AKT pathway. Transcription regulated by NFκB then triggers proliferation, survival or tubulogenesis (Trusolino, Bertotti, and Comoglio 2010).

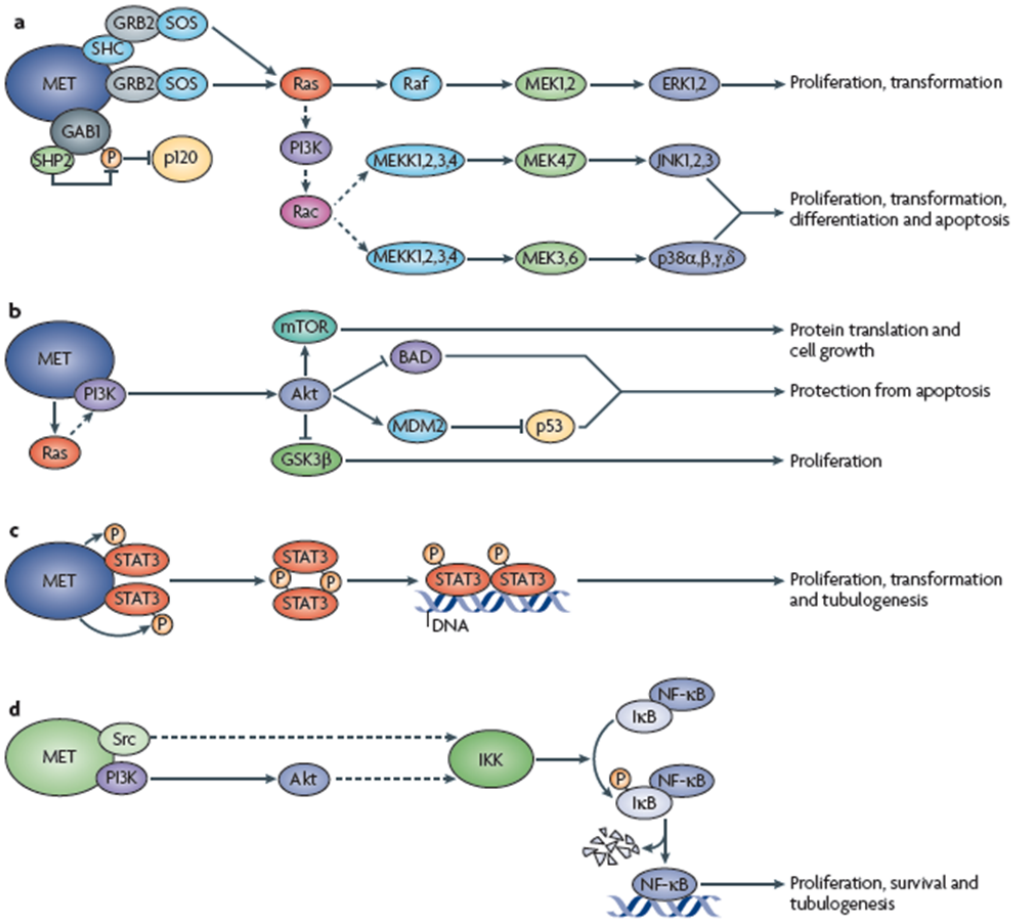

Figure 1-3: HGF-induced Met signaling pathways

The cellular responses and the components involved are very diverse. Four main downstream pathways can be activated by Met according to (Trusolino, Bertotti, and Comoglio 2010). A) MAPK cascade that induces proliferation, migration, apoptosis, and differentiation. B) PI3K-AKT signaling, which causes cell growth, survival, and proliferation. C) STAT3 induces the transcription of proliferative and tubulogenetic genes. D) IKK and NFκB lead to the activation of genes triggering proliferation, survival, and tubulogenesis.

How Met is able to activate different cascades specifically remains to be studied in detail. For example, only selected downstream effectors might be recruited at one time, because the receptor is unequally distributed on the cellular surface and would activate selected downstream effectors dependent on its spatial localization (Trusolino, Bertotti, and Comoglio 2010). Furthermore, due to steric reasons, only

one protein can attach to the effector binding site of Met. That would enable the receptor to differentially trigger downstream signaling branches (Birchmeier et al. 2003).

Additionally, the complex Met machinery has to be tightly regulated with regard to shutting down the signal. After HGF stimulation, Met gets also autophosphorylated at pY^{1003}, which recruits the E3 ubiquitin ligase CBL and causes Met's multi-monoubiquitination (Peschard et al. 2001). CBL can also be activated indirectly through GRB2, which is in turn bound to pY^{1356} of Met. Following ubiquitination, Met is internalized through clathrin-dependent endocytosis. The early endosomes including Met are translocated to the perinuclear compartment and fused with sorting endosomes. This is followed either by receptor recycling or fusion with lysosomes to eliminate Met signaling by its degradation. When trafficking in endosomes, Met is still able to induce downstream signaling components like STAT3 that localizes in the perinuclear region. Despite ligand-induced degradation, Met can also be proteolytically cleaved by caspases during apoptosis and by ADAM10 to mediate receptor shedding. The proteoglycan Decorin can bind to the extracellular part of Met, but is unable to induce downstream cascades. However, it causes Met downregulation by endocytosis, comparable to HGF (Lefebvre et al. 2012).

1.3 Met signaling is deregulated in cancer

Cancer is characterized as a set of cells displaying a higher proliferation rate as the surrounding tissue without any time-restriction. Tumors originating from these cells have escaped the control of the organ and exhibit progressive self-disorganization (Clark 1995).

The causes of cancer are as diverse as their tissue origin and include environmental as well as hereditary factors (Ames, Swirsky, and Willettt 1995). During the transformation of healthy tissue into cancer cells, more than one genetic change is necessary to acquire the characteristic uncontrolled growing phenotype. Generally, several subsequent mutations cause this development (Solomon, Borrow, and Goddard 1991). On the one hand, proliferative signaling, replicative immortality, and angiogenesis, as well as invasion and genetic

instability are enhanced. On the other hand, growth suppression, apoptosis, and destruction through the immune system are inhibited (Hanahan and Weinberg 2011).

Although cancer development is due to genetic changes, the manifestation of these mutations takes place on the protein level. As a consequence, several cellular processes are deregulated in cancer. Notably, the Met receptor is among the affected proteins and even was first identified as proto-oncogene. It is deregulated in a number of different cancers types and its expression in tumors often correlates with poor prognosis (Birchmeier et al. 2003). For example, the receptor is overexpressed in musculoskeletal tumors and melanoma, and activated in small-cell lung cancer as well as renal papillary carcinoma by point mutations. Furthermore, fusion with protein TPR causes its deregulation in gastric cancer (Krause and Van Etten 2005). Met has also been found overexpressed in 44-83% of prostate cancers (Van Leenders et al. 2002) and in 60% of patients with cervical cancer (Baykal et al. 2003). As Met is transcriptionally induced by inflammatory cytokines and pro-angiogenetic factors, it is likely that Met promotes cancer at a late state when the cells have already become malignant. This fact is further supported by its involvement in the activation of EMT as a requisite for invasion (Thiery 2002). In general, the receptor triggers proliferation, survival, and migration (Trusolino, Bertotti, and Comoglio 2010).

Like its receptor, HGF is overexpressed in many cancers. Furthermore, proteases activating the growth factor are also upregulated, resulting in an increased amount of active HGF compared to healthy tissues (Trusolino, Bertotti, and Comoglio 2010). Furthermore, the paracrine regulation of Met activity through HGF is lost in cancer cells, because the receptor is stimulated in an autocrine manner (Nakamura et al. 2011).

1.4 *Listeria monocytogenes* exploits Met signaling by activation through internalin B

Besides HGF, a further factor is able to bind and activate the Met receptor through its extracellular domain. This protein is called internalin B (InlB) and is located on the surface of *Listeria monocytogenes*. The latter is a facultative anaerobic rod-

shaped bacterium, which is found ubiquitously in soil, water, food, and in the feces of humans and animals. It is pathogenic and able to live intracellularly. The bacterium causes listeriosis in immune-compromised humans, pregnant women and newborns as well as in other vertebrates like domesticated mammals. Usually, the pathogen is ingested via contaminated food, survives the gastric acid, and finally reaches the intestine. There, it is able to cross the intestinal barrier, invades neighboring cells, and spreads through the blood to lymph nodes and spleen. Most bacteria reach the liver where *L. monocytogenes* multiplies and can cause hepatitis. As the bacterium is able to also cross the blood-brain and the feto-placental barrier, it can invade the tissues behind, which may lead to meningitis and miscarriage, respectively (Vazquez-Boland et al. 2001; Hamon, Bierne, and Cossart 2006).

The intracellular life cycle of *L. monocytogenes* enables the organism to escape the host's humoral immune system (Gouin et al. 2010). During evolution, the pathogen developed several virulence factors permitting the organism to invade and live in its host. On the one hand, the pathogen is able to survive phagocytosis by macrophages. Even more strikingly, it induces its internalization in usually non-phagocytic cells like fibroblasts, hepatocytes, endothelial and epithelial cells. In a first step, *L. monocytogenes* adheres to host cells via surface proteins, which trigger the invasion of the bacterium through a zipper-like mechanism involving the clathrin-dependent endocytosis machinery (Figure 1-4) (Lefebvre et al. 2012; Ireton 2007; Cossart and Veiga 2008). Yet before the fusion of the phagosome with the lysosomal compartment, the pathogen escapes the vacuole via listeriolysin O (LLO) and the phospholipases PlcA and PlcB that lyse the membrane. The cytoplasmic *Listeria* cells are now free and start to proliferate. Furthermore, the bacterial protein ActA acts as a nucleation factor for F-actin. These filaments polymerize at one pole of the rod, forming a tail that enables *Listeria* to move through the cell. By chance, it is propelled to the cytoplasmic membrane from where it invades neighboring cells. This process is comparable to the initial internalization, except that now the bacterium is surrounded by two membranes. Utilizing the membrane lysing virulence factors LLO and particularly the Plcs, the pathogen once more escapes the phagosome to start a further infection cycle (Hamon, Bierne, and Cossart 2006; Vazquez-Boland et al. 2001).

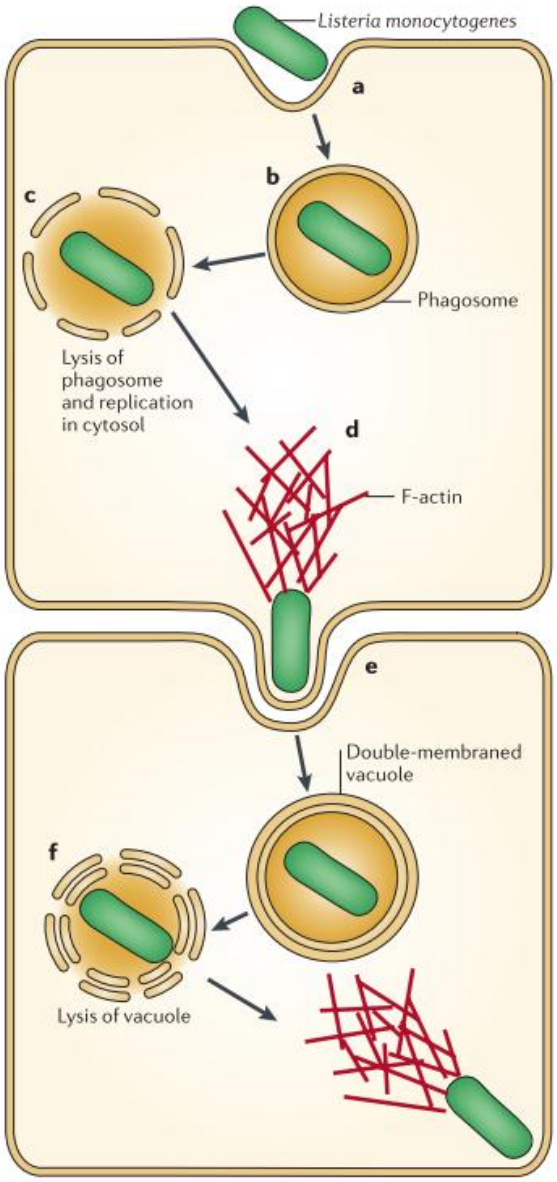

Figure 1-4: Intracellular infection cycle of *Listeria monocytogenes*

A) Adhesion and induced invasion of the pathogen is initiated by InlA or InlB. B) Listeria is incorporated in a phagosome. C) The bacterium is able to lyse the membrane of the vacuole with listeriolysin O and phospholipases PlcA and PlcB. Free intracellular *Listeriae* multiply and D) move through the cell by polymerizing actin at one pole with ActA. E) Neighboring host cells are invaded, resulting in the bacterium localized in a double-membrane vacuole. F) Lysis of the membranes, particularly via PlcA and B, where the cycle restarts again. Figure taken from (Hamon, Bierne, and Cossart 2006).

The crucial step for the intracellular life of *L. monocytogenes* is the adhesion to and invasion into its host cell. This is mediated by two proteins of the invasin family, namely internalin A (InlA) and B (InlB). While InlA binds to E-cadherin and facilitates the internalization into a small number of different cell types, InlB activates the Met receptor, triggering its endocytosis into a variety of cell types

(Hamon, Bierne, and Cossart 2006). Furthermore, InlB is sufficient to promote the entry of non-invasive bacteria and even of inert latex beads into mammalian cells (Braun, Ohayon, and Cossart 1998).

InlB is a 630 amino acid residue surface-associated protein of *L. monocytogenes* that can also be released to the surrounding medium. Like all other members of the internalin family, it comprises an N-terminal internalin domain, which consists of a helical Cap domain, a leucine-rich repeat (LRR), and an interrepeat region (IR) (Figure 1-5). The first two parts, until residue 241, are sufficient to bind to the Met receptor. However, addition of the IR domain ($InlB_{321}$) is required to activate the host receptor. Following the internalin domain, InlB consists of a poorly characterized B-repeat and three C-terminal GW domains, which are structurally related to SH3-domains that mediate protein-protein-interactions. The GW domain mediates binding to the bacterial surface, but is also able to interact with the mammalian surface proteins complement component receptor gC1qR and different Heparan Sulfate Proteoglycans (HSPGs) (Niemann 2011; Niemann et al. 2007).

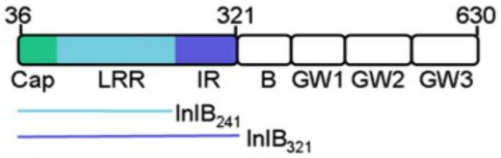

Figure 1-5: Domain structure of internalin B

Internalin B is an invasine of the internalin family consisting of 630 amino acids. It is composed of an internalin domain consisting of an N-terminal cap, a leucine-rich, and an interrepeat region. The protein also contains a B-repeat and three C-terminal GW domains. While cap and LRR are sufficient to bind the Met receptor, addition of the IR part (amino acids 1-321) successfully stimulates it. The GW domains link InlB to the bacterial surface and are able to bind to the host protein gC1qR and HSPGs. Figure taken from (Niemann et al. 2007).

In conclusion, both external ligands of Met - HGF and InlB – exhibit no structure homologies and also bind to Met at different sites. Obviously, the cellular response to stimulation is clearly different, too. Thus, the question arises to what extent HGF and InlB trigger similar signaling pathways downstream of Met and are utilizing same components. Several studies provide hints to comparable signaling mechanisms. InlB activates the PI3K and the MAPK pathways, which are known to

be part of HGF-induced signal transduction. Nevertheless, InlB causes only transient Met autophosphorylation while HGF promotes a sustained activation. Furthermore, the MAPK cascade appears to be stronger activated in response to the bacterial protein (Hamon, Bierne, and Cossart 2006; Y. Shen et al. 2000). A proteome study investigating the $InlB_{321}$-induced kinome also identified several similarly and differentially regulated signaling components compared to HGF/Met (Reinl et al. 2009).

1.5 Signaling cascades and post-translational modifications

Signaling pathways are induced by environmental changes or other extracellular stimuli. These are recognized by specific receptors that transduce the signal through the cell involving a diverse network of proteins, and finally results in specific cellular responses. It is believed that every eukaryotic cell utilizes comparable mechanisms in signal transduction, but the inputs and outputs are cell type-specific. How these signaling cascades and their cross-reaction are coordinated is poorly understood so far. As mentioned above, HGF and InlB induce Met-dependent signaling cascades involving numerous proteins. The different components not only recognize and transmit signals within one cell, but also amplify, multiply, and integrate them (Jordan, Landau, and Iyengar 2000; Keshet and Seger 2010).

Signal transduction induced by Met is mainly mediated by phosphorylation cascades. As at least 30% of all proteins in a cell are phosphorylated at one time point, it is clearly a general and important regulating instrument (Hubbard and Cohen 1993). Phosphorylation is the transfer of the terminal phosphate group of ATP to the hydroxyl group of the amino acids serine, threonine and tyrosine. Arginine, histidine, aspartic and glutamic acid may also be modified; however, this occurs seldom in vertebrates and is more common in prokaryotes. Phosphorylation of these uncharged amino acids incorporates a negative charge into the modified protein sequence at neutral pH due to the charge of two oxygen atoms of the phosphate group (Figure 1-6 A). Thereby, the conformation of the protein is affected by electrostatic interactions and hydrogen bonds between the phosphate group and the neighboring residues. When the three-dimensional

structure of the protein is affected, phosphorylation may influence its activity, stability, and association with other proteins (Dissmeyer and Schnittger 2011; Manning 2005).

Enzymes that are able to transfer a phosphate group from ATP to another protein are called kinases (Figure 1-6). With more than 500 members, it is one of the largest enzyme families encoded by the eukaryotic genome (Manning 2005). Dependent on their preferred amino acid substrates, they are classified as Ser/Thr- and Tyr-kinases. Most protein kinases are themselves targets for upstream kinases resulting in a consecutive chain of signaling molecules (Dissmeyer and Schnittger 2011). Because kinases are crucial for signal transduction and many of them have been implicated in different types of cancer, this group is now more and more targeted in cancer therapy. For example, Imatinib was the first kinase-targeting drug and has been shown to inhibit the oncogenic BCR-ABL in chronic myeloid leukemia (Krause and Van Etten 2005).

Protein phosphatases also play an important role in signaling as they act as antagonists of kinases by removing phosphate groups from signaling components (Figure 1-6). In doing so, they interfere with induced cascades and diminish signaling. That is an important mechanism to tightly regulate the response to extracellular stimuli. As for kinases, two different groups exist, distinguished by their preferences in hydrolyzed residues. Serine/threonine-phosphatases act as large, multi-subunit complexes, which mediate dephosphorylation of a broad spectrum of substrates (Figure 1-6 B). About 30 different genes encoding catalytic subunits are known. With about 100 genes encoding Tyr-phosphatases, the group is much bigger and is comparable to that of the Tyr-kinases. In contrast to the protein kinases that share a common structure, phosphatases have developed separately and share no sequence homologies (Cohen 2004; Tonks 2006).

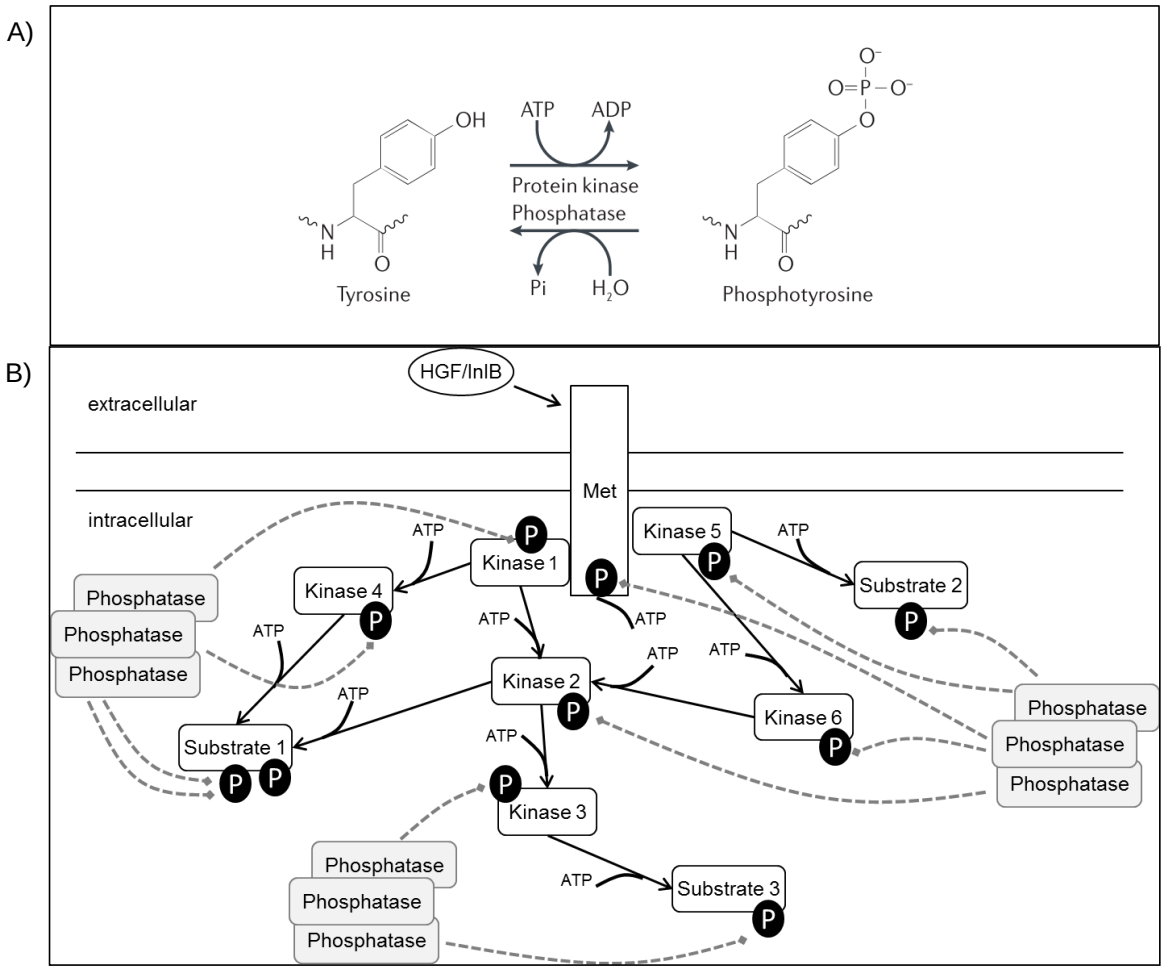

Figure 1-6: Protein phosphorylation and dephosphorylation in Met signaling

A) Using the example of tyrosine modification, phosphorylation by protein kinases and dephosphorylation by protein phosphatases is illustrated. The phosphate group is taken from ATP, thereby producing ADP and a modified, polar amino acid residue that may influence the protein's three-dimensional structure and function. Figure taken from (Seet et al. 2006). B) Balance between phosphorylation by kinases and dephosphorylation by phosphatases in Met signaling. Kinases amplify, multiply, and integrate the signal intracellularly. Substrate proteins may be transcription factors or cytoskeleton-associated proteins that, in response to HGF, regulate gene expression and morphologic alterations, respectively.

One further class of transducers in Met signaling is the small GTPases, which catalyze the conversion of bound GTP to GDP while activating downstream components. They, in turn, are regulated by GAP proteins that stimulate their GTPase activity, and GEFs, which exchange bound GDP to GTP. Furthermore, adapter and scaffold proteins act downstream of Met. Although they are unable to transmit signals on their own, they provide multiple docking sites, which recruit several effector proteins at once in order to bring them in close contact. These

complexes assure fast, localized, and directed transduction reactions (Pawson and Nash 2000).

Besides phosphorylation, about 300 other post-translational modifications are known, some of them also taking part in signaling. Furthermore, interaction of different types of PTMs in regulation of cellular processes is also possible (Seet et al. 2006). Activated Met, for example, gets phosphorylated at pY^{1003}, which recruits ubiquitin ligase Cbl, followed by Met multimono-ubiquitination and degradation through the proteasomal pathway (Lefebvre et al. 2012; Peschard et al. 2001). Thus, the combination of phosphorylation and ubiquitination is one method to regulate RTK signaling.

For the cell, the advantage of phosphorylation in signaling - compared to gene expression - is the immediate recognition and fast processing of a signal (Deribe, Pawson, and Dikic 2010). This mechanism enables the cell to adapt to changes in its environment in a short period of time. Thus, in order to identify and study early events triggered by HGF or InlB after Met-binding, monitoring the phosphorylation pattern of a cell is the method of choice.

1.6 Proteomic strategies to characterize phosphorylation patterns

In order to screen novel phosphoproteins, only proteome research based on mass spectrometry provides a broad overview of all modified proteins affected by an outside signal.

2D gel electrophoresis (2D-GE) in combination with Matrix-Assisted Laser Desorption/ Ionization Mass Spectrometry (MALDI-MS) has long been the proteomic standard to decomplex a sample and identify proteins. Using staining methods for phosphorylated proteins like ProQ diamond or radio-labeling (^{32}P), revealed several new modifications at once. However, these strategies lack the sensitivity for low-abundant proteins and slight changes in the often substoichiometric phosphorylation pattern, which is the case for signaling components. Thus, underrepresented phosphoproteins have to be enriched to improve resolution and a subsequently obtain higher amounts of identified phosphoproteins. Due to biochemical properties, which are more diverse on

protein level, this is easier when done on the level of peptides. Furthermore, only peptide sequencing reveals the exact localization of a phosphorylation site (Olsen et al. 2006; Kosako and Nagano 2011).

In contrast, gel-free Liquid Chromatography-tandem Mass Spectrometry (LC-MS/MS) in combination with effective phosphopeptide enrichment provides a robust high-throughput method to analyze the phosphoproteome even of a complex sample. Several approaches have been developed to purify phosphopeptides, including affinity-based methods as the most common ones (Figure 1-7). Antibodies against phosphorylated tyrosine have been shown to act very specific in immunoprecipitation (Rosenqvist, Ye, and Jensen 2011). Nevertheless, with a fraction below 1% in a mixture of phosphorylated peptides (Hunter and Sefton 1980; Olsen et al. 2006), phosphotyrosine is comparatively rare. Therefore, a general approach requires other methods that also capture serine and threonine phosphorylation. Affinity chromatography using metal oxides (MOAC), like TiO_2 has been shown to be very efficient and specific for every phosphorylation type. Here, the option to change the charge of the phosphate group at different pHs is utilized. At low pH, phosphopeptide anions bind to the surface of TiO_2, while they can be eluted at higher pH and neutral charge. However, this method is selective for mono-phosphorylated peptides (Larsen et al. 2005). Because multiple phosphorylations play an important role in signaling – kinases for example have to be phosphorylated at two distinct nearby sites to get active – TiO_2 is also not the method of choice for a phosphoproteome approach. Strong Cation eXchange chromatography (SCX) is often used in gel-free proteomic studies to reduce the complexity of a given sample. By increasing the salt concentration in the liquid phase, positively charged peptides that interact with the negatively charged resin are eluted depending on their isoelectric point. As phosphopeptides exhibit a negative charge, they are not retained on the column and elute in the first fractions. The advantage of SCX in phosphoproteomics is its application in experiments with large protein amounts. However, SCX is obviously not a specific method when used alone thus, it is often combined with other enrichment strategies (Grimsrud et al. 2010; Rosenqvist, Ye, and Jensen 2011). One of them is the Immobilized Metal Affinity Chromatography (IMAC), which takes advantage of positively charged metal ions binding to negative phosphate groups of peptides. Like for metal oxides, buffers with low and high pH affect the

binding or the elution of the peptides from the resin, respectively. IMAC is commonly carried out with Fe^{3+} or Ga^{3+} ions and purifies mono as well as multiply phosphorylated peptides. A disadvantage here is that it also binds to acidic peptides as they are negatively charged at low pH as well (Ndassa et al. 2006; Leitner, Sturm, and Lindner 2011; Villén and Gygi 2008).

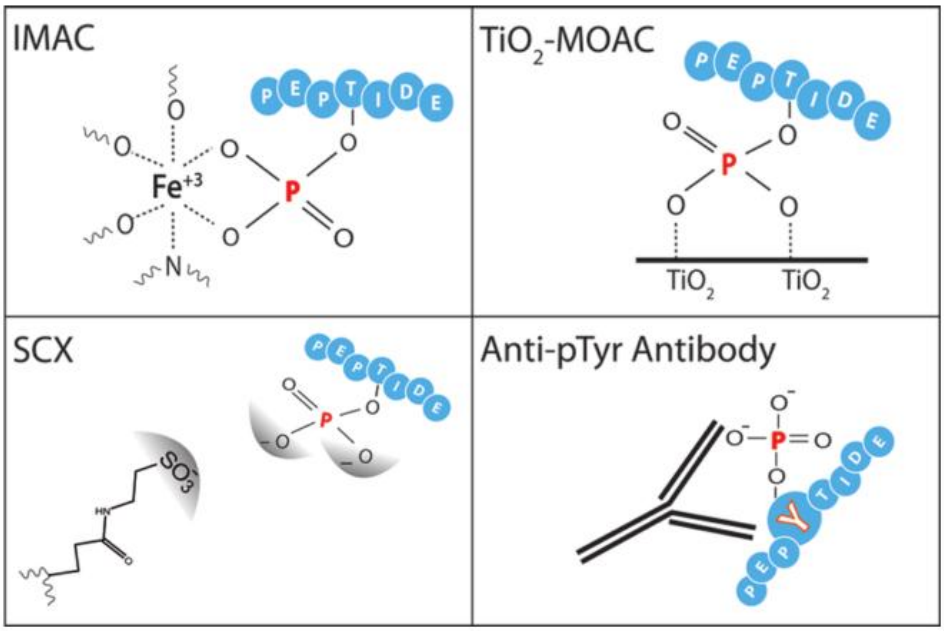

Figure 1-7: Commonly used phosphopeptide enrichment strategies

IMAC via positively charged metal ions binds phosphate groups at low pH and releases them at higher pH. Phosphopeptides are eluted early in SCX, because they do not bind to the negatively charged column resin. Charged phosphate groups are retained on TiO_2 at low pH. Antibodies against phosphorylated tyrosines specifically purify this type of modification. Figure taken from (Grimsrud et al. 2010).

The enriched phosphorylated peptides are then measured by LC-MS/MS in order to determine the peptide sequence and the phosphorylation site. ElectroSpray Ionization (ESI) allows coupling to an upstream reverse phase chromatography, which provides a continuous flow of peptides for detection by MS. The peptide sequence is determined by a second MS after fragmentation of the mother ions. During this collision, the peptide backbone is split into fragments, which are detected by their characteristic masses. Furthermore, modifications appear as increased masses in the peptide spectrum. Phosphorylations cause a mass shift of 80 Da of the modified amino acid. While the phosphate group is mostly lost from serine and threonine during fragmentation, causing a mass shift of -98 (loss of

H_3PO_4), the modification of tyrosine is comparatively stable. Stepwise calculation of the mass differences between neighboring peaks in the peptide spectrum then yields the amino acid sequence of a peptide including its phosphorylation sites (Leitner, Sturm, and Lindner 2011; Boersema, Mohammed, and Heck 2009).

1.7 Strategies for quantitative labeling

A certain amount of phosphorylated proteins is present even in non-stimulated cells. This phosphorylation pattern is changed in response to a stimulus. Thus, in order to identify phosphorylations that are caused or abolished by stimulation, the patterns of the treated and the non-treated sample have to be compared by phosphoproteomics. Quantitative analysis provides a robust strategy to get reliable data from different samples on the basis of peptide ion intensities. Label-free approaches utilize either the evaluation of ion currents or spectral counting and are becoming more and more popular for comparative proteomic studies. Nevertheless, they remain to be validated in phosphoproteomics (Rosenqvist, Ye, and Jensen 2011).

More commonly used are labeling strategies where several samples are marked, pooled and then measured together. Labeling with stable isotopes does not change the characteristics of a peptide, but slightly varies the mass. Approaches like ICAD rely on chemical tags with different masses. Those marked peptides elute in parallel from the LC, but display a mass shift in the peptide spectrum due to the isotope composition. This method of “light” and “heavy” peptides is also used in metabolic labeling. But in contrast to ICAD, no tags are applied, but amino acids consisting of different isotopes are directly incorporated during cell culture (SILAC, Stable Isotope LAbeling in Cell culture). SILAC is used frequently for phosphoproteomics approaches, because it provides comparable labeling from the beginning and therefore reduces technical variability. However, it is only applicable for samples for growing cells or organisms. In contrast to isotope-based strategies, isobaric labeling is not limited in sample number. For iTRAQ (isobaric Tags for Relative and Absolute Quantification), up to 8 different labels are available. This well-established method uses isobaric tags that are usually incorporated on the peptide level (Figure 1-8). These tags have the same masses, but during MS fragmentation dissociate into so-called balancer and reporter ions, with the latter

displaying different masses during MS/MS. The reporter ions are detected in the low mass range of the peptide spectrum. Most common are four labels that dissociate to fragment ions of 114, 115, 116, and 117 Da. Subsequently, the intensities of these fragment ions can be compared and the ratio of the peptide in all samples is calculated (Grimsrud et al. 2010; Schreiber et al. 2008; Timms and Cutillas 2010).

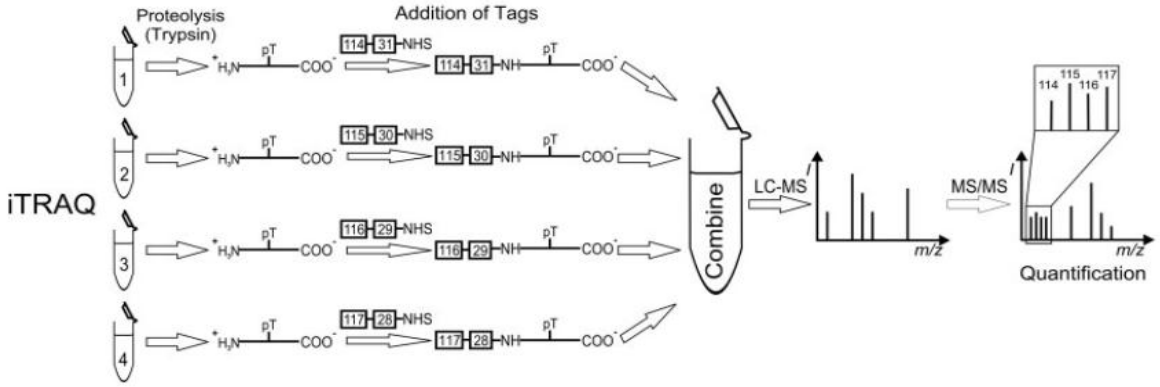

Figure 1-8: Isobaric labeling strategy using iTRAQ

Peptides are iTRAQ-labeled with tags having same masses and samples are combined afterwards. During MS/MS, tags are split into balancer groups and reporter ions with distinct masses. The reporters display the masses 114, 115, 116, and 117, which can be seen in the low mass range of a peptide spectrum. The intensities of the reporters then allow a comparative analysis of peptide amounts in different samples. Figure taken from (Schreiber et al. 2008)

2 Aim of this work

HGF/Met-induced signaling controls a variety of different cellular responses ranging from proliferation, migration, and survival to apoptosis or morphogenesis. Many studies have investigated the components downstream of Met and tried to separate them into several distinct pathways (Trusolino, Bertotti, and Comoglio 2010; Organ and Tsao 2011; Rosário and Birchmeier 2003). However, currently only speculations exist as to how one growth factor binding to one receptor can produce several outputs and how this “decision” is regulated. The high rate of phosphorylation on proteins suggests a more complex view on signal transduction and processing, because a single modification may not always affect protein function, while a multi-phosphorylation can have a dramatic change of the protein’s behavior. That indicates that regulation of some signaling components is not controlled simply by one upstream protein, but rather by a combination of several factors. Obviously, downstream of multifunctional receptors like Met, there are signaling networks existing, which are highly interconnected. Signaling nodes are supposed to play important roles in the integration of stimuli and their processing to one clear, unmistakable cellular reaction out of a set of different possibilities. This thesis aimed to characterize Met signaling from a more integrative point of view using global “omics” technologies in combination with traditional biochemical methods.

Proteomic approaches so far concentrated on the description of kinases or tyrosine phosphorylations involved in Met-induced signaling (Ma et al. 2007; Organ et al. 2011; Hammond et al. 2010; A. Guo et al. 2008). Here, the whole phosphoproteome after stimulation should be identified and characterized in the first 20 min after a stimulus. Using a time course of 3, 6, and 20 min should cover early as well as late events to increase the number of detected differentially regulated phosphoproteins in response to Met activation. Furthermore, it should allow characterizing the dynamics of regulated phosphorylation sites over time. The cell line DU145 was chosen because it is an accepted model for prostate cancer and Met is expressed at high levels. Additionally, it is known to respond to HGF stimulation with increased motility (Johnson, Hershberger, and Trump 2002; Humphrey et al. 1995).

Besides the global phosphorylation pattern affected by HGF, single components, which are potential signal integrators and their functions in Met signaling should be studied in detail. Those hubs are supposed to cause a significant cellular effect in response to HGF, revealing its regulation of crucial Met-induced pathways. Therefore, RNAi approaches in combination with gene expression arrays were designed that should clarify the role of these potential hubs in the processing of the HGF/Met signal into cellular reactions.

As the first parts aimed for a better understanding of the complex signal networks triggered by HGF, the last part of this thesis should highlight the impact of *Listeria monocytogenes* virulence factor InlB on Met-dependent signaling. Binding of InlB to Met induces the uptake of the pathogenic bacterium through the endocytotic pathway within 10 minutes (Cossart and Veiga 2008). However, proximal signaling in the first 5 min after InlB-Met contact has not been analyzed so far by phosphoproteomics. The experiment was performed in HeLa S3 cells that have often been used as infection model for *Listeria*, because they do not express E-cadherin, which binds to InlA (Shimabukuro et al. 2001).

3 Materials and Methods

3.1 Chemicals, reagents, and buffers

Table 3-1: Materials and reagents

Chemical	Catalog number	Company
1,4-Dithiothreitol ≥99% (DTT)	20710	Serva
2-Mercaptoethanol	444203	Calbiochem
Acetonitrile (ACN)	9017	J.T.Baker
Bovine serum albumin ≥98% (BSA)	A7906	Sigma
Formic acid (FA)	1.00264.0100	Merck
Ammonia anhydrous ≥99.99%	294993	Sigma
Ammonium dihydrogen phosphate ($NH_4H_2PO_4$)	1126	Merck
Ammonium phosphate (APS)	A1292	Sigma
Bromophenol blue	B0126	Sigma
Chloroform	7386	J.T.Baker
Complete Protease Inhibitor Cocktail	04693116001	Roche
Coomassie Brilliant Blue G250	17524	Serva
Diammonium sulfate ($(NH_4)_2SO_4$)	3746.4	Roth
Dipotassium hydrogen phosphate (K_2HPO_4)	P749.2	Roth
Disodium hydrogen phosphat (Na_2HPO_4)	1.06580.1000	Merck
Dimethyl sulfoxide (DMSO)	A994.2	Roth
Iron(III) chloride ($FeCl_3$)	P742.1	Roth
Acetic acid	3738.5	Roth
Ethanol (EtOH)	8006	J.T.Baker
HEPES Buffer ≥99.5%	9105.3	Roth
Gallium nitrate ($Ga(NO_3)_3$)	289892	Aldrich
Glycine ≥99% p.A.	3908.2	Roth
Glycerole ~86% p.A.	4043.5	Roth
Potassium chloride ≥99.5% p.A. (KCl)	6781.1	Roth
Potassium dihydrogen phosphate (KH_2PO_4)	3904.1	Roth
Magnesium chloride ($MgCl_2$)	2189.1	Roth
Skim milk powder	70166	Fluka

Methanol (MeOH)	8045	J.T.Baker
Sodium chloride ≥99.5% (NaCl)	3957.1	Roth
Sodium dodecyl sulfate (SDS)	CN30.3	Roth
Sodium fluoride 99.99 Suprapur® (NaF)	1610302	Merck
Sodium orthovanadate ≥90% (Na_3VO_4)	S6508	Sigma
Phosphatase Inhibitor Cocktail 1	P2850	Sigma
Phosphatase Inhibitor Cocktail 2	P5726	Sigma
Orthophosphoric acid (H_3PO_4) 85%	9079.2	Roth
Rotiphorese gel 30 (37.5:1), Acrylamide	3029.1	Roth
Hydrochloric acid (HCl)	1.09060.1000	Merck
TEMED 99% p.A.	2367.1	Roth
Thiazolyl Blue Tetrazolium Bromide (MTT)	M2128	Sigma
Triethylammonium bicarbonate buffer for HPLC (TEAB)	17902	Fluka
Trifluoroacetic acid Uvasol (TFA)	1.08262.0100	Merck
Triton X-100	T9284	Sigma
TRIS ≥99.5%	T1503	Sigma
Tween 20	9127.1	Roth

Table 3-2: Used buffers in this study

Buffer	Composition	Concentration
4x SDS sample buffer, pH 6.8	TRIS	0.24 M
	Glycerine	40% (v/ v)
	2-Mecaptoethanol	12% (v/ v)
	SDS	0.27 M
	Bromophenol blue	0.004% (w/ v)
Blot buffer, pH 8.3	TRIS	25 mM
	Glycerine	192 mM
	SDS	3.5 mM
	MeOH	20% (v/ v)
Coomassie silver	H_3PO_4	10% (v/ v)
	$(NH_4)_2SO_4$	10% (w/ v)
	MeOH	20% (v/ v)

	Coomassie BB G250	0.12% (w/ v)
Digest buffer	TEAB	50 mM
	ACN	10% (v/ v)
	Phosphatase Inhibitor Cocktail 1	1:100
	Phosphatase Inhibitor Cocktail 2	1:100
Gel fixing solution	EtOH	30% (v/ v)
	Acetic acid	10% (v/ v)
IMAC elution buffer, pH 4.5	$NH_4H_2PO_4$	0.1 M
IMAC wash buffer, pH 2.8	MeOH	27% (v/ v)
	ACN	27% (v/ v)
	Acetic acid	20% (v/ v)
Lysis buffer, pH 7.5	HEPES	50 mM
	NaCl	1 M
	$MgCl_2$	10 mM
	Complete Protease Inhibitor	1tablet/ 50 ml
	NaF	10 mM
	Na_3VO_4	2.5 mM
	Phosphatase Inhibitor Cocktail 1	1:100
	Phosphatase Inhibitor Cocktail 2	1:100
	Glycerine	5% (v/ v)
	Triton X-100	1% (v/ v)
PBS, pH 7.4	NaCl	137 mM
	KCl	2.7 mM
	Na_2HPO_4	10 mM
	KH_2PO_4	2 mM
RP elution buffer	MeOH	60% (v/ v)
	TFA	0.5% (v/ v)
RP wash buffer	TFA	60% (v/ v)
SCX buffer A	FA	0.065% (v/ v)
	CAN	25% (v/ v)
SCX buffer B	FA	0.065% (v/ v)
	ACN	25% (v/ v)
	KCl	0.5 M

SDS buffer A,	TRIS	1.5 M
pH 8.8	SDS	14 mM
SDS buffer B,	TRIS	0.5 M
pH 6.8	SDS	14 mM
SDS running buffer,	Glycine	199 mM
pH 8.9	TRIS	24 mM
	SDS	3.5 mM
TBS-T	TRIS	20 mM
	NaCl	137 mM
	Tween 20	0.1% (v/ v)
TBS-T/ NaCl	TBS-T +	
	NaCl	0.5 M
TBS-T/ Triton X-100	TBS-T +	
	Triton X-100	0.5% (v/ v)
UPLC buffer A	FA	0.1% (v/ v)
UPLC buffer B	FA	0.1% (v/ v)
	ACN	99.9% (v/ v)
WB blocking	TBS-T +	
solution 1	Skim milk powder	5% (w/ v)
WB blocking	TBS-T +	
solution 2	BSA	5% (w/ v)

All used buffers and solutions were prepared with ddH_2O water. To set the pH value, HCl, NaOH, ammonia, or acetic acid were used.

3.2 Recombinant proteins

Hepatocyte growth factor (HGF) and Internalin B (InlB) were kindly provided by Dr. Jörn Kraußе and Dr. Joop van den Heuvel from the Molecular Structural Biology Department of the Helmholtz Center for Infection Research.

HGF was recombinantly expressed in CHO insect cells in a 2.5 l fermenter. As the protein was secreted, the concentrated supernatant could directly be applied onto a heparin column where the protein was purified. Afterwards, it was activated by

digestion with hepatocyte growth factor activator (HGFA), bound to a strong cation exchange column, and eluted at about 750 mM NaCl in HEPES buffer. HGF was stored at 4 °C to maintain the conformation and activity of the protein.

Internalin B full length (InlB) was recombinantly expressed in CHO cells with a GST-tag. The cells were pelleted, lysed by homogenization, and the supernatant was loaded onto a glutathione sepharose (GST) column. PreScission protease was added to cut off InlB, and the protein was eluted. To further purify the product, strong cation exchange chromatography was applied and the protein was eluted during an NaCl gradient. InlB was aliquoted and stored at -80°C to decrease protein degradation.

To check purity of the recombinant proteins, SDS gels were run and stained with Coomassie blue. If the correct bands appeared on the gel, proteins were tested for activity as illustrated in section 3.3.2.

3.3 Cell culture

3.3.1 Splitting and storage of cells

Table 3-3: Cell lines used in this study

Cell line	Origin	Properties
HeLa S3	Human cervix adenocarcinoma	Epithelial, adherent
DU145	Human prostate carcinoma	Epithelial, adherent

Standard medium HeLa S3: Dulbecco's Modified Eagle's Medium (Gibco DMEM, #31885, Invitrogen) was combined with 10% Fetal bovine serum (FBS Gold, #A15151, PAA Laboratories), 1x Pen/Strep (#15070-063, Invitrogen), 2 mM L-Glutamine (#25030, Invitrogen).

Minimal medium HeLa S3: Dulbecco's Modified Eagle's Medium (Gibco DMEM, #31885, Invitrogen) was combined with 1x Pen/Strep (#15070-063, Invitrogen).

Standard medium DU145: Roswell Park Memorial Institute 1640 medium (Gibco RPMI, #21875, Invitrogen) was combined with 10% Fetal bovine serum (FBS

Gold, #A15151, PAA Laboratories), 1x Pen/Strep (#15070-063, Invitrogen), 2 mM L-Glutamine (#25030, Invitrogen).

Minimal medium DU145: Roswell Park Memorial Institute 1640 medium (Gibco RPMI, #21875, Invitrogen) was combined with 1x Pen/Strep (#15070-063, Invitrogen).

DU145 and HeLa S3 cells were cultivated to a confluence of 80-90% at 37 °C and 7.5% CO_2 in their medium, respectively. Before splitting, the cells were washed three times with PBS and removed from the culture dish with Trypsin-EDTA solution (#25300, Invitrogen). The reaction was stopped by adding standard medium. The cells were pelleted at 200 g for three minutes, resuspended in standard medium, and diluted from 1:20 to 1:100 in a new Petri dish with fresh medium.

In order to store the human cells, their concentration was determined in a Neubauer counting chamber and the cells were diluted to a final concentration of $2*10^6$ cells/ ml in 1:1 standard medium with 10% DMSO in 1 ml aliquots. The cells were afterwards frozen at -80 °C and stored in liquid nitrogen. When needed one aliquot was thawed at 37 °C, washed with fresh medium and seeded in a 10 cm Petri dish.

3.3.2 Preparation of human cells for experiments

For functional testing of the recombinant HGF protein, 10^5 DU145 cells were seeded in 3 cm dishes in duplicates and cultured overnight in standard medium. The next day, cells were serum-starved with minimal medium for 24 h. Then, the first half was stimulated for 5 min with 0, 0.02, 0.2, 2, 20, or 200 nM HGF and harvested with 50 µl SDS sample buffer supplied with 1 µl Benzonase (#1.01695.001, Merck) by scraping on ice. The second half of the cells was stimulated for 20 h with the same concentrations. The HGF-induced motility was then monitored by microscopy with an Axiovert100 (Zeiss) and documented by taking pictures with a digital camera (DXM1200, Nikon).

For the phosphoproteome experiments, three 15 cm dishes per sample were seeded with $3*10^6$ cells and cultured overnight in standard medium. After 24 h of starvation in minimal medium, the cells were stimulated with 2 nM HGF for 3, 6, 20

min, or with 10 nM InlB for 5 min. The medium was drained off and the cells were harvested with 500 µl lysis buffer by scraping on ice. Lysis was carried out for 30 min on ice and supported by vortexing and sonication in a water bath for 5 min.

3.4 RNAi approaches

3.4.1 Proliferation Assay

For the proliferation assay of HeLa S3 cells in response to NEK9 knockdown and HGF, 1000 cells per well were seeded into a 96-well plate and transfected with both NEK9 siRNAs in combination or left untreated. All samples were starved with DMEM minimal medium for 24 h and then stimulated with 2 nM HGF for 6 d. Every 24 h, cells were treated with 20µl of 5 mg/ ml MTT in PBS, which is reduced by living cells to the purple-colored formazan. After incubation for 2 h in the incubator, cells were washed with PBS and then incubated with isopropyl-HCl (0.13% HCl in isopropyl alcohol) while shaking, approximately for 10 -30 min, until the small crystals of the stain were dissolved. Afterwards, the absorbance was measured at 595 nm with an Infinite M200 ELISA reader (Tecan).

Table 3-4: Nek9 transfection solution for a 3 cm dish (3 ml volume)

Reagent	Catalog number	Company	Amount
NEK9 siRNA 5	SI02622459	Qiagen	10 nM
NEK9 siRNA 7	SI02660476	Qiagen	10 nM
Or nonsense siRNA	1022076	Qiagen	10 nM
HiPerFect	301705	Qiagen	12 µl
DMEM minimal medium	See 3.3.1	See 3.3.1	100 µl

3.4.2 Gene expression arrays

For NEK9 and HGF-dependent gene expression profiling, 8 plates with $3*10^5$ HeLa S3 cells per 10 cm petri dish were seeded and transfected either with 10 nM nonsense siRNA or NEK9 siRNAs 5 and 7 the next day. After 24 h, the medium was changed to DMEM minimal medium and cells were starved for additional 24

h. One half of the plates were afterwards treated with 2 nM HGF for 18 h, the others left untreated as a control. The experiment was performed in duplicates.

Table 3-5: Samples for RNA array with Nek9 knockdown

Samples	Cell line	Condition	Treatment
1	HeLa S3	Nonsense siRNA	-
2	HeLa S3	NEK9 siRNAs 5+7	-
3	HeLa S3	Nonsense siRNA	2 nM HGF, 18 h
4	HeLa S3	NEK9 siRNAs 5+7	2 nM HGF, 18 h
5-8	second replicate		

For the EPHA2 gene expression array, 36 dishes each with $3*10^5$ DU145 cells were seeded in 10 cm plates. In parallel, the transfection solutions with 100 nM nonsense siRNA, EphA2 siRNAs 5 or 7, respectively, were prepared and applied to the cells. After 1 d, cells were starved with RPMI minimal medium for 24 h and two-thirds of the plates were treated with 2 nM HGF for 1 h or 4 h. The experiment was performed in triplicates.

For subsequent RNA isolation, cells were washed two times with ice-cold PBS and harvested with 350 µl RLT buffer (Qiagen, RNA extraction kit) by scraping on ice. RNA extraction and microarray analysis (Agilent.SingleColor.14850) was performed by the Array Facility of Dr. Robert Geffers at the HZI.

Table 3-6: EphA2 transfection solution for a 10 cm dish (5 ml volume)

Reagent	Catalog number	Company	Amount
EPHA2 siRNA 5	SI00300181	Qiagen	100 nM
Or EPHA2 siRNA 7	SI02223508	Qiagen	100 nM
Or Nonsense siRNA	1022076	Qiagen	100 nM
HiPerFect	301705	Qiagen	25 µl
RPMI minimal medium	See 3.3.1	See 3.3.1	500 µl

Table 3-7: Samples for RNA array with EphA2 knockdown

Samples	Cell line	Condition	Treatment
1	DU145	Wildtype	-
2	DU145	Nonsense siRNA	-
3	DU145	EPHA2 siRNAs 5	-
4	DU145	EPHA2 siRNAs 7	-
5	DU145	Wildtype	2 nM HGF, 1 h
6	DU145	Nonsense siRNA	2 nM HGF, 1 h
7	DU145	EPHA2 siRNAs 5	2 nM HGF, 1 h
8	DU145	EPHA2 siRNAs 7	2 nM HGF, 1 h
9	DU145	Wildtype	2 nM HGF, 4 h
10	DU145	Nonsense siRNA	2 nM HGF, 4 h
11	DU145	EPHA2 siRNAs 5	2 nM HGF, 4 h
12	DU145	EPHA2 siRNAs 7	2 nM HGF, 4 h
13-24	second replicate		
25-36	third replicate		

3.5 General biochemical Methods

3.5.1 Determination of the protein concentration

The protein concentration of cell lysates was determined according to Bradford (Bradford 1976). A small aliquot of the sample was diluted 1:10, 1:15, and 1:20 with ddH_2O, mixed with BioRad Protein Assay reagent (#5000006, Bio-Rad), and absorption was measured in triplicates by an Infinite M200 Elisa reader (Tecan) at 595 nm. Several dilutions (0.1-1 mg/ml) of bovine serum albumin in ddH_2O were used to create a calibration curve.

3.5.2 SDS-PAGE

Separation of protein samples according to molecular mass (Laemmli 1970) was performed in an SDS-PAGE system of Biometra (86*77*1 mm). Stacking and separating gels were prepared as described in Table 3-8 and polymerized at least overnight at 4 °C. In most cases, 10% SDS gels with 10 pockets were used. The

samples were mixed with 4x SDS sample buffer, boiled for 3 min at 95 °C, and centrifuged for 1 min at 13,000 rpm to pellet insoluble particles.

Table 3-8: SDS gel preparation

Solution	Stacking gel 4.2% SDS	Separating gel 10% SDS
SDS buffer A	-	2.5 ml
SDS buffer B	2.5 ml	-
ddH_2O	6.1 ml	4.2 ml
Rotiphorese gel 30	1.4 ml	3.3 ml
TEMED	30 µl	20 µl
APS, 10% solution	60µl	50 µl

10–20 µl sample per gel pocket was loaded on an SDS gel and run for about 90 min at 120 V until Bromophenol Blue reached the bottom of the gel. PageRuler Prestained Protein Ladder (#26616, Fermentas) was used as molecular mass standard.

3.5.3 Immunoblotting

After gel electrophoresis, the proteins were transferred to a PVDF membrane (Immun-Blot PVDF Membrane, 0.2 µm, #162-0177, Bio-Rad). Therefore, the SDS gel, the membrane, and the Whatman paper were equilibrated in Blot buffer for 15 min and the proteins were transferred at 55 mA and 25 V for 1 h by a Semi-dry transfer cell (Trans-Blot SD, #170-3940, Bio-Rad). After that, the membrane was saturated either with WB blocking solution 1, or, in case of phospho-specific antibodies, with WB blocking solution 2 for 1 h. The membrane was incubated with primary antibody in blocking solution overnight at 4 °C with gentle agitation, washed with TBS-T, TBS-T/NaCl, TBS-T/Triton X-100, and once again with TBS-T. Afterwards, it was incubated with secondary antibody (1:2,000) in blocking solution for 1 h at room temperature. The membrane was washed three times with TBS-T. Detection was carried out by applying Lumi-Light Western Blot Substrate (#12015200001, Roche). Chemiluminescence was then detected by a CCD camera (Fujifilm LAS3000, Raytest).

Table 3-9: Applied antibodies

Directed protein	Reactivity	Dilution	Catalog number	Company
Actin	Mouse	1:5,000	A5441	Sigma
Actin	Rabbit	1:5,000	A5060	Sigma
EGFR	Rabbit	1:1,000	4267	Cell Signaling
GAPDH	Mouse	1:2,000	MCA4740	ABD Serotec
HSP90	Goat	1:1,000	AF3286	R&D Systems
NEK9	Mouse	1.3,000	H00091754-A01	Abnova
NEK9	Rabbit	1:5,000	(Roig et al. 2002)	
pEPHA2 (S897)	Rabbit	1:1,000	CY1108	Cell Applications
pERK1,2 (T202/Y204)	Mouse	1:1,000	9106	Cell Signaling
pMet (Y1234/Y1235)	Rabbit	1:1,000	3126	Cell Signaling

3.5.4 Coomassie staining of SDS gels

SDS gels were stained either directly after SDS-PAGE to estimate the amount of protein in cell lysates or after Western Blot to check the efficiency of the protein transfer to the blotting membrane. Therefore, gels were immersed in Gel fixing solution for at least 1 h and then stained overnight with Coomassie silver while shaking. To decrease background, gels were unstained by washing with H_2O for several times. Afterwards, gels were scanned by a ScanMaker 9800XL (1108-03-360072, Microtek) and saved as 16-bit grayscale pictures.

3.6 Quantitative phosphoproteome analysis

3.6.1 Protein precipitation

Proteins from DU145 cells stimulated 0, 3, 6, and 20 min with HGF and those stimulated 0, and 5 min with InlB in HeLa S3 cells were precipitated according to Wessel and Flügge (Wessel and Flügge 1984). In short, one volume of the sample was mixed with four volumes of methanol and one volume of chloroform, and then three volumes of H_2O were added. After vortexing and centrifugation, the protein

pellet, localized in the interphase, was washed with three volumes of Methanol and dried at room temperature. For each phosphoproteome sample 4 mg of protein were used.

3.6.2 Tryptic digest

For digesting of the proteins to peptides, Trypsin (sequence grade, bovine, #V511A, Promega) had to be activated in 100 µl Trypsin resuspension solution (#V542A, Promega) for 15 min at 37 °C. Next, the protein pellet was resuspended in 1.5 ml of digestion buffer by sonication and 40 µg Trypsin (corresponding to 200 µl) were added. The tryptic digest was performed overnight at 37 °C.

3.6.3 Purification of peptides via Bakerbond columns

For purification of the peptides C_{18} reverse phase (RP) chromatography was utilized. LiChroprep RP-18 (25-40 µm, #1.09303.0100, Merck) resin was mixed with RP elution buffer and pipetted to a Bakerbond column (#7121-01, J.T. Baker) to a filling level of 3-5 mm. The resin was equilibrated three times with 600 µl elution buffer and three times with wash buffer by gently blowing nitrogen through the column. After that, the samples were acidified with 10% TFA and loaded ten times. By adding three times RP wash puffer, the peptides on the column were desalted. For elution, 600 µl RP elution buffer was applied to the resin, peptides were collected below and the eluted fraction was dried in a centrifugal evaporator.

3.6.4 Isolation of phosphopeptides

For phosphoproteome analyses the phosphopeptides have to be enriched by Immobilized Metal Affinity Chromatography (IMAC) as they are underrepresented in cell lysates and non-phosphopeptides also disturb the ionization during mass spectrometric measurements. Using the Ga-IDA Phosphopeptide Enrichment Kit (#89853, Thermo-Pierce, not available anymore), which is based on Ga^{3+} ions binding to phosphate groups, it was possible to purify phosphopeptides from whole cell lysates. Therefore, the peptides were resuspended in 50 µl IMAC wash buffer, mixed with the swell gel of the kit, which contains the Ga resin, and incubated overnight at 4 °C. The next day, the resin was transferred into the supplied centrifugation columns and washed five times with 100 µl IMAC wash buffer to

flush out the non-phosphopeptides. To elute phosphopeptides, the resin was incubated 5 min with IMAC elution buffer and centrifuged afterwards. This was repeated four times to dissolve all phosphorylated peptides from Ga-resin. The flow-through was collected as well and used for a subsequent IMAC. This procedure was repeated until no phosphopeptides were enriched anymore. All dried samples were stored at -80 °C.

3.6.5 iTRAQ labeling of phosphorylated peptides

Before labeling of the peptides they first have to be purified by RP chromatography with Bakerbond columns as described above. The labeling was done with iTRAQ® Reagents Multiplex Kit (#4352135, AB Sciex) according to the manufacturer's advices. In short, purified peptides were resuspended in 40 µl Dissolution Buffer. The four labels with different reporters available in the kit (114.1, 115.1, 116.1, 117.1) were reconstituted in 70 µl ethanol and transferred to the sample. The incubation was done for 2 h at room temperature in the dark. Once the peptides were labeled, all samples of one experiment were pooled together and dried.

Table 3-10: iTRAQ Labeling scheme

Experiment	Sample	Label
HGF time course	0 min	114.1
	3 min	115.1
	6 min	116.1
	20 min	117.1
InlB stimulation	0 min	115.1
	5 min	117.1

3.6.6 Fractionation of phosphopeptides

The peptides were purified once again by RP chromatography with Bakerbond columns as described above. After that, fractionation by Strong Cation eXchange chromatography (SCX) was performed to decomplex the samples for mass spectrometry and to further purify phosphopeptides from acidic peptides. Therefore, 45 µl SCX buffer A was added to the peptides, the samples were ultracentrifuged (Sorvall Discovery MS120E, Hitachi, rotor S100AT3-308) for 20

min at 50,000 rpm and the supernatant was transferred into an Ettan-microLC system. The peptides were separated on a Mono S PC1.6/ 5 column (#17-0672-01, GE Healthcare) by a linear gradient (0–35% SCX buffer B, 15 min, 150 µl/ min flow rate). One fraction per minute was collected, in total 30 fractions were analyzed. The identification of peptide-containing fractions was supported by measuring the absorbance at 214 nm.

3.6.7 Purification of peptides using pipette tips

After fractionation the amount of phosphopeptides in each fraction is very low, however, for mass spectrometry, the samples need to be desalted again. Therefore, purification was done with RP resin containing pipette tips (ZipTip Pipette Tips 0.6 µl, # ZTC18S008, Millipore). As for the Bakerbond columns, the resin was first washed five times with RP elution buffer, then five times with RP wash buffer, and the sample was loaded ten times by gently pipetting the solutions up and down. Washing was done ten times; finally, the peptides were eluted in 30 µl RP elution buffer. The eluted phosphopeptides were then dried and stored at -80 °C until they were measured by mass spectrometry.

3.6.8 Mass spectrometry analysis

The purified samples were resuspended in 10 µl RP wash buffer, floating particles were pelleted by ultracentrifugation at 50,000 xg for 15 min and the phosphopeptides were applied to an Ultimate 3000 RSLCnano system (Thermo) with a C18 precolumn (Acclaim PepMap100 C18 nano-Trap Column, #164535, Thermo) for washing with UPLC buffer A. The separation took place on the analytic column (Acclaim PepMap RSLC, #164536, Thermo) with UPLC buffer B and a flow rate of 350 nl / ml with a 30–120 min gradient. The connected mass spectrometer was an Orbitrap Velos (Thermo), which was operated with Xcalibur (version 2.1, Thermo). The measurement parameters included dynamic exclusion (Table 3-11).

Table 3-11: Parameters for dynamic exclusion

Parameter	Setting
Repeat count	2
Repeat duration	20 sec
Exclusion duration	120 sec
Exclusion mass width	By mass
- Low	1.1
- High	1.6
Exclusion list size	500
Early expiration	Enabled
Count	3
S/ N threshold	2.0

3.6.9 Identification of proteins by database search

The resulting spectra from mass spectrometry (MS) provide the masses of the mother ions and after a further fragmentation step (MS/MS) show the fragment ions of the mother ions. These were sent against Mascot (version 2.3, Matrix Science), a database consisting of theoretically calculated masses, and were matched with the current UniProt database. The parameters chosen for the identification of the peptides and their corresponding proteins are shown in Table 3-12. Furthermore, Mascot is also able to identify phosphorylation sites. Those of the significantly regulated phosphopeptides were later checked manually together with Dr. Manfred Nimtz.

Table 3-12: Parameters for identification of peptides/ proteins

Parameter	Setting
Taxonomy	Homo sapiens (human)
Database	SwissProt
Fixed modifications	CarboxyMethyl (C)
Variable modifications	iTRAQ4plex (K), iTRAQ4plex (N-term.), iTRAQ4plex (Y), Oxidation (M), Phospho (ST), Phospho (Y)
Enzyme	Trypsin

Max. missed cleavages	2
Peptide charge	2+ and 3+
Peptide tol. +/ -	5 ppm
Data format	Sequest (.DTA)
Decoy database	Enabled
Monoisotopic	Enabled
MS/ MS search	Enabled
MS/ MS tol. +/ -	0.02 Da
Instrument	ESI-FTICR

3.6.10 Analysis of regulated peptides

The normalization of the samples was carried out with Prof. Dr. Frank Klawonn. For quantitative analysis of the different samples, the peptides were labeled with iTRAQ. The labels' reporters can be found in the peptide spectra in the low mass range. The intensities of the reporters were then used to compare the amount of the associated peptide between the samples. ITRAQassist, an in-house bioinformatics software (Hundertmark et al., 2009; Reinl et al., 2009) calculated regulation factors of the peptides on the basis of Mascot result files (dat-file). Firstly, the program corrected for the contamination of the labels' isotopes, secondly, estimated the instrument's specific background noise, and finally calculated the most probable Regulation Factor (RF) for a peptide group. The parameters were set to a minimum peptide score of 20, the regulation base was 114.1 (unstimulated control), only unique peptides were considered and peptide view was selected. The results were then exported into an Excel sheet and also as Likelihood plots. These curves illustrate the reliability of the calculated RFs, which is demonstrated by the Interval of Robustness (IoR).

To separate identified phosphopeptides from non-modified ones, the iTRAQassist results were loaded into MassCluster (version 1.2.3., in-house bioinformatics software), which then resulted in an Excel sheet showing only the phosphopeptides and their RFs in $\log_2$ scale.

This table was further processed together with Prof. Dr. Frank Klawonn to calculate significantly regulated phosphopeptides by multiple testing. Therefore, it

was assumed that regulation factors follow a normal distribution and that the significantly regulated peptides should exceed a theoretical calculated threshold within all experiments of the triplicate. The probability of a significant regulation was represented by a p-value above 95%, which corresponded to a $\log_2$ regulation factor of about 0.6.

3.6.11 Applied further software

To visualize all identified proteins and their peptide spectra, Mascot results were directly imported into Scaffold Q+ (version 3-00-01).

UniProt (www.uniprot.org) was used for annotation of single proteins, synonyms, functions, and interaction partners. For deeper literature studies PubMed (www.ncbi.nlm.nih.gov/pubmed) was searched.

As iTRAQassist and MassCluster provide only Protein Identifiers, but not UniProt Accession Numbers, StrAP 1.0 (www.downloadplex.com/Scripts/Matlab/Development-Tools/strap-clustering-data-streams-with-affinity_445041.html) was used for fetching those numbers. The program also added GO Annotations and is able to visualize data.

Java Treeview was utilized to illustrate regulated peptides or genes as a heatmap.

To get an overview of identified and regulated peptides, the belonging proteins were loaded into DAVID Bioinformatics Resources 6.7 (Database for Annotation, Visualization and Integrated Discovery, www.david.abcc.ncifcrf.gov). This online tool clusters and visualizes proteins by functional annotation (GO Annotation) or by pathways (KEGG pathway maps).

An alternative tool for pathway mapping and gathering protein information is GeneGo (www.genego.com). This commercial database also provides network building from experimental data and prediction of modulated transcriptions factors for example.

The expression of proteins in cell lines and tissues was queried with BioGPS (www.biogps.org).

Whether an identified phosphorylation site is known and functionally characterized was checked in several phosphorylation databases. The most complete and well-arranged ones were PhosphoNet (Kinexus, www.phosphonet.ca) and PhosphoSitePlus (Cell Signaling, www.phosphosite.org). PHOSIDA (www.phosida.com) and Phospho.ELM (www.phospho.elm.eu.org) were also utilized.

4 Results

Growth factor receptor signaling is a dynamic process, which is mediated by protein-protein interactions that depend on post-translational modifications. The transfer of phosphate groups amongst others between proteins influences their activity, interaction and localization and thus is an important mechanism for signal transduction and the regulation of cellular responses. However, analysis of the phosphoproteome by mass spectrometry requires an efficient enrichment method for phosphopeptides, as they are underrepresented in whole cell extracts (Hubbard and Cohen 1993).

Using state-of-the-art phosphoproteomics, this study was supposed to characterize HGF/Met signaling in a time-dependent manner to better understand the coordination of induced physiological processes, e.g. during wound healing and embryogenesis. As the cascades are also strongly activated in cancer and the experiments were performed in a cancer cell line, the approach might also reveal activities that take place during tumor growth and metastasis. How this physiological signaling is influenced by a pathogen during infection was examined in the second part of this work. As an example, the impact of the bacterium *Listeria monocytogenes* was determined by stimulation of cells with the pathogenic surface-located invasion protein InlB that is also able to activate Met (Hamon, Bierne, and Cossart 2006; Reinl et al. 2009).

4.1 Establishment of the phosphoproteome workflow

Several different phosphosproteome workflows have been described in the current literature. Most of them utilize SCX and subsequent metal ion chromatography for enrichment of phosphopeptides in combination with SILAC (Macek, Mann, and Olsen 2009; Rosenqvist, Ye, and Jensen 2011). As iTRAQ labeling and subsequent quantitative analysis supported by iTRAQassist were already established in this group (Hundertmark et al. 2009; Reinl et al. 2009) and future studies might include primary patient material, iTRAQ was chosen as the preferred labeling strategy. In order to improve the yield of identified phosphopeptides and to

cover all significant downstream pathways, several parts of the workflow had to be optimized.

First of all, the cell line DU145 was chosen for the HGF/Met study, because it is an accepted prostate cancer model and Met is expressed in high amounts to guarantee significant Met signaling. Furthermore, the cells show increased motility after HGF-stimulation, which could easily be used as control for a physiological response (Johnson, Hershberger, and Trump 2002; Humphrey et al. 1995).

An effective workflow for phosphoproteome isolation and characterization had to be established next. The aim was to identify as many phosphopeptides as possible, equivalent to current reports where thousands of sites have been published from one phosphoproteomic study (P. H. Huang 2011). Figure 4-1 illustrates the experimental strategy to investigate Met signaling in DU145 cells. The cells were starved for 24 h, followed by cell lysis and tryptic digestion of different amounts of protein. In the next step, phosphorylated peptides were enriched by IMAC. For sequencing, phosphopeptides were analyzed by LC-MS/MS. Corresponding proteins and their phosphorylation sites were then identified supported by the database Uniprot.

Within distinct pre-experiments, one parameter each was varied in order to improve efficiency of the described workflow. First of all, two IMAC strategies were compared, because isolation of phosphopeptides by IMAC is the most crucial step. Secondly, the initial amount of protein was increased in order to check for limitations. Finally, phosphopeptides after 1-dimensional IMAC separation were compared to those additionally fractionated in a 2-dimensional workflow using IMAC and SCX.

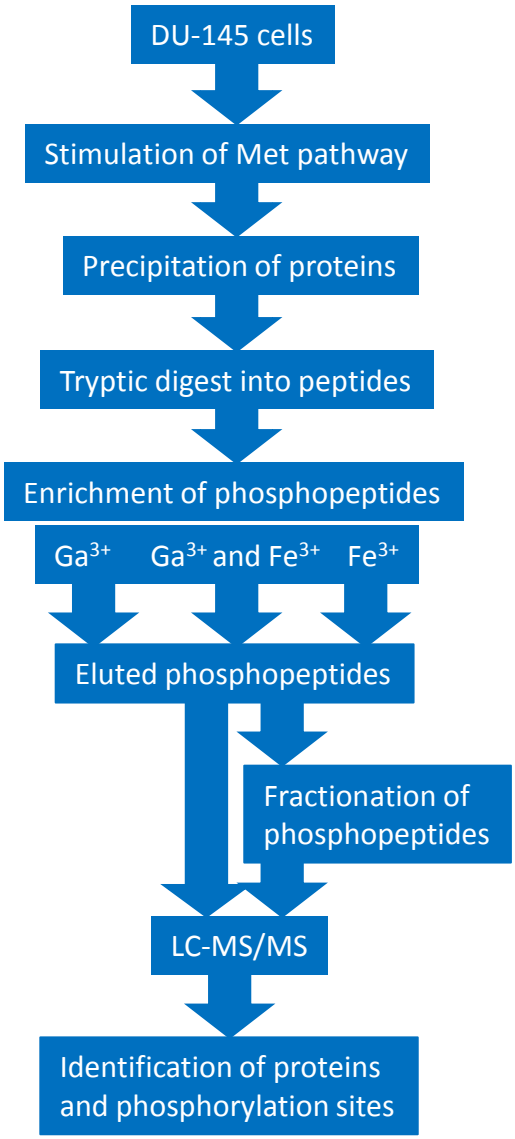

Figure 4-1: Experimental strategy for pre-experiments for the optimization of phosphopeptide enrichment

Human DU145 cells were stimulated with serum and lysed to extract proteins. For mass spectrometry, the samples were digested to peptides. Phosphopeptides were enriched by IMAC followed by fractionation via SCX. LC-MS/MS and database search were then performed to identify proteins and phosphorylation sites.

Specific phosphopeptide enrichment is the crucial step in the whole workflow. IMAC can be prepared with different types of metal ions and every material is known to have characteristic binding preferences (Mann et al. 2002). This experiment was designed to check whether IMAC via Fe^{3+} or Ga^{3+} ions produced a comparable number of phosphorylated peptides and whether a combination of both can improve selectivity or yield. To reduce experimental effort, only 2 mg of protein were utilized. It turned out that about 125 phosphopeptides were enriched

by both methods but Ga-IMAC isolated additionally almost 5-fold more phosphorylated peptides than Fe-IMAC with only 28 (Figure 4-2). Figure 4-2B shows the number of enriched peptides when the flow-through of Ga-IMAC is applied onto a Fe^{3+} column. In this case, no further phosphopeptides could be enriched by Fe-IMAC in comparison to the Ga-IMAC elution. These data illustrated clearly that IMAC with Ga^{3+} ions alone represented the method of choice for all further experiments.

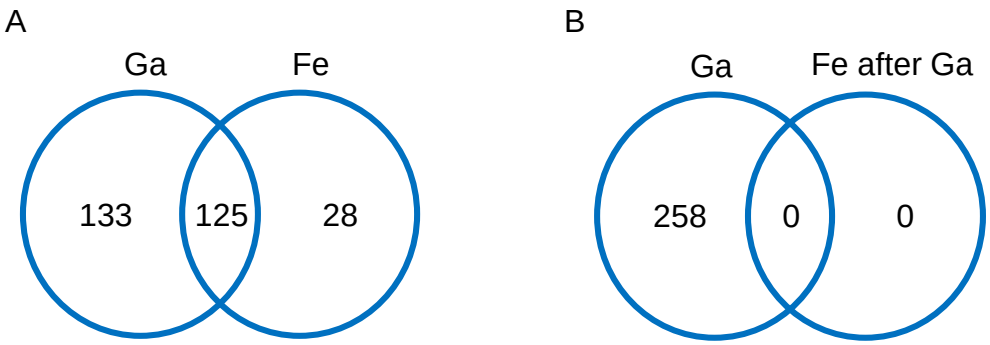

Figure 4-2: Comparison of different IMAC materials

A) Peptides from DU145 cells were either enriched by Ga- or by Fe-IMAC, and identified by LC-MS/MS. B) Phosphopeptides were first purified with Ga-IMAC, the eluate was measured by mass spectrometry, and the flow through was applied to Fe-IMAC. The number of identified unique phosphopeptides by each enrichment method is shown.

Next, the amount of protein required to produce a maximum number of phosphopeptides through this workflow was determined. For that, the protein quantity from serum-stimulated DU145 cells was varied from 300 µg to 4,000 µg and the resulting number of phosphopeptides after digestion, Ga-IMAC and LC-MS/MS was determined. While only 78 unique phosphopeptides were identified from 300 µg protein, the quantity increased more than 8-fold to 668 for 4,000 µg (Figure 4-3). Thus, increasing the amount of protein produced a greater number of identified phosphopeptides by LC-MS/MS and there was no negative effect of higher protein concentrations observable. In the main experiments, iTRAQ was planned as 4-plex labeling for a time course analysis. Therefore, all four samples would be combined before LC-MS/MS measurement and it was assumed that the number of phosphopeptides would further increase, because 16 mg of protein extract were used in total. The limit of 4 mg for each sample was chosen to

maintain experimental practicability, as this amount already requires the preparation of 3 – 4 large petri dishes (diameter: 15 cm).

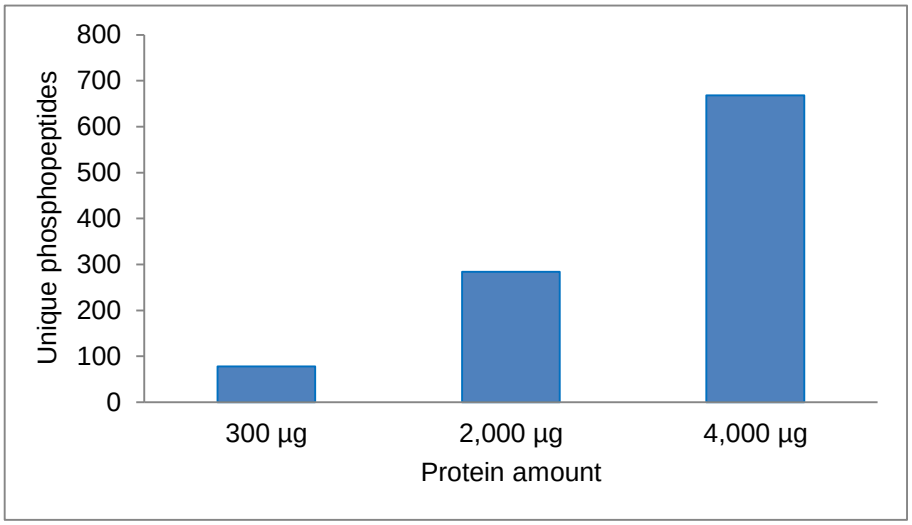

Figure 4-3: Determination of relation of protein amount to phosphopeptide recovery

Indicated amounts of protein were digested, phosphopeptides were enriched by Ga-IMAC, and analyzed by LC-MS/MS. Shown are the identified unique phosphopeptides of each sample.

So far, pre-experiments examined the efficiency of the workflow by improving 1-dimensional separation techniques. However, only the largest peptide ions in a sample are chosen for further identification during LC-MS/MS, which results in a low identification rate of ions with lesser intensity. Therefore, an additional separation of phosphopeptides via strong cation exchange chromatography (SCX) was tested next to improve the resolution of the phosphopeptides during LC-MS/MS. Ga-IMAC enriched phosphopeptides were separated on a SCX column to gain 2-dimensional-resolved peptides. One fraction per minute was collected during a 15 min salt gradient and the eluted peptides were monitored by absorption at 214 nm (Figure 4-4). The gradient (yellow curve) started during fraction 15, had a plateau between fractions 25-30 at 40% SCX buffer B, and increased then to 100% SCX buffer B at fraction 40. The absorption (blue curve) of fraction 17 displayed the most prominent peak, while fractions 18 to 25 and 35 to 42 also showed noteworthy absorbance, indicating peptide-containing fractions.

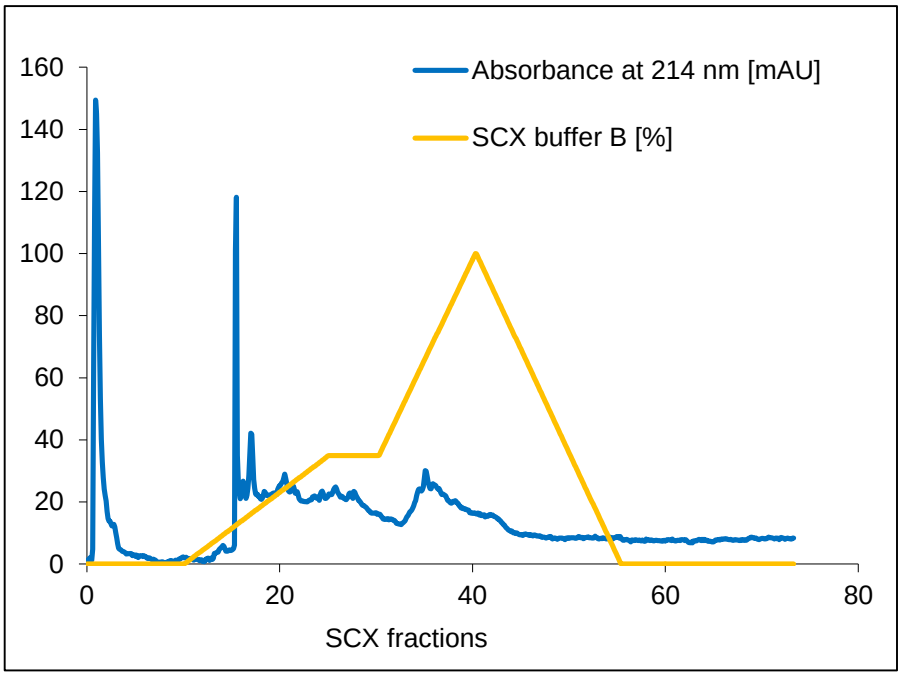

Figure 4-4: SCX chromatogram

IMAC-enriched phosphopeptides were labeled with iTRAQ, pooled and fractionated by SCX. The orange curve shows the increasing concentration of SCX buffer B during the gradient. The blue curve corresponds to milli absorbance units (mAU) of the eluted peptides detected at 214 nm.

Following, the ratio of phosphopeptides to non-phosphopeptides after SCX was calculated. Figure 4-5 shows the amount of identified peptides per SCX fraction. Non-phosphorylated peptides mainly eluted from fractions 18 to 25 corresponding to the detected absorbance in the SCX chromatogram. In contrast, phosphorylated peptides eluted earlier, namely from 8 to 27 with a maximum in fraction 16. This characteristic distribution of modified and non-modified peptides illustrated the potential of SCX in further separating phosphopeptides from non-modified ones. Therefore, only the first phosphopeptides-containing fractions 1 to 22 were analyzed by LC-MS/MS in this study in order to reduce the number of unmodified peptides in the further analyses.

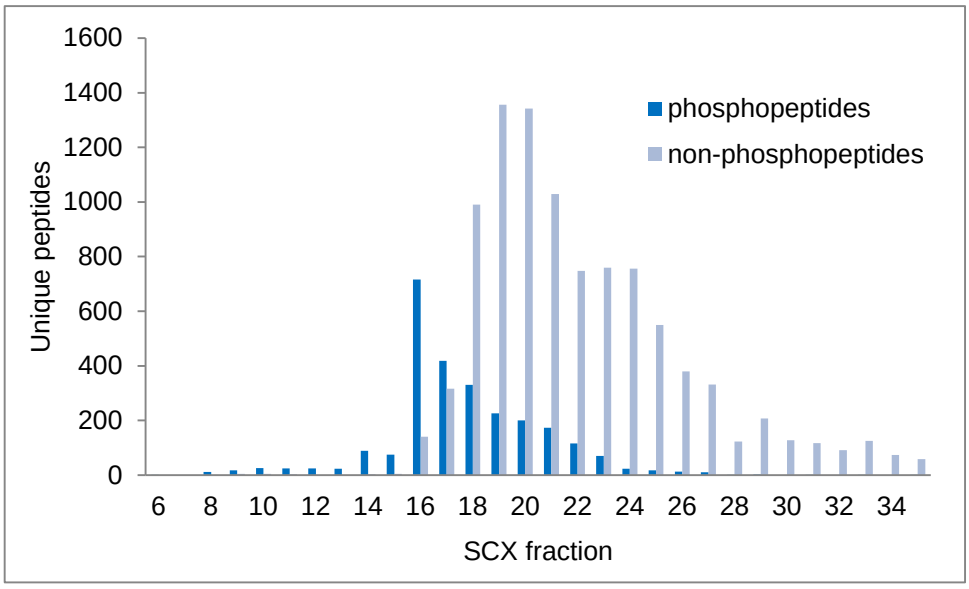

Figure 4-5: Distribution of phosphopeptides and non-phosphopeptides in SCX fractions

The total amount of LC-MS/MS-identified unique peptides for each fraction (6-35 analyzed) is shown. Light blue bars correspond to non-phosphopeptides, while the blue ones represent identified phosphopeptides. For further analyses the resulting raw-files were merged.

Furthermore, the number of phosphopeptides resulting from 2-dimensional Ga-IMAC and SCX were compared to those, from samples not further fractionated. Indeed, SCX increased the number of identified unique phosphopeptides more than 2-fold up to approximately 1,400 (Figure 4-6). However, the number of fractions collected is limited by the time these samples need for measurement by LC-MS/MS as one fraction already takes about 150 min to be analyzed.

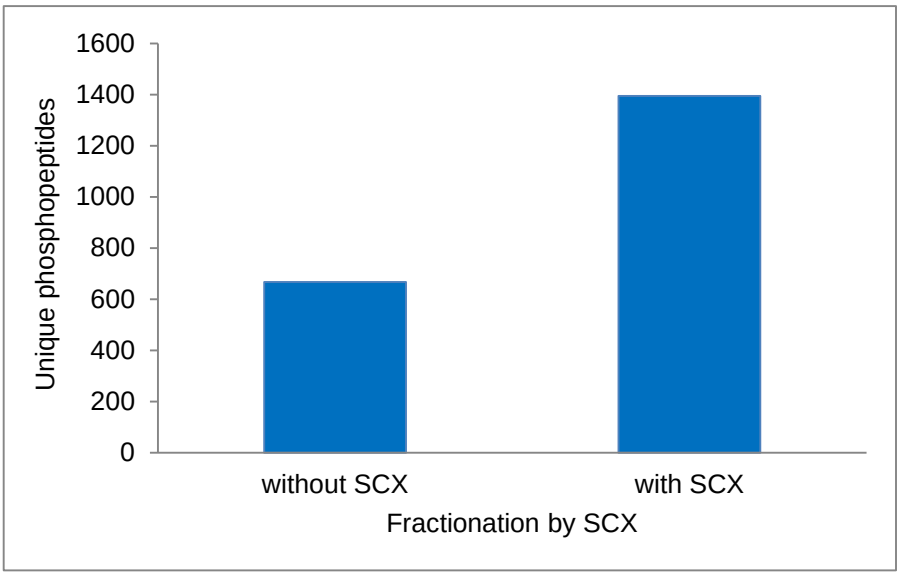

Figure 4-6: SCX increased the number of identified phosphopeptides

Phosphopeptides from digested proteins were purified by Ga-IMAC and identified by LC-MS/MS. Additional SCX fractionation after IMAC produced more identified unique phosphopeptides.

Screening the resulting list of phosphorylated proteins revealed that many essential signaling components were identified by this method. For example, mitogenic protein kinases like NEK9 and some CDKs as well as survival-regulating kinases like ABL-2 were detected by their phosphorylated peptides. The motogenic response was shown by the phosphorylation of several PAKs and some activating proteins of the small GTPases like RHG29 and RHG32. Several of the antagonists of kinases in signaling, the protein phosphatases PP4R2 and PTN12, were also identified. Furthermore, the transcription factors BCLF1, TCF20, and TF3C1 were observed. All of these mentioned proteins have in common that they belong to the low abundance proteins (Beck et al. 2011). Thus, this workflow was sensitive enough to even detect phosphorylations of proteins that show a small copy number per cell.

Taken together, the established workflow was able to extract a high amount of phosphopeptides out of 4 mg protein, enriched by Ga-IMAC and SCX. Remarkably, it provided access to many signaling components, and is therefore a suitable and sensitive method for the analysis of Met-dependent signaling.

4.2 Characterization of the physiological HGF/Met signaling

4.2.1 HGF-activated Met signaling and scattering of DU145 cells

Hepatocyte growth factor (HGF) was used to stimulate Met signaling in DU145 cells. It was recombinantly expressed in CHO cells and purified by the Molecular Structural Biology Department of the HZI. To ascertain the purity and functionality of the protein, three different tests were performed. First, a small aliquot was applied on an SDS gel to check for contaminations with other proteins. Second, DU145 cells were stimulated with different concentrations of HGF and the phosphorylation response of known pathway components was investigated by immunoblotting. Finally, DU145 cells were stimulated with the different concentrations of HGF and monitored for increased motility.

As described above, HGF was separated on an SDS gel with reducing sample buffer. As shown in Figure 4-7, elution fractions from SCX purification produced two bands of about 50 and a double band at 30 kDa, corresponding to the alpha and beta chains of the heterodimeric protein. A small portion of undigested pre-HGF was detected as a light band of 80 kDa. As this precursor only occurred in a low concentration, it was supposed to not influence the stimulation. The most concentrated HGF-containing fractions 5-10 were pooled and stored at 4°C until usage.

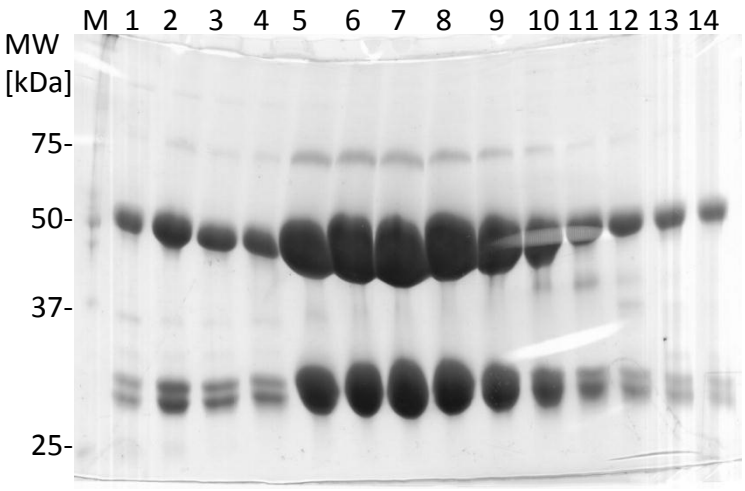

Figure 4-7: Control of purified HGF

HGF was recombinantly expressed in CHO insect cells and purified by affinity chromatography. Aliquots of the SCX fractions 1-14 were applied to an SDS gel, and stained with Coomassie brilliant blue. M: Precision Plus protein standard.

Two further approaches with different HGF concentrations (0, 0.02, 0.2, 2, 20, 200 nM) were carried out to determine the minimal concentration required for triggering Met signaling. The first experiment was designed as activity test for known phosphorylation sites downstream of Met. Therefore, cells were stimulated for 5 min with different concentrations of the growth factor and then analyzed for the presence of phospho-Met (pT^{1234}/pY^{1235}), phospho-ERK1 (MK03, pT^{202}/pY^{204}) and phospho-ERK2 (MK01, pT^{185}/pY^{187}) with specific antibodies. As illustrated in Figure 4-8, the Met receptor as well as the MAP kinases ERK1 and ERK2 were activated at 0.2 nM HGF and higher. These results proved the ability of the recombinant HGF to stimulate a significant phosphorylation response in the Met pathway.

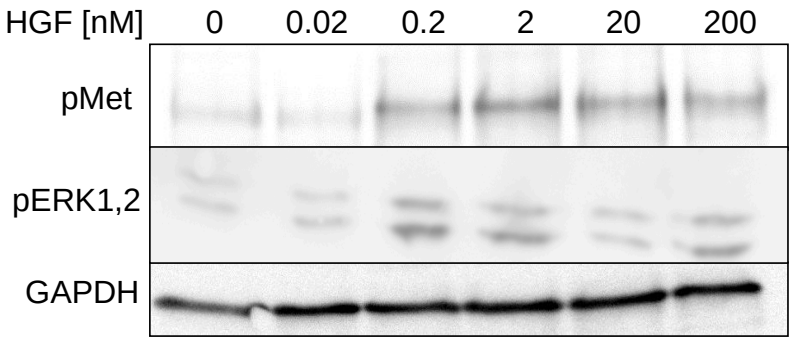

Figure 4-8: Activation of the Met pathway by HGF stimulation

DU145 cells were stimulated for 5 min with indicated concentrations of HGF. Samples were analyzed by Western blotting with antibodies against phospho-Met (pY^{1234}/pY^{1235}) and phospho-ERK1 (pT^{202}/pY^{204}) and phospho-ERK2 (pT^{185}/pY^{187}). GAPDH served as control.

Additionally, the ability of HGF to induce Met-dependent cell scattering (Humphrey et al. 1995) was tested. DU145 cells were stimulated with the same concentrations of HGF as for the phospho-specific immunoblot and monitored under a microscope after 24 h. Without HGF, DU145 cells grew in clusters, adherent to the surface of the dish. Stimulation with increasing concentrations of the growth factor up to 0.2 nM HGF resulted in increased motility (Figure 4-9, first row). Above 0.2 nM, the scattering of cells decreased again, but no negative effects could be observed by microscopy (Figure 4-9, second row).

Taken together, a concentration of 0.2 nM HGF is sufficient to trigger Met-induced signaling and for inducing a motoric response of DU145 cells. To ensure a reliable stimulation of the cells in the main experiments and because no negative effect was determined above, a HGF concentration of 2 nM HGF was chosen for further studies.

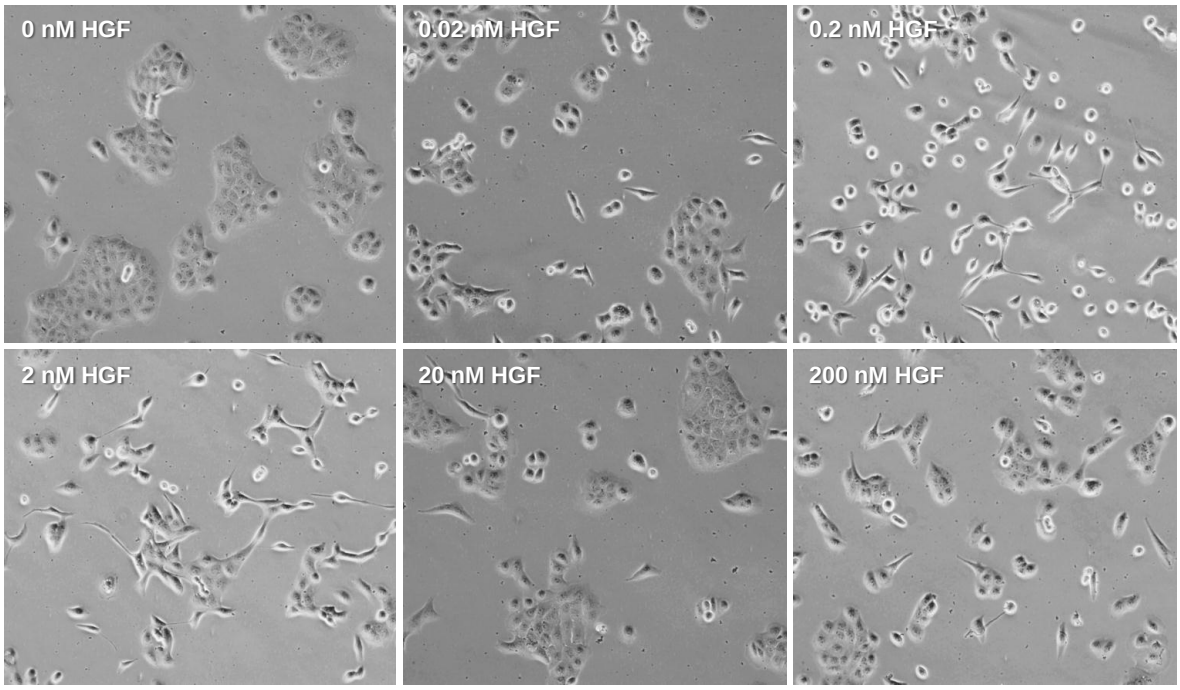

Figure 4-9: Activation of HGF-induced cell scattering

100-fold magnification of DU145 cells stimulated for 24 h with indicated concentrations of HGF. Images were taken with a digital camera under a transmitted light microscope (see 3.3.2).

4.2.2 The HGF/Met-induced phosphoproteome

Following the purity and functional activity of the HGF protein used for stimulation, main studies analyzing the HGF-induced phosphoproteome were performed. Therefore, activation of known pathway components after the chosen time points was checked first by immunoblotting with phospho-specific antibodies. Afterwards, all identified phosphopeptides were investigated concerning their functional classification as well as their composition of modified amino acids. Quantitative analysis of the different samples was performed subsequently.

In order to investigate HGF/Met signaling, the cell line DU145 was selected, because it provides an accepted model system for Met and cancer studies (Johnson, Hershberger, and Trump 2002). As the peak of Met activation is at 5 min and that of the MAP kinases at 15 min (Ozen et al. 2012), time points 3, 6, and 20 min were chosen for stimulation with HGF. A fourth sample, consisting of non-stimulated DU145 cells, served as a control. This time course ensured covering of very early as wells as sustained or late signaling events.

The workflow for these experiments was mainly as for the pre-experiments. Instead of serum, HGF was used for stimulation. In order to monitor the phosphorylation pattern over a time course, cells were stimulated for the three indicated time points and compared to non-stimulated cells. Furthermore, the samples were labeled with the four iTRAQ reagents in contrast to the non-tagged samples of the pre-experiments.

DU145 cells were stimulated for 0, 3, 6, and 20 min with 2 nM HGF-HEPES in RPMI minimal medium. Stimulation was controlled using immunoblots, and the same amount of HEPES buffer in medium were applied to cells in parallel samples. Afterwards, the cells were harvested and lysed for phosphoproteome analyses. One aliquot of each sample was analyzed by immunoblotting for presence of phospho-Met (pT^{1234}/pY^{1235}), and phospho-ERK1 and 2 (alias MK03, MK01, pT^{202}/pY^{204}, pT^{185}/pY^{187}). As shown in Figure 4-10, cells treated with only buffer showed no phosphorylation of either Met or ERK1 and ERK2. Light bands could be found for phospho-Met, though, but it is rather typical background of the antibody. That is also true for the 0 min time point of the HGF-stimulated sample, which was also treated with buffer and displayed a light band for Met. Importantly, after 3 min with HGF, Met was activated at pY^{1234}/pY^{1235}, and the phosphorylation of the MAP kinases ERK1/2 was also induced after 3 to 20 min. These observations proved the successful stimulation of the HGF samples, which could afterwards be further processed to enrich phosphopeptides.

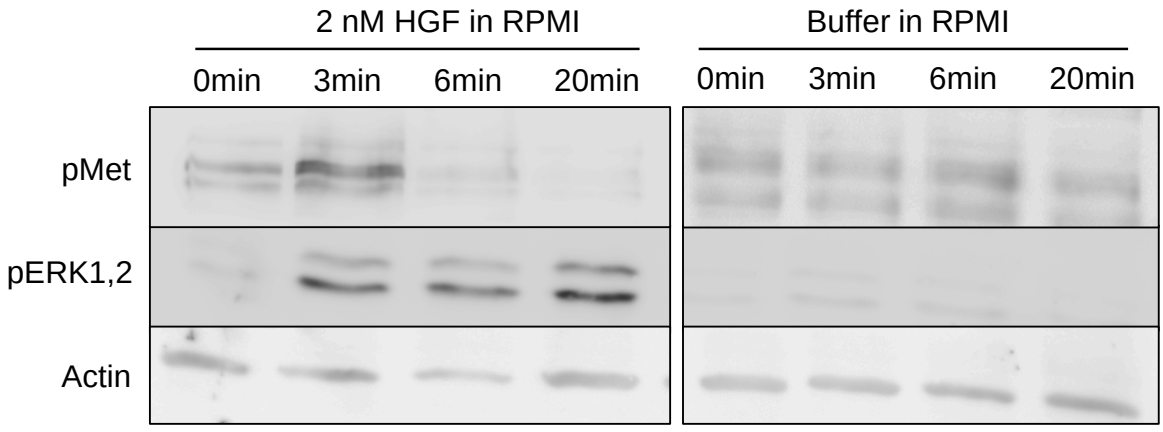

Figure 4-10: Stimulation control for phosphoproteome analyses

DU145 cells, either treated with HGF or with buffer in RPMI medium, were harvested, lysed and an aliquot was applied to SDS-PAGE and immunoblotted against phospho-Met (pT^{1234}/pY^{1235}) and phospho-ERK1, 2 (alias MK03, MK01, pT^{202}/pY^{204}, pT^{185}/pY^{187}). Actin served as loading control.

After LC-MS/MS, peptide sequences were obtained from the distance between peaks in the resulting fragment ion spectra (three examples are depicted in Figure 4-11). The mass difference between two peaks corresponds to the mass of the amino acids. In the same way, other modifications, like phosphorylations, could be detected. As the phosphate ion (PO_4^{3-}) has a molecular weight of 80 Da, this modification causes a mass shift of the modified amino acid. However, serine and threonine phosphorylations are often eliminated during fragmentation, resulting in a 98 kDa loss of phosphoric acid (H_3PO_4). The remaining products are dehydro-alanine for serine and dehydro-aminobutyric acid for threonine, with a specific mass of 69 Da and 83 Da, respectively. Tyrosine phosphorylations, however, are more stable due to the robust aromatic ring structure of the tyrosine side chain and can be confirmed via the characteristic immonium ion with a specific mass of 216 Da. Thus, these characteristics enable the identification of the phosphorylation site within a peptide sequence.

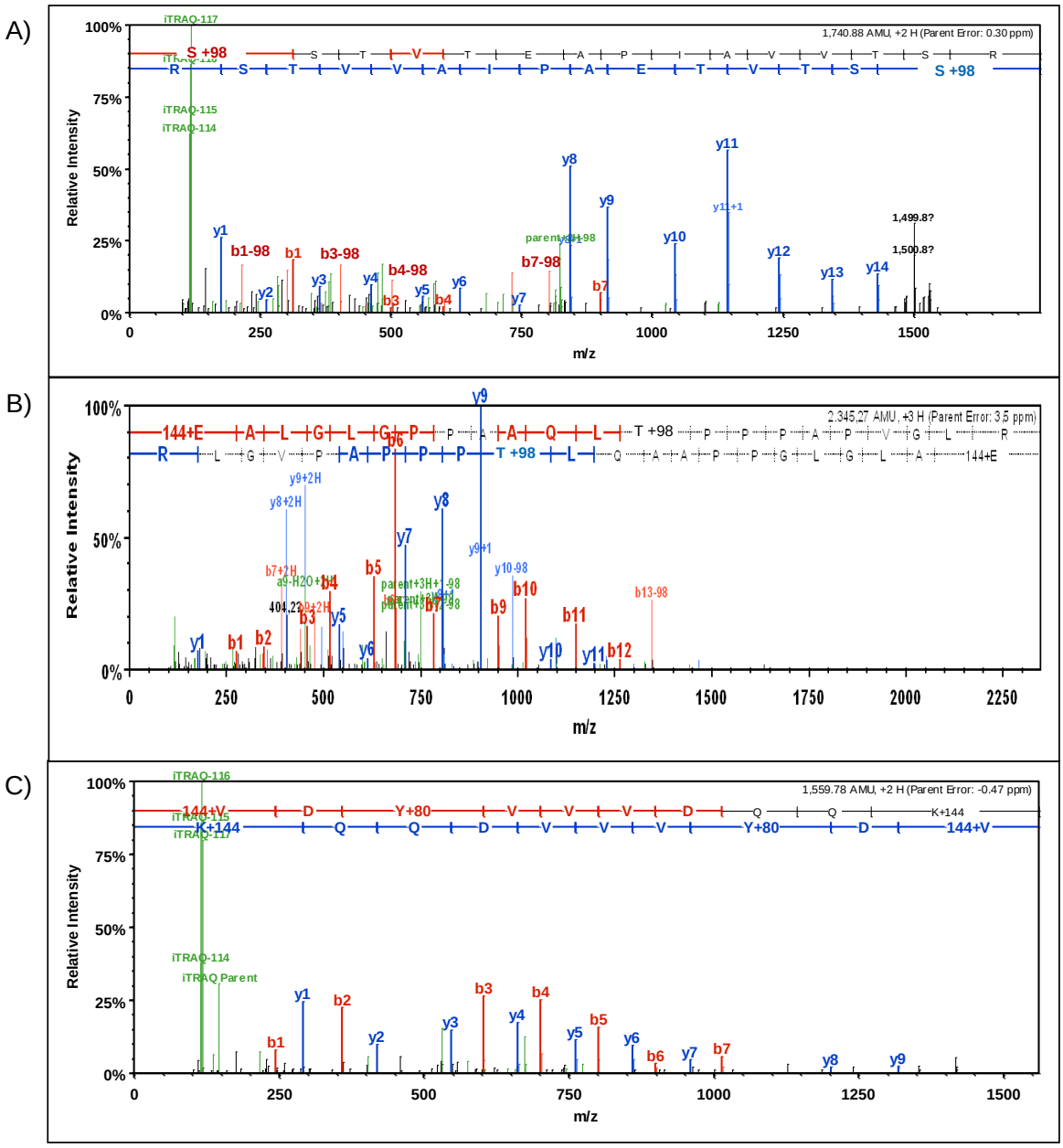

Figure 4-11: Fragment ion spectra of phosphorylated peptides

The mass difference between two peaks corresponds to the mass of one specific amino acid. If one is phosphorylated, it can be detected by a 80 Da shift. In the case of S/T phosphorylation, the elimination of phosphoric acid (-98 kDa) is frequently observed. In contrast, Y phosphorylation is very stable and does not eliminate phosphoric acid. Sequences are calculated from both sides: b ions (forwards, red) and y ions (backwards, blue). iTRAQ reporters can be found in the low mass range of the spectra. For identification, spectra were compared to theoretical computed ones of known protein sequences in the database UniProt. Examples for each of the three phosphorylation types at serine (A) pSSTVTEAPIAVVTSR of NEK9), threonine (B) EAGLELGPPAAQLpTPPPAPVGLR of RAVR1), and tyrosine (C) VDpYVVVDQQK of GAB1) are shown.

Summarizing all three biological and technical replicates, phosphoproteomics identified 7,996 different phosphopeptides corresponding to 2,592 proteins. These proteins were analyzed supported by StrAP to obtain Gene Ontology data (GO annotations, Figure 4-12) to get a global functional overview of the identified phosphorylated proteins. For 2,260 of the 2,592 proteins, localization information was available. With about 1,300 members, the most prominent portion of proteins was annotated in the nucleus. The second largest group localized in the cytoplasm. Additionally, more than 500 proteins were identified from different organelles like peroxisomes, mitochondria, endosomes, and ER. Of course, highly abundant ribosomal as well as cytoskeleton-associated proteins were also found in the phosphoproteome. Thus, the localization of the identified proteins reflected a representative distribution of proteins within the different cellular compartments. As signal transduction takes place mainly from the plasmamembrane to the cytoplasma into the nucleus and these groups were the three largest, this provided excellent conditions to analyze the Met signaling.

2,153 phosphoproteins identified in this study were clustered according to their molecular function (Figure 4-12B). For 1,952 of them, interaction with other cellular component was known (“binding”) and 200 to 700 were described to have catalytic activity (“enzyme regulator activity”, “catalytic activity”). However, 75 were assigned to be part of signal transduction processes (“molecular transducer activity”). Thus, the majority were signal effectors, demonstrating the importance of this class of proteins.

2,009 proteins of the dataset were assigned to biological processes (Figure 4-12C). 227 play a role during development that is also affected by Met signaling. Importantly, 135 were already known to “respond to a stimulus” and might therefore be signal transducers or substrates of Met signaling. However, this number of proteins is very low compared to the response known for signaling processes and illustrates the lack of knowledge of proteins involved in signaling cascades like those induced by HGF/Met.

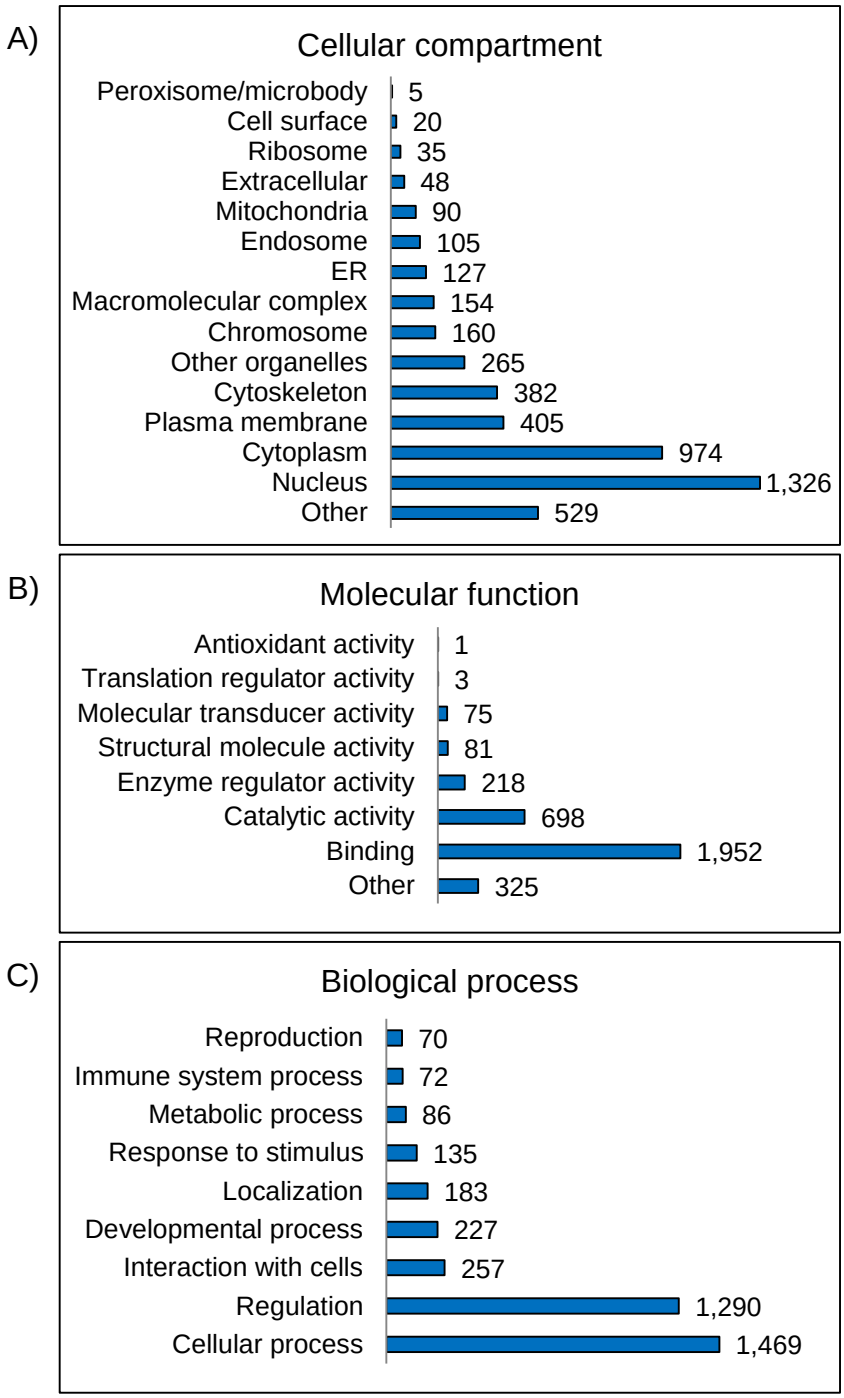

Figure 4-12: GO annotations of identified phosphoproteins

All identified phosphoproteins were loaded into the software StrAP and annotated automatically by Gene Ontology. For cellular localization 2,260 of 2,592 identified proteins were annotated, for molecular function 2,153, and for biological process 2009 proteins.

In addition to the functional overview of purified phosphoproteins, the characteristics of the corresponding peptides were further examined. As every serine, threonine, and tyrosine can be phosphorylated, peptides happen to carry multiple modifications at once. The majority, with more than 85% of identified

peptides, was phosphorylated at one site, while 13.9% carried two, and 0.4% even three phosphate groups (Figure 4-13). Several phosphorylation sites in close proximily to each other increase the effect on structural rearrangements of the proteins and offer more possibilities to regulate the protein through several layers in case of signal integration. The distribution of phosphorylated amino acids was very disparate. As only 0.9% was tyrosine, and 15.5% threonine phosphorylation, the most prominent proportion by far was modified serine with 83.6%. This ratio is consistent with other phosphoproteome studies (Olsen et al. 2006; Hunter and Sefton 1980) and validates the ability of this workflow based on Ga-IMAC to purify all three common types in human cells representatively.

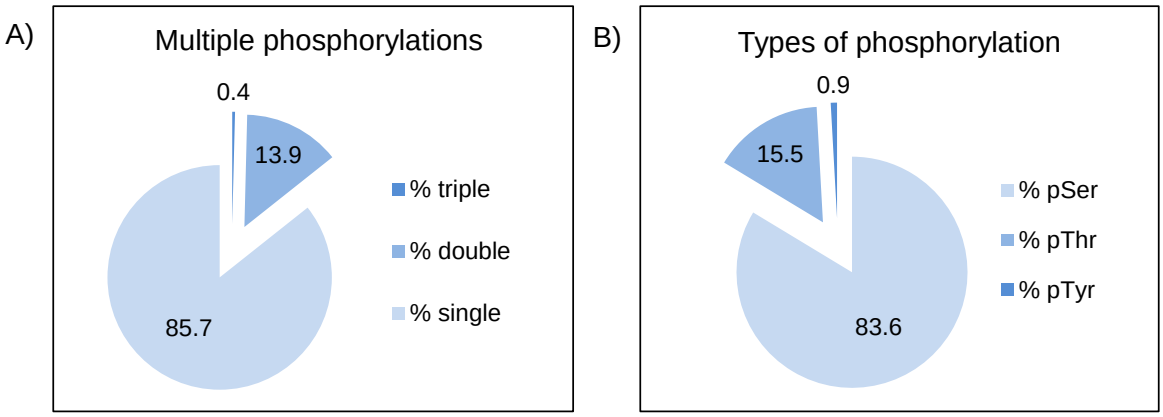

Figure 4-13: Composition of phosphopeptides

A) All 7996 identified phosphopeptides were sorted according to their phosphorylation state. Single, double, and triple phosphorylations occurred in this study. B) The proportion of serine, threonine, and tyrosine phosphorylations of the identified peptides is shown.

Normalization of the phosphopeptide regulation data was carried out to ascertain the comparability of the samples. For each of the three independent experiments and time points one boxplot was generated to check and compare the distribution of regulation factors in comparison to the non-treated control (Figure 4-14). All boxes located in the range of -0.3 to 0.3, with the median around 0. The 20 min-sample of experiment 1 showed the broadest box, while experiment 2 after 6 min revealed the smallest one. Nevertheless, all boxes were located in the unregulated range between -0.5 and 0.5. Few extreme values occurred in different samples, but taken together, all boxplots exhibit similar patterns concerning their regulation factor distribution, which ensures that the samples were comparable.

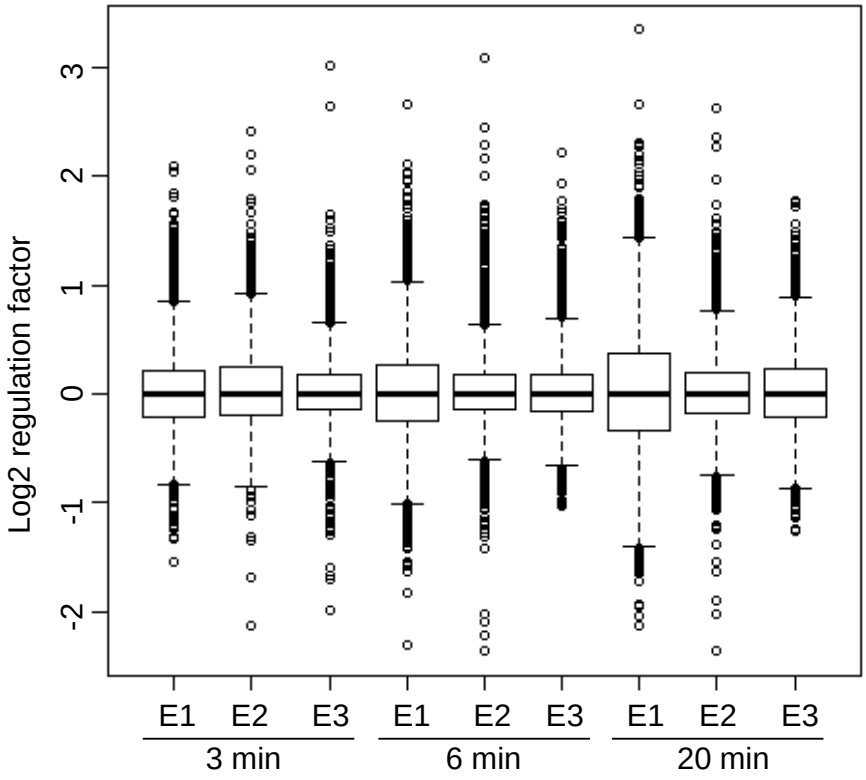

Figure 4-14: Boxplot of samples after normalization

Regulation factors for every experiment (E1-E3) and time point were normalized and their distribution was illustrated by boxplots. The line in the middle of the box represents the median, the box includes 50% of the data, and antennae show the 1.5-fold range of the box. Dots represent extreme regulation factors. The range between the two external dots corresponds to 100% of all identified regulation factors for one sample.

4.2.3 Quantitative analysis of time-resolved HGF/Met signaling

So far, the whole identified phosphoproteome after HGF stimulation was regarded. In the next step, quantitative analysis was performed with the non-stimulated sample as control to calculate regulated phosphopeptides in response to HGF. Furthermore, the regulated peptides were not only separated into up and downregulated, but were also clustered more detailed according their phosphorylation dynamics over the time course.

Of 8,000 phosphopeptides detected in three replicates, 2,311 were identified reproducibly in all three replicates. Only these were taken into account for the

extraction of significantly regulated phosphopeptides from the regulation factors calculated from the iTRAQ reporter ion intensities.

For quantitative comparison of the different samples of the HGF time course, the peptides had been labeled with the iTRAQ reagent. During MS/MS, the four iTRAQ reporters were split from its associated peptide and detected in the low mass range at 114, 115, 116, and 117. The relative intensities of the iTRAQ ions represent the amount of the corresponding peptide in one sample compared to the control. This analysis was supported by the in-house bioinformatics tool iTRAQassist. Figure 4-15 shows one peptide spectrum of the Met adapter protein GAB1 including all four iTRAQ reporters in the low mass range as an example. Based on the reporter intensities, less peptide occurred in the control, while it increased until 6 min HGF stimulation and decreased after 20 min. Supported by the software iTRAQassist, the intensities of all identified peptides were processed and the corresponding regulation factors were calculated.

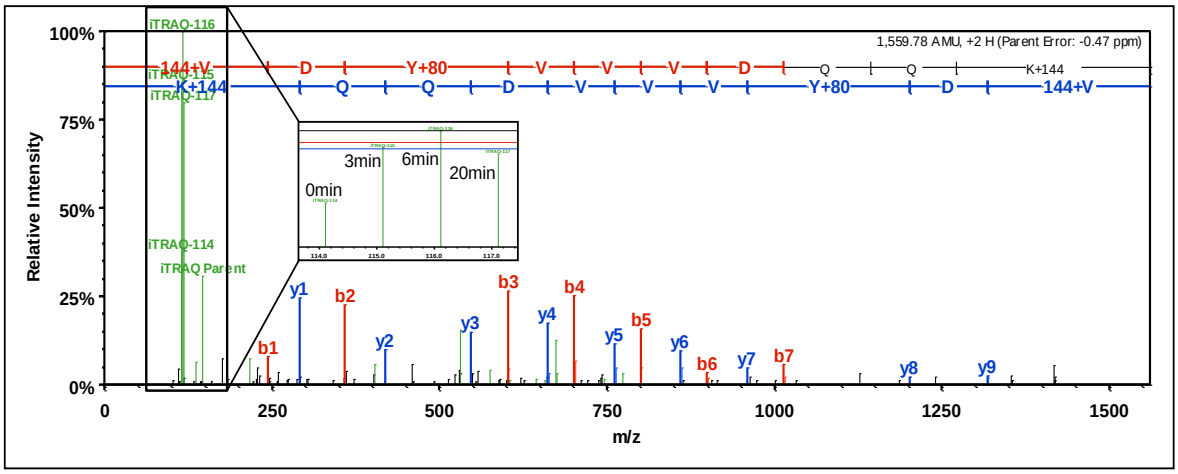

Figure 4-15: Regulation analysis with iTRAQ

The intensities of the iTRAQ reporters reflect the ratio of peptides in the different samples. Spectrum of the peptide VDpYVVVDQQK of the adapter protein GAB1 is shown here. The low mass range between 113 and 118 Da is enlarged to illustrate iTRAQ reporters of the samples. 114.1: unstimulated control, 115.1: 3 min HGF, 116.1: 6 min HGF, 117.1: 20 min HGF.

For the calculation of significantly regulated phosphopeptides, a normal distribution was supposed and multiple testing was utilized. Based on that, a theoretical threshold was calculated, which should be exceeded at one time point in all three replicates. Those peptides considered significantly regulated exhibited

a p-value below 0.05 and correlated with a $\log_2$ RF threshold of at least +/-0.5 in all three replicates, which is consistent with other proteome studies using iTRAQ. Furthermore, regulated peptides were additionally validated by checking their MS/MS spectra and their Interval of Robustness (calculated by iTRAQassist, section 3.6.10), which measures the reliability of a given regulation factor.

According to these criteria, 95 phosphopeptides were found to be significantly regulated at least at one time point of HGF stimulation (Figure 4-16, and appendix Table 8-1). These peptides corresponded to 80 proteins. Interestingly, 82 phosphopeptides exhibited a positive regulation, in contrast to only 13 peptides being downregulated. Furthermore, 19 phosphopeptides were regulated after 3 min, 36 after 6 min, and even 81 after 20 min, demonstrating the broadening of the signal network over time. The heatmap clearly depicts the diverse regulation patterns of the phosphorylated peptides. While some phosphopeptides were regulated throughout, others displayed significant regulation only at one or two time points. Furthermore, the regulation factors of one peptide often slightly differed from each other within the triplicate. This clearly illustrated the fast and transient characteristic of these modifications, which resulted in shifted phosphorylation dynamics.

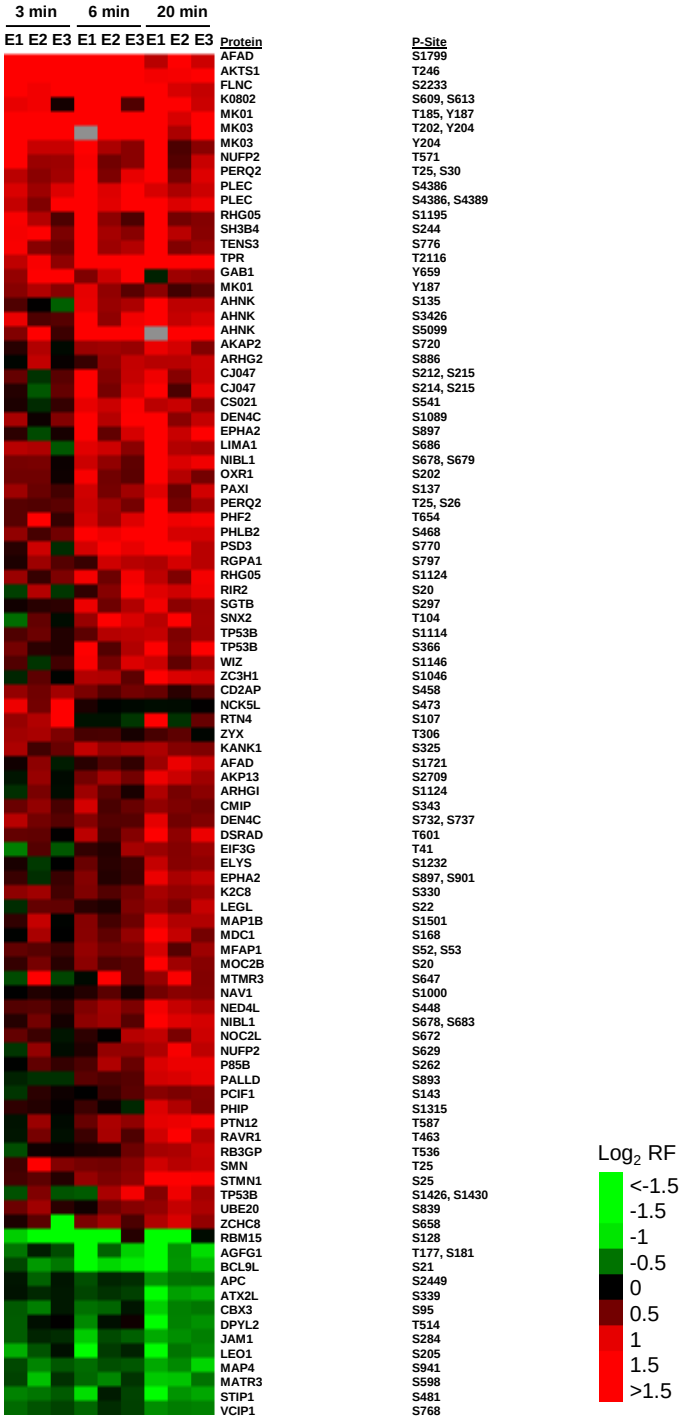

Figure 4-16: Heatmap of all HGF-regulated phosphopeptides

Regulation factors of significantly regulated peptides were illustrated as heatmap with Java Treeview. Peptides are shown in rows and the samples in columns. The color code illustrates regulation factors in $\log_2$ scale. Red boxes indicate upregulated, green downregulated, black non-regulated, and grey missing values. P-Site: phosphorylation site.

Each regulated peptide in every replicate exhibited a characteristic regulation behavior over the three different time points. Nevertheless, the phosphopeptides could be clustered according to their dynamics. Supposing 4 regulation factors per peptide (one for 0, 3, 6, 20 min each), clustering was performed depending on the order of absolute values of the regulation factors. This resulted in 24 possible clusters. For example, a peptide phosphorylated gradually over time exhibited the order 1<2<3<4 (in short: ord1234), with the lowest value after 0 min, and the highest after 20 min. In contrast, a phosphopeptide increasing until 6 min and then decreasing until 20 min might have the order 1243 and so forth. Importantly, those peptides being clustered together displayed a similar phosphorylation behavior and thus, were regulated in the same manner in response to HGF. Similar regulation therefore indicated the participation in the same biological process and might also hint at the regulation by the same upstream kinase subset.

Of the 24 possible clusters, the four orders 2341, 2431, 3412, and 4213 were not reflected by any regulated phosphopeptide in this study. This is not surprising since these dynamics are very inconsistent over time. As some of the remaining 20 clusters showed very similar regulation dynamics , these were further combined in a second step. As indicated by the representative schemes 1-4 in Figure 4-17 and Figure 4-18, phosphorylations were regulated either early, or late, constant, oscillating, or in between. This second “clustering” was only supposed to clarify the distinct phosphorylation dynamics and sometimes is ambiguous as several options may be possible (Figure 4-17, Figure 4-18). An overview of which phosphorylation sites was integrated in which cluster is illustrated in Table 8-2 and Table 8-3 in the appendix.

Most strikingly, more than 50% of the regulated peptides concentrated in the 3 clusters ord1234 (Figure 4-17 F), ord1243 (Figure 4-18 A), and ord2134 (Figure 4-17 G). Thus, the three large clusters seem to be common phosphorylation dynamics of peptides in response to HGF.

Furthermore, peptides regulated early were almost exclusively upregulated and also stayed regulated over time. Thus, the majority of early responders was sorted into the cluster with constant behavior (Figure 4-18 A+B), while 7 phosphopeptides (Figure 4-17 A-C) were only upregulated after 3 min. Among the group of phosphopeptides only regulated early were all three peptides of the functionally

uncharacterized protein NCK5L modified at pS^{473}. The sites pY^{659} of the Met adapter GAB1, pY^{204} of the kinase MK03, and pS^{458} of the membrane-bound adapter CD2AP were upregulated with a maximum after 3 min HGF, but still stayed slightly regulated until 20 min (Figure 4-17 D). In contrast, gradually upregulated phosphorylation sites included pS^{1124} of Rac1-GAP RHG05, pS^{137} of the actin-membrane linker PAXI, and pS^{1000} of the cytoskeleton-associated protein NAV1. Additionally, pS^{448} of the E3 ubiquitin ligase NED4L, pS^{609}/pS^{613} of the uncharacterized protein K0802, and pS^{897} of the receptor tyrosine kinase EPHA2 were sorted into this group of late upregulated responders (Figure 4-17 F-H). In comparison, late downregulated phosphopeptides were pS^{2449}, as well as pS^{284} and pS^{941} on cytoskeleton-associated proteins APC, JAM1 and MAP4, respectively (Figure 4-17 I-J).

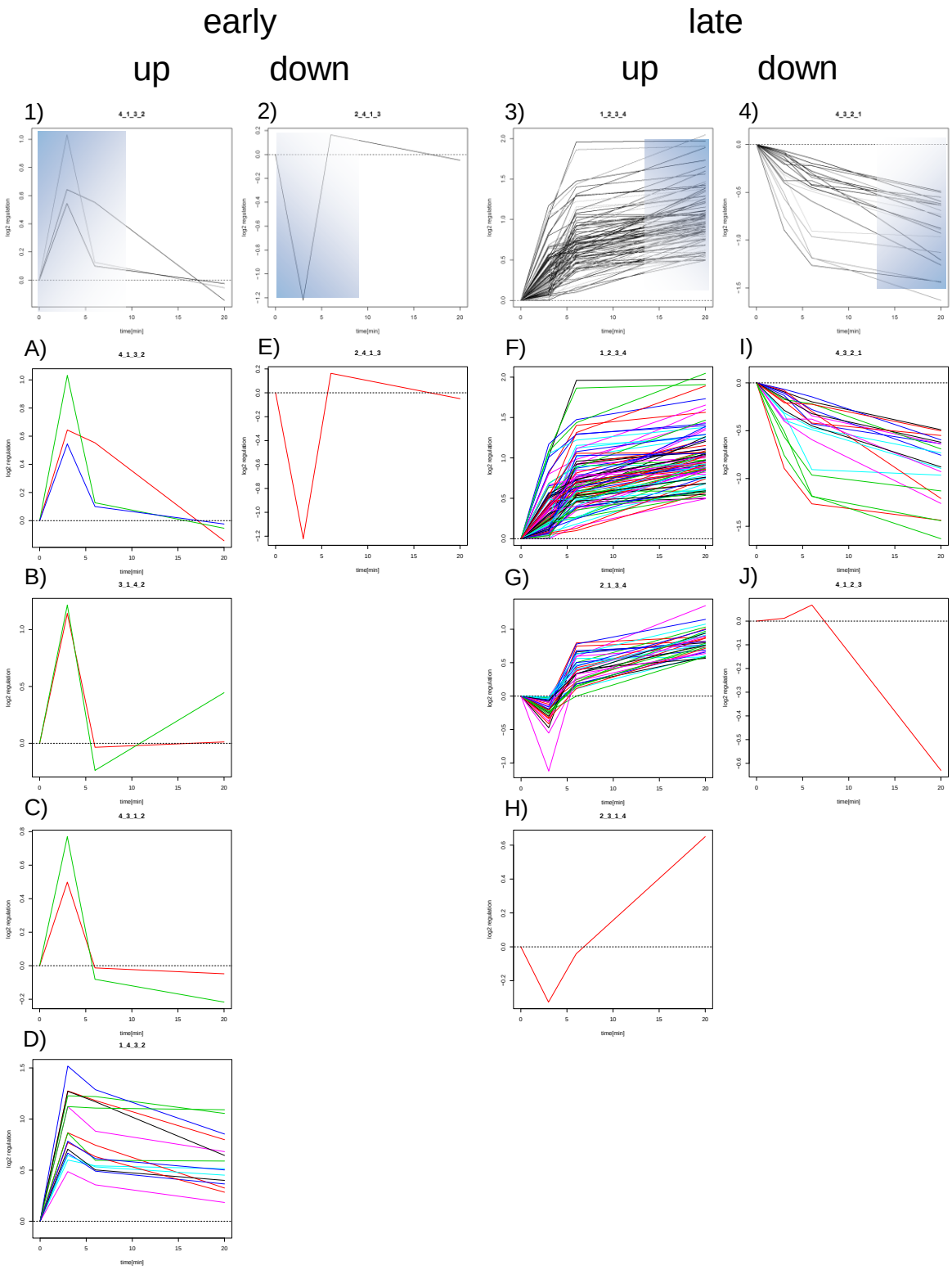

Figure 4-17: Phosphopeptides regulated early and late in response to HGF

Regulated phosphopeptides were clustered according to their rate of regulation over time. Phosphopeptides with maximal regulation after 3 min (early) and after 20 min (late) are illustrated. Clusters were generated corresponding to the orders A) ord4132, B) ord3142, C) ord4312, D) ord1432, E) ord2413, F) ord1234, G) ord2134, H) ord2314, I) ord4321, J) ord4123 ,where the first value reflects the lowermost and the last represents the topmost regulation in the time course. The clusters 1-4) are representatives for each group of regulated phosphopeptides and mark the time point of maximal regulation. Connecting the

values of one phosphopeptide was only used for better illustrating the dynamics. Of course, it is not known what happened to the phosphopeptides between the time points. See Table 8-2 in the appendix for information, which phosphorylation site was integrated in which cluster.

Three phosphopeptide clusters exhibited sites that were upregulated almost immediately after HGF stimulation and maintained there until 20 min (Figure 4-18 A-C). Among them were pT^{185}/pY^{187} and pT^{202}/pY^{204} of the MAP kinases MK01 and MK03, respectively, as well as pT^{246} of the AKT1 substrate AKTS1. Furthermore, pS^{1146} of the nuclear protein WIZ and pS^{2116} of the nuclear pore complex protein TPR were clustered together. Furthermore, the constant upregulated phosphopeptides included also the sites pS^{541} and pS^{1089} of the uncharacterized proteins CS021 and DEN4C.

On the contrary, the next group of phosphorylation sites was not constantly regulated, but showed oscillating modification (Figure 4-18 D-F). Among the upregulated sites after 3 and 20 min were pS^{839} of the E2 ubiquitin conjugase UBE2O and pT^{306} of the adhesion protein ZYX. Furthermore, the sites pS^{132}/pS^{137} and pS^{672} of the uncharacterized proteins DEN4C and NOC2L also showed this dynamics. However, phosphorylation sites that were regulated inconstantly included pS^{95} of the transcriptional regulator CBX3 and pS^{768} of the deubiquitinating enzyme VCIP1 (Figure 4-18 G).

Additionally, phosphopeptides that were significantly regulated only after 6 min were almost not identified. Nevertheless, all three peptides of the signaling protein BCL9L modified at pS^{21} exhibited this dynamics (Figure 4-18 H-J).

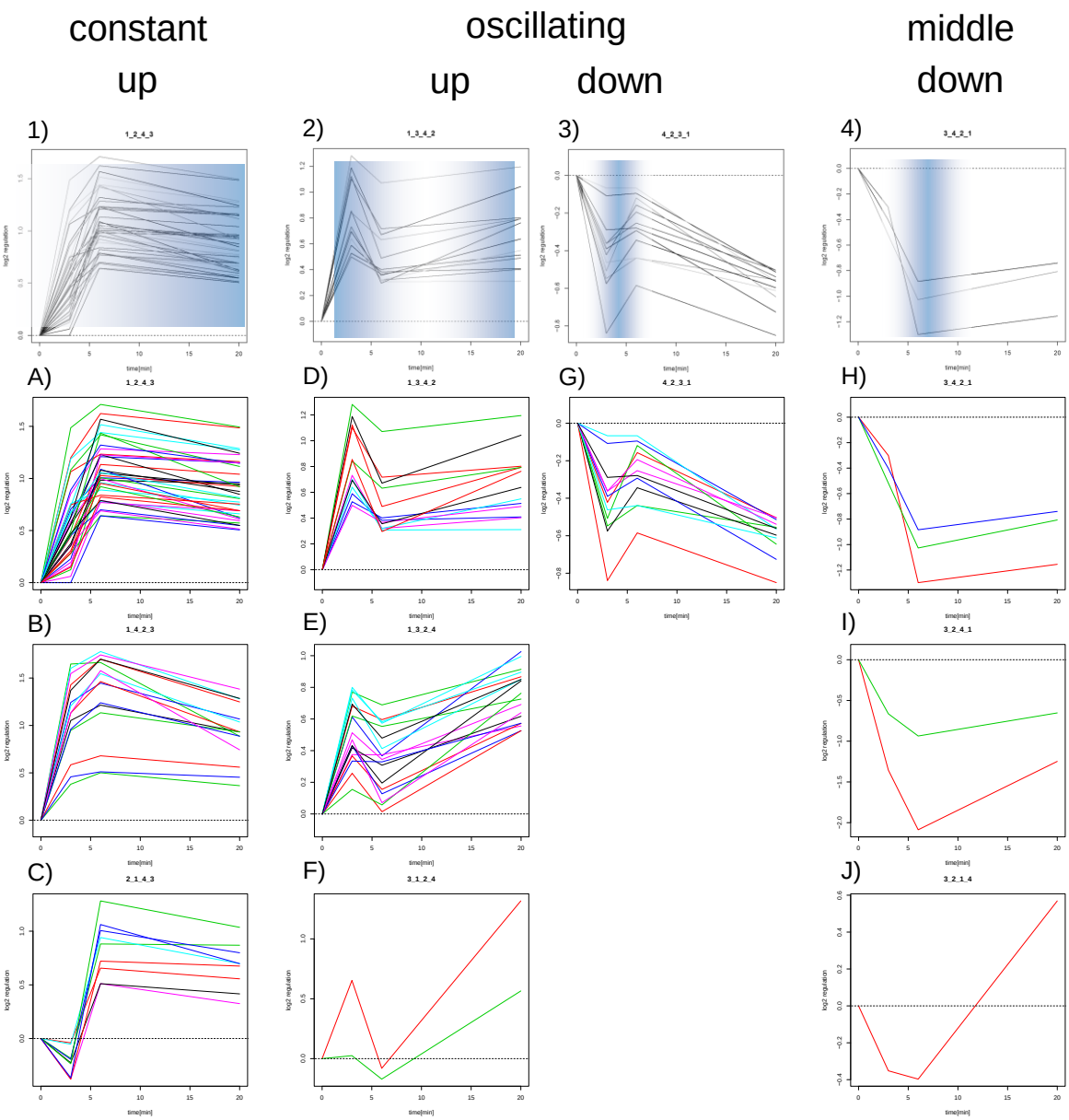

Figure 4-18: Phosphopeptides with other dynamics in response to HGF

Cluster of regulated phosphopeptides with different dynamics than early and late response. Shown are phosphopeptides regulated constantly over the time points, oscilliating and those with a maximum after 6 min. Clusters were generated corresponding to the orders A) ord1243, B) ord1423, C) ord2143, D) ord1342, E) ord1324, F) ord3124, G) ord4231, H) ord3421, I) ord3241, J) ord3214, where the first figure reflects the lowermost and the last represents the topmost regulation in the time course. The clusters 1-4) are representatives for each group of regulated phosphopeptides and mark the time point of maximal regulation. Table 8-3 in the appendix shows, which phosphorylation site was integrated in which cluster.

While most of the 95 phosphopeptides were only regulated at one or two time points, some peptides were significantly regulated throughout. Examples among the 9 allover regulated phosphorylation sites were known components like

pT^{185}/pY^{187} of MK01, but also novel like pT^{246} of AKTS1, pS^{2233} of FLNC, and pT^{2116} of TPR. The permanent regulation indicates that they are particular important signaling components downstream of HGF/Met.

All differentially regulated phosphopeptides comprised 101 phosphorylation sites as some peptides exhibited double phosphorylations. Comparing the regulated phosphorylation sites with the current phosphorylation databases PhosphoSitePlus and PhosphoNet uncovered that the majority of sites were known but not functionally characterized. However, the sites pS^{720} of AKAP2, and pS^{343} of CMIP were not listed in the databases and are thus novel identifications (Figure 4-19).

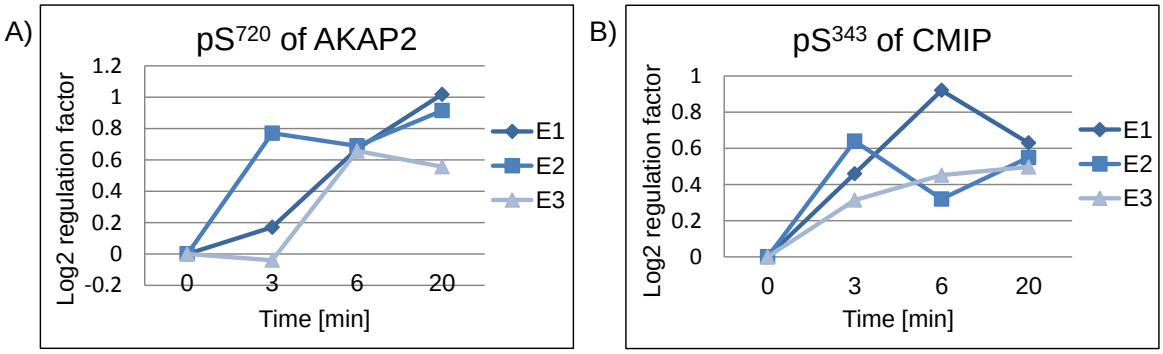

Figure 4-19: Regulation dynamics of novel phosphorylation sites

Screening all regulated phosphorylation sites in the databases PhosphoSitePlus and PhosphoNet revealed these two sites of AKAP2 and CMIP as novel. The graphs A) and B), illustrate their phosphorylation dynamics in response to 3, 6, and 20 min of HGF. Each curve corresponds to the phosphopeptide identified in one of the three replicates (E1-E3).

In contrast, for 9 regulated phosphorylation sites, further information was available in the databases (Table 4-1). For example, pT/pY double phosphorylations of the MAP kinases MK01 and MK03 increase their enzymatic activity. The site Y^{659} of the adapter protein GAB1 is known to trigger cell proliferation in response to growth factors. Furthermore, the novel component AKTS1 was phosphorylated at T^{246} that is known to be caused by AKT1, one of the key players in growth factor signaling. All these components confirmed the activation of the HGF/Met cascade.

Additionally, the physiological effects of signaling could also be monitored by the differential modification of several novel Met pathway candidates. For example, pS^{25} of STMN1 is responsible for rearrangements of the cytoskeleton during cell

cycle progression. Furthermore, pS^{886} of ARHG2 recruits the protein to microtubules where it is able to activate Rho GTPases. SGK1 phosphorylates S^{448} of the E3 ubiquitin ligase NED4L and thus, changes its binding preferences from inhibiting SCNNA to 14-3-3 proteins. It is also known that pS^{284} of the tight junction protein JAM1 alters its cellular localization. Phosphorylation of pS^{897} of the EPHA2 receptor by AKT1 influences cell motility.

Table 4-1: Regulated phosphorylation sites with known function

HGF-regulated phosphorylation sites were matched with entries in the databases PhosphositePlus and Phospho.NET. For those listed here, further functional characterization was provided. P-Site: phosphorylation site. Regulation direction for every time point is indicated by arrows.

Protein	P-Site	Regulation (3, 6, 20 min)	Upstream Kinase	Function / effect of P-Site
AKTS1	T246	↑↑↑	AKT1	Interaction with 14-3-3β
MK01	T185/Y187	↑↑↑	MEK1, JAK2	Activity, signal transduction
MK03	T202/Y204	↑↑↑	MEK1+2, JAK2	Activity, signal transduction
GAB1	Y659	↑↑→	EGFR, InsR	Cell cycle regulation
NED4L	S448	→↑↑	SGK1	Activates SCNNA
STMN1	T25	→↑↑	CDK1, PKCB	Cytoskeleton reorganization
ARHG2	S886	→→↑	PAK1	Relocalization of 14-3-3 to microtubules
EPHA2	S897	→→↑	AKT1	Motility regulation
JAM1	S284	→→↓	PKCA	Relocalization

Proteins that exhibited regulated phosphorylation sites were further analyzed by GeneGo to get an overview of the HGF-affected processes. Mapping the experimental data onto canonical pathway maps revealed mainly cascades triggering cell adhesion, development, and cytoskeleton reorganization. Only 6 of

the 80 identified phosphoproteins could be integrated, because the majority was not present on the canonical pathway maps.

However, functional data was available for 71 differentially phosphorylated proteins. These were classified according to their task in signaling or as substrates to uncover affected mechanisms in the cell. The first group comprised the signaling molecules. As part of these, the serine/threonine protein kinases MK01 and MK03, and the receptor tyrosine kinase EPHA2 have been identified. As protein phosphatases, MTMR3 and tyrosine phosphatase PTN12 were found. The regulated dataset also included the signaling adapter proteins GAB1, AHNK, AKP13, and P85B. Signaling via small GTPases was also influenced by HGF stimulation. The GAPs RHG05, RGPH1, and RB3GP, as well as the GEFs ARHG2, ARHGI, and PSD3 displayed significantly regulated phosphopeptides. The deubiquitinating enzymes also take part in signaling and were represented by one regulated phosphorylation site of VCIP1. The second group consisted of signaling substrates. The transcription factor ELYS was found to be phosphorylated after HGF treatment. The function of the site is unknown, but it is likely that this phosphorylation influences the protein's transcription activity in response to HGF. Other differentially phosphorylated nuclear proteins have also an effect on transcriptional progression (e.g. PCIF1, BCL9L, CBX3) or support the cytoplasma-nucleus transport (e.g. TPR). Other acceptors of signaling are proteins that, once phosphorylated, directly affect cellular processes. For example, adhesion-associated proteins like AFAD, ZYX, and JAM1 appeared to be modified here. Cytoskeletal proteins like FLNC, PLEC, TENS3, PAXI, PALLD, APC, and CD2AP are likely to be involved in HGF-mediated migration or proliferation as well as receptor internalization. In the dataset, ubiquitin ligases were regulated via phosphorylation, which mediates degradation and thus stops signaling via ubiquitin-labeled proteins. Here, E3 ubiquitin ligase NED4L, and E2 ubiquitin conjugase UBE2O were found with one regulated phosphorylation site each.

4.2.4 The role of EPHA2 in HGF/Met signaling

The EPH receptor family is the largest group in tyrosine kinase-mediated signaling (Bush and Soriano 2012). The family member EPHA2 can be activated by its ligands Ephrin A1, A2, A3, A4, A5, and A6 and is involved in angiogenesis,

branching morphogenesis, and epithelial proliferation. Deregulated EPHA2 is known for many cancer types, both, as tumor inhibitor, and accelerator, which is supposed to be mediated by the presence and absence of its ligand (Miao and Wang 2012; Pasquale 2008).

Interestingly, the site pS^{897} of EPHA2 was identified in this study by phosphoproteomics to be regulated after HGF stimulation (Figure 4-20). The phosphorylation of this site increased gradually in the first 20 min after HGF. As EPHA2 is also regulated ligand-independently, this phosphorylation confirmed a receptor crosstalk between Met and EPHA2. Therefore, the receptor tyrosine kinase became an interesting candidate for studying the role of EPHA2 in Met-dependent signaling.

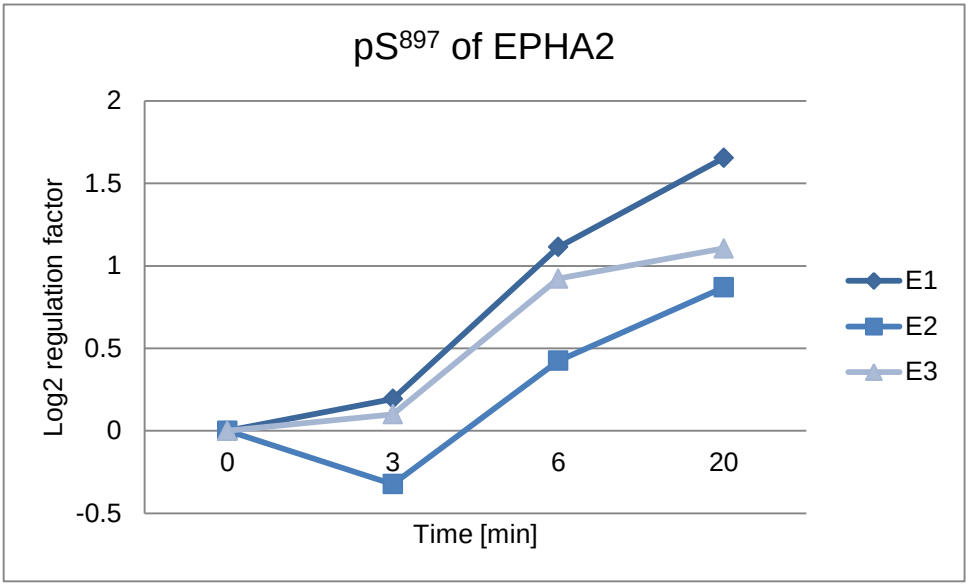

Figure 4-20: Phosphorylation dynamics of pS^{897} of EPHA2 in response to HGF

Phosphoproteomics revealed a modified and gradually increasing phosphorylation of this site of the receptor tyrosine kinase EPHA2 in the first 20 min after HGF/Met-activation. Curves E1- E3 represent the three replicates.

First of all, EPHA2 knockdown was established and different siRNAs were tested for adequate efficiency. Afterwards, gene expression dependent on HGF stimulation in DU145 wildtype cells was investigated in order to check for proof-of-concept data. Finally, the influence of EPHA2 knockdown on HGF-stimulated gene expression was studied in detail. Therefore, genes affected by the EPHA2 knockdown were compared to the HGF/Met transcription response in wildtype

cells in order to determine important HGF/Met-regulated genes that are controlled by EPHA2.

In order to investigate a potential EPHA2-dependent Met response, EPHA2 knockdown was established in DU145 cells, and gene expression was compared to the wildtype. In order to exclude off-target effects of the siRNA, two different sequences were used separately to create the knockdown; one binding to the 5' region (siRNA5) and the second one aiming at the 3' end (siRNA7) of the EPHA2 mRNA. Furthermore, a nonsense siRNA control was added as fourth sample to exclude site effects due to the transfection reagents besides the siRNAs. All four samples were stimulated with HGF and were compared to their unstimulated counterparts. Moreover, two different time points for the stimulation with HGF were selected to cover immediate as well as later gene expression and compared to the unstimulated control. After 1 h, first transcripts of HGF/Met signaling were supposed that could provide information of induced upstream pathways. The transcripts of regulators of the cellular response were thought to be produced after 4 h of HGF stimulation. Thus, in total, 12 different samples were analyzed by a microarray in triplicate.

Before considering the gene expression, an immunoblot against activated Met and the EPHA2 protein in all samples was performed as a control. Afterwards, genes regulated by HGF in the wildtype were determined to check the HGF/Met response for known targets and ensure a physiological effect of stimulation. Only after all these necessary controls were considered, the actual influence of EPHA2 knockdown on the HGF/Met-induced gene expression was analyzed.

As described above, aliquots of the samples for the microarray were first analyzed by immunoblot to ensure an efficient EPHA2 knockdown by each of the siRNAs and a sufficient stimulation of Met by HGF stimulation. Figure 4-21 A shows this immunoblot of all samples analyzed in the microarray. Met's activation loop was phosphorylated on pY^{1234}/pT^{1235} after 1 h HGF stimulation, and still slightly after 4 h. Importantly, Met was not affected by the EPHA2 knockdown. Furthermore, EPHA2 was detected equally in the wildtype and nonsense samples, while the protein concentration was lower in the siRNA-treated samples. Noteworthy, knockdown by siRNA7 was more efficient than by siRNA5. Quantification of the EPHA2 bands of the immunoblot clearly demonstrated a reduction of EPHA2

protein in the samples treated with siRNA (Figure 4-21 B). The amount of EPHA2 protein was decreased down to 60% through siRNA5 and to 33% through siRNA7 compared to the wildtype. Thus, knockdown mediated by siRNA7 was almost 2-fold more efficient than that of siRNA5.

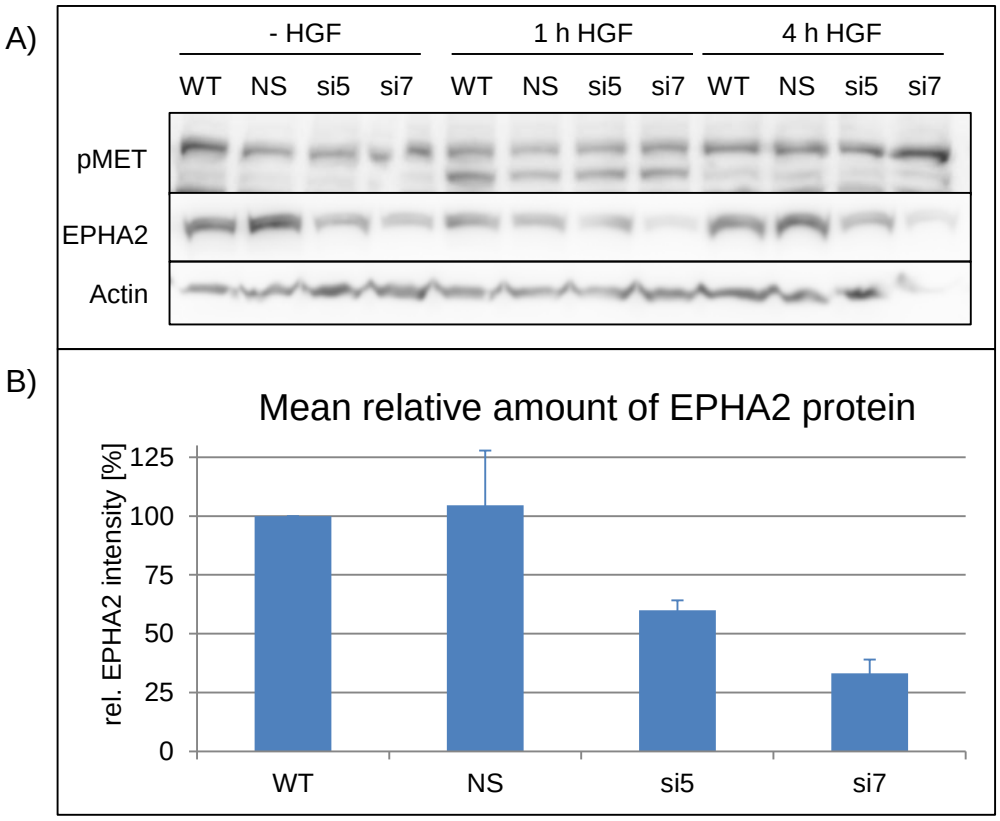

Figure 4-21: EPHA2 knockdown efficiency in microarray samples

A) Immunoblot against phospho-Met (pY^{1234}/pT^{1235}) and EPHA2 showing Met activation and EPHA2 knockdown efficiency in samples used for the microarray. DU145 cells were treated with nonsense (NS) RNA, EPHA2 siRNA5 (si5), or EPHA2 siRNA7 (si7) and were stimulated for 1 h and 4 h with 2 nM HGF. These samples were compared to non-stimulated cells, which serve as a control. B) Quantification of the EPHA2 protein intensities calculated from the EPHA2 bands on the immunoblot. Shown is the mean of the three samples each (for - HGF, 1 h HGF, 4 h HGF). The histogram proves the successful knockdown of EPHA2 and illustrates the different EPHA2 knockdown efficiencies by the two siRNAs.

Using an Agilent chip, expression of more than 41,000 genes from three biologically independent experiments were compared. The nonsense siRNA control exhibited comparable behavior as the wildtype, ensuring no side effects of the transfection besides the siRNAs. Therefore, siRNA-treated samples could be compared directly to the wildtype. Only genes regulated in all three replicates more than 2-fold were considered. The usual threshold of 5-fold for gene

expression analyses could not be applied here, because it resulted in a very low amount of regulated genes. This might be due to the comparatively early time points for the analysis of transcripts in this experiment (compared to NEK9 study, section 4.2.5).

First, genes regulated in the DU145 wildtype during HGF stimulation compared to non-stimulated cells were considered to reveal proof-of-concept data. After 1 h HGF, 656 genes were affected, and 1,072 after 4 h. Each list was evaluated with the help of GeneGo to detect genes that are known to be influenced by HGF/Met and therefore serve as proof-of-concept. Genes corresponding to transcription factors EGR1, EGR3, FOSB, and JUNB as well as the receptor LDLR were clearly upregulated at the first time point. Later, genes of integrin ITA2 and transcriptional regulator SOX9 were also induced. No further genes as these 7 were found that were regulated in the wildtype and are listed in GeneGo to be known as targets of HGF and Met. This is perhaps due to the fact that data in GeneGo also refers to other cell lines or even different organisms. However, there were no genes in the dataset disagreeing with former data, by either being regulated in the opposite direction as described, or being unregulated but should be regulated according to literature. Additionally, GeneGo (using the tool “Which are the key transcription factors and target genes in my data”) supported the identification of transcription factors that led to the expression of genes regulated in this dataset. Noteworthy, 9 of 31 known transcription factors for HGF and Met were retrieved - amongst them prominent ones like JUN, MYC, and STAT3, but also cell-cycle regulating E2F1 and developmental factor SOX9. These results proved the activation of the HGF/Met-dependent gene expression machinery.

To answer the question whether there is an EPHA2-dependent Met signaling after HGF stimulation, growth factor regulated genes of DU145 wildtype were compared to those regulated by HGF in EPHA2-knockdown cells (Figure 4-22). Therefore, only genes behaving the same in the two knockdown samples siRNA5 and siRNA7 in response to HGF stimulation were considered. The knockdown through siRNA7 was more efficient (Figure 4-21) than that of siRNA5. Therefore, genes were considered as regulated if they exhibited a fold change more than 2-fold in the siRNA7 sample, compared to the wildtype, and were regulated in the siRNA5 sample at least in the same direction.

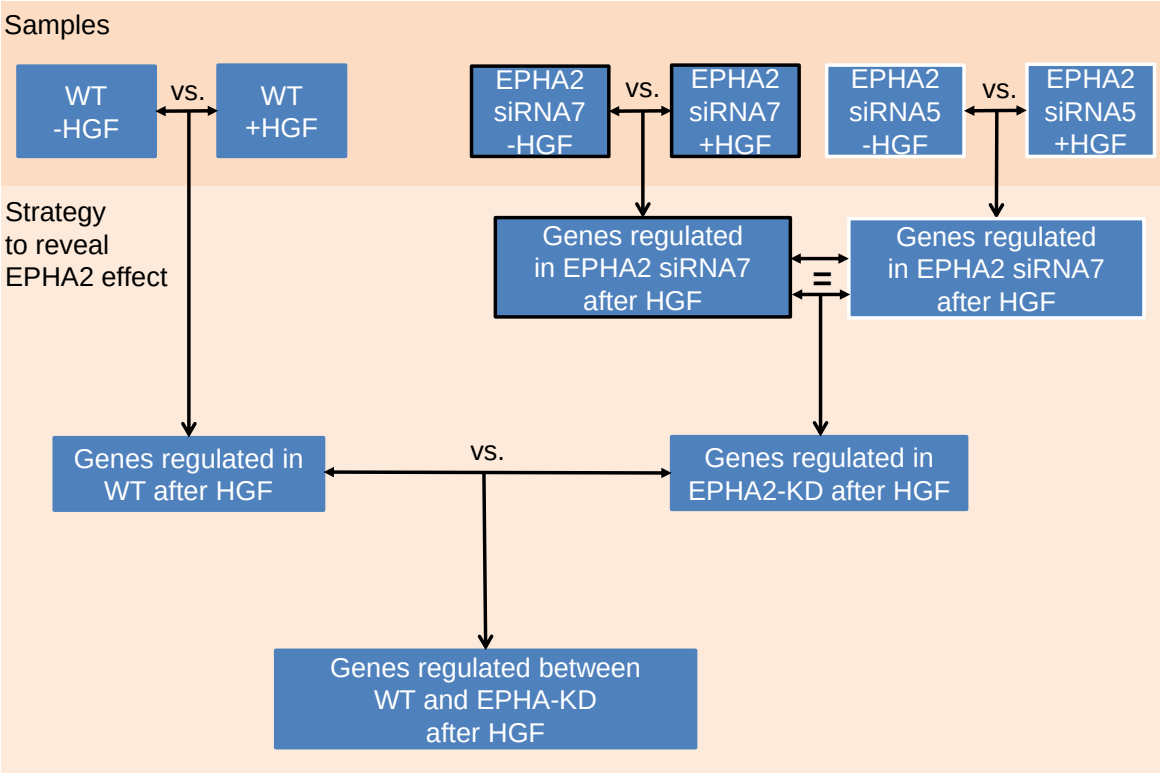

Figure 4-22: Strategy to uncover EPHA2-dependent effect on HGF/Met-response

First, genes regulated by HGF in the wildtype were extracted. Second, genes affected in both EPHA2 siRNAs (5 and 7) by HGF were calculated and those regulated similarly (see: =) were selected. Finally, ratios between regulation values of wildtype (WT) and EPHA2 knockdown (KD) were computed to identify genes that are regulated by EPHA2 in response to HGF. Because the knockdown of siRNA7 was more efficient, this was preferentially considered. As a regulation threshold, a fold change of +/-2 was considered each time. This procedure was done for both time points: after 1 h and 4 h of HGF stimulation.

70 genes behaved differently in wildtype and both types of EPHA2 knockdown cells in response to HGF (Figure 4-23). After 1 h of stimulation, 44 genes were affected, with a majority of 91% being upregulated in the knockdown. Correspondingly, after 4 h, 31 genes were affected of which 74% were upregulated. Conversely, this indicates for the wildtype that most gene expression is usually inhibited or decreased by EPHA2 in DU145 cells during HGF stimulation.

Figure 4-23: Heatmap of EPHA2-regulated genes during HGF stimulation

Two different siRNAS against EPHA2 were used for EPHA2 knockdown. Genes regulated by HGF in DU145 wildtype and knockdown cells were compared. The fold change between these two values is illustrated as boxes, respectively. A) 44 genes regulated in the EPHA2 knockdown compared to WT after 1 h HGF. B) 31 genes regulated in EPHA2-knockdown with WT as basis after 4 h HGF. C) Legend for fold change regulation factors. Upregulated values are red, while downregulated are green. Si5: EPHA2-siRNA5, si7: EPHA2-siRNA7, WT: wildtype DU145.

To figure out, which genes in the important HGF/Met response are affected by EPHA2, the 70 genes differentially regulated in knockdown and wildtype were matched with genes top-regulated in the wildtype. Importantly, 13 of the 70 genes were highly regulated in the wildtype and appear to be particularly under the control of EPHA2 (Figure 4-24).

After 1 h HGF stimulation, 7 regulated genes were affected by EPHA2 knockdown during HGF stimulation. All of them are so called “immediate-early genes” (IEGs) and they were upregulated in the wildtype in response to stimulation, but even more in the EPHA2 knockdown (Figure 4-24 A). Only two of them, namely EGR1 and Fos, are known transcriptional targets of HGF/Met. IEGs usually respond to different kinds of signals by rapid and transient induction. Many of them - like here *egr1-4* and *fos* - are encoding transcription factors. Their transcription is usually very low but they get activated within minutes after transcription (Tullai et al. 2007; Sukhatme 1990).

In comparison, after 4 h HGF stimulation, only 3 genes are up- and 4 downregulated in an HGF- and EPHA2-dependent manner (Figure 4-24 B). EGR4 is still activated, though not as strong as after 1 h. Furthermore, the potassium channel KCNK12 is highly upregulated in the wildtype, while in EPHA2 knockdown it is only slightly affected. This protein has not been implicated in growth factor receptor signaling so far. NPY5R (neuropeptide Y receptor Y5) is downregulated in the wildtype and upregulated in the EPHA2 knockdown, which means that EPHA2 strongly limits its expression in DU145 cells in response to HGF. Furthermore, SPSB4 is more upregulated in wildtype than in the EPHA2 knockdown and the protein is able to bind Met (Wang et al. 2005).

Three further regulated genes, *c12orf67, c5orf58*, and *c14orf105*, and their corresponding protein products CL067, CE058, and CN105 have not been described functionally so far. The first two are upregulated about 8-fold in the wildtype, but only 3-fold in the EPHA2 knockdown. The latter one is downregulated 8-fold in the wildtype, but only 3-fold in the EPHA2 knockdown samples. Obviously, those proteins are expressed in response to HGF and are influenced by the EPHA2 knockdown.

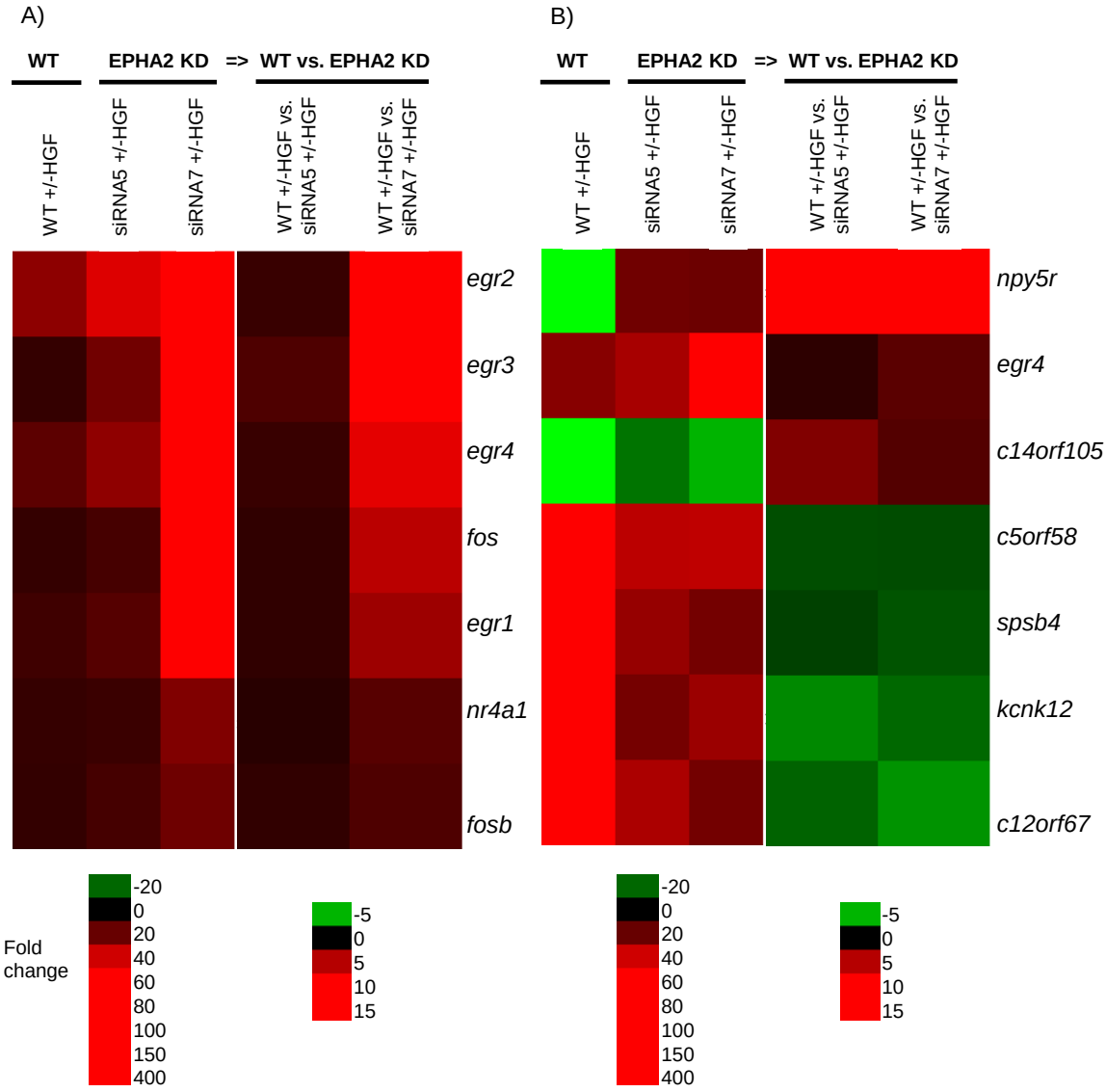

Figure 4-24: Regulation profiles of EPHA2- and HGF-dependent genes

Illustrated genes are part of the main HGF expression response in the wildtype and are at least 2-fold influenced by EPHA2. Fold changes are encoded by colored boxes of a heatmap, where red is upregulated and green is downregulated. A) shows 7 regulated genes after 1 h HGF stimulation and B) the affected genes after 4 h HGF. The color code of the boxes is illustrated below heatmaps. WT: DU145 wildtype; KD: EPHA2 knockdown, realized with two different siRNAs: 5 und 7.

4.2.5 The kinase Nek9 in HGF/Met signaling

The protein kinase NEK9 belongs to the NIMA family of cell cycle regulators (Roig et al. 2002). Previous work identified NEK9 as part of the Met-dependent signaling as it was phosphorylated at pT^{333} after 4 min of InlB stimulation (Reinl et al. 2009).

Since HGF/Met triggers proliferation and NEK9 was known to be a mitotic kinase, a role of NEK9 in physiological signaling was apparent.

Indeed, in this study, the site pT^{333} of NEK9 was regulated after HGF stimulation (Figure 4-25). The phosphorylation was identified in only one of three replicates (E3), probably due to the absence of a kinase-specific enrichment step in this phosphoproteome workflow in contrast to Reinl et al., 2009. Nevertheless, pT^{333} of NEK9 was identified clearly with a peptide score of 57 and exhibited a maximum regulation factor of 1.3 in $\log_2$ scale after 6 min HGF.

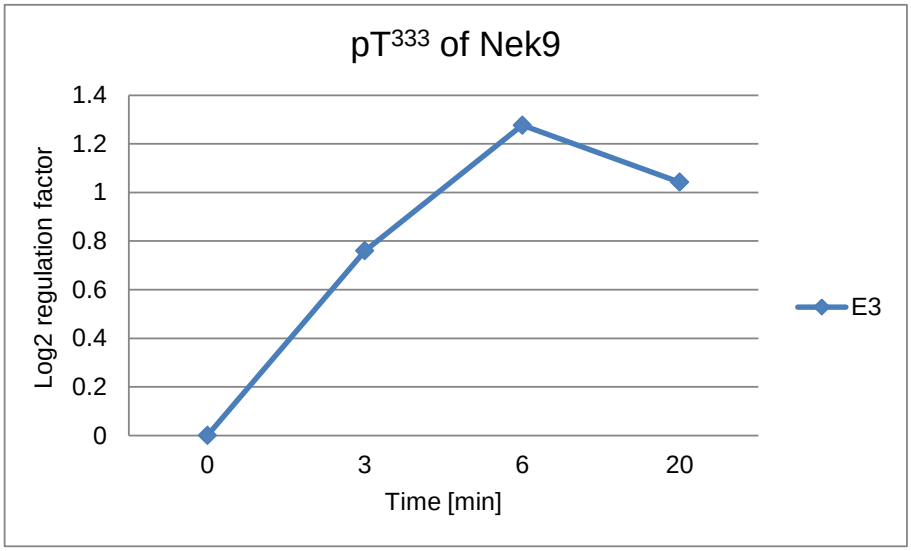

Figure 4-25: Dynamic regulation of pT^{333} of the kinase NEK9 after HGF stimulation

The $\log_2$ regulation factors of NEK9 pT^{333} after HGF stimulation for 3, 6, and 20 min of DU145 cells is illustrated for replicate 3 (E3). The phosphopeptide was not found in replicates 1 and 2 (E1, E2).

As Met regulates proliferation and NEK9 plays a role in mitosis, a liekly function of the kinase NEK9 in the HGF/Met response should be investigated. Therefore, different siRNAs against NEK9 were tested to establish an efficient NEK9 knockdown. After that, the effect of the NEK9 knockdown during HGF stimulation was characterized by proliferation and motility assays. In order to investigate its influence on the transcription of HGF/Met target genes, gene expression analysis was performed next. Proof-of-concept data of HGF-affected genes in the HeLa S3 wildtype were tested first to confirm physiological response. Afterwards, genes regulated by NEK9 knockdown during HGF stimulation were calculated to investigate the role of NEK9 in HGF/Met-induced gene regulation.

In order to test siRNAs for their NEK9 knockdown efficiency, two different sequences against the NEK9 mRNA were used either separate or in combination. While the siRNA5 binds to the middle region of the NEK9 mRNA, the siRNA7 aims at the first third of the 5' end. The resulting knockdown was monitored by immunoblotting against NEK9. Figure 4-26 shows the immunoblot against Nek9 in the Hela S3 wildtype and in the siRNA-treated samples. While a clear band was visible in the wildtype cells, the separate siRNAs provided a NEK9 knockdown of about 80% each. However, the knockdown efficiency was further increased by the combination of both siRNAs to over 90%. In order to ensure efficient NEK9 knockdown, all characterization studies on NEK9 were therefore performed with both siRNAs in combination and compared to the wildtype.

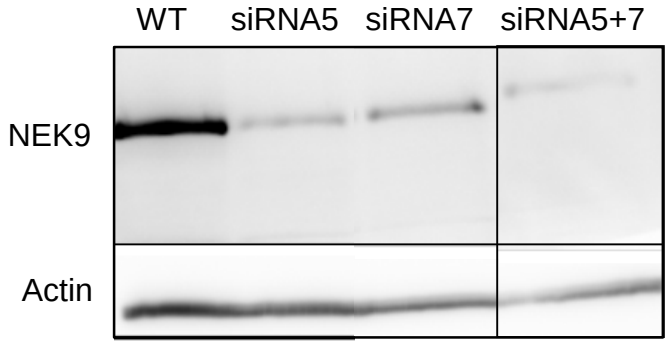

Figure 4-26: Knockdown efficiency of NEK9 siRNAs

HeLa S3 cells were treated with siRNA5 and 7, separate and combined, against NEK9 in order to test knockdown efficiency. The expression of NEK9 was compared with the wildtype 72 h after transfection and actin served as loading control.

As mentioned above, NEK9 was annotated as a mitotic kinase. Therefore, a proliferation assay (MTT assay) was performed in a cell line that was known to respond HGF/Met rather with proliferation than with scattering as DU145 does. Thus, HeLa S3 cells were transfected with the two siRNAs against NEK9 in combination and were compared to non-transfected cells. The subsequent proliferation was documented over 6 days in response to HGF stimulation in comparison to non-stimulated cells. During the first 72 h, no significant proliferation could be observed for all samples (Figure 4-27). After 96 h and 120 h, all cells had increased in number as indicated by a higher absorbance at 595 nm due to a larger amount of formazan produced by living cells. HGF stimulation in wildtype and NEK9 knockdown samples had a positive effect on proliferation, although non-

stimulated cells also exhibited a small increase in number. Even though the effect of HGF was similar in wildtype and knockdown cells, the total amount of cells in the NEK9 knockdown was overall 50% smaller. This could be due to increased cell death after transfection with siRNA against NEK9. Taken together, NEK9 knockdown did not affect the responsiveness of HeLa S3 cells in proliferating after HGF stimulation.

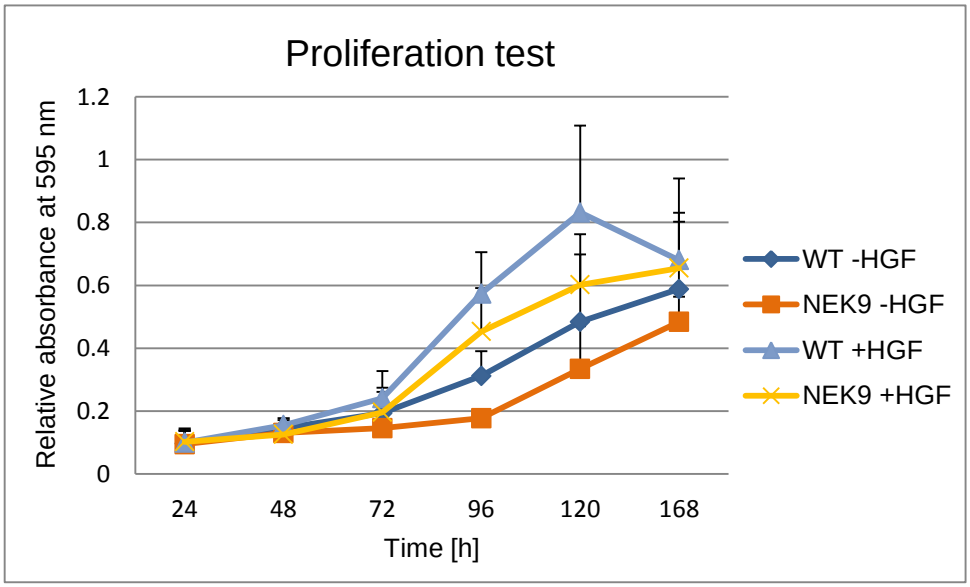

Figure 4-27: Influence of NEK9 on proliferation of Hela S3 cells in response to HGF

The effect of NEK9 knockdown via two siRNAs and stimulation with 2 nM HGF was monitored over 168 h. Absorption of living cells was detected by staining with MTT and subsequent measurement at 595 nm. WT: wildtype Hela S3; NEK9: NEK9 knockdown cells; combination of two siRNAs used for efficient knockdown.

To further examine the role of NEK9 in HGF/Met signaling, HeLa S3 and DU145 cells transfected with the two NEK9 siRNAs were tested on their migration behavior in response to HGF. Wildtype DU145 cells without HGF formed compact clusters on the surface of the petri dish (Figure 4-28). Treatment with either NEK9 or nonsense siRNA revealed less cell-cell contacts. This phenotype was possibly caused by dying of several cells in the clusters throughout the treatment. Once stimulated for 18 h with HGF, all samples exhibited a scattered phenotype as expected for the motile DU145 cell line. A difference regarding motility between wildtype and NEK9 knockdown was not detected for DU145 cells.

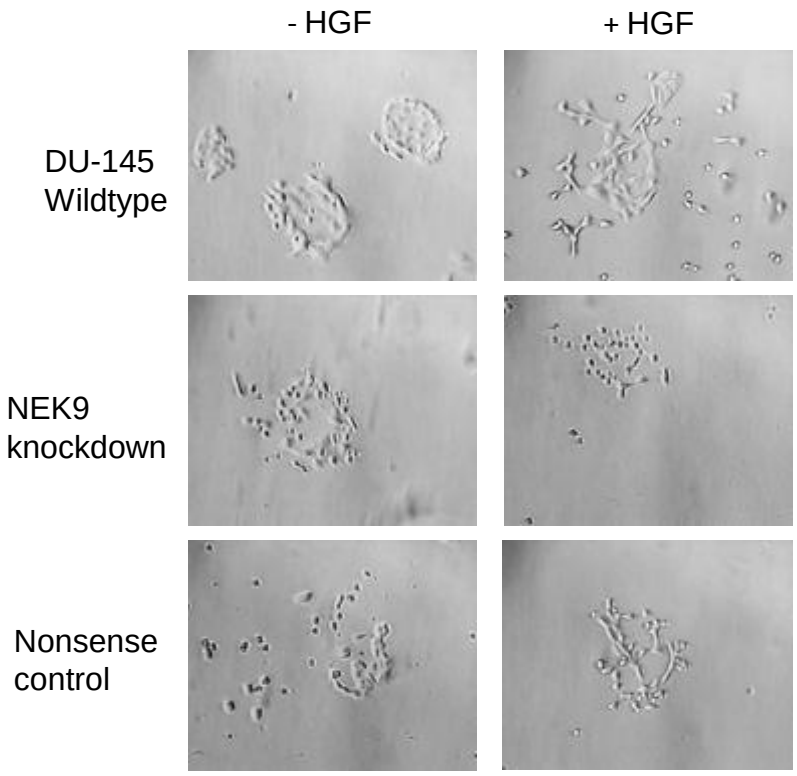

Figure 4-28: Effect of NEK9 knockdown on DU145 cells

DU145 wildtype, NEK9 knockdown, and nonsense-treated cells were stimulated for 18 h with 2 nM HGF and screened for morphological changes in comparison to the non-stimulated control.

Without stimulation, wildtype HeLa S3 cells grew in close clusters (Figure 4-29). As for DU145, some cells died during siRNA treatment, resulting in less compact clusters. Wildtype and nonsense-treated cells behaved similar after 18 h of HGF stimulation. Surprisingly, HeLa cells with NEK9 knockdown and HGF in combination displayed an impressive scatter phenotype. The cell-cell contacts have been abrogated, and the cells were released from the clusters. Furthermore, the cells spread in every direction, thereby changing their globular morphology into a stretched ellipsoid shape with long, thin filopodia in the front and rear. Usually, this cell line is proliferating after HGF/Met-induction and is not known to respond growth factor stimulation with scattering. Therefore, this monitored motile phenotype of HeLa S3 cells with NEK9 knockdown is novel and very remarkable.

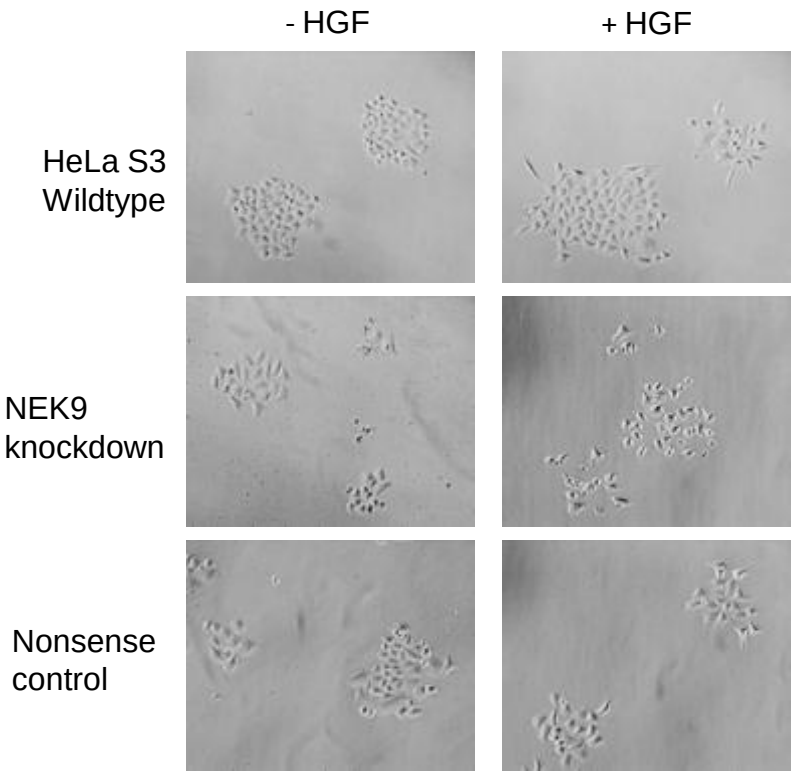

Figure 4-29: Effect of NEK9 knockdown on HeLa S3 cells

NEK9 or nonsense siRNA transfected and wildtype HeLa S3 cells were stimulated with 2 nM HGF. After 18 h, they were screened for phenotypic alterations by monitoring the cells under a microscope.

Based on the previous observation that NEK9 knockdown dramatically effects motility of HeLa S3 cells, a gene expression array with these cells was performed to investigate whether NEK9 participates in gene regulation or directly controls signaling components to result in such an intense phenotypic alteration. For that, wildtype HeLa S3 cells were compared to cells treated with the two NEK9 siRNAs in combination. Furthermore, a nonsense siRNA was added as third sample to exclude side effects of the transfection reagent. Each sample was either stimulated for 18 h with HGF or left unstimulated. In total, two replicates were performed in order to ensure reproducibility.

First of all, gene expression data of the two replicates should be compared and only those genes regulated in the same direction were considered. Next, proof-of-concept data from the HeLa S3 wildtype with and without HGF should be investigated and confirmed. Only after that, the effect of NEK9 knockdown on the HGF/Met-dependent gene expression after HGF stimulation was analyzed.

In total, more than 41,000 different genes were analyzed on a gene expression chip. After deletion of outliers and those genes exhibiting strong variances within the replicates, 3,334 genes remained for further analyzes. As the nonsense siRNA sample showed comparable gene expression as the HeLa S3 wildtype, the latter one was used as regulation basis. A minimum fold change of ≥5 in comparison to the unstimulated wildtype was assumed as significant regulation, resulting in 336 genes fulfilling these criteria.

First of all, genes in the HeLa S3 wildtype affected by HGF were investigated. Only 56 were downregulated, while 280 were upregulated. Affected genes included proof-of-concept data as the transcriptional regulator EGR1, which activates genes responsible for mitogenesis and differentiation. The cell adhesion proteins ITA2 and LAMC2 are also known to be transcriptional targets of HGF/Met signaling and influence cell-cell contacts as well as migration. The determination of transcriptions factors that lead to the expression of HGF-regulated genes in the HeLa S3 wildtype was supported by GeneGo. Indeed, 47 key transcription factors were identified that control the transcription of the regulated genes in this study. Of them, 11 (of 28 established) were known for HGF/Met signaling, among them FOS, FOSB, JUN, and GATA-4.

Analysis of the dependency of the NEK9 knockdown during HGF stimulation that caused the altered phenotype was performed in two steps. First, the fold changes of genes between the wildtype with and without HGF as well as the NEK9 knockdown with and without HGF were calculated. Second, the fold change between these two values was computed (analogous to the EPHA2 array, Figure 4-22). The regulated genes were affected by NEK9 during HGF stimulation. 170 genes were considered, of which 48 exhibited no regulation between wildtype and knockdown. Of the remaining 122 genes, 73 were up- and 49 downregulated through NEK9 dependent on HGF. Most affected genes were collagen degrading protein MMP-3, the purine receptor P2RY8, functionally unknown LRC36, nuclear pore protein NAV3, and the ubiquitin ligase TRI63 - all about 20 fold upregulated in the NEK9 knockdown.

Searching for altered gene expression, which could be responsible for the observed migration, the list of 122 was sorted by function. Indeed, 22 genes were found associated with motility and migration in pathways provided by GeneGo

(Table 4-2). For example, FLRT3 causes dynamin-dependent internalization of c-cadherin resulting in decreased cell contacts. Matrix metallopeptidases MMP1 and MMP3 as well as PAI1 cleave the extracellular matrix. Furthermore, EGR1 induces the transcription factor SNAI1, which regulates genes involved in motility. Also genes coding for cytoskeletal proteins were affected by the NEK9 knockdown. The tubulin TBAL3, linker protein DYST, and actin-modulator SYP2L were upregulated. PLEK2 is involved in the formation of lamellipodia and was also found upregulated. Additionally, genes for small GTPases or their regulators were also affected by the NEK9 knockdown in HeLa S3 cells. Notably, the gene coding for RAC2 was upregulated more than 10-fold. RAPGEF3 activates the GTPase RAP and triggers motility through this pathway. IL8 stimulates cascades involving RAC and RHO as well as PI3K to enhance cellular movement. In contrast, genes expressing proteins for cellular adhesion were negatively affected by NEK9 knockdown. Downregulated ID2 inhibits e-cadherin expression and CLN1 eliminates cell adhesion. Furthermore, the gene coding for a 2ABB, which is involved in cell cycle progression, was downregulated. In contrast, upregulated genes of RGS2 and CDN1A are known to inhibit proliferation.

Table 4-2: NEK9- and HGF-regulated genes associated with motility.

22 genes occur in GeneGo pathways related to motility and migration and were found among 122 genes differentially regulated in NEK9 knockdown cells in comparison to the wildtype depending on HGF stimulation. WT: wildtype HeLa S3 cells; KD: NEK9 knockdown HeLa S3 cells.

Gene	Protein name	Fold Change (WT +/- HGF) vs. (KD +/- HGF)	NEK9 knockdown effect
mmp3	Matrix Metallopeptidase 3	28.0	Cleaves ECM
p2ry8	Purinergic receptor 8	27.3	Receptor family triggers motility
coha1	Collagen type17, alpha 1	13.7	Regulates MAPK-induced migration
mmp1	Matrix Metallopeptidase 1	12.4	Cleaves ECM
Inhba	Inhibin/activin, beta A chain	11.2	Activates MAPK-induced migration
rac2	Ras-related C3 botulinum toxin substrate 2	10.5	Cytoskeletal reorganization

gpr56	G protein coupled receptor 56	9.1	Regulates migration
flrt3	Fibronectin leucine rich transmembrane protein 3	7.8	C-cadherin internalization
cdn1a	Cyclin-dependent kinase inhibitor 1A	7.0	Inhibits cyclin-CDK complexes, cell cycle
rapgef3	Rap guanine nucleotide exchange factor 3	4.9	Cytoskeletal reorganization
egr1	Early growth response 1	4.0	Activates SNAI1
syp2l	Synaptopodin 2-like	3.6	Cytoskeletal reorganization
pgh2	Prostaglandin-endoperoxide synthase 2	3.3.	Affects migration
tbal3	Tubulin, alpha-like 3	3.2	Cytoskeletal reorganization
plek2	Pleckstrin 2	2.8	Formation of lamellipodia
dyst	Dystonin	2.4	Cytoskeletal reorganization
rgs2	Regulator of G protein signaling 2	2.4	Inhibitor of proliferation
il8	Interleukin 8	2.1	Cytoskeletal reorganization
pai1	Serpin peptidase inhibitor, clade E	2.0	Disrupts cell contacts
id2	Inhibitor of DNA-binding 2	-2.4	Inhibits e-cadherin expression
2abb	Protein phosphatase 2, subunit B	-3.1	Affects cyclin through GSK3β
cln1	Claudin 1	-8.4	Eliminates cell adhesion

4.3 The effect of *Listeria* InlB on Met signaling

4.3.1 The phosphoproteome triggered by InlB/Met

The growth factor HGF is the only physiological ligand known, which binds and activates Met, inducing cascades for proliferation, migration, and survival. Nevertheless, internalin B of the pathogenic bacterium *Listeria monocytogenes* is also able to externally bind and stimulate the Met receptor.

To compare induced pathways of HGF and InlB in this study, phosphoproteomics was applied to cells stimulated with the bacterial surface protein. Human cervix cancer line HeLa S3 is the common model for infection studies and was used in these experiments. In contrast to the HGF-study, only one time point was selected to reduce time and effort. A maximum stimulation of known pathway components was supposed to happen during the first minutes (Reinl et al. 2009).

First of all, the purity and activity of the InlB protein was tested by gel electrophoresis and immunoblot against known signaling proteins of the Met pathway. After that, the phosphoproteome of InlB-stimulated HeLa S 3 cells was investigated. Regulated phosphopeptides after 5 min InlB stimulation were calculated next. These were compared to phosphopeptides affected by HGF (from section 4.2.3) to determine the influence of the pathogenic protein on the physiological signaling.

SCX elution fractions of InlB recombinantly expressed InlB in CHO cells were loaded on a SDS gel to control the purity of the protein. All lanes showed a thick band at 70 kDa which corresponds to the InlB chain (Figure 4-30). Fractions 1-7, and 12-14 exhibited three slightly smaller bands, perhaps variants of the protein with different glycosylation patterns. Additionally, most fractions contained a faint band at 20 kDa. For the stimulation experiments, InlB of fraction 10 was used, because it was one of the purest.

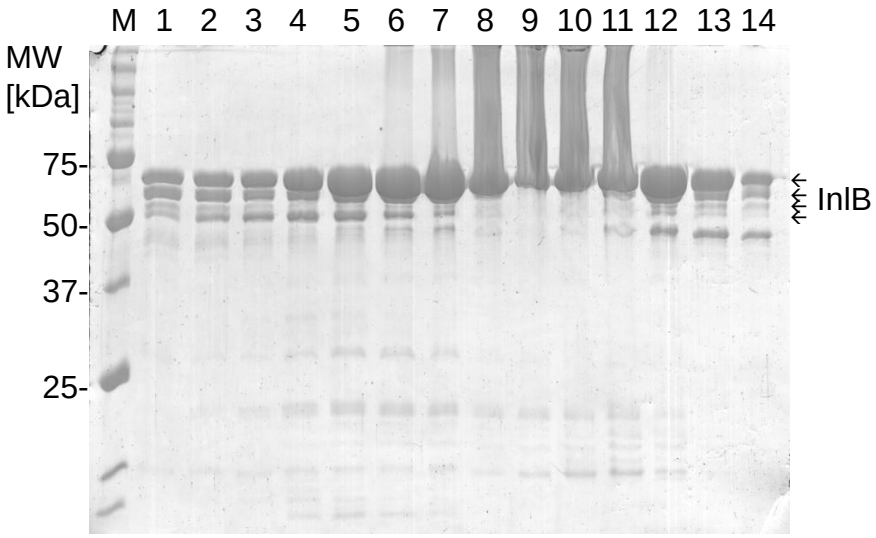

Figure 4-30: Elution fractions of recombinantly expressed InlB

The protein was expressed in CHO cells and purified. Elution fractions of the SCX were applied to an SDS gel to control purity. Protein of fraction 10 was chosen for further experiments.

Second, the activity of the protein was checked testing whether it was able to induce Met-dependent signaling. To determine an InlB concentration which is sufficient to induce signaling cascades downstream of Met, HeLa S3 cells were treated with 7 and 10 nM InlB. Three different stimulation times (2, 6, 20 min) were compared to identify the time point with maximal stimulation.

According to the loading control HSP90, all samples contained equal amounts of protein (Figure 4-31). In non-stimulated controls (lanes 1, 2) no signal was detected with phospho-specific antibodies against pY^{1234}/pY^{1235} of Met as well as pT^{185}/pY^{187} and pT^{202}/pY^{204}, of MK01 (ERK2) and MK03 (ERK1), respectively. In contrast, every time point and every concentration of InlB caused the phosphorylation of MK01 and MK03. Met phosphorylation was also induced by InlB, particularly at 10 nM after 2 and 6 min. Based on these results, stimulation with 10 nM InlB for 5 min was selected for the phosphoproteome study.

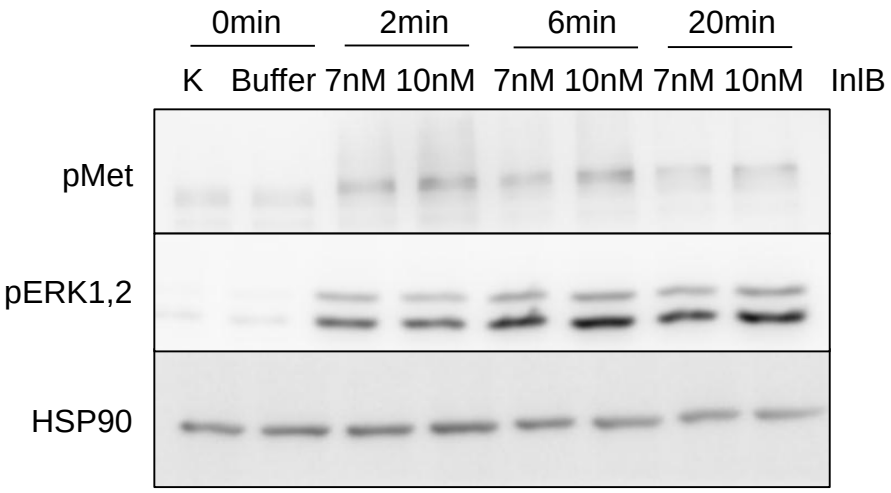

Figure 4-31: InlB is able to stimulate Met-pathway

HeLa S3 cells were stimulated as indicated with InlB or MES buffer and activation of Met as well as MK01 (ERK2), MK03 (ERK1) was evaluated with phospho-specific antibodies. Heat shock protein 90 (HSP90) was utilized as loading control.

Human cervix cancer line HeLa S3 was stimulated for 5 min with *L. monocytogenes* surface protein InlB and compared to the non-treated control. Following stimulation and harvest, aliquots of cell lysates were immunoblotted to check for the stimulation of Met-pathway components via phospho-specific antibodies. Loading control GAPDH exhibited similar bands, proving equal amounts of proteins applied per sample (Figure 4-32). Activation sites pY^{1234}/pY^{1235} of Met was found to be phosphorylated after 5 min InlB as well as double sites of the MAP kinases ERK1 (MK03) and ERK2 (MK01).

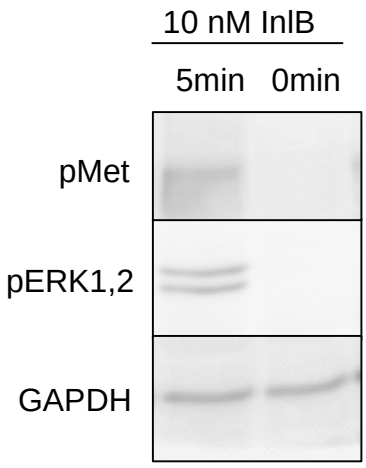

Figure 4-32: Stimulation control for phosphoproteomics

Aliquots of the stimulated cell lysates for phosphoproteomics were applied to immunoblotting. With phospho-specific antibodies against pY^{1234}/pY^{1235} of Met as well as pT^{202}/pY^{204} and pT^{185}/pY^{187} of ERK1 (MK03) and ERK2 (MK01), respectively, the activation of the Met cascade was tested. GAPDH served as loading control.

Phosphoproteomics of the two samples carried out as duplex iTRAQ labeling with three replicates each, identified 2,784 phosphopeptides belonging to 1,299 phosphorylated proteins. The data were processed as shown and described in detail for the HGF/Met phosphoproteome. In this approach, 387 phosphopeptides were detected in all three experiments and 28 of them were considered as significantly regulated after 5 min InlB-treatment.

Regulated phosphopeptides were illustrated in a heatmap (Figure 4-33) and further information is illustrated in the appendix (Table 8-4). The 20 upregulated peptides were marked again by red boxes, while the green boxes indicated the 8 downregulated phosphopeptides. As for the HGF phosphoproteome, regulation directions within the triplicate were the same, but the regulation factors varied due to the fast phosphorylation dynamics. The activation sites pT^{185}/pY^{187} and pT^{202}/pY^{204} of the MAP kinases MK01 and MK03 were upregulated clearly. The adapter protein AHNK exhibited several upregulated phosphorylations. Further, the site pS^{801} of the motor protein KIF4A, which plays a role in cytokinesis, was modified as well. The kinase PKN2 was phosphorylated at pS^{583} after 5 min with InlB. Notably, the site pT^{693} of the growth factor receptor EGFR was found to be upregulated, revealing potential receptor crosstalk between Met and EGFR in response to InlB. Phosphorylation sites for Met were not detected, perhaps due to

a lack of kinase enrichment. OSTF1, a protein probably involved in signaling was found to be dephosphorylated at pS^{213} in response to InlB. The site pS^{134} of the p53- and NF-k-interacting protein IASPP was downregulated as well. Surprisingly, a protein involved in immune response, namely TRAD1, was also affected by InlB-stimulation by downregulation of pS^{415}.

As previously mentioned, InlB is supposed to activate signaling cascades comparable to HGF. Therefore, proteins corresponding to the 28 regulated peptides were checked for known functions in Met signaling. The majority of these has not been published and is therefore detected in this context for the first time. The proteins MK01, MK03, and EGFR were already described as part of this cascade and thus constitute proof-of-concept. The first two are among the most well-known signal transducers in Met-dependent signaling (Birchmeier et al. 2003) and even served as stimulation control for HGF and InlB in this study. The EGF receptor is closely related to Met and shares several downstream components. Furthermore, it has been shown to occur in complexes with Met, at least in cancer cells (Mueller et al. 2010). Met was first identified as an oncogenic fusion protein together with TPR, resulting from a chromosomal rearrangement. This construct forms dimers through TPR located in the cytoplasm and leads to continuous and ligand-independent Met dysregulated signaling in affected cells (Peschard and Park 2007). Here, TPR was identified with two upregulated phosphorylation sites.

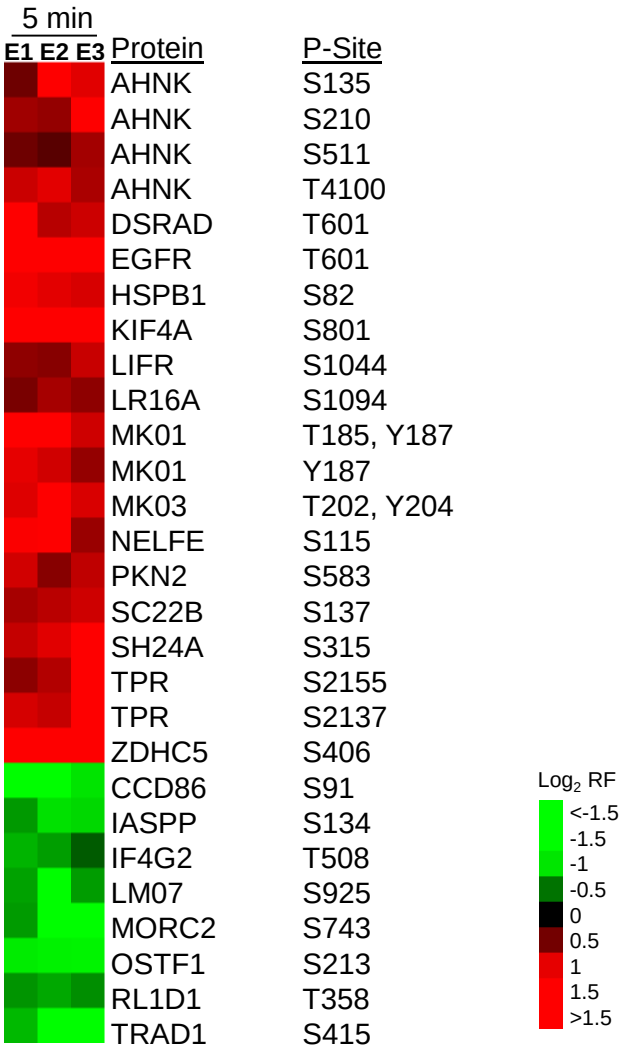

Figure 4-33: Phosphopeptides regulated after 5 min stimulation with InlB.

Heatmap of significantly regulated phosphopeptides after InlB treatment. Green boxes illustrate downregulations, while red boxes stand for upregulated peptides. Values of regulation factors are shown in $\log_2$ scale. P-Site: phosphorylation site.

All regulated phosphorylation sites were already described in human cells, except for pS^{406} of the palmitoyltransferase ZDHC5. This site is only predicted from mouse in the databases PhosphoSitePlus and PhosphoNet. Phosphoproteomics revealed this modification to be upregulated after 5 min of InlB stimulation (Figure 4-34).

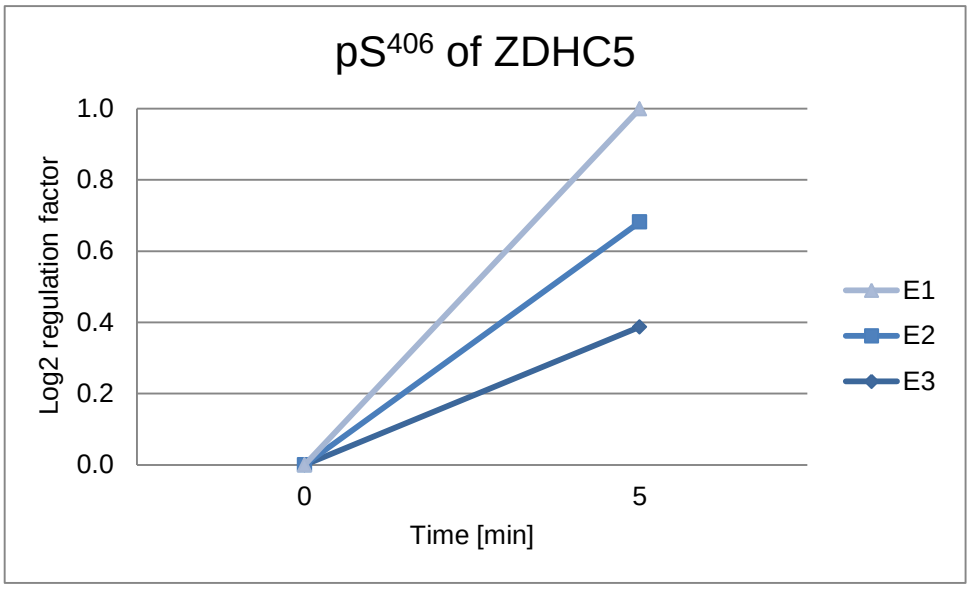

Figure 4-34: Regulation of the novel phosphorylation site pS^{406} of ZDHC5

Phosphorylation sites regulated in response to InlB were looked up in the current databases PhosphoSitePlus and PhosphoNet. All sites were found, besides pS^{406} of palmitoyltransferase ZDHC5. This novel modification of unknown function was upregulated in all three replicates (E1-E3).

Further functional information was available for only 5 of the 28 phosphopeptides regulated after InlB-stimulation,. The protein kinases MK01 and MK03 with their phosphorylation sites at pT^{185}/pY^{187} and pT^{202}/pY^{204} are key players of several signaling cascades. They are activated through the identified double modifications caused by MP2K1 (MEK1), MP2K2 (MEK2), and JAK2. MK01 and MK01 are also able to phosphorylate pS^{1044} of LIFR, which inhibits this protein. EGFR was phosphorylated at pT^{693} by the MAP kinases leading to its internalization. Furthermore, modification of pS^{82} of heat shock protein HSPB1 causes the dissociation of chaperone complexes and triggers cytoskeletal rearrangements by binding to TPM1. Several kinases are able to phosphorylate this site, which also inhibits interaction of HSPB1 with TRAF6 and AKT1.

4.3.2 Influence of *Listeria monocytogenes'* InlB on physiological Met signaling

The growth factor HGF and the *L. monocytogenes* surface protein InlB both bind to and activate the Met receptor, triggering comparable signaling cascades on the kinase level (Reinl et al. 2009). Nevertheless, they produce different kinds of

cellular responses: While HGF stimulates proliferation, migration, and survival, InlB induces the bacterium's uptake into the host cell. In this study, HGF- and InlB-regulated phosphopeptides have been identified and characterized (see 4.2.3 and 4.3), and thus can be compared in order to find similarities and differences in these phosphoproteomes.

Comparable to the kinase data, the majority of regulated phosphorylation sites were not known to play a role in Met signaling before. Besides that, 25 phosphopeptides were regulated after HGF and were detected after InlB stimulation, but were not regulated in the InlB dataset. However, it has to be taken into account that for InlB only the 5 min time point was analyzed. Thus, all late responders in HGF signaling were not considered when matching both datasets. That resulted in 11 phosphopeptides, which were only regulated by HGF, but were detected after InlB stimulation (Table 4-3). Several proteins possessing HGF-regulated sites seemed to be involved in progression of the cell cycle. While TP53B is a transcriptional regulator, which induces mitosis, NUFP2 changes its localization in a cell cycle-dependent manner, indicating an associated function. RIR2 is a regulator of Wnt-signaling, taking part in several processes, including mitosis and establishing cell polarity. Furthermore, the regulated site pS^{20} is phosphorylated by CDK1 and CDK2 that are key players of the cell cycle. Other proteins with regulated phosphorylation sites only after HGF stimulation influence cytoskeleton reorganization, which is necessary for cell division or migration. Rho-GEF ARHG2 regulates signaling via small GTPases, which activate rearrangements of the cytoskeleton. TENS3 and LIMA1 are responsible for reformation and polymerization of actin fibers. The protein NIBL1, however, is supposed to suppress apoptosis.

In conclusion, phosphopeptides regulated only in the HGF dataset correspond to proteins involved in the physiological response of Met signaling like mitosis, migration, and survival.

Table 4-3: Phosphorylation sites regulated only by HGF after 3 and 6 min

Listed sites were regulated after 3 or 6 min of HGF stimulation, but displayed no response in the InlB dataset. Protein functions were retrieved from the Uniprot database. Arrows illustrate the regulation direction of the phosphorylation site after 3 and 6 min HGF treatment. The 20 min time point was not taken into account for this comparison, because InlB was only stimulated for 5 min.

Protein	P-Site	Regulation (3, 6min)	Protein function
NUFP2	pT571	↑↑	Relocalization during cell cycle
SH3B4	pS244	↑↑	Transferrin receptor internalization
TENS3	pS776	↑↑	Reorganization cytoskeleton
TPR	pT2116	↑↑	Nuclear pore, protein import
RTN4	pS107	↑↔	Regulation in development
ARHG2	pS886	↔↑	Rho-GEF
LIMA1	pS686	↔↑	Formation of actin fibers
NIBL1	pS678/pS679	↔↑	Anti-apoptosis signal
OXR1	pS202	↔↑	Oxygen stress response
RIR2	pS20	↔↑	Inhibits Wnt-signaling
TP53B	pS1114	↔↑	Transcription, Mitosis

On the other hand, 13 phosphopeptides were regulated after InlB, but not HGF stimulation, although they had been detected there (Table 4-4). The adapter protein LMO7 exhibited modified sites in response to InlB as well as the transcriptional regulators NELFE and MORC2. Compared to HGF, the involvement of these components implicates at least a slightly altered signaling after contact with this isolated pathogenic factor. Interestingly, three proteins of TRAF6-NFκB-signaling appeared differentially phosphorylated in this dataset. The heat shock protein HSPB1 was modified at pS^{82}, which inhibits interaction with the signaling adapter TRAF6. Second, pS^{134} of phosphatase IASPP was downregulated. The protein interacts with the transcription factor p53, but also negatively regulates NFκB. A phosphorylation site of TRAD1, a protein involved in the negative feedback in immune response, was downregulated in response to InlB.

Table 4-4: Phosphorylation sites regulated only by InlB

Illustrated phosphorylation sites were regulated only in response to InlB after 5 min and were not affected in the HGF-dataset. The regulation direction of the phosphorylation site is indicated by arrows. Functional protein information was retrieved from the Uniprot database.

Protein	P-Site	Regulation (5 min)	Protein function / effect
AHNK	pS210	↑	Adapter in development
HSPB1	pS82	↑	Heat shock, actin reorganization
LR16A	pS1094	↑	Actin polymerization
NELFE	pS115	↑	Transcription
SC22B	pS137	↑	Vesicle trafficking
SH24A	pS315	↑	Inhibits proliferation
CCD86	pS91	↓	Unknown
IASPP	pS134	↓	Interaction with p53, NFκB
IF4G2	pT508	↓	Translation
LMO7	pS925	↓	Adapter protein
MORC2	pS743	↓	Inhibits transcription
RL1D1	pT358	↓	Unknown
TRAD1	pS415	↓	Inhibits immune response

In contrast, 5 of 28 phosphorylation sites affected by InlB were significantly regulated in both datasets. 19 further sites were significantly regulated after HGF stimulation and were affected by InlB, although not significantly. Thus, 24 phosphorylation sites on 21 proteins were similar in both signaling cascades, indicating – at least in part - comparable downstream components for both ligands. Among those regulated sites were the activation sites of the MAP kinases MK01 and MK03, as well as pT^{246} of the AKT1 target protein AKTS1 and pS^{262} of the PI3K subunit P85B. Furthermore, phosphorylation sites pS^{893} and pS^{137} of the actin-associated proteins PALLD and PAXI and pT^{587} of the phosphatase PTN12 were also regulated by both ligands. In conclusion, the pathogen-derived protein InlB activates also signaling cascades induced by HGF/Met, although it is structurally unrelated and binds to different regions on the Met receptor.

5 Discussion

Intracellular signal transduction processes utilize phosphorylation to transmit and process information. Addition of a phosphate group to serine, threonine, or tyrosine affects the protein's interactions, activity, stability or localization. Kinases transduce those signals from one to another, thereby spreading, enhancing, or integrating them within minutes. The mechanism is antagonized and tightly regulated by phosphatases, which dephosphorylate their substrates. The flexibility and rapidity of this processes enables cells to respond immediately to environmental changes by regulating target gene expression or protein activity (Jordan, Landau, and Iyengar 2000). One of the most important signaling pathways for embryogenesis and wound healing, but also during cancer progression, was investigated in this study. Signaling by the Met receptor was either stimulated by binding of the growth factor HGF or of the surface-located invasin InlB of *Listeria monocytogenes,* which triggers the pathogen's invasion (Birchmeier et al. 2003; Ireton 2007). Although the downstream signaling cascades of Met have been studied for two decades, recent proteomic approaches allow for a comprehensive overview and a more precise characterization of involved proteins and substrates.

5.1 Successful strategy to uncover the phosphoproteome from cell lines

Traditional 2D gel electrophoresis in combination with phospho-staining can be utilized to identify phosphorylated proteins. However, in a current study using 2D gels stained with Pro-Q Diamond to identify regulated phosphoproteins in response to wounding in maize leaves, the limitations of the technique became obvious. The authors identified 270 proteins in total, of which 41 were regulated and could be identified by MALDI-MS. Nearly all proteins were already known in this context before and phosphorylation sites were not determined (Lewandowska-Gnatowska et al. 2011). As most signaling molecules like kinases and transcription factors are among the low abundance proteins, there is a need for an efficient phosphoproteome enrichment strategy. Ruan and co-workers recently proved that

purification of phosphoproteins previous to two-dimensional difference gel electrophoresis (2D-DIGE) improves the sensitivity for signaling proteins. They were able to identify 28 phosphoproteins differentially regulated in response to EGF in CNE2 cells, but the method used by them did also not provide information about the location of the phosphorylation sites (Ruan et al. 2011). Thus, in order to additionally localize phosphorylation sites, this work utilized LC-MS/MS, where peptide sequencing is performed in the second MS. Indeed, phosphopeptide enrichment by affinity chromatography using metal ions (IMAC) followed by strong cation exchange chromatography (SCX) and LC-MS/MS as established in this study successfully enriched and identified more than 3,000 phosphopeptides in the preliminary studies including those of low-expressed signaling components. Furthermore the technique provided reliable phosphorylation site information for all identified proteins.

Initial experiments in this study were designed to establish a robust and effective workflow to characterize the Met-induced phosphoproteome. Results showed that Ga^{3+}-based IMAC purified phosphopeptides more efficiently than IMAC using Fe^{3+}-ions. Furthermore, applying the Ga-IMAC flow-through onto Fe^{3+}-resin did not result in additional enriched peptides. Thus, Ga-based IMAC was sufficient to purify phosphopeptides from a complex cell lysate. Increasing the amount of protein from cell lysate resulted in a larger number of identified peptides. Notably, no negative effect was observed concerning binding characteristics of the Ga-resin. Of course, the binding sites for phosphopeptides on the IMAC material were limited, but could be expanded by using larger amounts of Ga^{3+}. The limiting factor was rather the amount of cells prepared for the experiment, as 4 mg of protein required already more than 10^7 cells for each sample. IMAC binds acidic peptides as well, because they also interact with positively charged metal ions at low pH as phosphopeptides do. Therefore, enriched peptides were fractionated via SCX, where the resin interacts with cations, while phosphorylated peptides are not retained during elution. The ability of SCX to further separate phosphorylated from non-modified peptides was clearly demonstrated by their distinct distributions in the eluted SCX fractions. However, not all currently available phosphopeptide enrichment strategies were compared in the pre-experiments due to time limitations. Olsen and co-workers for example were successful using SCX followed by TiO_2 (Olsen et al. 2006), which was not examined here.

In the first main study, the phosphoproteome isolated after HGF stimulation over a time course consisted of about 7,996 different phosphopeptides from three independent experiments. Comparable studies investigating tyrosine receptor signaling resulted in similar peptide amounts, reflecting the efficiency of the utilized workflow. For example, the mentioned TiO_2 approach by Olsen et al. resulted in 10,000 phosphopeptides after 5 and 10 min EGF stimulation of HeLa cells. In comparison, strategies with anti-phosphotyrosine antibodies revealed up to about 250 tyrosine phosphorylation sites when cell lines were stimulated by HGF (Hammond et al. 2010; Organ et al. 2011). The recent publication of Organ has to be compared to the results of this study, because it is highly equivalent. They screened the colorectal cancer cell model DLD1 to analyze the cellular response after 10 and 60 min HGF stimulation. Utilizing phosphotyrosine-specific antibodies, they identified 266 phosphorylation sites on 168 proteins and performed regulation analysis with label-free quantification (Organ et al. 2011). However, the authors achieved access to only tyrosine phosphorylations that represent 1-2% of a complex phosphoproteome.

Furthermore, the ratio of the phosphorylated amino acids (pS:pT:pY) 84:15:1 in this work was analogous to data from other phosphoproteome studies. Olsen et al. published 86:12:2 for the distribution of phosphorylated serine, threonine, and tyrosine, and Hunter found 90:10:0.05 by radioactive-labeling with ^{32}P (Hunter and Sefton 1980), reflecting the comparability of this enrichment workflow with other methods.

In contrast, the phosphoproteome after InlB stimulation only yielded 2,784 modified peptides in total. The striking difference to the HGF-dataset might be caused by several factors. Firstly, only 8 mg instead of 16 mg of protein were applied to the workflow due to iTRAQ duplex labeling of two instead of four samples in comparison. During the first MS run only peptide ions with certain intensity are further processed and sequenced to decrease the false discovery rate. Therefore, it is likely that a smaller amount of peptides resulted in a lower number of identified peptides in total. Furthermore, no phosphopeptides were detected as regulated after more than 5 min InlB which decreases the total amount of identifications compared to the HGF time course. Nevertheless, biological reasons could also play a role. HGF might be able to induce a broader response

resulting in more phosphorylated proteins. Furthermore, the threshold for inducing downstream pathways could vary depending on the concentration of the ligand. In the stimulation control, phosphorylation of Met as well as MK01 and MK03 (alias ERK2 and ERK1) was monitored only in a qualitative manner; therefore no quantitative comparison of the activation of these proteins by the different ligands is available from this work. Thus, it is possible that an increase of the concentration of InlB might have caused an analogous stimulation, resulting in a comparable amount of identified phosphopeptides. However, the most likely reason for the differences between the two datasets are the unlike amounts of peptides applied to mass spectrometry and the resulting ion shadding by highly abundant peptides.

Time-resolved analyses of RTK signaling allow covering of several intermediate states during the process of signal transduction. In order to quantitatively compare these states with each other or with the non-stimulated condition, the samples were labeled. Here, iTRAQ was used for tagging, because it has been successfully used in several investigations of Met (T. Guo et al. 2010; Reinl et al. 2009) or RTK signaling (Lim et al. 2009; Zhang et al. 2010; Zhang et al. 2005). The strategy provided relative quantification data based on the regulation factors of HGF-activated samples compared to the non-stimulated control. As the distribution of regulation factors in all samples after normalization was comparable, the triplicate was performed without any major sources of error. However, cell lines were used to extract proteins, which could have been compared also with SILAC. In this case, inter-experimental variations might have been almost completely abolished because of the earlier labeling on the level of intact cells. Biological variances between cells, however, still cannot be eliminated by either technique. Furthermore, results of this work established a robust and comparable workflow using iTRAQ labeling. Additionally, the workflow can now be easily adapted to clinical human tissue samples, where SILAC labeling is not possible.

Phosphorylation events were monitored during the first 20 min after stimulation, because the modification cascade is fast. For example, Met was phosphorylated after 1 min (Y. Shen et al. 2000), while the MAP kinases MK01 and MK03 were shown to be activated after 5 min (Wells et al. 2005) or even earlier (see Figure 4-10). Generally, no significant change in the concentration of proteins identified

during this time span can be expected. As first transcripts occur after 30 min at the earliest, protein synthesis is usually much slower than phosphorylation. Thus, it can be assumed that no increase in protein amount might influence the upregulation of a phosphopeptide. The contrary mechanism, decreasing the amount of protein through degradation, will also take some time and can be expected to play a minor role after 3 and 6 min, when a downregulation of a phosphopeptide is monitored. Nevertheless, Goormachtigh et al. investigated the degradation time of GAB1 in HeLa cells and demonstrated that already after 15 min HGF stimulation there is a decrease of the protein's amount in the cell. However, this was not the case for Met and the MAP kinases, which did not show degradation within the first 2 h after stimulation (Goormachtigh et al. 2011). Therefore, it has to be taken into account that phosphopeptide downregulation might be due to a decreased protein amount and not due to a regulation of the phosphorylation site. In this case, additional immunoblots against the whole protein have to be performed to ascertain no change in the protein level. In contrast, for all other regulated sites, no influence of the corresponding protein concentration should be expected.

Taken together, the established strategy was able to identify, quantify and compare thousands of phosphopeptides from the cell lines DU145 and HeLa S3 after stimulation with HGF or InlB. With this, the HGF study was one of the most extensive investigations of RTK signaling and the largest of the HGF/Met-induced phosphoproteome so far. Although fewer phosphopeptides were found for the InlB-induced signaling, this work was the first phosphoproteomic study that investigated the host response after stimulation with a specific pathogenic effector molecule.

5.2 Activation of known HGF/Met pathway components

The majority of previous approaches to analyse HGF/Met signaling have not been global, but instead concentrated on single proteins or complexes that could play a role in this context. Main pathway components were identified using hypothesis-driven and targeted traditional biochemical methods against a limited amount of candidate proteins that have been implicated in certain phenotypes involving Met. For example, the Ras-Raf-MEK-ERK cascade has been known to trigger motility,

was therefore screened by phospho-immunoblots during Met activation and confirmed as part of the downstream network (Jeffers et al. 1998). Additionally, one of the first interaction partners of Met, PI3K, was identified by co-immunoprecipitation with the receptor after HGF stimulation (Graziani et al. 1991).

Nowadays, these techniques are still important to characterize a protein or its interactions, but signaling cascades are rather screened by proteomic approaches. This enables researchers to get a comprehensive overview and provides many potential pathway components from one experiment. In this study, 80 proteins were identified as part of this pathway by their regulated phosphorylation sites in response to HGF stimulation. Notably, among them were 6 known proteins of the HGF/Met pathway that were integrated into the established signaling network.

5.2.1 The GAB1-MAPK-PAXI cascade

The essential and direct Met adapter GAB1 was phosphorylated on pY^{659} with a maximum in the first 6 minutes. The phosphorylation site is known to be modified by several growth factor receptors and leads to the activation of the MAPK cascade (Onishi-Haraikawa et al. 2001; Ingham et al. 1998). Members of this cascade, namely MK01 and MK03, were identified in this by their known activating double phosphorylations on tyrosine and threonine. Those were significantly upregulated in response to HGF with a maximum after 6 min. Furthermore, as one target of MK01, PAXI exhibited increased phosphorylation after 6 and 20 min. Although, the site pS^{137} on PAXI is not functionally characterized so far, it is likely that the MAP kinase modifies this site in response to HGF. PAXI is a protein localized in the focal adhesions and is supposed to play a role in cell migration (Schaller 2001). The GAB1-MAPK-PAXI cascade is a perfect example of a signal being transmitted stepwisely through the cell in the first 20 min of HGF stimulation (Figure 5-1). This pathway might regulate cellular motility in response to activated Met.

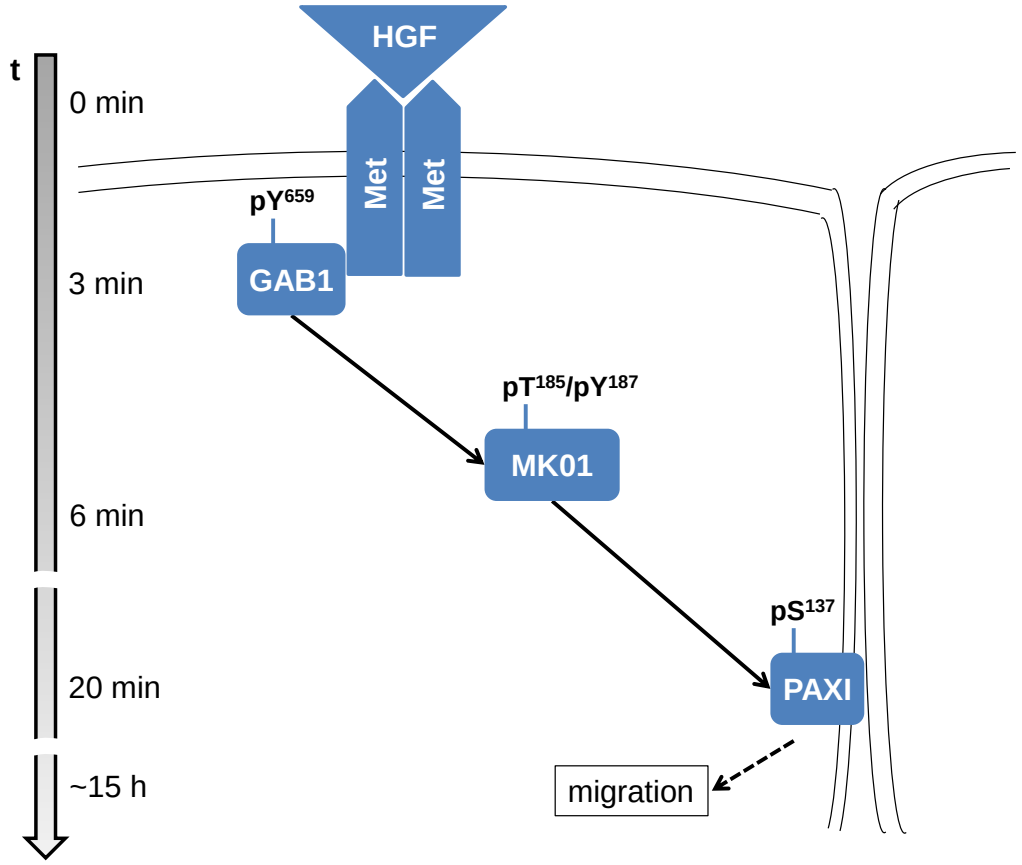

Figure 5-1: GAB1-MAPK-PAXI signaling cascade

In response to HGF stimulation, the indicated phosphorylations sites of the known Met pathway members GAB1, MK01, and PAXI were upregulated one after another within the first 20 min. When activated, the adhesion protein PAXI regulates migration.

5.2.2 The PI3K-AKT1 axis

GAB1 acts as adapter for the kinase PI3K, which is also able to bind to Met directly. Binding of PI3K to Met is mediated via its SH2 domain-containing p85 subunit (Ponzetto et al. 1994) that was identified by phosphoproteomics in this study. P85B is the adapter unit of the kinase complex that transmits the signal from Met to AKT1 thereby triggering several distinct pathways leading to proliferation and protection from apoptosis (Rosário and Birchmeier 2003). The site pS^{262} was found upregulated after 20 min of HGF stimulation, but is not functionally characterized yet. As PI3K belongs to the proximal Met signaling, an activating phosphorylation might occur earlier than that. Thus, the function of this site could be inhibitory in order to stop PI3K-AKT1 signaling.

Small GTPases like RAC1 and CDC42 mediate HGF/Met-induced migration (Wells et al. 2005). Although these proteins could not been identified in this study because they are not controlled by phosphorylation, another known regulator of cell motility that interacts with GTPase signaling was detected by its phosphorylation site. The Adenomatous Polyposis Coli (APC) protein accumulates in lamellipodia and membrane ruffles in HeLa cells stimulated by HGF. Under these conditions, it co-localizes with the Rho-GEF SPT13 and the phosphatase complex scaffold protein NEB2, which both are required for migration in response to HGF (Sagara et al. 2009). SPT13 again activates RAC1 and CDC42 in a PI3K-AKT1-dependent manner. Binding of APC to SPT13 increases its GEF activity thereby enhancing this pathway (Kawasaki et al. 2007). As the phosphorylation site on APC was downregulated after 20 min of HGF stimulation, the modification might affect the interaction with SPT13 and thus, regulate the migratory pathway.

5.2.3 Where are the proof-of-concept data?

Of course, more than these proteins are known as members of Met signaling, but obviously have not been identified here. To consider the reasons, one should keep in mind that, phosphorylation of the components was monitored at only three time points. Additionally, peptides that reacted differently in one experiment were ignored due to the stringent statistic parameters applied during quantitative analysis. Furthermore, those hypothetically regulated before, in between, or after the chosen time points could not be detected either. As phosphorylations are highly dynamic, this time course is only able to provide snapshots of the phosphorylation pattern at the investigated moments after HGF stimulation. Incidentally, this is also true for the phosphorylation dynamics monitored for each significantly regulated peptide. How one site is modified off-time points cannot be said. Therefore, the lines in the presented figures (see section 4.2.3) connecting the regulation values in the phosphorylation dynamics of the exemplified peptides are a simplification and rather serve as a better illustration. In order to circumvent this problem, many more time points have to be chosen resulting in a dramatic increase in experimental complexity and sample number. Furthermore, the quantification strategy would need to be redesigned according to the high amount of samples.

Other known Met downstream proteins might not be identified due to the enrichment method. Proteins that function as substrates are more likely to be detected, because phosphorylations on these signal acceptors might be more sustained compared to the highly dynamic regulation of kinases for example. These transducers are among the low abundant proteins and might still be underrepresented in the phosphoproteome due to a lower concentration of their phosphorylation sites. Finally, known signaling components of Met signaling have been detected in a large number of different cell types ranging from cancer tissues to cell lines. It is obvious that every cell type might express or use different sets of proteins involved in Met signaling. That is a problem when comparing experimental data with the literature or databases. For example, GeneGo interactions collected in the database originate from studies performed in different cell lines or even distinct organisms. Thus, in a phosphoproteome approach like this, which was done in one cell line, it cannot be expected that all known interactions can be matched to the experimental data.

In conclusion, only 6 of 80 proteins that exhibited regulated phosphorylation sites after HGF stimulation are currently known components of the Met downstream signaling. Notably, that means vice versa that the majority of proteins differentially modified in response to the stimulus has not been described in this context so far. This fact clearly demonstrates how incomplete the knowledge of the HGF/Met pathway components was prior to this study, although it has been investigated for a long time.

5.3 Characterization of novel pathway components and substrates of HGF/Met signaling

40 of 74 proteins that have not been described before in HGF/Met signaling are likely to have a function in this pathway (marked with ** in Table 8-1 in the appendix), because they were differentially phosphorylated in response to HGF stimulation and are known to interact with established pathway members or they participate in cellular rearrangements known for Met (Figure 5-2). These candidates of Met signaling were additionally compared to the publication of Organ et al., as they performed the only other phosphoproteomics screen on HGF/Met signaling so far (Organ et al. 2011).

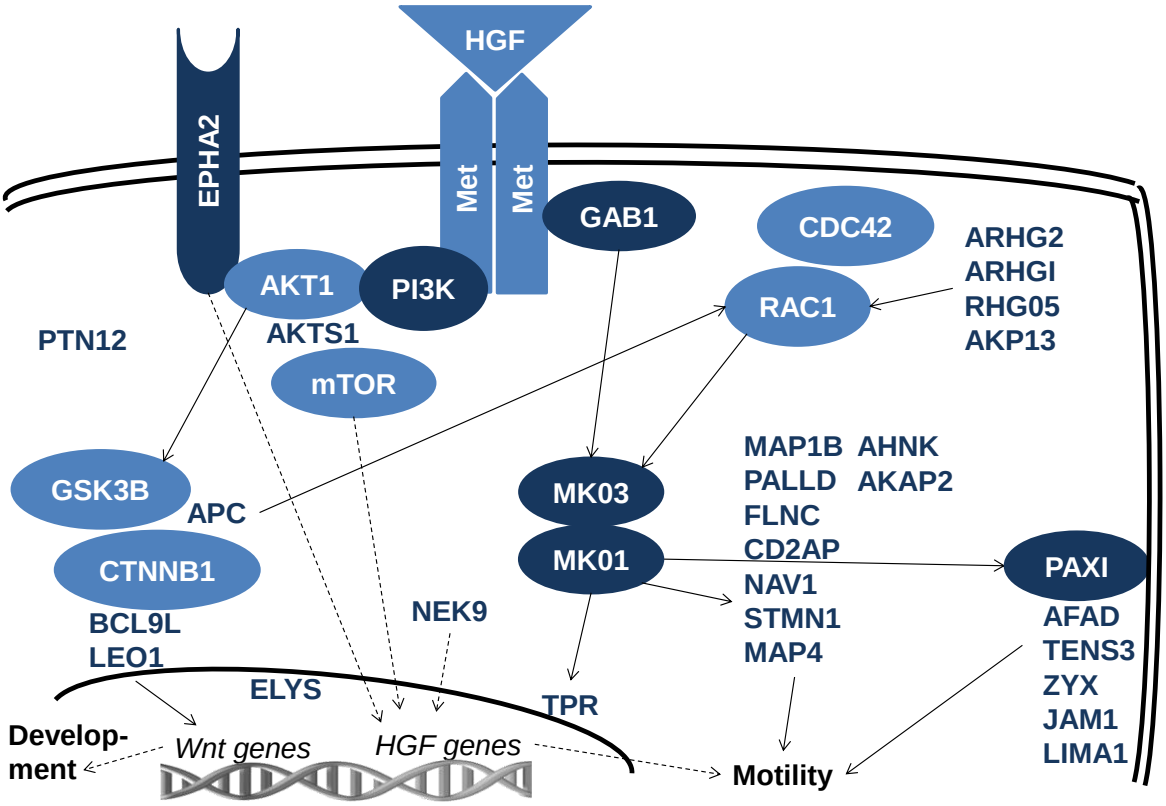

Figure 5-2: Novel proteins in the Met pathway

Dark blue protein names mark the novel HGF/Met signaling substrates identified by phosphoproteomics in this work and which are described in the subsection below. Established proteins of the pathway are illustrated by light blue ovals, with those identified here marked in dark blue. The known components are not completely depicted to improve clarity. Only those exhibiting interactions with novel proteins are mentioned.

5.3.1 Signaling molecules

One of the main signaling components of HGF/Met is the kinase AKT1 that was not regulated here. However, its substrate AKTS1 was detected with the upregulated site pT^{246} that is known to be modified by AKT1. AKTS1 interacts with mTOR in a complex called mTORC1 that triggers protein synthesis (Sancak et al. 2007). As mTOR is a target of Met signaling through the PI3/AKT1 axis (Trusolino, Bertotti, and Comoglio 2010), AKTS1 is likely to be involved in this pathway as well.

Furthermore, another target of AKT1 was gradually phosphorylated in response to HGF. The receptor tyrosine kinase EPHA2 was modified at S^{897}, a site that was previously described by Miao and co-workers. They discovered this phosphorylation and monitored the migration of PC-3M and U373 cells in

response to different growth factors. When the cells were co-stimulated with the EPHA2 ligand Ephrin A1 (EFNA1), migration was abolished as well as the phosphorylation at pS^{897} (Miao et al. 2009). Therefore, EPHA2 might be involved in HGF-induced cell motility. Additionally, three tyrosine-modifications on EPHA2 were identified by Organ and co-workers that were upregulated after 60 min HGF stimulation (Organ et al. 2011). Thus, EPHA2 is an interesting novel candidate in Met signaling. The role of EPHA2 in the HGF/Met pathway was therefore analyzed further in this study and is discussed in detail in the following chapter (see section 5.4).

PI3K and AKT1 also mediate signaling via small GTPases that trigger cell motility. These proteins were not identified by phosphoproteomics, because they are regulated by binding to GTP and GDP and not by phosphorylation sites. However, 7 of their regulators - GEFs and GAPs – were differentially modified in response to HGF. ARHGI and ARHG2 interact with Rac1 (Niu et al. 2003; Ren et al. 1998), which is one of the most prominent proteins in Met signaling and belongs to the Rho family of small GTPases. The regulated site pS^{886} is known to be phosphorylated by PAK1, which recruits 14-3-3 proteins to the microtubules (Zenke et al. 2004). Furthermore, AKP13 acts also as a GEF for Rho family members (Diviani, Soderling, and Scott 2001), while RHG05 functions as GAP for these proteins (Burbelo et al. 1995). They all were identified by a phosphorylation site upregulated after 6 or 20 min HGF.

As the example of GAB1 illustrates (see section 5.2.1), scaffold proteins play a major role in signaling by supporting the formation of protein complexes. The adapter AHNK and the anchor protein AKAP2 are two such scaffolds that may take part in HGF/Met signaling. They are phosphorylated with a maximum after 20 min of HGF stimulation, indicating rather a secondary role in the cellular response than an important function during signal transduction.

Furthermore, the phosphatase PTN12 was phosphorylated on T^{587} after 20 min HGF. As this protein removes phosphorylations on tyrosine kinases, the regulation might be a negative feedback loop of HGF/Met signaling.

5.3.2 Transcription factors and nuclear proteins

After Met activation, the signal is also transmitted into the nucleus where gene expression is modified by activation or inhibition of different transcription factors. The translocation is accomplished by components of the nuclear pore complex (NPC) that shuttles its substrates into the nucleus. TPR and ELYS are nucleoporins that were phosphorylated in response to HGF. ELYS was first proposed as transcription factor in mice and was shown later to be responsible for postmitotic NPC assembly in HeLa and *Xenopus* cells (Franz et al. 2007). TPR has been characterized as MK01 substrate and nuclear shuttle (Vomastek et al. 2008). In this thesis, an uncharacterized phosphorylation site on TPR was upregulated at every time point after HGF stimulation. Therefore, TPR is likely to play an important role in HGF/Met-induced translocation of the signal into the nucleus (Figure 5-3).

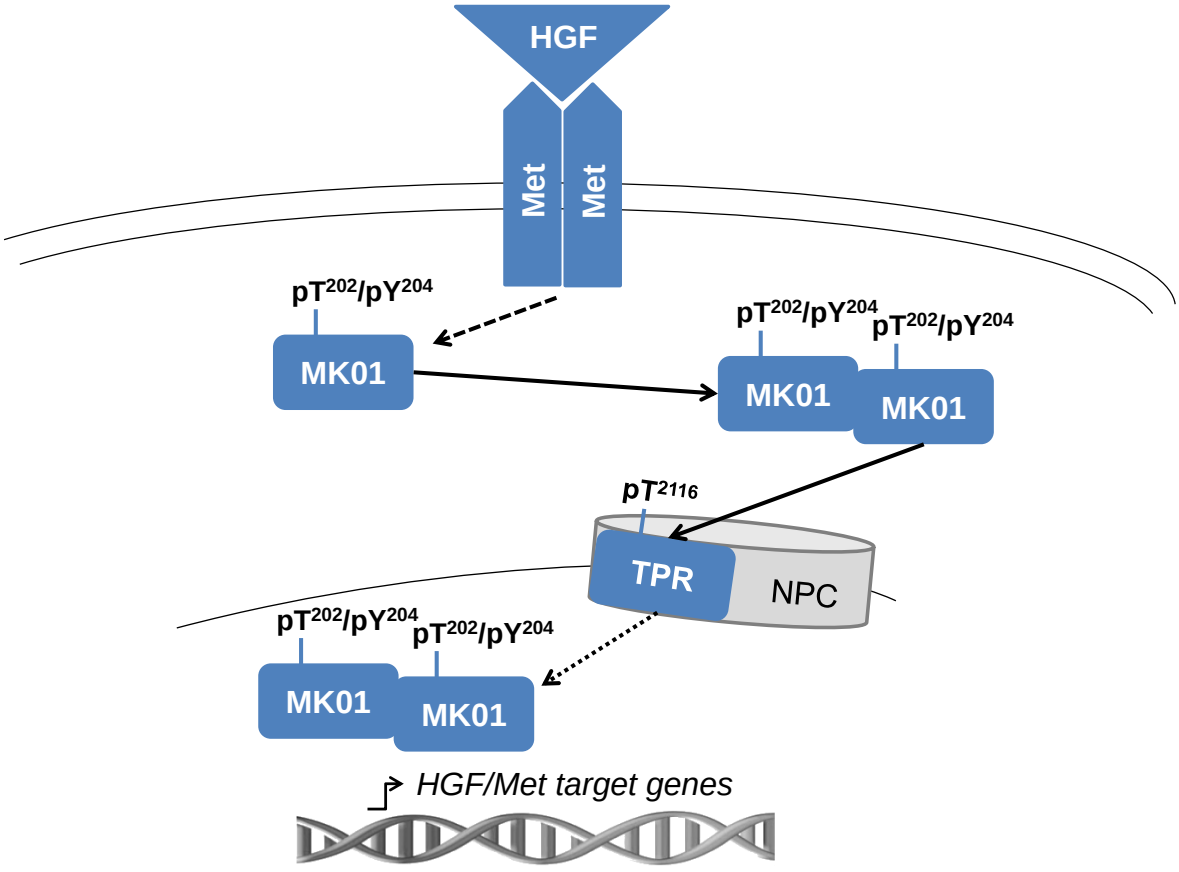

Figure 5-3: TPR is responsible for MK01 translocation into the nucleus

After HGF stimulation, the MAP kinase MK01 is activated by double phosphorylation and dimerizes in the cytosol. MK01 phosphorylates the protein TPR of the nuclear pore complex (NPC), which induces MK01's translocation into the nucleus.

5.3.3 Crosstalk with Wnt signaling

In response to HGF stimulation, three proteins involved in Wnt signaling were differentially phosphorylated. Wnt signaling is induced by receptors of the Frizzled (FDC) family and is characterized by inhibition of GSK3β and APC resulting in elevated levels of β-catenin (CTNNB1). CTNNB1 again is induced to interact with BCL9L that together promote the transcription of Wnt target genes through a complex involving LEO1. Subsequent gene expression promotes the production of proteins involved in development and cancer invasion (Akiyama 2000; Chaudhary et al. 2007; Brembeck et al. 2004). As GSK3β and APC are also described in Met signaling (Papkoff and Aikawa 1998; Sagara et al. 2009), a crosstalk between both pathways is obvious and was previously proposed (Boccaccio and Comoglio 2006; Papkoff and Aikawa 1998; Huang et al. 2012). A crosstalk is further supported by the observed phosphorylations on the three proteins APC, BCL9L and LEO1 after HGF stimulation in this phosphoproteome analysis.

5.3.4 Cell adhesion and motility apparatus

Among other processes, HGF/Met controls cellular movement of DU145 cells that is accompanied by regulation of the cytoskeleton and cell adhesion (Humphrey et al. 1995; Organ and Tsao 2011). During HGF stimulation of DU145 cells, linkage protein E-cadherin is lost from cell-cell junctions, which allows migration (Wells et al. 2005). Furthermore, E-cadherin interacts with nectin that has been shown to regulate E-cadherin endocytosis. This process involves afadin (AFAD), another adherence junction protein that links nectin to the actin cytoskeleton (Hoshino et al. 2005). In this study, AFAD was phosphorylated on serine in response to HGF, indicating a role for AFAD in Met-mediated dissociation of cell-cell adhesion. TENS3, a focal adhesion protein, was phosphorylated on serine after 6 and 20 min HGF. Although it is not known in Met signaling, it has been implicated in the EGF response in MDA-MB-468 epithelial cells. After stimulation, it also gets phosphorylated and occurs in a complex with FAK1 and BCAR1, which are both implicated in cell migration (Cui, Liao, and Lo 2004). As Met and EGFR utilize comparable downstream cascades and TENS3 is modified by both pathways, it is likely that the protein is part of Met signaling and might regulate migration there. This is also supported by the finding of Organ and co-workers, who identified this

site as upregulated after 10 and 60 min HGF as well (Organ et al. 2011). Other junction proteins like LIMA1, ZYX, and JAM1 were also differentially modified after growth factor stimulation and might therefore have a function in the downregulation of cell adhesion. The regulated site pS284 of JAM1 is phosphorylated by PKCA and causes clustering of the protein to cell-cell adhesions (Ozaki et al. 2000). Interestingly, Organ also identified a tyrosine phosphorylation on JAM1 that is only 4 amino acids apart from the serine modification that was regulated in this study. Once the cellular junctions have been abolished, the cells are able to move freely. The movement is mediated by stretching and contraction of the cytoskeleton. Several proteins unknown in HGF/Met signaling but regulating the cell's motility apparatus were identified by phosphoproteomics in this work. One example is MAP1B that binds to microtubules and enhances their dynamic stability. Further evidence for the protein being part of the Met response is its phosphorylation by GSK3β (Goold, Owen, and Gordon-Weeks 1999) and its involvement in the migration of neurons (González-Billault et al. 2005). Palladin (PALLD) is an actin-associated protein that binds to a large set of other actin-interacting proteins like VASP and PROF1 (Dixon et al. 2008). Furthermore, it has been described as direct target of the kinase AKT1 and contributes to motility of breast cancer cell lines (Chin and Toker 2010). Here, it was identified by its upregulated serine phosphorylation after 20 min HGF stimulation and might therefore play a role as regulator of Met-induced motility. Other potentially novel cytoskeleton-associated proteins acting in Met signaling are FLNC, CD2AP, NAV1, STMN1, and MAP4.

5.3.5 Crosstalk with the ubiquitin system

The phosphorylation and ubiquitination systems act hand in hand as is known for example in Met signaling during receptor degradation and recycling. While activating (E1), conjugating (E2), and ligating enzymes (E3) are required for ubiquitination, the reverse process is mediated by deubiquinating enzymes (DUBs). Just like for phosphorylation, ubiquitination is tightly controlled by balancing these enzymatic activities. In addition to determining a protein's fate, this modification also contributes to signaling pathways by regulating protein activity, interaction, and localization. Ubiquitin ligases are often activated by phosphorylation (Grabbe, Husnjak, and Dikic 2011). In contrast, modification of

DUBs is known for some examples, but mostly the effects are unknown (Reyes-Turcu, Ventii, and Wilkinson 2009).

Here, three members of the ubiquitin apparatus were differentially phosphorylated after prolonged HGF stimulation (20 min). The E2 enzyme UBE2O is an exceptionally large conjugase that transfers ubiquitin to its substrates without any involvement of an E3 ligase (Van Wijk and Timmers 2010). The detected phosphorylation site on pS^{839} was also identified after 15 min EGF stimulation (Cantin et al. 2008), but is not functionally described yet. Nevertheless, it seems to be a conserved modification site in GFR signaling. The second enzyme of the ubiquitin system identified here is the E3 ubiquitin ligase NED4L. The regulated site pS^{448} is known to inhibit interaction with ENaC, a channel protein, which stabilizes and promotes Na^{2+} transport (Snyder et al. 2004). No direct link between HGF/Met signaling and sodium channels is published, but the MAPK cascade is supposed to downregulate the channel's activity. Furthermore, stimulation of cystic fibrosis airway cells with HGF resulted in a reduction of the Na^{2+} transport (B. Q. Shen, Widdicomb, and Mrsny 1999). The third protein differentially phosphorylated in response to HGF is the DUB VCIP1. In a RNAi approach targeting several DUBs, it was identified as 1 of 12 members that affect HGF-mediated scattering of A549 cells (Buus et al. 2009) and might therefore be a crucial component in Met-induced motility.

In conclusion, the majority of proteins that were identified here as differentially phosphorylated in response to HGF were not known to take part in Met signaling before. However, in accordance with their described function, they are likely to play a role as signal transducers or effectors. Comparison with the phosphotyrosine approach of Organ revealed only one shared phosphorylation site among the novel HGF/Met candidates (Organ et al. 2011). Thus, their study should not be regarded as competitive, but rather as complementary, because they found more than 150 new tyrosine phosphorylations.

There were 10 uncharacterized proteins that exhibited differential phosphorylation sites after HGF stimulation. Due to a lack of information about their function, structure and interactions, they could not be integrated into any cascade downstream of Met. However, this fact even increases the possibility for these

proteins to be novel components of HGF/Met signaling, because they might not have been discovered so far.

More than half of the proteins affected by HGF could not be integrated into canonical pathways. One reason is that many proteins are not well-characterized concerning their function or involvement in pathways. Additionally, pathway maps provided by specialized databases like GeneGo are highly conservative to improve clarity. While this is an advantage for getting a first overview of a certain pathway, an illustration is not able to reflect the actual complexity of signaling networks.

5.3.6 Benefits and limitations of time-resolved studies

In this study, phosphorylations were analyzed during the first 20 min after HGF stimulation. Because this modification is highly transient and is adjusted within seconds, monitoring several time points improves the number of identified phosphopeptides. Only coverage of many time points during signaling will provide a comprehensive overview of involved proteins. However, the sample number is of course limited by practicability of the experiment and the type of labeling utilized. Importantly, time-resolved analyses do not only increase the number of potential signal components, but also provide quantitative information about changes of the phosphopeptides from one time point to another. This phosphorylation dynamics was monitored in the HGF study after 3, 6, and 20 min of stimulation. For all regulated peptides, the change of regulation factors over time was determined. Clustering according to these dynamics uncovered peptides regulated in the same manner and allowed drawing conclusions on effected regulatory networks (see previous sections 5.2 and 5.3). However, the heatmaps illustrating regulated phosphopeptides already indicated a problem with this transient modification. The reproducibility of the values of regulation factors within the three replicates was sufficient to draw conclusions, but it differed from one experiment to another. This might be affected by slightly different stimulation times and by experimental variation during processing of the samples. However, it might also be affected by slightly different stimulation times. Phosphorylation reactions are considered as fast and thus, seconds might influence the sum of identified phosphopeptides at a certain time point. Furthermore, variation between biological samples concerning the speed or magnitude of signal processing may also cause this discrepancy.

These effects obviously result in three different phosphorylation patterns for the triplicate that are shifted, for example, by some seconds on the time-scale.

Supported by Prof. Frank Klawonn, a promising strategy was set up to calculate a temporal correction factor for the triplicate (Klawonn et al. 2012). So far, the attempt was only computed for the proof-of-concept data. Nevertheless, this strategy is a new chance to reduce intra-experimental variations. Biological variation and individual cell responsiveness may also cause the observed variation and are therefore difficult to factor in. As the strategy was not applied to the whole dataset, it had no effect on the quantitative analyses.

5.4 The EPHA2 receptor regulates HGF/Met gene expression

Met utilizes a large network of downstream proteins to process the HGF signal and produce the required cellular effects. Notably, the network seems to include another membrane-bound receptor that usually exhibits an own signaling when triggered by its extracellular ligands. The EPHA2 receptor can be activated by membrane-bound Ephrin A family ligands and is involved in axon guidance during the development of the nervous system (Mori et al. 1995). Unlike other EPH receptors, it is additionally found in adult epithelial cells, where it regulates cell growth, migration and invasion (Lindberg and Hunter 1990). Once stimulated by its main ligand Ephrin A1, it binds to SHP-2, SHC, SLAP, GRB2, and PI3K (Kinch and Carles-Kinch 2003). Interestingly, the MAPK cascade was either published as up- or downregulated, depending on the receptor’s downstream interaction partners (Lin et al. 2010). Target proteins of EPHA2 signaling are integrin and CLD4, which are involved in cell adhesion, indicating a role for EPHA2 in regulating this process (Miao and Wang 2012). Additionally, EPHA2 is downregulated by degradation after Ephrin A1 stimulation. As Ephrin A1 is localized in the membrane of surrounding cells, an increased cell density results in lower amount of EPHA2 on the surface (Walker-Daniels, Riese, and Kinch 2002). On the other hand, there are hints that the EPHA2 receptor can be activated in a ligand-independent manner, because EPHA2 was shown to also promote cancer progression in the absence of Ephrin A1 (Wykosky and Debinski 2008).

Interestingly, EPHA2 was phosphorylated at S^{897} after 20 min HGF stimulation in this study, which indicates a downstream role of EPHA2 in Met signaling. As this phosphorylation site was already published to affect HGF-induced motility (Miao et al. 2009), the role of EPHA2 downstream of Met became especially interesting. In order to examine the effect of EPHA2 knockdown on the cellular output of HGF/Met signaling, gene expression analyzes were performed.

Gene arrays concerning the Met pathway have been completed before. *In vivo* approaches include data from Siltanen and co-workers who examined the effect of human HGF overexpression in rat myoblasts and Factor et al. who compared the transcriptome of murine liver cells with and without Met knockout (Siltanen et al. 2011; Factor et al. 2010). Additionally, primary hepatocytes were stimulated for 30 min, as wells as 2, 12, and 24 h with HGF and wildtype cells were compared to Met knockout cells (Kaposi-Novak et al. 2006). Two studies performed in the canine cell line MDCK illustrated the HGF response after 3 and 24 h and influenced by the MAPK inhibitors UO126, PD09859 (Hellman et al. 2008; Balkovetz et al. 2004). However, only two arrays were performed so far in human cell lines. The first one by Olivero and co-workers stimulated ovarian cancer cells (SK-OV-3) for 6 h with HGF. Nevertheless, their results cannot be compared here, because the scientists co-treated the cells with cisplatin, a drug usually applied in chemotherapy.

Van Leenders and co-workers recently published an array analysis using prostate cancer DU145 cells. They stimulated the cells for 2, 8, and 24 h with HGF and analyzed the resulting gene expression compared to the non-stimulated control (Van Leenders et al. 2011). Although van Leenders et al. used the same cell line their analysis concentrated on the 24 h time point, while the study performed in this thesis focused on earlier gene expression. After 1 h of stimulation, the first wave of target genes is expressed, while after 4 h first actors of the cellular response are induced.

5.4.1 Early target genes of HGF/Met signaling in DU145 cells

In the wildtype, microarray results revealed 656 genes as regulated after 1 h and 1,072 genes after 4 h HGF consistent in the triplicate. Among them, proof-of-concept data were found that verified the activation of the HGF/Met pathway.

Importantly, of 31 known target genes for HGF and Met, 11 were regulated in the dataset (see Table 8-5 in the appendix). For example, after 1 h genes of the transcription factors FOSB and JUN (Deleu et al. 1999) were upregulated. After 4 h, genes coding for the integrin ITA2 (Liang and Chen 2001; van Leenders et al. 2011) and the transcription factor SOX9 (Van Leenders et al. 2011) were affected. The latter two were also identified by van Leenders and are described in the publication as two stem-cell markers important during prostate development.

However, about 99% of the regulated genes are not described as transcriptionally regulated by HGF/Met, which is consistent with data from other publications. For example, Kaposi-Novak identified 730 regulated genes after 0.5, 2, 12, and 24 h HGF stimulation, but they name only 5 genes as known HGF/Met targets, and Balkovetz *et al.* found 8 (Kaposi-Novak et al. 2006; Balkovetz et al. 2004). These data clearly illustrate the great lack of knowledge of the HGF/Met pathway and especially its target genes.

5.4.2 EPHA2-mediated control of HGF/Met target genes

In contrast to the above mentioned gene expression arrays addressing the HGF response, this work was the first focusing on the effect of the receptor EPHA2 on HGF/Met signaling. With this aim, it was also the first study characterizing a potential HGF/Met pathway component by RNAi in combination with expression analyses.

In total, 70 genes were affected by EPHA2 knockdown during HGF stimulation (see Figure 4-23). The majority of them were upregulated in the EPHA2 knockdown (91% after 1 h, 74% after 4 h HGF). This means vice versa that EPHA2 *in vivo* predominantly negatively regulates the HGF/Met response.

In order to clarify the role of EPHA2 in the HGF/Met response, those genes top-regulated in the wildtype by HGF and those affected by the EPHA2 knockdown were matched. After 1 h of HGF stimulation, 7 genes fulfilled these criteria (see Figure 4-24 A). All of them were higher upregulated in the EPHA2 knockdown compared to the wildtype. Furthermore, all genes were transcription factors and so-called immediate-early genes (IEGs). These genes are expressed early after growth factor stimulation or other outside signals like stress or injury. The IEGs

were examined in detail during neuronal development, where they regulate key targets for dramatic phenotypic changes of the cell (Dijkmans et al. 2009). In general, IEGs connect late signaling events to gene expression. Therefore, most of the IEGs are coding for transcription factors, controlling the expression of different sets of target genes. However, cytoplasmic proteins like the phosphatase DUS1 and secreted effectors like cytokines belong to that group (Pérez-Cadahía, Drobic, and Davie 2011).

The best-characterized IEG is FOS, which was also identified in this study as regulated by EPHA2 knockdown and is a known HGF/Met target (Boccaccio et al. 1994). Molecular changes of the *fos* promotor region in response to post-translational modifications like SUMOylation or phosphorylation cause the activation of proteins responsible for *fos* gene expression. Already 30 to 60 min later, the expression is stopped by several feedback mechanisms. This process ensures a transient but strong FOS activity (O'Donnell, Odrowaz, and Sharrocks 2012). Interestingly, Irie and co-workers described the EPHA2 receptor as a target of FOS in osteoblasts (Irie et al. 2009). Thus, HGF/Met activates FOS expression and this subsequently induces the production of EPHA2. Moreover, this mechanism is controlled by EPHA2 itself by negatively affecting FOS expression. In this manner, the concentration of EPHA2 in the cell might be regulated by its current abundance of the protein.

Additionally, the *egr1-4* genes of the HGF/Met response were strongly affected by the EPHA2 knockdown. With a more than 13-fold upregulation in the EPHA2 knockdown compared to the wildtype after 1 h HGF stimulation, EGR2 was the most affected one. In a recent publication by Zaman, *egr2* was discovered to be regulated by the MK01/MK03 pathway (Zaman et al. 2012). However, no direct link between HGF/Met and EGR2 expression is described so far. The same is true for *egr3* and *egr4*. Interestingly, EGR1, which was also affected by EPHA2 knockdown, was found before by Ozen and co-workers to be regulated by HGF in hepatocellular carcinoma (HCC). In their publication, the authors describe the effect of HGF stimulation on the expression of EGR1 with an *egr1* mRNA peak after 1 h. Furthermore, they link HGF/Met-induced EGR1 expression to matrix-metalloproteases (MMPs) activation, followed by induced cancer invasion in HCC (Ozen et al. 2012). As Met controls, among others, invasion and migration, the

regulation of EGR1 in this study might also affect motility of DU145 cells through EPHA2. No effect on the expression of MMPs was detected here. However, Ozen and co-workers characterized the effect of MMPs after 24 h; thus, the chosen time points 1 and 4 h were probably too early to detect the expression of these proteins.

Taken together, HGF induces the expression of known immediate-early genes after 1 h of stimulation, which is negatively controlled by EPHA2 in the wildtype. The genes activated by HGF and subsequent expression of this group influence motility and development, but also a large number of other cellular effects like survival or proliferation (Ozen et al. 2012). Therefore, it is difficult to conclude, which Met-induced phenotypes might be controlled by EPHA2 at this time point.

Similar to the 1 h time point, 7 genes were regulated EPHA2-dependently after 4 h HGF stimulation (see Figure 4-24 B). However, in this case, 3 were up- and 4 were downregulated between EPHA2 knockdown and wildtype in response to HGF. One of them was *egr4* that was already found after 1 h, where it was more strongly induced. The lower regulation of EGR4 and the absence of other IEGs after 4 h confirm the transient expression of this group of proteins. Furthermore, three genes coding for the proteins CL067, CE058, and CN105 were not described functionally in the literature. Therefore, they could not be integrated into any process. However, the corresponding genes *c12orf67, c5orf58*, and *c14orf105* were regulated nearly 3-fold between EPHA2 knockdown and wildtype. Thus, it is obvious that they play a role in the HGF/Met response, because they are among the top-regulated genes by HGF in the wildtype. Interestingly, they are controlled by EPHA2, which makes them exciting candidates for further studies of EPHA2-dependent Met signaling.

Furthermore, the potassium channel gene *kcnk12* is highly upregulated in the wildtype, while it is only slightly affected in the EPHA2 knockdown. Thus, EPHA2 usually promotes the expression of the gene in wildtype cells. However, as this protein has not been implicated in growth factor-induced processes so far, it is very difficult to speculate about its role in the HGF/Met response. Usually, potassium channels play a role in neuronal conduction of stimuli where they create

action potentials by translocating K^+ ions. However, the protein coded by *kcnk12* has been shown to be expressed in a wide range of cell types (Patel and Lazdunski 2004). Besides its pore-forming ability in neuronal cells, it might act as plasma membrane-bound component of cell adhesion in epithelial cells, for example. Moreover, the gene corresponding to the neuropeptide receptor NPY5R was downregulated in the wildtype, but upregulated in the EPHA2 knockdown in response to HGF. Therefore, in the wildtype, EPHA2 usually significantly limits the expression of NPY5R. The protein was shown to activate the MAP kinases and through them, to induce cell growth in BT-549 cells and motility in MDA MB-231 breast cancer cells (Sheriff et al. 2010). Therefore, the regulation of EPHA2 on NPY5R likely is involved in a negative feedback loop downregulating the MAPK-effect after 4 h HGF. Furthermore, the gene corresponding to SPSB4 was more upregulated in wildtype than in the EPHA2 knockdown. It might directly interact with the Met receptor, because the protein was co-immunoprecipitated with Met by Wang et al. (Wang et al. 2005). However, the effect of the interaction is unknown. 4 h after HGF stimulation, this ubiquitin E3 ligase (Kamura et al. 2004) might be activated in an EPHA2-dependent manner and mediate ubiquitin-associated degradation of Met, which is still membrane-localized. The dynamics of Met incorporation and degradation after HGF stimulation was investigated by Jeffers and co-workers in several cell lines. They showed that degradation of Met starts after 1 h, but with a maximum after 8 h (Jeffers et al. 1997). Therefore, it might still be early enough for the cell to express SPSB4 after 4 h HGF in order to stop Met signaling by receptor endocytosis and degradation (Figure 5-4).

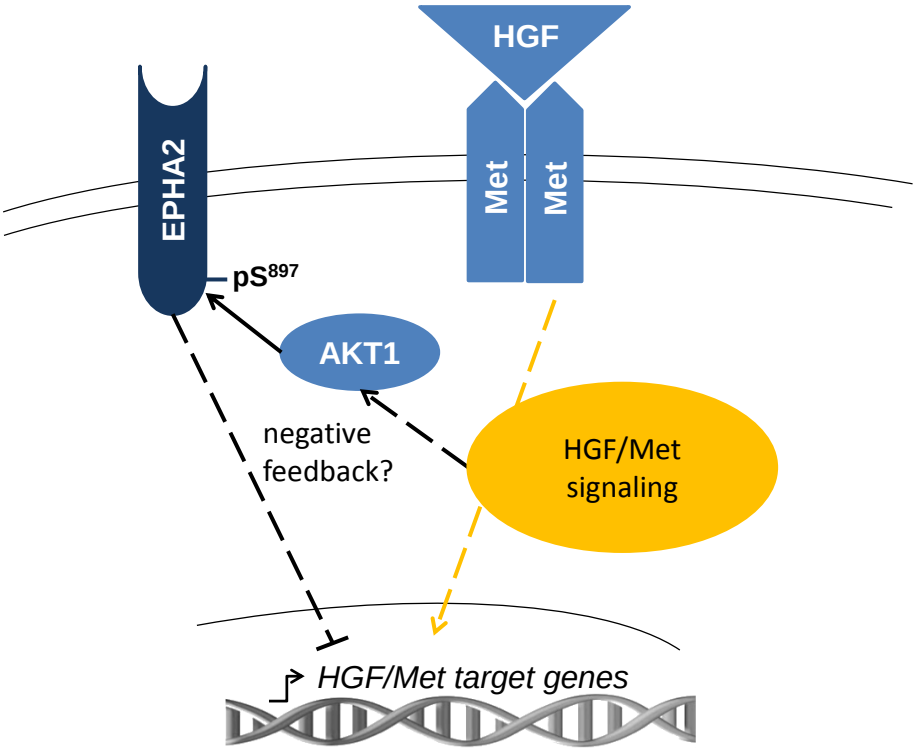

Figure 5-4: EPHA2 controls HGF/Met-induced gene expression

20 min after HGF stimulation, the site pS^{897} of the receptor EPHA2 is upregulated by the known Met pathway member AKT1. Knockdown of EPHA2 revealed an inhibitory role of EPHA2 on the expression of HGF/Met target genes. Therefore, it is likely that EPHA2 is involved in a negative feedback loop controlling the HGF-induced genetic program.

Taken together, many cellular processes induced by HGF/Met are negatively controlled by EPHA2. This is confirmed by the expression of immediate-early genes shortly after HGF stimulation, but also by the regulation of effectors of Met receptor degradation or phenotypic changes after 4 h. In agreement with Miao et al., there is definitely a regulatory role of EPHA2 in growth factor signaling (Miao et al. 2009). However, they described the negative effect on cell migration and invasion only during co-stimulation with the EPHA2 ligand Ephrin A1 and not in the wildtype, as identified here. Nevertheless, the inhibitory effect of EPHA2 on migration during Ephrin A1-HGF co-stimulation could not be reproduced in this thesis either. The choice of different cell lines might also influence the results. While the authors used U373 cells for their migratory experiments, motile cell lines DU145, A549, HepG2 and Caco-2 were utilized in this work to reproduce the results, but none of them exhibited the effect described by Miao et al..

5.4.3 EPHA2-Met receptor crosstalk

Results of EPHA2 knockdown on the transcriptional level in this study convincingly indicate a regulatory role of the EPHA2 receptor in the HGF/Met response. From the point of signal integration, the role of receptor crosstalk is evident. As a cell *in vivo* is usually exposed to a variety of different signals at once, its response has to be processed and balanced in order to create the appropriate cellular reaction. Furthermore, many different signals may be necessary to produce one particular phenotypic change.

EPHA2 is not the only receptor or transmembrane protein that interferes with Met signaling. Other members of the tyrosine kinase receptor family like EGFR, RON and RET can also affect a trans-phosphorylation of Met and vice versa. Furthermore, GPCRs associated with their ligands may cause phosphorylation of Met, as well as CD44 and the integrins α6β1 and α6β4. Likewise, class B plexins stimulate Met activation. However, except for RET, which activates Met through SRC, all described cross-talking proteins directly interact with the Met receptor (Lai, Abella, and Park 2009). In the publication of Miao et al., the authors describe AKT1 as the EPHA2-phosphorylating kinase of the site pS^{897} (Miao et al. 2009). Since this phosphorylation site was identified by phosphoproteomics in this work as upregulated only after 20 min of HGF stimulation, a direct interaction of EPHA2 and Met is unlikely. Additionally, no direct interaction, for example by co-immunoprecipitation has been published so far. Therefore, EPHA2 and RET obviously play slightly different roles in Met signaling as they interfere with the downstream signaling and not with the receptor itself.

How cells can realize signal integration was illustrated by preliminary experiments after this work. As previously described, the two siRNAs utilized created a differently efficient EPHA2 knockdown. While siRNA7 was very effective with a reduction of EPHA2 of 70%, the siRNA5 caused a reduction of only 40% in the protein level of EPHA2 compared to the wildtype. Interestingly, scatter assays performed with these samples after 24 h HGF stimulation indicated that limited loss of EPHA2 leads to increased motility, compared with the wildtype. In contrast, efficient EPHA2 knockdown seemed to stimulate apoptosis. This hypothesis is supported by the gene expression discrepancies between siRNA5 and 7. Efficient knockdown of EPHA2 by siRNA7 significantly increased the expression of three

genes associated with apoptosis. Their corresponding proteins TNF10, CASP1 and BMF have been shown to induce programmed cell death (Wiley et al. 1995; Alnemri, Fernandes-Alnemri, and Litwack 1995; Puthalakath et al. 2001). Thus, the amount of EPHA2 seems to have crucial impact on the regulated genes, as well as the phenotypic result. In conclusion, EPHA2 might be a brilliant example for signal integration and this should be investigated in further studies.

Regarding the effect of EPHA2 in Met signaling, EPHA2 has the capacity to limit the cellular response. This mechanism makes especially sense when a cell is deregulated, for example in the context of cancer. Indeed, HGF/Met signaling is upregulated in many types of cancer and supports survival, proliferation, invasion and metastasis (Trusolino, Bertotti, and Comoglio 2010; Birchmeier et al. 2003). In contrast, the role for EPHA2 in cancer is still unclear. Although it is found upregulated in many cancers, it may not necessarily trigger the disease. Remarkably, EPHA2 is often regarded even as cancer inhibitor (Pasquale 2010). Thus, in the context of this work, EPHA2 might tightly control Met signaling as a checkpoint agent that limits the impact of deregulated Met activity. The serum-free conditioning combined with the constant stimulation with HGF might create such a scenario for the cells.

5.5 NEK9: never in mitosis, but in migration?

The kinase NEK9 was first described in the mitotic context. Like other members of the Never In Mitosis A-related (NIMA-like) family, it was activated during mitosis. Furthermore, it was shown to bind to the highly homologous protein NEK6 and to the GTPase Ran. Since overexpression of this protein caused cell cycle arrest, a function of NEK9 as mitotic checkpoint was suggested (Roig et al. 2002). However, Reinl and co-workers identified a novel phosphorylation site of NEK9 on pT^{333} during stimulation of HeLa S3 cells with the bacterial surface protein InlB of *L. monocytogenes*. This suggested a role for NEK9 as effector during bacterial invasion, in addition to its mitotic function (Reinl et al. 2009). Because the phosphorylation site was further confirmed in this study during HGF stimulation of DU145 cells, the role of NEK9 in Met signaling was characterized.

Surprisingly, knockdown of NEK9 did not affect the proliferation rate. However, NEK9 knockdown and stimulation with HGF for 14-20 h resulted in a dramatic phenotypic change of HeLa S3 cells. While this cell line is usually non-motile and responds to HGF with proliferation, the NEK9 knockdown significantly increased the motility of HeLa cells in response to HGF. Likewise, cell adhesion was reduced and typical HeLa clusters were resolved, while cells moved away from each other. The subsequently performed microarray analysis provided evidence for the involvment of NEK9 in HGF/Met-induced gene expression causing the discovered phenotype (Figure 5-5).

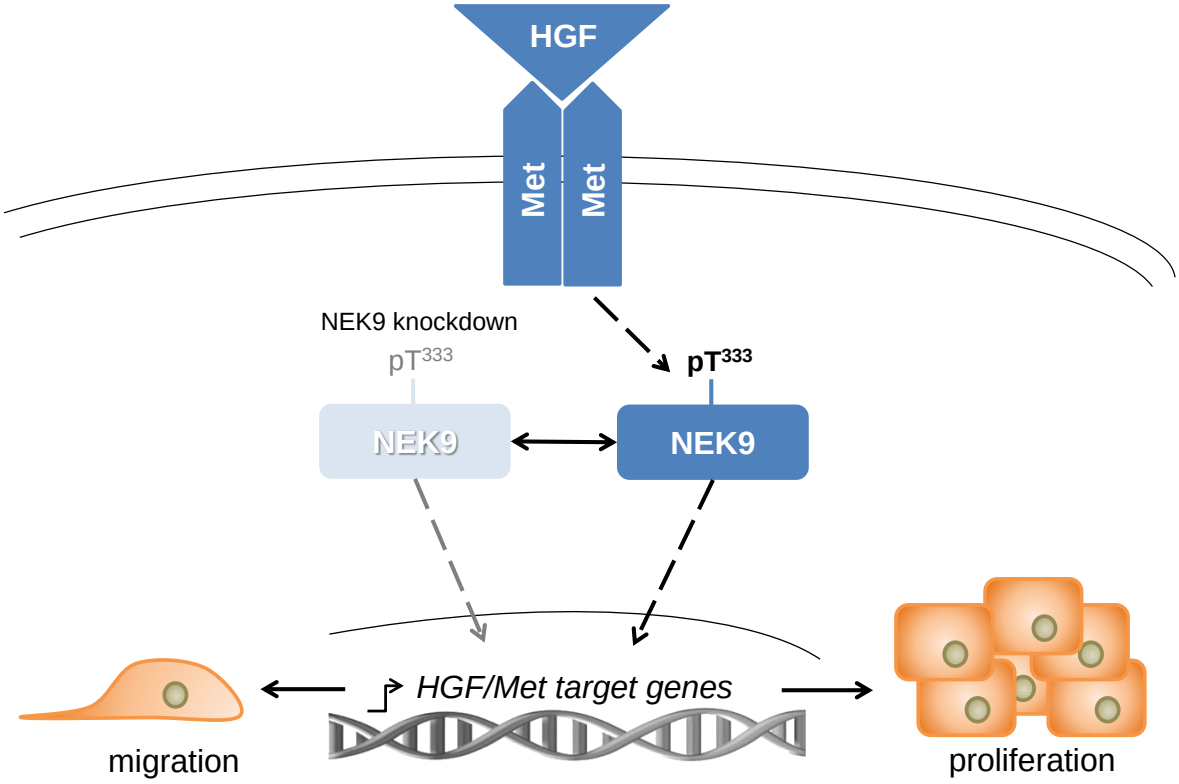

Figure 5-5: NEK9 regulates HGF/Met-induced motility

The site pT^{333} of the kinase NEK9 was upregulated in response to HGF stimulation, suggesting a role for NEK9 in Met signaling. NEK9 knockdown cells did not proliferate, but significantly increased the expression of motility-associated proteins and showed a scatter phenotype when stimulated by HGF. Thus, NEK9 seems to be a switch between proliferation and motility.

Remarkably, migratory pathways affected by NEK9 knockdown during HGF stimulation can be assigned to epithelial-mesenchymal transition (EMT). This process is characterized by an increase in motility of usually stationary, tissue-bound cells and is especially important during embryogenesis and wound healing.

Notably, cancer cells exploit EMT to propagate from their area of origin to the whole body to create metastases (Figure 5-6). The transition is regulated by several signaling pathways that induce the activity of developmental transcriptions factors. These in turn induce the expression of proteins that trigger the loss of adherence junctions, the degradation of the extracellular matrix, the motility-associated cytoskeleton, and the resistance to apoptosis.

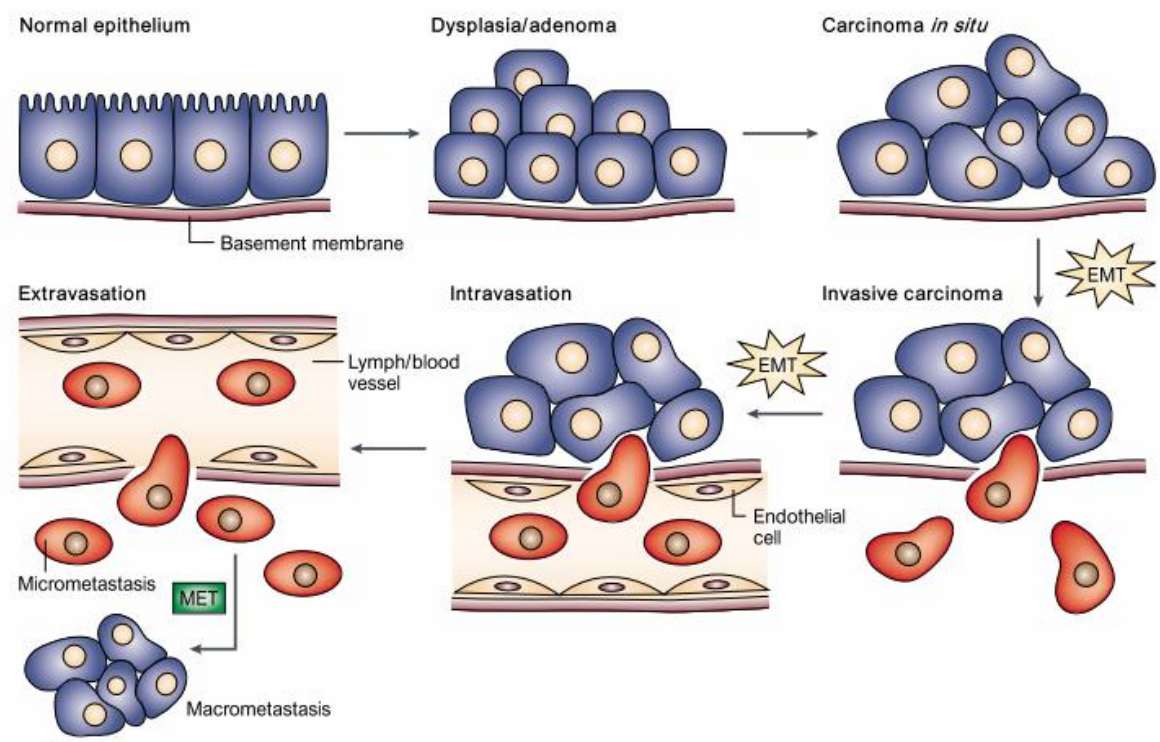

Figure 5-6: Epithelial-mesenchymal transition during cancer invasion

Carcinoma cell can undergo EMT, resulting in cells becoming motile are spreading through the whole body and invade other tissues. Eventually, mesenchymal-epithelial transition (MET) takes place, which allows cells to become adherent again and grow as a metastasis. Figure taken from (Thiery 2002).

For example, upregulated extracellular protein PAI1 was shown by Freytag and co-workers to trigger TGFβ 1-EGR-induced EMT, monitored by cell invasion into a three-dimensional matrix (Freytag et al. 2010). Experiments performed by Grotegut et al. investigated the upstream initiation of SNAI1, one major activator of EMT, after HGF stimulation. Dominant negative expression of the transcription factor EGR1 inhibited SNAI1 expression in HepG2 cells. Furthermore, expression of *egr1* and *snai1* was dependent on the stimulation of the MAPK cascade (Grotegut et al. 2006). Therefore, EGR1, in addition to being regulated in the

EPHA2 knockdown was also influenced by NEK9 knockdown in this work, was revealed as important regulator of HGF/Met-mediated EMT.

All NEK9-regulated genes involved in the processes necessary for cell migration also fit well into the EMT context, where non-motile tissue cells decrease their contacts and start to move. These processes include the abrogation of cell-cell contacts, the dissolving of the extracellular matrix around the cells, as well as the upregulation of components necessary for migration. The latter are cytoskeleton-associated proteins and those activating the rearrangements of the cytoskeleton. Additionally, there is evidence that cells are not able to move and divide in parallel (Makagiansar et al. 2007). Accordingly, genes coding for mitotic proteins should be downregulated in the NEK9 knockdown. Indeed, the results of the gene expression analysis depending on NEK9 and HGF confirmed this assumption.

FLRT3, which was described by Ogata et al. as a factor abolishing cell adhesion, was nearly 8-fold upregulated in response to HGF and NEK9. Loss-of-function experiments revealed that FLRT3 causes dynamin-mediated endocytosis of cadherin in frog embryos. Thus, the lack of cadherin on the cell surface led to increased migration of embryonic cells (Ogata et al. 2007). The two matrix metallopeptidases MMP1 and MMP3 were among the top 5 upregulated genes. As their names indicate, those proteins degrade the extracellular matrix and provide the room for migration of the cells. Interestingly, both proteins are known targets of HGF/Met during EMT. Jinnin and co-workers demonstrated that MMP1 is regulated via the MK01/MK03 pathway in human fibroblasts (Jinnin et al. 2005). Very recently, Lee and co-workers proved the HGF-induced expression of MMP3 by RT-PCR, but did not characterize the upstream regulatory pathways (Lee, Park, and Rah 2011). Upregulation of cytoskeleton modulators SYP2L and PLEK2 and small GTPase RAC2 further supported the EMT-inducing effect of NEK9 knockdown. In contrast, expression of the gene coding for cell adhesion protein CLN1 was downregulated, proving the abrogation of cell-cell contacts. Additionally, an inhibitor of the cyclin-CDK complex, CDNA1, was upregulated in NEK9 knockdown cells, thus verifying the inhibition of mitotic processes during EMT.

Both utilized siRNAs against NEK9 were added in combination and not separately to improve the efficiency of the NEK9 knockdown. Therefore, off-target effects of

one of the siRNAs cannot be ruled out completely for all experiments. Future investigations controlling the monitored motility effect will elucidate whether the presented results are due to NEK9-deficiency or are influenced by side effects. Nevertheless, if those results confirm the remarkable effects of NEK9 knockdown, this would clearly illustrate the importance of Met signaling in regulating crucial phenotypic processes.

Furthermore, the initially apparent discrepancy between the described role of NEK9 during cell cycle progression and the novel migratory effect of this protein makes sense when considering it more thoroughly. First, motility was observed in the NEK9 knockdown, revealing an inhibitory effect of NEK9 on cell motility in the wildtype. Second, cells either proliferate or migrate; a mixture of both opposed processes in parallel is unlikely (Makagiansar et al. 2007). Therefore, NEK9 seems to control both, motility-inhibition and cell cycle progression in HeLa cells. Which function is activated at a given time point, might be regulated through the localization of the protein. As NEK9 was found in the cytoplasm and the nucleus (Tan and Lee 2004), spatial distribution of the protein may decide on the protein's effect. Furthermore, NEK9 is phosphorylated on pT^{210} during mitosis, while it was modified at pT^{333} after HGF stimulation in HeLa cells. These different sites may each activate a separate function.

Taken together, NEK9 was shown to play a central role in regulating HGF/Met-induced cell migration in HeLa cells. Met signaling balances proliferation and motility - as well as survival and apoptosis in healthy cells. In contrast, these processes are deregulated in cancer, where Met signaling is permanently activated and causes EMT that supports metastasis. Although no studies have investigated the expression or activity of NEK9 in cancer compared to healthy cells so far, results of this work indicate that NEK9 has to be considered and investigated as a tumor suppressor.

5.6 InlB-induced signaling of Met

Met-dependent phosphorylation induced by HGF has been characterized in detail in the previous chapters. These studies contributed significantly to the current knowledge of HGF/Met signaling and its targets, Furthermore, they provided a

prerequisite to analyze the impact of a pathogen's interference with host cell signaling. As an example, the invasin InlB of *Listeria monocytogenes* was used to characterize Met-dependent signaling during pathogen infection.

Importantly, 13 of 28 sites were differentially phosphorylated after InlB stimulation, but not affected in the HGF dataset (Figure 5-7 and see Table 4-4). Obviously, these candidates seem to be the basic InlB-dependent Met response. However, different cell lines and stimulation times were utilized in the two studies. Each analysis was performed in the appropriate model cell line, but protein composition or phosphorylation responsiveness of the cells might differ. The lack of phospho-specific antibodies against the identified InlB-specific candidates hampered the verification of phosphoproteomic results in different cell lines. Considering the different time points used for stimulation with InlB and HGF, it has to be kept in mind that these modifications happen fast and are extremely transient. Therefore, the one-minute difference between the InlB and HGF datasets may have an influence on the phosphorylation pattern. In addition, signaling dynamics induced by the two factors might also be different; independent from the same stimulation time. Thus, results could vary for this reason as well. Indeed, two publications illustrate different phosphorylation kinetics of the two ligands. Shen and co-workers, who first identified InlB as agonist for Met, observed that tyrosine phosphorylation of Met in T47D cells was at least 4 times prolonged after HGF stimulation, compared to InlB (Y. Shen et al. 2000). In contrast, InlB caused a more intense Ras-MAPK activation than HGF in Vero cells (Copp et al. 2003). Both effects were shown to be concentration-independent. As HGF and InlB are structurally unrelated and even bind to different sites of the Met receptor, discrepancies in signal intensity and kinetics are very likely anyway.

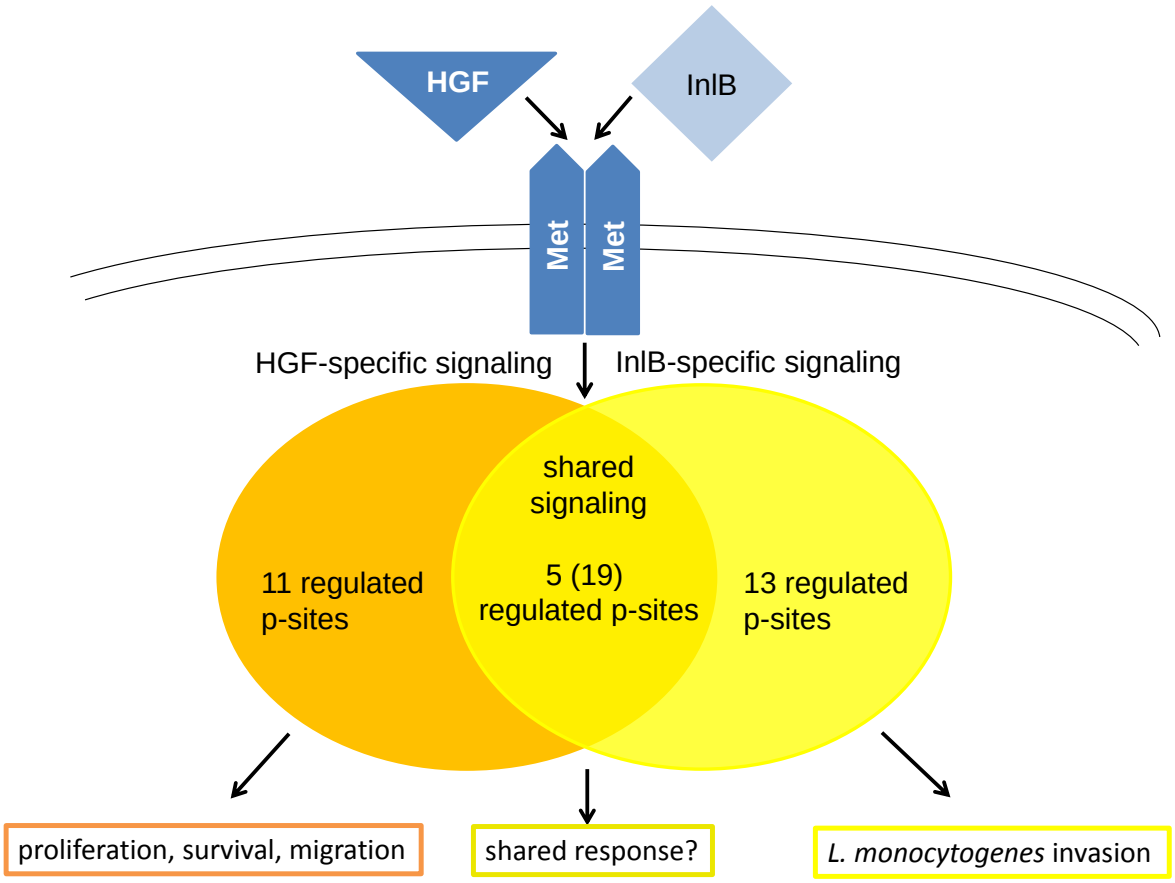

Figure 5-7: Comparison of HGF and InlB signaling

Comparing the regulated phosphorylation sites of the HGF dataset (after 3 and 6 min) with those affected by InlB (after 5 min) revealed specific pathway members for each ligand. These might cause the known cellular responses proliferation, survival and migration in response to HGF, and invasion of the pathogen *L. monocytogenes* in response to InlB. However, 5 sites were significantly regulated similar in both datasets. Further 19 phosphorylation sites were significantly regulated after HGF stimulation and were also affected by InlB, although not significantly. Thus, HGF and InlB share some downstream pathway members and might, in part, induce similar cellular responses.

5.6.1 InlB influences immune-associated proteins in its host

Assuming that the candidates only affected by InlB are validated correctly, the InlB-induced signaling involves proteins regulating cellular immunity. TRAD1 participates in Toll-like receptor (TLR) signaling and Mashima and co-workers showed that the protein is part of a negative feedback loop that downregulates NFκB signaling. When TLRs are activated following pathogen contact, a conserved canonical cascade is induced, which includes the E3 ubiquitin ligase TRAF6. This protein activates kinases that finally trigger the transcription factor NFκB to relocate into the nucleus, where it activates the transcription of pro-

inflammatory genes (Lang and Mansell 2007). Mashima et al. showed that TRAD1 interacts with TRAF6 in HEK-293T cells and that TRAD1, when overexpressed, inhibits NFκB-mediated gene expression. However, they did not describe the mechanism, which regulates TRAD1-TRAF6 interaction (Mashima et al. 2005). Nevertheless, results of this work indicate that TRAD1 activation might be controlled by the phosphorylation on pS^{415} that was downregulated after 5 min of InlB stimulation. This phosphorylation site has been identified before, e.g. during the stimulation of HeLa cells with the cytokine TNFα (Nabetani et al. 2009). However, the function of the site is still unknown. Interestingly, besides TRAD1, Nabetani et al. identified two proteins affected by the cytokine that were also differentially phosphorylated by InlB in this work. The phosphatase IASPP and heat shock protein HSPB1 were regulated by TNFα (Nabetani et al. 2009), and also after 5 min of InlB. Furthermore, like TRAD1, they are part of the TRAF6 network in TLR signaling. While IASPP interacts with the subunit TF65 of NFκB and is able to inhibit its transcriptional activity (Yang et al. 1999), HSPB1 interacts directly with TRAF6 and supports its ubiquitination. When cytokine-stimulated in HeLa cells, HSPB1 is phosphorylated at pS^{78} and pS^{82}, resulting in the dissociation from TRAF6 and subsequently causing decreased TRAF6 downstream signaling (Wu et al. 2009). Notably, the site pS^{82} was also upregulated after InlB stimulation in this work, proposing a downregulation of TRAF6-NFκB signaling in response to contact with the pathogenic protein. The second site was not detected here, but might be essential for the inhibitory effect (Figure 5-8).

The identified phosphorylation sites of TRAD1 and IASPP are not characterized functionally yet. Thus, direction of regulation does not provide information on the proteins' activity. They may be activated or inhibited by the modification, and therefore the immune response might be up- or downregulated. This study only proves that the TRAF6-NFκB pathway is influenced by InlB. In fact, InlB was already shown by Mansell and co-workers to trigger an NFκB-mediated immune response through PI3K in the macrophage-like cell line J774 (Mansell et al. 2000).

Interestingly, other virulence factors of *L. monocytogenes* directly affect the immune response. Purified extracellular Listeriolysin O stimulates the regulator of NFκB and thereby activates this pathway in HEK-293 (Kayal et al. 2002).

However, intracellular produced InlC downregulates this pathway through interaction with IKK, the regulator of NFκB, in HEK-293 and HeLa cells (Gouin et al. 2010). These obvious discrepancies between the activation and the downregulation of NFκB signaling by different proteins of *L. monocytogenes* illustrate well the complexity of signaling networks. Perhaps, time-dependent activation may explain this problem. For example, InlB effects were investigated after minutes, while the downregulation by InlC was monitored only 4 h after stimulation. Furthermore, Mansell and colleagues proposed different possibilities of the NFκB effect. Firstly, immune response may be upregulated by bacterial particles, proving the ability of host cells to defend against pathogens. Secondly, *Listeria* might downregulate NFκB signaling in order to dampen the pro-inflammatory response. Finally, NFκB signaling can avoid apoptosis of the host cell and would therefore support the pathogen's survival (Mansell et al. 2000). In either way, future studies will shed light on these currently still contradictory observations. Nevertheless, *L. monocytogenes* infection clearly affects the NFκB pathway through several bacterial proteins. Furthermore, the observed upregulation of the site pS^{82} of HSPB1 might hint at an inhibitory function of InlB in this context.

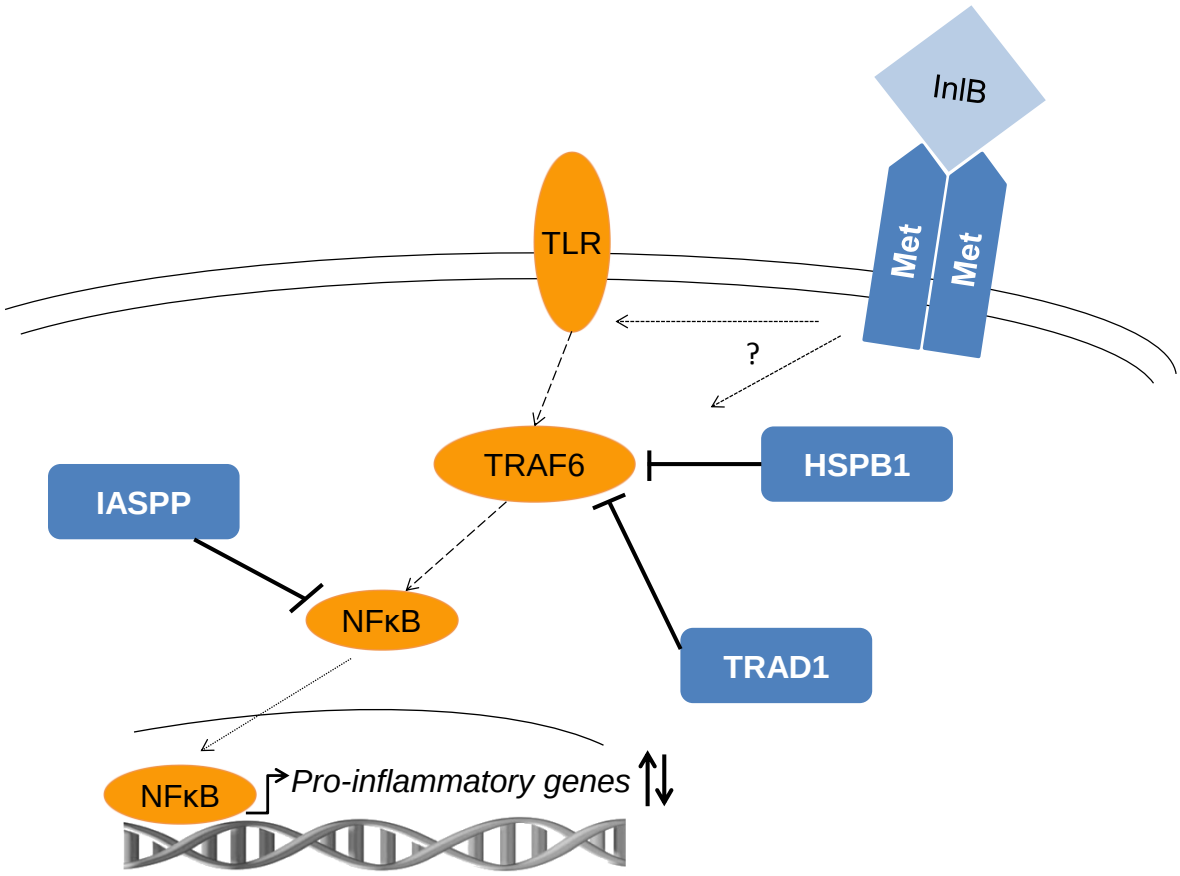

Figure 5-8: InlB affects its host's immune response

The proteins differentially phosphorylated after 5 min InlB (blue rectangles) belong to a negative feedback loop that abolishes TRAF6-NFκB signaling. Phosphorylated HSPB1 and TRAD1 inhibit TRAF6 signal transduction, while the phosphatase IASPP prevents transcriptional activity of NFκB (yellow ovals). This cascade is usually stimulated by Toll-like receptors (TLRs) after pathogenic contact and includes TRAF6 activation and NFκB translocation into the nucleus. The latter protein induces the transcription of pro-inflammatory genes in response to the stimulus. As the monitored phosphorylation sites on the three effectors are not characterized, the transcription of pro-inflammatory genes might be either up- or downregulated. Furthermore, which proteins are involved in the regulation of these sites after InlB stimulation is unknown.

In conclusion, TRAD1, IASPP and HSPB1 belong to a negative feedback loop of the TRAF6 network and negatively control the gene expression of pro-inflammatory genes. Stimulation of cells by InlB might downregulate innate immunity and would support *Listeria* infection. Surprisingly, this was observed in epithelial HeLa cells, and not in immune cells that are specialized for TLR signaling and the activation of an immune response. Nevertheless, there are hints for the involvement of non-immune cells in the activation of the immune system. For example, TLRs and other innate pattern recognition receptors (PRRs) are not only expressed in immune cells like dendritic cells or macrophages, but also in

fibroblasts and epithelial cells like HeLa. Furthermore, even in the non-immune cells, the transcription of pro-inflammatory genes is activated in response to pathogenic contact (Aoki et al. 2012; Takeuchi and Akira 2010). Therefore, InlB stimulation might really affect immunity in HeLa cells via the downregulation of TRAF6-mediated signaling. That indicates that *L. monocytogenes* might promote its own survival already at an early stage of infection, when the pathogen is still extracellular. At that time point, the bacterium is especially vulnerable, because it can be easily detected and eliminated by the immune system. Therefore, it might protect itself by downregulating the immune response of all surrounding cells. Moreover, InlB has been shown to be not only bound to the bacterial surface, but also occurs in a soluble form (Ireton 2007; Trost et al. 2005), which might particularly promote the inhibitory effect in a larger expense in the surrounding tissues.

5.6.2 Side effects of *L. monocytogenes* infection

The second half of the proteins affected by InlB was comparable to the HGF data (see Table 8-6 in the appendix). The large size of this subset supports the theory that InlB mainly mimics HGF signaling and not all induced cascades are crucial for the invasion of *L. monocytogenes*. These additional cascades are induced by InlB, but might not be an advantage for the pathogen, but rather side effects that at least do not hamper invasion and survival of the bacterium. Nevertheless, although likely unimportant for the bacterium, many host cell processes are deregulated by the induced signaling. As the Met pathway usually regulates a great amount of crucial cellular responses, a deregulation might have enormous consequences on host cell homeostasis.

One mechanism induced by Met is apoptosis. However, *Listeria* needs an intact host cell for proliferation, therefore the induction of apoptosis - even by chance - would not support the bacterium’s life cycle. In contrast, the opposite signal for host cell survival, which is also controlled by Met, maintains the status-quo for the pathogen and would support its life in the host. Notably, prolonged host cell survival is also one of the characteristics of cancer cells. The question arises whether *L. monocytogenes* infection affects cancer-associated processes. Although the ability of *L. monocytogenes* to trace cancer tissues and to induce

inflammatory responses that support cancer therapy was investigated (Guirnalda, Wood, and Paterson 2012), there are no hints for a correlation between listeriosis and development of cancer yet. However, the causes of cancer induced by viral or bacterial infections might be difficult to define due to the long time interval between the two diseases. For those infections that are already known to cause cancer, patient samples included the pathogens, thus a correlation was more or less obvious. *Helicobacter pylori* infection, for example, was shown in 1984 to be one cause of gastric cancer by a screening of gastric biopsy samples (Marshall and Warren 1984). Thereby, the virulence factor CagA of *H. pylori* translocates into the host cell upon cellular adhesion. Interestingly, Churin et al. demonstrated that this CagA binds and activates the Met receptor intracellularly, causing increased host cell motility, which may be associated with cancer development (Churin et al. 2003). Furthermore, in 1983, the group of zur Hausen identified human papilloma virus (HPV) DNA in biopsy samples of invasive cancers, thereby proving that HPV infection may induce cervical cancer (Dürst et al. 1983).

In contrast, most infections with *L. monocytogenes* in otherwise healthy humans mostly cause inconspicuous symptoms like mild diarrhea. Thus, many cases may not be diagnosed and therefore complicate the identification of a correlation between a *Listeria* infection and cancer development.

5.6.3 Does InlB mimic HGF?

InlB induces many signaling cascades similar to HGF. However, the example of the differentially regulated TRAF6-NFκB pathway has demonstrated that InlB indeed uses specific signaling molecules to promote its survival in the host. Moreover, several hints in the literature show that duration of Met activation is different, as well as the strength of induced MAPK signaling (Y. Shen et al. 2000; Copp et al. 2003). This is not unexpected as HGF and InlB are structurally unrelated and bind to different domains of the Met receptor. Therefore, InlB does not mimic HGF, but rather acts like an independent factor that is able to mediate specific downstream pathways. Similar signaling pathways downstream of Met induced by both ligands might only be side effects of InlB, It is likely that these are not essential for the pathogen’s survival, proliferation and spreading in the host, but might cause significant attendant symptoms during and after *Listeria* infection.

6 Outlook

As the HGF study was performed in DU145 and InlB in HeLa S3 cells, it is necessary that the monitored differences between the regulated phosphorylation sites are not cell type-specific. Therefore, all proteins regulated only after HGF or InlB stimulation have to be examined via immunoblot against their regulated phosphorylation sites. The reason why that was not performed during this work was the lack of phospho-specific antibodies against these sites. Thus, it may be necessary to produce the required antibodies by immunization of mice or rabbits in order to get specific polyclonal antisera. Furthermore, promising candidates should also be additionally immunoblotted against the whole protein, to ascertain the presence of a constant level of the protein in all samples. In some cases, protein degradation might have caused a “downregulation” of the phosphorylation site, although the amount of protein had decreased in fact.

Using phosphoproteomics, this work identified more than 60 proteins downstream of Met that were differently phosphorylated in response to HGF or InlB. Through their known interaction partners or their involvement in Met-induced processes there is evidence that these proteins take part in Met signaling or are substrates of involved components. However, only the functional characterization of the regulated phosphorylation sites will provide reliable information. Therefore, site-specific mutagenesis in combination with interaction studies using co-immunoprecipitation, co-localization, e.g. by fluorescence imaging, and *in vitro* kinase assays are necessary. These experiments will show whether a regulated phosphorylation site is functional in response to stimulation or not, and where the protein has to be integrated into the Met pathway. Additionally, the TRAF6-NFκB network that was influenced by InlB stimulation is worth verification. Also in this case, functional characterization of the regulated phosphorylation sites will show, through which intermediate proteins InlB regulates modification of these immune signaling molecules. Furthermore, in order to answer the question whether InlB activates or downregulates the immune response of the host cell, gene expression arrays might be performed to investigate the impact of InlB on its host’s genetic program. Additionally, InlB-stimulated cells could be screened for the production of

pro-inflammatory factors like cytokines. These should be produced, only if InlB upregulates the immune response of the cell.

As InlB has been shown to trigger many side effects that could lead to the development of cancer, this correlation might be studied in the future. Therefore, extensive epidemiological screens among cancer patients should be performed. Additionally, infection studies with mice might also prove if there is a higher probability for these animals to develop tumors later on.

As kinases are still underrepresented in the phosphoproteome after HGF and InlB stimulation, further experiments enriching the kinome as realized by Reinl and co-workers should be performed using the same conditions as in this work (Reinl et al. 2009). Kinome and phosphoproteome data integration by systems biology will further contribute to the knowledge of the complex regulation of the Met signaling networks.

Although microarrays demonstrated a regulatory role for the EPHA2 receptor in HGF/Met-induced gene expression, the molecular mechanism of regulation is still unclear. The identified phosphorylation on pS^{897} should be investigated by site-specific mutagenesis to verify its participation in controlling the expression of target genes. As this site is modified by AKT1, that has several other targets besides EPHA2, regulation of this kinase is also worth investigation. Additionally, the pathway downstream of EPHA2, which leads to the inhibitory effect on HGF/Met-induced gene expression might be studied by phosphoproteomics in future. As the amount of EPHA2 in the cell seems to influence the phenotypic response as well, signal integration should be considered including protein quantity. Most interesting is a comparison of pathways downstream of EPHA2 induced either indirectly by HGF or directly by its actual extracellular ligand Ephrin A1.

Cell type-specific effects also might have caused the inability to reproduce inhibition of scattering by HGF through co-stimulation with Ephrin A1 as described in the publication of Miao (Miao et al. 2009). Therefore, the U373 cell line used by the authors should be tested as well as their self-made Ephrin A1, which could have also prevented the inhibitory phenotype of the co-stimulation. Additionally, experiments should be performed, in which the receptor is stimulated by the

membrane-bound ligand, because this is its naturally occurring form. Many studies done so far used an artificial soluble Ephrin A1, which might not act exactly like the bound form.

Preliminary data of this thesis to elucidate the effect of EPHA2 knockdown on HGF-induced scattering of DU145 cells 24 h after stimulation indicated that the amount of EPHA2 defines the phenotypic response. Once the effects are confirmed, long-term gene expression monitored after 24 h HGF will reveal genes responsible for the discovered differential phenotypes of EPHA2 knockdown. As *epha2* certainly is a target gene of HGF/Met signaling, the knockdown stability should be tested by immunoblot over the whole time span. Additionally, EPHA2 overexpression studies might be performed in order to investigate whether the inhibitory effect on HGF-induced gene expression can be increased beyond the level observed and a clear dose-response relationship exits.

NEK9 investigations illustrated that this kinase might regulate HGF/Met-activated motility. As all experiments were performed with the two siRNAs in combination, off-target effects of one of the siRNAs cannot be excluded. Therefore, data should be improved using the siRNAs separately in order to verify the monitored impressive effect on cell migration. Once NEK9 is verified as important inhibitor of scattering, its cellular protein level should be compared within different cell lines. Motile cells like DU145, HepG2, and A549 might contain less NEK9 compared to non-motile ones like HeLa or Hep3B. Interestingly, this correlation could also be investigated in primary cancer cells. Tissues originating from metastases might show lower levels of NEK9 than those of healthy or non-metastatic tissues. In this case, NEK9 would be a promising target for cancer therapy. Nevertheless, not only the protein level, but also the activity of the NEK9 protein might determine cell migration. Therefore, the regulated phosphorylation site pT^{333} on NEK9 should be investigated by site-directed mutagenesis combined with functional studies in order to clarify the role of this site in Met signaling. Additionally, overexpression of NEK9 should increase its inhibitory effect on cell motility of usually migrating cell lines. If this is indeed correct, DU145 cells, for example, will show no response to HGF, proving an important role for NEK9 in controlling cellular motility.

7 Summary

Met is a receptor tyrosine kinase that is located on the surface of vertebrate epithelial cells. The main ligand of Met is hepatocyte growth factor (HGF), a mesenchymal-derived growth factor, which activates several signaling cascades downstream of Met that regulate proliferation, motility as well as apoptosis and survival. Therefore, HGF/Met plays an important role during embryogenesis, but also during wound healing in adults. However, HGF and Met are deregulated in cancer accompanied with poor prognosis and metastasis. Furthermore, the pathogenic bacterium *Listeria monocytogenes* exploits the Met receptor for invasion into its host cell through binding with the surface protein internalin B (InlB). Infection with the food-borne pathogen might cause meningitis and miscarriage in pregnant women. Both Met ligands induce signaling cascades that are mediated via phosphorylations, which are transmitted by kinases and are removed by phosphatases. Phosphorylation of a protein can affect its activity, interaction with other proteins, or even its localization. Therefore, the analysis of the phosphorylation pattern after activation of Met by one of its ligands is a suitable method to identify novel proteins involved in these signaling cascades.

The first aim of this work was to characterize the physiological Met signaling in DU145 cells. Subsequently, this knowledge was utilized as prerequisite to understand the influence of the pathogen *L. monocytogenes* by stimulation of Met with bacterial InlB.

Phosphoproteomics using Ga-based IMAC phosphopeptide enrichment, followed by fractionation via SCX and LC-MS/MS measurement provided access to 7,996 different phosphopeptides from a triplicate. Quantitative analyses resulted in 95 phosphopeptides that were significantly regulated in the first 20 min of HGF stimulation. This work found 80 proteins that were differentially phosphorylated in response to HGF. Although the HGF/Met pathway has been studied for two decades, 40 of them are novel pathway components acting downstream of the Met receptor. Furthermore, signaling dynamics of all regulated phosphorylation sites was characterized.

In this study, the function of two novel proteins was studied more detailed to determine their roles in HG/Met signaling. Scatter assay and gene expression analyses using RNAi revealed the kinase NEK9 as an important regulator of cellular motility in response to HGF. Furthermore, knockdown of the receptor tyrosine kinase EPHA2 illustrated its role in controlling the HGF/Met-induced target gene expression. Thus, besides its receptor function, which is activated by Ephrin A proteins, EPHA2 acts as downstream signaling component of HGF/Met. Both proteins, NEK9 and EPHA2, could be key components of Met signaling that might play an important role as cancer suppressors in healthy tissue.

When cells were stimulated with the pathogenic InlB and analyzed by phosphoproteomics, about 50% of the differentially phosphorylated proteins were similar to the physiological signaling induced by HGF. Nevertheless, the other half was only regulated after InlB stimulation, indicating crucial components necessary for *L. monocytogenes* infection. Among those were proteins that act as negative effectors of cellular immunity, complementing our knowledge how *L. monocytogenes* subverts host cell's defense during infection.

7.1 Zusammenfassung

Met ist eine membranständige Rezeptor-Tyrosine-Kinase, die sich auf der Zelloberfläche von Epithelzellen von Wirbeltieren findet. Der Hauptligand von Met ist der Wachstumsfaktor HGF, der den Rezeptor aktiviert und damit mehrere Signalkaskaden unterhalb von Met induziert, die Proliferation und Motilität, sowie Apoptose und Überleben der Zelle regulieren. Daher spielen HGF und Met eine wichtige Rolle in der Embryonalentwicklung, aber auch während der Wundheilung bei Erwachsenen. Allerdings sind diese Proteine in Krebs dereguliert, was mit einer schlechten Prognose, sowie Metastasierung in Zusammenhang gebracht wird. Weiterhin nutzt das pathogene Bakterium *Listeria monocytogenes* den Met-Rezeptor als Eintrittspforte in seine Wirtszelle, indem es Met mit dem Oberflächenprotein Internalin B (InlB) bindet und aktiviert. Infektion mit diesem über kontaminierte Nahrung aufgenommenen Bakterium können zu Meningitis und Fehlgeburt führen. Beide Liganden des Met-Rezeptors induzieren Signalkaskaden, die durch Phosphorylierung von Kinasen vermittelt, und durch Phosphatasen gegenreguliert werden. Phosphorylierung eines Proteins kann seine Aktivität, die Interaktion mit anderen Proteinen, als auch seine Lokalisierung beeinflussen. Daher ist die Analyse des Phosphorylierungsmusters, welches durch einen der beiden Liganden induziert wird, eine geeignete Methode um neue Proteine zu identifizieren, die im Met-Signalweg eine Rolle spielen.

Das erste Ziel dieser Arbeit war es den physiologischen HGF/Met-Signalweg in DU145-Zellen zu charakterisieren. Nachfolgend diente dieses Wissen als Basis für die Analyse des Einflusses einer Infektion mit *L. monocytogenes*, welcher nach InlB-Stimulation untersucht wurde.

Phosphoproteomische Analysen mittels Anreicherung der Phosphopeptide durch Ga-basiertes IMAC, folgende SCX-Fraktionierung und Messung durch LC-MS/MS ermöglichten die Identifizierung von 7.996 verschiedenen Phosphopeptiden aus drei Replikaten. Durch quantitativen Vergleich konnten 95 Phosphopeptide gefunden werden, die in den ersten 20 min nach HGF-Stimulation signifikant reguliert waren. Damit ermöglichte diese Arbeit eine Identifizierung von 80 neuen Komponenten stimuliert durch HGF. Obwohl der HGF/Met-Signalweg schon seit zwei Dekaden untersucht wird, wurden 40 Proteine gefunden, die unterhalb des

Met-Rezeptors agieren. Zudem konnte die Phosphorylierungsdynamik aller regulierten Phosphorylierungsstellen innerhalb der ersten 20 min nach Stimulation aufgeklärt werden.

Nachfolgend wurden zwei neue Proteine genauer untersucht, um ihre Rolle im Met-Signalweg zu bestimmen. Migrationsstudien und die Analyse der Genexpression mit Hilfe der RNAi-Technik ließen eine Funktion der Kinase NEK9 bei der Inhibition von HGF-induzierter Zellmotilität vermuten. Außerdem zeigte der Knockdown von EPHA2, dass dieses Protein die Regulation von HGF/Met-Zielgenen beeinflusst. Neben seiner Rolle als Rezeptor für Ephrin A-Proteine wurde EPHA2 daher als Signalweg-Bestandteile unterhalb von HGF/Met identifiziert. Daher können beide Proteine, NEK9 und EPHA2, Schlüsselbestandteile des Met-Signalwegs sein, welche im gesunden Gewebe als Tumor-Suppressoren wirken.

Phosphoproteomische Analysen von Zellen, die mit dem pathogenen Protein InlB stimuliert wurden, zeigten 50% Ähnlichkeit der regulierten Phosphopeptide, verglichen mit dem physiologischen HGF/Met-Signalweg. Hingegen war die andere Hälfte nur nach InlB-Stimulation reguliert, was spezifische Signalweg-Komponenten für InlB vermuten lässt, die die Invasion von *L. monocytogenes* ermöglichen. Unter diesen wurden Proteine gefunden, die innerhalb eines Feedback Loops die Immunantwort regulieren. Daher könnte das Pathogen *L. monocytogenes* die Abwehr seines Wirts während der Invasion gezielt unterwandern, um sein Überleben zu sichern.

8 Appendix

8.1 Additional tables

Table 8-1: List of all 95 HGF-regulated phosphorylation sites

Significantly regulated phosphorylation sites after 3, 6, or 20 min of HGF stimulation in DU145 cells. Log_2 regulation factors of the triplicate E1, E2, and E3 are illustrated. Significant RFs possess a pval (p-value) of below 0.05 (marked as bold letters). Proteins that are novel members, but are likely involved in Met signaling are marked by **

Uniprot ID	Protein	P-Site	E1_3min	E2_3min	E3_3min	E1_6min	E2_6min	E3_6min	E1_20min	E2_20min	E3_20min	pval3	pval6	pval20
P55196	AFAD**	S1799	1.275	1.428	1.648	1.181	1.699	1.664	0.798	1.248	0.887	**1.30E-18**	**6.03E-16**	**4.94E-07**
P55196	AFAD**	S1721	0.076	0.613	-0.122	0.181	0.367	0.214	0.679	1.026	0.867	1	1	**6.81E-05**
P52594	AGFG1	T177,S181	-0.508	-0.131	-0.327	-1.182	-0.428	-0.907	-1.63	-0.637	-0.965	1	0.249823418	**0.000330069**
Q09666	AHNK**	S135	0.343	0.01	-0.414	1.013	0.661	0.748	1.254	0.822	0.819	1	**0.00013518**	**1.93E-07**
Q09666	AHNK**	S3426	1.02	0.342	0.375	1.96	0.623	1.051	1.972	0.85	0.938	1	**0.000547508**	**4.64E-08**
Q09666	AHNK**	S5099	0.559	1.17	0.26	1.941	1.474	1.122	NA	1.733	1.285	1	**2.28E-14**	1
Q9Y2D5	AKAP2**	S720	0.17	0.77	-0.04	0.671	0.689	0.656	1.018	0.914	0.556	1	**0.00016313**	**0.005476067**
Q12802	AKP13**	S2709	-0.093	0.654	-0.04	0.501	0.717	0.502	1.033	0.878	0.69	1	**0.030962004**	**4.45E-05**
Q96B36	AKTS1**	T246	1.227	1.243	1.602	1.22	1.447	1.779	1.055	1.067	1.28	**3.16E-17**	**4.98E-17**	**1.14E-12**
P25054	APC	S2449	-0.093	-0.422	-0.094	-0.344	-0.157	-0.198	-0.638	-0.504	-0.49	1	1	**0.043129258**
Q92974	ARHG2**	S886	-0.025	0.843	0.038	0.246	0.632	0.848	0.789	0.793	0.873	1	1	**7.35E-07**
Q6ZSZ5	ARHGI**	S1124	-0.206	0.527	-0.053	0.68	0.402	0.111	0.762	0.514	0.605	1	1	**0.020839877**
Q8WWM7	ATX2L	S339	-0.079	-0.175	-0.108	-0.299	-0.218	-0.279	-1.209	-0.691	-0.757	1	1	**4.28E-05**
Q86UU0	BCL9L	S21	-0.301	-0.664	-0.518	-1.299	-0.936	-1.027	-1.155	-0.653	-0.807	1	**6.94E-10**	**0.000182745**
Q13185	CBX3	S95	-0.39	-0.548	-0.108	-0.489	-0.439	-0.095	-0.894	-0.555	-0.514	1	1	**0.020839877**
Q9Y5K6	CD2AP**	S458	0.644	0.486	0.705	0.532	0.356	0.502	0.451	0.184	0.4	**0.048585075**	1	1
Q86WR7	CJ047	S212,S215	0.441	-0.218	0.385	1.134	0.563	0.854	1.04	0.583	0.86	1	**0.004342153**	**0.002221379**

Q86WR7	CJ047	T214,S215	0.159	-0.378	0.434	1.227	0.511	0.923	1.148	0.325	1	1	**0.022825495**	1
Q8IY22	CMIP	S343	0.46	0.64	0.314	0.921	0.32	0.452	0.63	0.549	0.497	1	1	**0.034980177**
Q8IVT2	CS021	S541	0.124	-0.184	0.228	1.006	0.881	1.089	0.806	0.869	0.621	1	**1.06E-08**	**0.000589022**
Q5VZ89	DEN4C	S1089	0.732	0.06	0.563	1.516	0.788	1.229	1.286	0.594	0.847	1	**7.67E-07**	**0.001523204**
Q5VZ89	DEN4C	S732,S737	0.8	0.499	0.375	0.573	0.367	0.374	0.995	0.49	0.556	0.98127857	1	**0.043129258**
Q16555	DPYL2	T514	-0.402	-0.067	0.012	-0.594	-0.067	0.068	-1.261	-0.564	-0.63	1	1	**0.004206287**
P55265	DSRAD	T601	0.432	0.418	0.012	0.814	0.308	0.573	1.222	0.617	1.03	1	1	**0.000679512**
O75821	EIF3G	T41	-0.553	0.367	-0.378	0.22	0.155	0.721	0.669	0.572	0.675	1	1	**0.003221361**
Q8WYP5	ELYS**	S1232	0.112	-0.251	0	0.458	0.181	0.273	0.85	0.583	0.621	1	1	**0.002221379**
P29317	EPHA2**	S897	0.193	-0.324	0.1	1.114	0.424	0.923	1.654	0.869	1.105	1	0.278168457	**1.89E-08**
P29317	EPHA2**	S897,S901	0.248	-0.201	0.25	0.573	0.155	0.263	1.025	0.733	0.84	1	1	**7.93E-06**
Q14315	FLNC**	S2233	1.546	1.052	1.518	1.744	1.214	1.287	1.383	0.932	0.853	**1.36E-12**	**7.34E-17**	**4.03E-08**
Q13480	GAB1	Y659	0.644	1.122	1.271	0.553	0.881	1.169	-0.143	0.681	0.644	**0.000255336**	**0.006032746**	1
Q9Y624	JAM1**	S284	-0.402	-0.158	-0.194	-0.884	-0.322	-0.42	-0.74	-0.621	-0.55	1	1	**0.006661181**
Q9Y4B5	K0802	S609,S613	1.007	1.052	0.088	1.29	1.22	0.347	1.423	1.378	0.88	1	1	**1.12E-08**
P05787	K2C8	S330	0.619	0.694	0.293	0.553	0.356	0.51	0.726	0.638	0.683	1	1	**0.000318208**
Q14678	KANK1	S325	0.748	0.281	0.453	0.839	0.642	0.699	0.753	0.572	0.548	1	**0.000274375**	**0.007108064**
Q3ZCW2	LEGL	S22	-0.192	0.432	0.424	0.181	0.127	0.558	0.659	0.526	0.86	1	1	**0.014343647**
Q8WVC0	LEO1	S205	-0.758	-0.362	-0.067	-1.188	-0.253	-0.146	-1.442	-0.504	-0.596	1	1	**0.028307432**
Q9UHB6	LIMA1**	S686	0.8	0.758	-0.378	0.983	0.889	0.596	1.44	0.773	0.735	1	**0.001419435**	**7.30E-06**
P46821	MAP1B**	S1501	0.216	0.855	-0.013	0.583	0.296	0.469	0.979	0.763	0.77	1	1	**2.26E-06**
P27816	MAP4**	S941	-0.314	-0.575	-0.378	-0.469	-0.344	-0.379	-0.732	-0.597	-0.929	1	1	**0.00137291**
P43243	MATR3	S598	-0.287	-0.839	-0.208	-0.449	-0.585	-0.224	-0.879	-0.85	-0.502	1	1	**0.030078974**
Q14676	MDC1	S168	-0.012	0.732	0	0.593	0.413	0.641	1.353	0.85	0.506	1	0.372446678	**0.026635355**
P55081	MFAP1	S52,S53	0.422	0.38	0.271	0.642	0.501	0.534	0.924	0.365	0.683	1	**0.030962004**	1
P28482	MK01	T185,Y187	1.199	1.131	1.486	1.623	1.463	1.71	1.485	0.932	1.493	**1.33E-14**	**1.60E-24**	**8.52E-10**
P28482	MK01	Y187	0.585	0.77	0.589	0.998	0.632	0.383	0.61	0.284	0.409	**0.0020759**	0.803345723	1
P27361	MK03	Y204	1.187	0.866	0.863	1.441	0.744	0.596	1.273	0.325	0.589	**2.52E-08**	**0.001419435**	1
P27361	MK03	T202,Y204	1.136	1.131	1.37	NA	1.578	1.699	1.317	0.743	1.285	**1.33E-14**	1	**5.24E-06**

O96007	MOC2B	S20	0.227	0.513	0.171	0.603	0.344	0.4	1.389	0.692	0.581	1	1	**0.002377678**
Q13615	MTMR3**	S647	-0.326	1.122	-0.302	-0.041	1.107	0.4	0.65	1.091	0.565	1	1	**0.004068994**
Q8NEY1	NAV1	S1000	0	0.145	0.051	0.155	0.39	0.1	0.495	0.594	0.573	1	1	**0.037145548**
Q9HCH0	NCK5L	S473	1.032	0.499	1.142	0.127	-0.013	-0.035	-0.054	-0.048	0.012	**0.032949808**	1	1
Q96PU5	NED4L	S448	0.363	0.38	0.205	0.553	0.708	0.542	1.055	0.859	0.756	1	**0.008615577**	**3.04E-06**
Q96TA1	NIBL1	S678,S679	0.515	0.527	0.051	0.881	0.632	0.409	1.468	0.949	1.048	1	0.413596601	**3.57E-10**
Q96TA1	NIBL1	S678,S683	0.159	0.499	0.088	0.613	0.689	0.374	1.347	0.967	0.919	1	1	**1.64E-09**
Q9Y3T9	NOC2L	S672	0.432	0.257	-0.094	0.195	0.014	0.796	0.841	0.526	0.887	1	1	**0.014343647**
Q7Z417	NUFP2	T571	1.281	0.667	0.681	1.071	0.49	0.596	1.195	0.365	0.867	**0.000107912**	**0.043071159**	1
Q7Z417	NUFP2	S629	-0.233	0.64	-0.053	0.141	0.642	0.634	0.762	1.075	0.819	1	1	**2.36E-06**
Q8N573	OXR1	S202	0.488	0.486	0.063	1.078	0.49	0.392	1.292	0.783	0.506	1	0.64056989	**0.026635355**
O00459	P85B	S262	-0.012	0.418	0.228	0.332	0.762	0.452	0.948	1.026	1.024	1	1	**3.76E-10**
Q8WX93	PALLD	S893	-0.149	-0.21	-0.208	0.39	0.332	0.374	0.908	0.941	1.006	1	1	**2.84E-09**
P49023	PAXI	S137	0.685	0.458	0.293	0.897	0.511	0.699	0.972	0.454	0.906	1	**0.022825495**	0.122247117
Q9H4Z3	PCIF1	S143	-0.233	0.189	0.063	0	0.259	0.392	0.59	0.537	0.581	1	1	**0.010125514**
Q6Y7W6	PERQ2**	T25,S30	0.808	0.599	0.705	1.402	0.542	1.006	1.564	0.514	0.963	**0.001281322**	**0.008615577**	**0.020839877**
Q6Y7W6	PERQ2**	T25,S26	0.373	0.354	0.395	0.873	0.689	0.51	1.113	0.514	0.69	1	**0.02353697**	**0.020839877**
O75151	PHF2	T654	0.373	1.188	0.228	0.913	0.671	0.959	1.6	1.043	1.071	1	**9.25E-05**	**2.25E-12**
Q8WWQ0	PHIP	S1315	0.204	0.155	0.025	0.259	0.057	-0.171	0.956	0.763	0.565	1	1	**0.004068994**
Q86SQ0	PHLB2	S468	0.628	0.305	0.491	1.568	1.028	1.435	1.241	0.923	0.919	1	**5.20E-12**	**1.64E-09**
Q15149	PLEC**	S4386	0.948	0.68	0.96	1.134	0.96	1.239	0.932	0.743	0.887	**6.56E-05**	**2.02E-10**	**5.24E-06**
Q15149	PLEC**	S4386,S4389	0.851	0.556	1.205	1.284	0.983	1.546	1.228	0.949	1.036	**0.005478526**	**6.00E-11**	**3.57E-10**
Q9NYI0	PSD3**	S770	0.17	0.889	-0.194	0.921	1.32	1.006	1.154	1.145	0.799	1	**1.48E-09**	**4.73E-07**
Q05209	PTN12**	T587	-0.079	0.667	-0.04	0.447	0.744	0.627	0.995	1.026	1.077	1	0.148482966	**3.16E-11**
Q8IY67	RAVR1	T463	-0.093	0.513	-0.067	0.259	0.726	0.338	0.9	1.205	0.763	1	1	**2.26E-06**
Q15042	RB3GP**	T536	-0.339	0.071	0.038	0.114	0.127	0.469	0.716	0.743	0.873	1	1	**1.58E-05**
Q96T37	RBM15	S128	-0.894	-1.355	-1.221	-1.265	-2.087	0.163	-1.437	-1.248	-0.049	**5.66E-09**	1	1
Q6GYQ0	RGPA1**	S797	0.124	0.68	0.365	0.246	0.897	0.796	0.762	0.923	0.799	1	1	**2.36E-06**
Q13017	RHG05**	S1124	0.669	0.234	0.545	1.057	0.468	1.057	0.815	0.549	1.065	1	0.081983242	**0.006881155**

Q13017	RHG05	S1195	1.082	0.783	0.334	1.436	0.613	0.329	2.047	0.502	0.573	1	1	**0.030078974**
P31350	RIR2**	S20	-0.274	0.783	-0.235	0.208	0.583	1.282	0.972	0.896	1.036	1	1	**5.13E-09**
Q9NQC3	RTN4	S107	0.653	0.77	1.216	-0.081	-0.081	-0.238	1.317	-0.217	0.445	**0.000182827**	1	1
Q96EQ0	SGTB	S297	0.076	0.177	0.194	1.028	0.479	0.769	1.055	0.606	0.69	1	0.059586719	**0.001002762**
Q9P0V3	SH3B4	S244	1.064	1.102	0.536	1.233	0.717	0.589	1.161	0.802	0.589	**0.010458308**	**0.001807009**	**0.001809447**
Q16637	SMN	T25	0.27	1.122	0.571	0.511	0.49	0.589	0.9	0.793	0.847	1	**0.043071159**	**6.16E-07**
O60749	SNX2	T104	-0.473	0.432	-0.053	0.661	1.155	0.941	0.798	1.248	0.698	1	**0.00013518**	**3.25E-05**
P31948	STIP1	S481	-0.564	-0.508	-0.39	-0.964	-0.119	-0.293	-1.13	-0.645	-0.726	0.675046158	1	**0.000245969**
P16949	STMN1**	S25	0.302	0.405	0.159	0.652	0.542	0.627	1.365	1.263	1.088	1	**0.008615577**	**1.71E-13**
Q68CZ2	TENS3**	S776	1.082	0.585	0.463	1.864	0.68	0.776	1.908	0.56	0.66	0.094777934	**6.55E-05**	**0.004801146**
Q12888	TP53B**	S1114	0.343	0.472	0.148	0.402	0.788	0.822	0.85	0.549	0.69	1	0.495999918	**0.006881155**
Q12888	TP53B**	S1426,S1430	-0.352	0.556	-0.365	-0.397	0.735	1.062	0.569	1.043	0.698	1	1	**0.003561541**
Q12888	TP53B**	S366	0.506	0.189	0.148	1.314	0.356	0.769	1.891	0.583	1.224	1	1	**0.002221379**
P12270	TPR**	T2116	0.83	1.082	0.623	1.296	1.419	1.209	1.4	1.115	1.15	**0.000548493**	**1.01E-16**	**3.47E-14**
Q9C0C9	UBE2O	S839	0.469	0.694	0.182	0.071	0.479	0.581	0.64	0.85	0.749	1	1	**0.000295707**
Q96JH7	VCIP1	S768	-0.462	-0.362	-0.289	-0.439	-0.194	-0.279	-0.612	-0.539	-0.561	1	1	**0.009498571**
O95785	WIZ	S1146	0.353	-0.226	0.282	1.078	0.511	0.953	0.875	0.416	0.69	1	**0.022825495**	0.34459738
O60293	ZC3H1	S1046	-0.163	0.405	-0.013	0.779	0.762	0.4	1.148	0.949	0.912	1	0.522218676	**2.33E-09**
Q6NZY4	ZCHC8	S658	0.124	0.393	-1.122	0.532	0.699	0.329	0.762	0.941	0.637	1	1	**0.000330069**
Q15942	ZYX**	T306	0.701	0.732	0.545	0.308	0.32	0.1	0.311	0.403	-0.024	**0.007836025**	1	1

Table 8-2: Clusters of HGF-regulated phosphopeptides

Significantly regulated peptides clustered according to their phosphorylation dynamics over the time course 3, 6, and 20 min. The table lists the peptides illustrated in Figure 4-17 as graphs. Due to the triplicate, every peptide occurs three times.

Figure 4-17A	
ord4132	GAB1_HUMAN@Y659
	NCK5L_HUMAN@S473
	ZYX_HUMAN@T306
Figure 4-17B	
ord3142	NCK5L_HUMAN@S473
	RTN4_HUMAN@S107
Figure 4-17C	
ord4312	NCK5L_HUMAN@S473
	RTN4_HUMAN@S107
Figure 4-17D	
ord1432	AFAD_HUMAN@S1799
	AKTS1_HUMAN@T246
	CD2AP_HUMAN@S458
	CD2AP_HUMAN@S458
	CD2AP_HUMAN@S458
	FLNC_HUMAN@S2233
	GAB1_HUMAN@Y659
	GAB1_HUMAN@Y659
	MK01_HUMAN@Y187
	MK03_HUMAN@Y204
	MK03_HUMAN@Y204
	MTMR3_HUMAN@S647
	NUFP2_HUMAN@T571
	PERQ2_HUMAN@T25.S30
	RHG05_HUMAN@S1195
Figure 4-17E	
ord2413	RBM15_HUMAN@S128
Figure 4-17F	
ord1234	AFAD_HUMAN@S1721
	AHNK_HUMAN@S135
	AHNK_HUMAN@S135
	AHNK_HUMAN@S3426
	AHNK_HUMAN@S3426
	AHNK_HUMAN@S5099
	AHNK_HUMAN@S5099
	AKAP2_HUMAN@S720
	AKP13_HUMAN@S2709
	ARHG2_HUMAN@S886
	CJ047_HUMAN@S212.S215
	CJ047_HUMAN@T214.S215
	CMIP_HUMAN@S343
	DSRAD_HUMAN@T601
	DSRAD_HUMAN@T601
	ELYS_HUMAN@S1232
	ELYS_HUMAN@S1232
	EPHA2_HUMAN@S897
	EPHA2_HUMAN@S897
	EPHA2_HUMAN@S897.S901
	EPHA2_HUMAN@S897.S901
Figure 4-17F	
ord1234	K0802_HUMAN@S609.S613
	K0802_HUMAN@S609.S613
	K0802_HUMAN@S609.S613
	K2C8_HUMAN@S330
	LEGL_HUMAN@S22
	LIMA1_HUMAN@S686
	MAP1B_HUMAN@S1501
	MFAP1_HUMAN@S52.S53
	MFAP1_HUMAN@S52.S53
	MOC2B_HUMAN@S20
	MOC2B_HUMAN@S20
	NAV1_HUMAN@S1000
	NAV1_HUMAN@S1000
	NAV1_HUMAN@S1000
	NED4L_HUMAN@S448
	NED4L_HUMAN@S448
	NED4L_HUMAN@S448
	NIBL1_HUMAN@S678.S679
	NIBL1_HUMAN@S678.S679
	NIBL1_HUMAN@S678.S679
	NIBL1_HUMAN@S678.S683
	NIBL1_HUMAN@S678.S683
	NIBL1_HUMAN@S678.S683
Figure 4-17F	
ord1234	NUFP2_HUMAN@S629
	OXR1_HUMAN@S202
	OXR1_HUMAN@S202
	OXR1_HUMAN@S202
	P85B_HUMAN@S262
	P85B_HUMAN@S262
	PAXI_HUMAN@S137
	PAXI_HUMAN@S137
	PCIF1_HUMAN@S143
	PCIF1_HUMAN@S143
	PERQ2_HUMAN@T25.S26
	PERQ2_HUMAN@T25.S26
	PERQ2_HUMAN@T25.S30
	PHF2_HUMAN@T654
	PHF2_HUMAN@T654
	PSD3_HUMAN@S770
	PTN12_HUMAN@T587
	RAVR1_HUMAN@T463
	RB3GP_HUMAN@T536
	RB3GP_HUMAN@T536
	RGPA1_HUMAN@S797
	RGPA1_HUMAN@S797
	RGPA1_HUMAN@S797

Table 8-3: Clusters HGF-regulated phosphopeptides, continued

The table lists the peptides illustrated in Figure 4-18 as graphs.

Figure 4-18A	
ord1243	AHNK_HUMAN@S3426
	CJ047_HUMAN@S212.S215
	CJ047_HUMAN@T214.S215
	CMIP_HUMAN@S343
	CS021_HUMAN@S541
	CS021_HUMAN@S541
	DEN4C_HUMAN@S1089
	DEN4C_HUMAN@S1089
	DEN4C_HUMAN@S1089
	KANK1_HUMAN@S325
	KANK1_HUMAN@S325
	KANK1_HUMAN@S325
	LIMA1_HUMAN@S686
	MDC1_HUMAN@S168
	MK01_HUMAN@T185.Y187
	MK01_HUMAN@T185.Y187
	MK01_HUMAN@Y187
	MK03_HUMAN@Y204
	PERQ2_HUMAN@T25.S26
	PERQ2_HUMAN@T25.S30
	PHLB2_HUMAN@S468
	PHLB2_HUMAN@S468
	PHLB2_HUMAN@S468
	PLEC_HUMAN@S4386

Figure 4-18A	
ord1243	PLEC_HUMAN@S4386.S4389
	PLEC_HUMAN@S4386.S4389
	PSD3_HUMAN@S770
	RHG05_HUMAN@S1124
	SGTB_HUMAN@S297
	SH3B4_HUMAN@S244
	TENS3_HUMAN@S776
	TP53B_HUMAN@S1114
	TP53B_HUMAN@S1114
	TPR_HUMAN@T2116
	TPR_HUMAN@T2116
	WIZ_HUMAN@S1146
	WIZ_HUMAN@S1146
Figure 4-18B	
ord1423	AFAD_HUMAN@S1799
	AFAD_HUMAN@S1799
	AKTS1_HUMAN@T246
	AKTS1_HUMAN@T246
	FLNC_HUMAN@S2233
	FLNC_HUMAN@S2233
	MFAP1_HUMAN@S52.S53
	MK01_HUMAN@T185.Y187
	MK03_HUMAN@T202.Y204
	MK03_HUMAN@T202.Y204

Figure 4-18B	
ord1423	PAXI_HUMAN@S137
	PLEC_HUMAN@S4386
	PLEC_HUMAN@S4386
	PLEC_HUMAN@S4386.S4389
	TENS3_HUMAN@S776
Figure 4-18C	
ord2143	AKAP2_HUMAN@S720
	CJ047_HUMAN@T214.S215
	CS021_HUMAN@S541
	EIF3G_HUMAN@T41
	PSD3_HUMAN@S770
	RIR2_HUMAN@S20
	SNX2_HUMAN@T104
	TP53B_HUMAN@S1426.S1430
	WIZ_HUMAN@S1146
Figure 4-18D	
ord1342	SH3B4_HUMAN@S244
	NUFP2_HUMAN@T571
	MK01_HUMAN@Y187
	ZYX_HUMAN@T306
	ZYX_HUMAN@T306
	PHF2_HUMAN@T654
	SMN_HUMAN@T25
	ARHG2_HUMAN@S886

Figure 4-18D	
ord1342	ARHGI_HUMAN@S1124
	CMIP_HUMAN@S343
	DEN4C_HUMAN@S732.S737
	K2C8_HUMAN@S330
	MAP1B_HUMAN@S1501
Figure 4-18E	
ord1324	AFAD_HUMAN@S1721
	AKAP2_HUMAN@S720
	DEN4C_HUMAN@S732.S737
	DEN4C_HUMAN@S732.S737
	DSRAD_HUMAN@T601
	EIF3G_HUMAN@T41
	K2C8_HUMAN@S330
	LEGL_HUMAN@S22
	MDC1_HUMAN@S168
	MOC2B_HUMAN@S20
	NOC2L_HUMAN@S672
	NOC2L_HUMAN@S672
	NUFP2_HUMAN@T571
	PHIP_HUMAN@S1315
	RHG05_HUMAN@S1195
	RIR2_HUMAN@S20
	UBE2O_HUMAN@S839
	UBE2O_HUMAN@S839

Figure 4-18F	
ord3124	PHIP_HUMAN@S1315
	RTN4_HUMAN@S107
Figure 4-18G	
ord4231	APC_HUMAN@S2449
	CBX3_HUMAN@S95
	CBX3_HUMAN@S95
	DPYL2_HUMAN@T514
	LEO1_HUMAN@S205
	MAP4_HUMAN@S941
	MATR3_HUMAN@S598
	STIP1_HUMAN@S481
	STIP1_HUMAN@S481
	VCIP1_HUMAN@S768
	VCIP1_HUMAN@S768
	VCIP1_HUMAN@S768
Figure 4-18H	
ord3421	BCL9L_HUMAN@S21
	BCL9L_HUMAN@S21
	JAM1_HUMAN@S284
Figure 4-18I	
ord3241	BCL9L_HUMAN@S21
	RBM15_HUMAN@S128
Figure 4-18J	
ord3214	TP53B_HUMAN@S1426.S1430

Table 8-4: List of all 28 InlB-regulated phosphorylation sites

Significantly regulated phosphorylation sites after 5 min of InlB stimulation in HeLa S3 cells. Log_2 regulation factors of the triplicate E1, E2, and E3 are illustrated. Significant RFs possess a pval (p-value) of below 0.05 (marked as bold letters).

Uniprot ID	Protein	P-Site	E1_5min	E2_5min	E3_5min	pval_5min
Q09666	AHNK	S135	0.477	1.131	0.977	**0.002146028**
Q09666	AHNK	S210	0.697	0.644	1.241	**2.61E-06**
Q09666	AHNK	S511	0.477	0.383	0.707	**0.046309956**
Q09666	AHNK	T4100	0.879	0.986	0.738	**2.89E-08**
Q9H6F5	CCD86	S91	-1.131	-1.906	-0.988	**1.35E-14**
P55265	DSRAD	T601	1.399	0.795	0.886	**1.45E-09**
P00533	EGFR	T693	1.642	2.065	2.443	**4.28E-39**
P04792	HSPB1	S82	1.049	0.986	0.932	**4.93E-13**
Q8WUF5	IASPP	S134	-0.666	-0.976	-0.939	**9.53E-07**
P78344	IF4G2	T508	-0.782	-0.687	-0.397	**0.030247431**
O95239	KIF4A	S801	1.526	1.784	1.602	**6.71E-34**
P42702	LIFR	S1044	0.62	0.586	0.867	**3.23E-05**
Q8WWI1	LMO7	S925	-0.703	-1.15	-0.678	**5.44E-07**
Q5VZK9	LR16A	S1094	0.526	0.721	0.619	**0.000354332**
P28482	MK01	T185,Y187	1.216	1.86	0.895	**4.77E-12**
P28482	MK01	Y187	0.997	0.903	0.642	**2.85E-06**
P27361	MK03	T202,Y204	0.962	1.917	0.941	**2.80E-13**
Q9Y6X9	MORC2	S743	-0.674	-1.202	-1.671	**6.56E-07**
P18615	NELFE	S115	1.091	1.349	0.664	**1.05E-06**
Q92882	OSTF1	S213	-1.024	-1.051	-1.059	**1.21E-15**
Q16513	PKN2	S583	0.907	0.586	0.829	**3.23E-05**
O76021	RL1D1	T358	-0.643	-0.73	-0.617	**8.62E-06**
O75396	SC22B	S137	0.719	0.805	0.895	**7.49E-08**
Q9H788	SH24A	S315	0.85	0.977	1.602	**6.75E-11**

P12270	TPR	S2155	0.608	0.774	1.226	**1.27E-05**
P12270	TPR	T2137	0.926	0.855	1.99	**5.06E-11**
O14545	TRAD1	S415	-0.802	-1.604	-1.243	**9.94E-10**
Q9C0B5	ZDHC5	S406	1.231	1.139	1.496	**3.17E-19**

Table 8-5: Proof-of-concept transcription factors

The list illustrates 11 of 31 known transcription factors of the HGF/Met response that regulated genes in the DU145 transcriptome in response to HGF stimulation. Data were taken from the EPHA2 expression array and compared to known factors involved in HGF/Met-induced gene expression in the GeneGo database.

Uniprot ID
CEBPA
CEBPB
JUN
MYC
E2F1
EGR1
EGR3
ETS1
ETV4
SOX9
STAT3

Table 8-6: Phosphorylation sites regulated similar in response to HGF and InlB

All significantly regulated phosphorylation sites identified by phosphoproteomics were compared. 5 sites were significantly regulated in both datasets and further 19 sites were significantly regulated in response to HGF and affected by InlB stimulation, although not significantly.

Uniprot ID	Protein	P-Site	Significantly regulated?
Q09666	AHNK	S135	yes
P55265	DSRAD	T601	yes
P28482	MK01	T185,Y187	yes
P28482	MK01	Y187	yes
P27361	MK03	T202,Y204	yes
Q09666	AHNK	S3426	only in HGF significant
Q9Y2D5	AKAP2	S720	only in HGF significant
Q12802	AKP13	S2709	only in HGF significant
Q96B36	AKTS1	T246	only in HGF significant
Q6ZSZ5	ARHGI	S1124	only in HGF significant
Q5VZ89	DEN4C	S1089	only in HGF significant
Q8WYP5	ELYS	S1232	only in HGF significant
Q14678	KANK1	S325	only in HGF significant
P27361	MK03	Y204	only in HGF significant
O00459	P85B	S262	only in HGF significant
Q8WX93	PALLD	S893	only in HGF significant
P49023	PAXI	S137	only in HGF significant
Q9H4Z3	PCIF1	S143	only in HGF significant
Q6Y7W6	PERQ2	T25,S26	only in HGF significant
Q05209	PTN12	T587	only in HGF significant
Q8IY67	RAVR1	T463	only in HGF significant
O60749	SNX2	T104	only in HGF significant
O95785	WIZ	S1146	only in HGF significant
Q15942	ZYX	T306	only in HGF significant

8.2 List of abbreviations

µM	Micromolar
APS	Ammonium persulfate
ATP	Adenosine triphosphate
BSA	Bovine serum albumin
cm	Centimeter
EDTA	Ethylenediaminetetraacetic acid
ELISA	Enzyme-linked immunosorbent assay
EMT	Epithelial-mesenchmal transition
EPHA2	Ephrin type-A-receptor 2
Fe	Iron
Ga	Gallium
GAP	GTPase activating protein
GAPDH	Glyceraldehyde 3-phosphate dehydrogenase
GDT	Guanosine diphosphate
GEF	Guanine nucleotide exchange factor
GO	Gene ontology
GTP	Guanosine diphosphate
h	Hour
HCl	Acetic acid
HGF	Hepatocyte growth factor
HZI	Helmholtz-Center for Infection Research
IMAC	Immobilized metal affinity chromatography
InlB	Internalin B
iTRAQ	Isobaric tags for relative and absolute quantitation
kDa	Kilodalton
LC-MS/MS	Liquid chromatography tandem mass spectrometry
m/z	Mass-charge ratio
MALDI	Matrix-assisted laser desorption/ionization
MAPK	Mitogen-activated protein kinase
mg	Milligram
min	Minute
MK01	Mitogen-activated protein kinase 1 (alias ERK2)
MK01	Mitogen-activated protein kinase 3 (alias ERK1)
ml	Milliliter
mM	Millimolar
mRNA	Messenger ribonucleic acid

MS	Mass spectrometry
MTT	Dimethyl thiazolyl diphenyl tetrazolium
nm	Nanometer
nM	Nanomolar
NS (siRNA)	Nonsense (siRNA)
PBS	Phosphate buffered saline
ppm	Parts per million
pS	Phosphoserine
P-Site	Phosphorylation site
pT	Phosphothreonine
pY	Phosphotyrosine
RF	Regulation factor
RNAi	RNA interference
rpm	Rounds per minute
RT	Room temperature
RTK	Receptor tyrosine kinase
SCX	Strong cation exchange chromatography
SDS	Sodium dodecylsulfate
SDS-PAGE	SDS polyacrylamide gel electrophoresis
sec	Second
si(-RNA)	Small interfering RNA
SILAC	stable isotope labeling with amino acids in cell culture
TEMED	Tetramethylethylenediamine
V	Volt
v/v	Volume per volume
w/v	Weight per volume
WT	Wildtype
xg	n-fold of standard gravity

8.3 List of tables

8.4 List of figures

8.5 List of references

Akiyama, Tetsu. 2000. “Wnt/β-catenin Signaling.” *Cytokine & Growth Factor Reviews* 11 (4) (December): 273–282. doi:10.1016/S1359-6101(00)00011-3. http://linkinghub.elsevier.com/retrieve/pii/S1359610100000113.

Alnemri, Emad S, Teresa Fernandes-Alnemri, and Gerald Litwack. 1995. “Cloning and Expression of Four Novel Isoforms of Human Interleukin-1β Converting Enzyme with Different Apoptotic Activities.” *The Journal of Biological Chemistry* 270 (9): 4312–17. doi:10.1074/jbc.270.9.4312. http://www.jbc.org/content/270/9/4312.long.

Ames, Bruce N, Lois Swirsky, and Walter C Willettt. 1995. “The Causes and Prevention of Cancer.” *Proceedings of the National Academy of Sciences of the United States of America* 92 (12): 5258–5265. http://www.pnas.org/content/92/12/5258.short.

Aoki, Maria Pilar, Eugenio Antonio Carrera-Silva, Henar Cuervo, Manuel Fresno, Núria Gironès, and Susana Gea. 2012. “Nonimmune Cells Contribute to Crosstalk Between Immune Cells and Inflammatory Mediators in the Innate Response to Trypanosoma Cruzi Infection.” *Journal of Parasitology Research* 2012 (January): 1–13. doi:10.1155/2012/737324. http://www.pubmedcentral.nih.gov/articlerender.fcgi?artid=3159004&tool=pmcentrez&rendertype=abstract.

Balkovetz, Daniel F, Edward R Gerrard, Shixiong Li, David Johnson, James Lee, John W Tobias, Katherine K Rogers, Richard W Snyder, and Joshua H Lipschutz. 2004. “Gene Expression Alterations During HGF-induced Dedifferentiation of a Renal Tubular Epithelial Cell Line (MDCK) Using a Novel Canine DNA Microarray.” *American Journal of Physiology. Renal Physiology* 286 (4) (April): F702–10. doi:10.1152/ajprenal.00270.2003. http://www.ncbi.nlm.nih.gov/pubmed/14665430.

Baykal, Cem, Ayse Ayhan, Atakan Al, Kunter Yüce, and Ali Ayhan. 2003. “Overexpression of the c-Met/HGF Receptor and Its Prognostic Significance in Uterine Cervix Carcinomas.” *Gynecologic Oncology* 88 (2): 123–129. doi:10.1016/S0090-8258(02)00073-2. https://connect.helmholtz-hzi.de/science/article/pii/,DanaInfo=.awxyCwholvloou4sr9Qu76+S0090825802000732.

Beck, Martin, Alexander Schmidt, Johan Malmstroem, Manfred Claassen, Alessandro Ori, Anna Szymborska, Franz Herzog, Oliver Rinner, Jan Ellenberg, and Ruedi Aebersold. 2011. “The Quantitative Proteome of a Human Cell Line.” *Molecular Systems Biology* 7 (549) (January): 1–8. doi:10.1038/msb.2011.82. http://www.ncbi.nlm.nih.gov/pubmed/22068332.

Birchmeier, Carmen, Walter Birchmeier, Ermanno Gherardi, and George F Vande Woude. 2003. “Met, Metastasis, Motility and More.” *Nature Reviews.*

Molecular Cell Biology 4 (12) (December): 915–25. doi:10.1038/nrm1261. http://www.ncbi.nlm.nih.gov/pubmed/14685170.

Boccaccio, Carla, and Paolo M Comoglio. 2006. “Invasive Growth: a Met-driven Genetic Programme for Cancer and Stem Cells.” *Nature Reviews. Cancer* 6 (8): 637–45. doi:10.1038/nrc1912. http://www.nature.com/nrc/journal/v6/n8/abs/nrc1912.html.

Boccaccio, Carla, Giovanni Gaudino, Giovanna Gambarotta, Francesco Galimi, and Paolo M Comoglio. 1994. “Hepatocyte Growth Factor (HGF) Receptor Expression Is Inducible and Is Part of the Delayed-early Response to HGF.” *The Journal of Biological Chemistry* 269 (17) (April 29): 12846–51. http://www.ncbi.nlm.nih.gov/pubmed/8175699.

Boersema, Paul J, Shabaz Mohammed, and Albert J R Heck. 2009. “Phosphopeptide Fragmentation and Analysis by Mass Spectrometry.” *Journal of Mass Spectrometry : JMS* 44 (6) (June): 861–78. doi:10.1002/jms.1599. http://www.ncbi.nlm.nih.gov/pubmed/19504542.

Bradford, M M. 1976. “A Rapid and Sensitive Method for the Quantitation of Microgram Quantities of Protein Utilizing the Principle of Protein-dye Binding.” *Analytical Biochemistry* 72 (May 7): 248–54. http://www.ncbi.nlm.nih.gov/pubmed/942051.

Braun, Laurence, Hélène Ohayon, and Pascale Cossart. 1998. “The InIB Protein of Listeria Monocytogenes Is Sufficient to Promote Entry into Mammalian Cells.” *Molecular Microbiology* 27 (5) (March): 1077–87. doi:10.1046/j.1365-2958.1998.00750.x. http://www.ncbi.nlm.nih.gov/pubmed/10540282.

Brembeck, Felix H, Thomas Schwarz-Romond, Jeroen Bakkers, Sabine Wilhelm, Matthias Hammerschmidt, and Walter Birchmeier. 2004. “Essential Role of BCL9-2 in the Switch Between Beta-catenin’s Adhesive and Transcriptional Functions.” *Genes & Development* 18: 2225–2230. doi:10.1101/gad.317604.GENES. http://genesdev.cshlp.org/content/18/18/2225.long.

Burbelo, P D, S Miyamoto, A Utani, S Brill, K M Yamada, A Hall, and Y Yamada. 1995. “p190-B, a New Member of the Rho GAP Family, and Rho Are Induced to Cluster After Integrin Cross-linking.” *The Journal of Biological Chemistry* 270 (52) (December 29): 30919–26. doi:10.1074/jbc.270.52.30919. http://www.ncbi.nlm.nih.gov/pubmed/8537347.

Bush, Jeffrey O, and Philippe Soriano. 2012. “Eph/ephrin Signaling: Genetic, Phosphoproteomic, and Transcriptomic Approaches.” *Seminars in Cell & Developmental Biology* 23 (1) (February): 26–34. doi:10.1016/j.semcdb.2011.10.018. http://www.ncbi.nlm.nih.gov/pubmed/22040918.

Buus, Richard, Monica Faronato, Dean E Hammond, Sylvie Urbé, and J Michael. 2009. “Deubiquitinase Activities Required for Hepatocyte Growth Factor-Induced Scattering of Epithelial Cells.” *Current Biology : CB* 19 (17) (February

7): 1463–1466. doi:10.1016/j.cub.2011.12.035. http://www.ncbi.nlm.nih.gov/pubmed/22337370.

Cantin, Greg T, Wei Yi, Bingwen Lu, Sung Kyu Park, Tao Xu, Jiing-dwan Lee, and John R Yates. 2008. “Combining Protein-based IMAC, Peptide-Based IMAC, and MudPIT for Efficient Phosphoproteomic Analysis.” *Journal of Proteome Research* 7 (3): 1346–1351. doi:10.1021/pr0705441. http://pubs.acs.org/doi/abs/10.1021/pr0705441.

Chaudhary, K, S Deb, N Moniaux, M P Ponnusamy, and S K Batra. 2007. “Human RNA Polymerase II-associated Factor Complex: Dysregulation in Cancer.” *Oncogene* 26 (54) (November 29): 7499–507. doi:10.1038/sj.onc.1210582. http://www.ncbi.nlm.nih.gov/pubmed/17599057.

Chin, Y Rebecca, and Alex Toker. 2010. “The Actin-bundling Protein Palladin Is an Akt1-specific Substrate That Regulates Breast Cancer Cell Migration.” *Molecular Cell* 38 (3) (May 14): 333–44. doi:10.1016/j.molcel.2010.02.031. http://www.pubmedcentral.nih.gov/articlerender.fcgi?artid=2872630&tool=pmcentrez&rendertype=abstract.

Churin, Yuri, Laila Al-Ghoul, Oliver Kepp, Thomas F Meyer, Walter Birchmeier, and Michael Naumann. 2003. “Helicobacter Pylori CagA Protein Targets the c-Met Receptor and Enhances the Motogenic Response.” *The Journal of Cell Biology* 161 (2) (April 28): 249–55. doi:10.1083/jcb.200208039. http://www.pubmedcentral.nih.gov/articlerender.fcgi?artid=2172921&tool=pmcentrez&rendertype=abstract.

Clark, H. 1995. “The Nature of Cancer : Morphogenesis and Progressive (self)-Disorganization in Neoplastic Development and Progression.” *Acta Oncologica* 34 (1): 3–21. http://informahealthcare.com/doi/abs/10.3109/02841869509093632.

Cohen, Patricia. 2004. “Overview of Protein Serine/threonine Phosphatases.” *Topics in Current Genetics* 5: 1–20. doi:10.1007/978-3-540-40035-6_1. http://link.springer.com/chapter/10.1007%2F978-3-540-40035-6_1?LI=true.

Copp, Jeremy, Michael Marino, Manidipa Banerjee, Partho Ghosh, and Peter van der Geer. 2003. “Multiple Regions of Internalin B Contribute to Its Ability to Turn on the Ras-mitogen-activated Protein Kinase Pathway.” *The Journal of Biological Chemistry* 278 (10) (March 7): 7783–9. doi:10.1074/jbc.M211666200. http://www.ncbi.nlm.nih.gov/pubmed/12488439.

Cossart, Pascale, and Esteban Veiga. 2008. “Non-classical Use of Clathrin During Bacterial Infections.” *Journal of Microscopy* 231 (3) (September): 524–8. doi:10.1111/j.1365-2818.2008.02065.x. http://www.ncbi.nlm.nih.gov/pubmed/18755008.

Cui, Yumin, Yi-Chun Liao, and Su Hao Lo. 2004. “Epidermal Growth Factor Modulates Tyrosine Phosphorylation of a Novel Tensin Family Member , Tensin3.” *Molecular Cancer Research : MCR* 2 (4): 225–32. http://mcr.aacrjournals.org/content/2/4/225.long.

Deleu, S, I Pirson, F Clermont, T Nakamura, J E Dumont, and C Maenhaut. 1999. “Immediate Early Gene Expression in Dog Thyrocytes in Response to Growth, Proliferation, and Differentiation Stimuli.” *Journal of Cellular Physiology* 181 (2) (November): 342–54. doi:10.1002/(SICI)1097-4652(199911)181:2<342::AID-JCP16>3.0.CO;2-K. http://www.ncbi.nlm.nih.gov/pubmed/10497313.

Deribe, Yonathan Lissanu, Tony Pawson, and Ivan Dikic. 2010. “Post-translational Modifications in Signal Integration.” *Nature Structural & Molecular Biology* 17 (6) (June): 666–72. doi:10.1038/nsmb.1842. http://www.ncbi.nlm.nih.gov/pubmed/20495563.

Dijkmans, T F, L W a van Hooijdonk, T G Schouten, J T Kamphorst, C P Fitzsimons, and E Vreugdenhil. 2009. “Identification of New Nerve Growth Factor-responsive Immediate-early Genes.” *Brain Research* 1249 (January 16): 19–33. doi:10.1016/j.brainres.2008.10.050. http://www.ncbi.nlm.nih.gov/pubmed/19013137.

Dissmeyer, Nico, and Arp Schnittger. 2011. *Plant Kinases: The Age of Protein Kinases*. Ed. Nico Dissmeyer and Arp Schnittger. *Methods*. Vol. 779. Totowa, NJ: Humana Press. doi:10.1007/978-1-61779-264-9. http://www.springerlink.com/index/10.1007/978-1-61779-264-9.

Diviani, D, J Soderling, and J D Scott. 2001. “AKAP-Lbc Anchors Protein Kinase A and Nucleates Galpha 12-selective Rho-mediated Stress Fiber Formation.” *The Journal of Biological Chemistry* 276 (47) (November 23): 44247–57. doi:10.1074/jbc.M106629200. http://www.ncbi.nlm.nih.gov/pubmed/11546812.

Dixon, Richard D S, Daniel K Arneman, Andrew S Rachlin, Naresh R Sundaresan, M Joseph Costello, Sharon L Campbell, and Carol a Otey. 2008. “Palladin Is an Actin Cross-linking Protein That Uses Immunoglobulin-like Domains to Bind Filamentous Actin.” *The Journal of Biological Chemistry* 283 (10) (March 7): 6222–31. doi:10.1074/jbc.M707694200. http://www.ncbi.nlm.nih.gov/pubmed/18180288.

Dürst, M, L Gissmann, H Ikenberg, and H zur Hausen. 1983. “A Papillomavirus DNA from a Cervical Carcinoma and Its Prevalence in Cancer Biopsy Samples from Different Geographic Regions.” *Proceedings of the National Academy of Sciences of the United States of America* 80 (12) (June): 3812–5. http://www.pubmedcentral.nih.gov/articlerender.fcgi?artid=394142&tool=pmcentrez&rendertype=abstract.

Factor, Valentina M, Daekwan Seo, Tsuyoshi Ishikawa, Pal Kaposi-Novak, Jens U Marquardt, Jesper B Andersen, Elizabeth a Conner, and Snorri S Thorgeirsson. 2010. “Loss of c-Met Disrupts Gene Expression Program Required for G2/M Progression During Liver Regeneration in Mice.” *PloS One* 5 (9) (January). doi:10.1371/journal.pone.0012739. http://www.pubmedcentral.nih.gov/articlerender.fcgi?artid=2940888&tool=pmcentrez&rendertype=abstract.

Franz, Cerstin, Rudolf Walczak, Sevil Yavuz, Rachel Santarella, Marc Gentzel, Peter Askjaer, Vincent Galy, Martin Hetzer, Iain W Mattaj, and Wolfram Antonin. 2007. “MEL-28/ELYS Is Required for the Recruitment of Nucleoporins to Chromatin and Postmitotic Nuclear Pore Complex Assembly.” *EMBO Reports* 8 (2) (February): 165–72. doi:10.1038/sj.embor.7400889. http://www.pubmedcentral.nih.gov/articlerender.fcgi?artid=1796766&tool=pmcentrez&rendertype=abstract.

Freytag, Jennifer, Cynthia E Wilkins-Port, Craig E Higgins, Stephen P Higgins, Rohan Samarakoon, and Paul J Higgins. 2010. “PAI-1 Mediates the TGF-beta1+EGF-induced ‘Scatter’ Response in Transformed Human Keratinocytes.” *The Journal of Investigative Dermatology* 130 (9) (September): 2179–90. doi:10.1038/jid.2010.106. http://www.ncbi.nlm.nih.gov/pubmed/20428185.

González-Billault, Christian, José a Del Río, Jesús M Ureña, Eva M Jiménez-Mateos, María J Barallobre, Marta Pascual, Lluís Pujadas, et al. 2005. “A Role of MAP1B in Reelin-dependent Neuronal Migration.” *Cerebral Cortex* 15 (8) (August): 1134–45. doi:10.1093/cercor/bhh213. http://www.ncbi.nlm.nih.gov/pubmed/15590913.

Goold, R G, R Owen, and P R Gordon-Weeks. 1999. “Glycogen Synthase Kinase 3beta Phosphorylation of Microtubule-associated Protein 1B Regulates the Stability of Microtubules in Growth Cones.” *Journal of Cell Science* 112 (October): 3373–84. http://www.ncbi.nlm.nih.gov/pubmed/10504342.

Goormachtigh, Gautier, Zongling Ji, Arnaud Le Goff, and Véronique Fafeur. 2011. “Degradation of the GAB1 Adaptor by the Ubiquitin-proteasome Pathway Hampers HGF/SF-MET Signaling.” *Biochemical and Biophysical Research Communications* 411 (4) (August 12): 780–5. doi:10.1016/j.bbrc.2011.07.024. http://www.ncbi.nlm.nih.gov/pubmed/21782801.

Gouin, Edith, Minou Adib-Conquy, Damien Balestrino, Marie-Anne Nahori, Véronique Villiers, Frédéric Colland, Shaynoor Dramsi, Olivier Dussurget, and Pascale Cossart. 2010. “The Listeria Monocytogenes InlC Protein Interferes with Innate Immune Responses by Targeting the I{kappa}B Kinase Subunit IKK{alpha}.” *Proceedings of the National Academy of Sciences of the United States of America* 107 (40) (October 5): 17333–8. doi:10.1073/pnas.1007765107. http://www.pubmedcentral.nih.gov/articlerender.fcgi?artid=2951401&tool=pmcentrez&rendertype=abstract.

Grabbe, Caroline, Koraljka Husnjak, and Ivan Dikic. 2011. “The Spatial and Temporal Organization of Ubiquitin Networks.” *Nature Reviews. Molecular Cell Biology* 12 (5) (May): 295–307. doi:10.1038/nrm3099. http://www.ncbi.nlm.nih.gov/pubmed/21448225.

Graziani, Andrea, Daniela Gramaglia, Lewis C Cantley, and Paolo M Comoglio. 1991. “The Tyrosine-phosphorylated Hepatocyte Growth Factor/Scatter Factor Receptor Associates with Phosphatidylinositol 3-Kinase.” *The Journal of Biological Chemistry* 266 (33): 22087–90.

Grimsrud, Paul A, Danielle L Swaney, Craig D Wenger, Nicole A Beauchene, and Joshua J Coon. 2010. “Phosphoproteomics for the Masses.” *ACS Chemical Biology* 5 (1): 105–119. doi:10.1021/cb900277e. http://pubs.acs.org/doi/pdf/10.1021/cb900277e.

Grotegut, Stefan, Dietrich von Schweinitz, Gerhard Christofori, and François Lehembre. 2006. “Hepatocyte Growth Factor Induces Cell Scattering Through MAPK/Egr-1-mediated Upregulation of Snail.” *The EMBO Journal* 25 (15) (August 9): 3534–45. doi:10.1038/sj.emboj.7601213. http://www.pubmedcentral.nih.gov/articlerender.fcgi?artid=1538570&tool=pmcentrez&rendertype=abstract.

Guirnalda, Patrick, Laurence Wood, and Yvonne Paterson. 2012. *Listeria Monocytogenes and Its Products as Agents for Cancer Immunotherapy. Advances in Immunology*. 1st ed. Vol. 113. Elsevier Inc. doi:10.1016/B978-0-12-394590-7.00004-X. http://www.ncbi.nlm.nih.gov/pubmed/22244580.

Guo, Ailan, Judit Villén, Jon Kornhauser, Kimberly a Lee, Matthew P Stokes, Klarisa Rikova, Anthony Possemato, et al. 2008. “Signaling Networks Assembled by Oncogenic EGFR and c-Met.” *Proceedings of the National Academy of Sciences of the United States of America* 105 (2) (January 15): 692–7. doi:10.1073/pnas.0707270105. http://www.pubmedcentral.nih.gov/articlerender.fcgi?artid=2206598&tool=pmcentrez&rendertype=abstract.

Guo, Tiannan, Yi Zhu, Chee Sian Gan, Sze Sing Lee, Jiang Zhu, Haixia Wang, Xin Li, et al. 2010. “Quantitative Proteomics Discloses MET Expression in Mitochondria as a Direct Target of MET Kinase Inhibitor in Cancer Cells.” *Molecular & Cellular Proteomics : MCP* 9 (12) (December): 2629–41. doi:10.1074/mcp.M110.001776. http://www.pubmedcentral.nih.gov/articlerender.fcgi?artid=3101852&tool=pmcentrez&rendertype=abstract.

Hammond, Dean E, Russell Hyde, Irina Kratchmarova, Robert J Beynon, Blagoy Blagoev, and Michael J Clague. 2010. “Quantitative Analysis of HGF and EGF-dependent Phosphotyrosine Signaling Networks.” *Journal of Proteome Research* 9 (5) (May 7): 2734–42. doi:10.1021/pr100145w. http://www.ncbi.nlm.nih.gov/pubmed/20222723.

Hamon, Mélanie, Hélène Bierne, and Pascale Cossart. 2006. “Listeria Monocytogenes: a Multifaceted Model.” *Nature Reviews. Microbiology* 4 (6) (June): 423–34. doi:10.1038/nrmicro1413. http://www.ncbi.nlm.nih.gov/pubmed/16710323.

Hanahan, Douglas, and Robert a Weinberg. 2011. “Hallmarks of Cancer: The Next Generation.” *Cell* 144 (5) (March 4): 646–74. doi:10.1016/j.cell.2011.02.013. http://www.ncbi.nlm.nih.gov/pubmed/21376230.

Hellman, Nathan E, June Spector, Jonathan Robinson, Xiaofeng Zuo, Sophie Saunier, Corinne Antignac, John W Tobias, and Joshua H Lipschutz. 2008. “Matrix Metalloproteinase 13 (MMP13) and Tissue Inhibitor of Matrix

Metalloproteinase 1 (TIMP1), Regulated by the MAPK Pathway, Are Both Necessary for Madin-Darby Canine Kidney Tubulogenesis." *The Journal of Biological Chemistry* 283 (7) (February 15): 4272–82. doi:10.1074/jbc.M708027200. http://www.ncbi.nlm.nih.gov/pubmed/18039671.

Hoshino, Takashi, Toshiaki Sakisaka, Takeshi Baba, Tomohiro Yamada, Toshihiro Kimura, and Yoshimi Takai. 2005. "Regulation of E-cadherin Endocytosis by Nectin Through Afadin, Rap1, and P120ctn." *The Journal of Biological Chemistry* 280 (25) (June 24): 24095–103. doi:10.1074/jbc.M414447200. http://www.ncbi.nlm.nih.gov/pubmed/15857834.

Huang, Fang-I, Yu-Ling Chen, Chih-Ning Chang, Ray-Hwang Yuan, and Yung-Ming Jeng. 2012. "Hepatocyte Growth Factor Activates Wnt Pathway by Transcriptional Activation of LEF1 to Facilitate Tumor Invasion." *Carcinogenesis* 33 (6) (June): 1142–8. doi:10.1093/carcin/bgs131. http://www.ncbi.nlm.nih.gov/pubmed/22436613.

Huang, Paul H. 2011. "Phosphoproteomic Studies of Receptor Tyrosine Kinases: Future Perspectives." *Molecular bioSystems* (December 2). doi:10.1039/c1mb05327b. http://www.ncbi.nlm.nih.gov/pubmed/22134727.

Hubbard, Michael J., and Philip Cohen. 1993. "On Target with a New Mechanism for the Regulation of Protein Phosphorylation." *Trends in Biochemical Science* 18 (5): 172–7. doi:10.1016/0968-0004(93)90109-Z. http://www.sciencedirect.com/science/article/pii/096800049390109Z.

Humphrey, P a, X Zhu, R Zarnegar, P E Swanson, T L Ratliff, R T Vollmer, and M L Day. 1995. "Hepatocyte Growth Factor and Its Receptor (c-MET) in Prostatic Carcinoma." *The American Journal of Pathology* 147 (2) (August): 386–96. http://www.pubmedcentral.nih.gov/articlerender.fcgi?artid=1869824&tool=pmcentrez&rendertype=abstract.

Hundertmark, Claudia, Roman Fischer, Tobias Reinl, Simone May, Frank Klawonn, and Lothar Jänsch. 2009. "MS-specific Noise Model Reveals the Potential of iTRAQ in Quantitative Proteomics." *Bioinformatics (Oxford, England)* 25 (8) (April 15): 1004–11. doi:10.1093/bioinformatics/btn551. http://www.ncbi.nlm.nih.gov/pubmed/18952628.

Hunter, T, and B M Sefton. 1980. "Transforming Gene Product of Rous Sarcoma Virus Phosphorylates Tyrosine." *Proceedings of the National Academy of Sciences of the United States of America* 77 (3) (March): 1311–5. http://www.pubmedcentral.nih.gov/articlerender.fcgi?artid=348484&tool=pmcentrez&rendertype=abstract.

Ingham, R J, M Holgado-Madruga, C Siu, a J Wong, and M R Gold. 1998. "The Gab1 Protein Is a Docking Site for Multiple Proteins Involved in Signaling by the B Cell Antigen Receptor." *The Journal of Biological Chemistry* 273 (46) (November 13): 30630–7. doi:10.1074/jbc.273.46.30630. http://www.ncbi.nlm.nih.gov/pubmed/9804835.

Ireton, Keith. 2007. “Entry of the Bacterial Pathogen Listeria Monocytogenes into Mammalian Cells.” *Cellular Microbiology* 9 (6) (June): 1365–75. doi:10.1111/j.1462-5822.2007.00933.x. http://www.ncbi.nlm.nih.gov/pubmed/17419717.

Irie, Naoko, Yasunari Takada, Yoshihiko Watanabe, Yumi Matsuzaki, Chie Naruse, Masahide Asano, Yoichiro Iwakura, Toshio Suda, and Koichi Matsuo. 2009. “Bidirectional Signaling Through ephrinA2-EphA2 Enhances Osteoclastogenesis and Suppresses Osteoblastogenesis.” *The Journal of Biological Chemistry* 284 (21) (May 22): 14637–44. doi:10.1074/jbc.M807598200. http://www.pubmedcentral.nih.gov/articlerender.fcgi?artid=2682911&tool=pmcentrez&rendertype=abstract.

Jeffers, Michael, Michele Fiscella, Craig P Webb, Miriam Anver, Shahriar Koochekpour, and George F Vande Wounde. 1998. “The Mutationally Activated Met Receptor Mediates Motility.” *Proceedings of the National Academy of Sciences of the United States of America* 95 (24): 14417–14422. doi:10.1073/pnas.95.24.14417. http://www.ncbi.nlm.nih.gov/pmc/articles/PMC24388/.

Jeffers, Michael, Gregory A Taylor, K Michael Weidner, Satoshi Omura, and George F Vande Woude. 1997. “Degradation of the Met Tyrosine Kinase Receptor by the Ubiquitin-proteasome Pathway.” *Molecular and Cellular Biology* 17 (2) (February): 799–808. doi:0270-7306/97/$04.0010. http://www.pubmedcentral.nih.gov/articlerender.fcgi?artid=231806&tool=pmcentrez&rendertype=abstract.

Jinnin, Masatoshi, Hironobu Ihn, Yoshihiro Mimura, Yoshihide Asano, Kenichi Yamane, and Kunihiko Tamaki. 2005. “Matrix Metalloproteinase-1 Up-regulation by Hepatocyte Growth Factor in Human Dermal Fibroblasts via ERK Signaling Pathway Involves Ets1 and Fli1.” *Nucleic Acids Research* 33 (11) (January): 3540–9. doi:10.1093/nar/gki648. http://www.pubmedcentral.nih.gov/articlerender.fcgi?artid=1156961&tool=pmcentrez&rendertype=abstract.

Johnson, Candace S, Pamela a Hershberger, and Donald L Trump. 2002. “Vitamin D-related Therapies in Prostate Cancer.” *Cancer Metastasis Reviews* 21 (2) (January): 147–58. http://www.ncbi.nlm.nih.gov/pubmed/12465754.

Jordan, J Dedrick, Emmanuel M Landau, and Ravi Iyengar. 2000. “Signaling Networks: The Origins of Cellular Multitasking.” *Cell* 103 (2) (October 13): 193–200. http://www.ncbi.nlm.nih.gov/pubmed/11057893.

Kamura, Takumi, Katsumi Maenaka, Shuhei Kotoshiba, Masaki Matsumoto, Daisuke Kohda, Ronald C Conaway, Joan Weliky Conaway, and Keiichi I Nakayama. 2004. “VHL-box and SOCS-box Domains Determine Binding Specificity Modules of Ubiquitin Ligases.” *Genes & Development* 18 (2): 3055–3065. doi:10.1101/gad.1252404.ferred. http://www.ncbi.nlm.nih.gov/pmc/articles/PMC535916/.

Kaposi-Novak, Pal, Ju-Seog Lee, Luis Gòmez-Quiroz, Cédric Coulouarn, Valentina M Factor, and Snorri S Thorgeirsson. 2006. “Met-regulated Expression Signature Defines a Subset of Human Hepatocellular Carcinomas with Poor Prognosis and Aggressive Phenotype.” *Journal of Clinical Investigation* 116 (6): 1582–95. doi:10.1172/JCI27236.1582. http://www.jci.org/articles/view/27236.

Kawasaki, Y, M Sagara, Y Shibata, M Shirouzu, S Yokoyama, and Tetsu Akiyama. 2007. “Identification and Characterization of Asef2, a Guanine-nucleotide Exchange Factor Specific for Rac1 and Cdc42.” *Oncogene* 26 (55) (December 6): 7620–267. doi:10.1038/sj.onc.1210574. http://www.ncbi.nlm.nih.gov/pubmed/17599059.

Kayal, Samer, Alain Lilienbaum, Olivier Join-Lambert, Xiaoxia Li, Alain Israël, and Patrick Berche. 2002. “Listeriolysin O Secreted by Listeria Monocytogenes Induces NF-kB Signalling by Activating the IkB Kinase Complex.” *Molecular Microbiology* 44 (5): 1407–1419. doi:10.1046/j.1365-2958.2002.02973.x. http://onlinelibrary.wiley.com/doi/10.1046/j.1365-2958.2002.02973.x/abstract.

Keshet, Yonat, and Rony Seger. 2010. “MAP Kinase Signaling Cascades: A System of Hundreds of Components Regulates a Diverse Array of Physiological Functions.” Ed. Rony Seger. *Methods in Molecular Biology* 661 (1): 3–38. doi:10.1007/978-1-60761-795-2. http://www.springerlink.com/index/10.1007/978-1-60761-795-2.

Kinch, Michael S, and Kelly Carles-Kinch. 2003. “Overexpression and Functional Alterations of the EphA2 Tyrosine Kinase in Cancer.” *Clinical & Experimental Metastasis* 20 (1) (January): 59–68. http://www.ncbi.nlm.nih.gov/pubmed/12650608.

Klawonn, Frank, Nada Abidi, Evelin Berger, and Lothar Jänsch. 2012. “Curve Fitting for Short Time Series Data from High Throughput Experiments with Correction for Biological Variation.” In *Advances in Intelligent Data Analysis XI*, ed. J. Hollmén, F. Klawonn, and A. Tucker, 150–160. Berlin: Springer. http://link.springer.com/chapter/10.1007/978-3-642-34156-4_15.

Kosako, Hidetaka, and Kohji Nagano. 2011. “Quantitative Phosphoproteomics Strategies for Understanding Protein Kinase-mediated Signal Transduction Pathways.” *Expert Review of Proteomics* 8 (1) (February): 81–94. doi:10.1586/epr.10.104. http://www.ncbi.nlm.nih.gov/pubmed/21329429.

Krause, Daniela S, and Richard a Van Etten. 2005. “Tyrosine Kinases as Targets for Cancer Therapy.” *The New England Journal of Medicine* 353 (2) (July 14): 172–87. doi:10.1056/NEJMra044389. http://www.ncbi.nlm.nih.gov/pubmed/16014887.

Laemmli, U. K. 1970. “Cleavage of Structural Proteins During the Assembly of the Head of Bacteriophage T4.” *Nature* 227: 680–685. doi:doi:10.1038/227680a0. http://www.nature.com/nature/journal/v227/n5259/abs/227680a0.html.

Lai, Andrea Z, Jasmine V Abella, and Morag Park. 2009. “Crosstalk in Met Receptor Oncogenesis.” *Trends in Cell Biology* 19 (10) (October): 542–51. doi:10.1016/j.tcb.2009.07.002. http://www.ncbi.nlm.nih.gov/pubmed/19758803.

Lang, Tali, and Ashley Mansell. 2007. “The Negative Regulation of Toll-like Receptor and Associated Pathways.” *Immunology and Cell Biology* 85 (6): 425–34. doi:10.1038/sj.icb.7100094. http://www.ncbi.nlm.nih.gov/pubmed/17621314.

Larsen, Martin R, Tine E Thingholm, Ole N Jensen, Peter Roepstorff, and Thomas J D Jørgensen. 2005. “Highly Selective Enrichment of Phosphorylated Peptides from Peptide Mixtures Using Titanium Dioxide Microcolumns.” *Molecular & Cellular Proteomics : MCP* 4 (7) (July): 873–86. doi:10.1074/mcp.T500007-MCP200. http://www.ncbi.nlm.nih.gov/pubmed/15858219.

Lee, Won Jai, Sang Eun Park, and Dong Kyun Rah. 2011. “Effects of Hepatocyte Growth Factor on Collagen Synthesis and Matrix Metalloproteinase Production in Keloids.” *Journal of Korean Medical Science* 26 (8) (August): 1081–6. doi:10.3346/jkms.2011.26.8.1081. http://www.pubmedcentral.nih.gov/articlerender.fcgi?artid=3154345&tool=pmcentrez&rendertype=abstract.

Van Leenders, Geert, Bianca van Balken, Tilly Aalders, Christina Hulsbergen-van de Kaa, Dirk Ruiter, and Jack Schalken. 2002. “Intermediate Cells in Normal and Malignant Prostate Epithelium Express c-MET: Implications for Prostate Cancer Invasion.” *The Prostate* 51 (2) (May 1): 98–107. doi:10.1002/pros.10073. http://www.ncbi.nlm.nih.gov/pubmed/11948964.

Van Leenders, Geert, Rajesh Sookhlall, Wilma J Teubel, Corrina M a de Ridder, Suzanne Reneman, Andrea Sacchetti, Kees J Vissers, Wytske van Weerden, and Guido Jenster. 2011. “Activation of c-MET Induces a Stem-like Phenotype in Human Prostate Cancer.” *PloS One* 6 (11) (January): e26753. doi:10.1371/journal.pone.0026753. http://www.pubmedcentral.nih.gov/articlerender.fcgi?artid=3215704&tool=pmcentrez&rendertype=abstract.

Lefebvre, Jonathan, Frédéric Ancot, Catherine Leroy, Ghaffar Muharram, Arnaud Lemière, and David Tulasne. 2012. “Met Degradation: More Than One Stone to Shoot a Receptor Down.” *The FASEB Journal : Official Publication of the Federation of American Societies for Experimental Biology* (January 12): 1–13. doi:10.1096/fj.11-197723. http://www.ncbi.nlm.nih.gov/pubmed/22223753.

Leitner, Alexander, Martin Sturm, and Wolfgang Lindner. 2011. “Tools for Analyzing the Phosphoproteome and Other Phosphorylated Biomolecules: a Review.” *Analytica Chimica Acta* 703 (1) (October 3): 19–30. doi:10.1016/j.aca.2011.07.012. http://www.ncbi.nlm.nih.gov/pubmed/21843671.

Lewandowska-Gnatowska, Elżbieta, Mark L Johnston, Wesner Antoine, Jadwiga Szczegielniak, Grażyna Muszyńska, and Ján a Miernyk. 2011. “Using Multiplex-staining to Study Changes in the Maize Leaf Phosphoproteome in Response to Mechanical Wounding.” *Phytochemistry* 72 (10) (July): 1285–92. doi:10.1016/j.phytochem.2011.01.030. http://www.ncbi.nlm.nih.gov/pubmed/21334701.

Liang, C C, and H C Chen. 2001. “Sustained Activation of Extracellular Signal-regulated Kinase Stimulated by Hepatocyte Growth Factor Leads to Integrin Alpha 2 Expression That Is Involved in Cell Scattering.” *The Journal of Biological Chemistry* 276 (24) (June 15): 21146–52. doi:10.1074/jbc.M010669200. http://www.ncbi.nlm.nih.gov/pubmed/11287413.

Lim, Simin, Lee-Yee Choong, Chong Poh Kuan, Chen Yunhao, and Yoon-Pin Lim. 2009. “Regulation of Macrophage Inhibitory Factor (MIF) by Epidermal Growth Factor Receptor (EGFR) in the MCF10AT Model of Breast Cancer Progression.” *Journal of Proteome Research* 8 (8): 4062–4076. doi:10.1021/pr900430n. http://pubs.acs.org/doi/abs/10.1021/pr900430n?ai=52caf=R.

Lin, Samantha, Kristin Gordon, Nihal Kaplan, and Spiro Getsios. 2010. “Ligand Targeting of EphA2 Enhances Keratinocyte Adhesion and Differentiation via Desmoglein 1.” *Molecular Biology of the Cell* 21 (22): 3902–3914. doi:10.1091/mbc.E10. http://www.molbiolcell.org/content/21/22/3902.long.

Lindberg, R A, and T Hunter. 1990. “cDNA Cloning and Characterization of Eck, an Epithelial Cell Receptor Protein-tyrosine Kinase in the Eph/elk Family of Protein Kinases.” *Molecular and Cellular Biology* 10 (12) (December): 6316–24. http://www.pubmedcentral.nih.gov/articlerender.fcgi?artid=362907&tool=pmcentrez&rendertype=abstract.

Ma, P C, M S Tretiakova, V Nallasura, R Jagadeeswaran, A N Husain, and R Salgia. 2007. “Downstream Signalling and Specific Inhibition of c-MET/HGF Pathway in Small Cell Lung Cancer: Implications for Tumour Invasion.” *British Journal of Cancer* 97 (3) (August 6): 368–77. doi:10.1038/sj.bjc.6603884. http://www.pubmedcentral.nih.gov/articlerender.fcgi?artid=2360323&tool=pmcentrez&rendertype=abstract.

Macek, Boris, Matthias Mann, and Jesper V Olsen. 2009. “Global and Site-specific Quantitative Phosphoproteomics: Principles and Applications.” *Annual Review of Pharmacology and Toxicology* 49 (January): 199–221. doi:10.1146/annurev.pharmtox.011008.145606. http://www.ncbi.nlm.nih.gov/pubmed/18834307.

Makagiansar, Irwan T, Scott Williams, Tomas Mustelin, and William B Stallcup. 2007. “Differential Phosphorylation of NG2 Proteoglycan by ERK and PKCalpha Helps Balance Cell Proliferation and Migration.” *The Journal of Cell Biology* 178 (1) (July 2): 155–65. doi:10.1083/jcb.200612084. http://www.pubmedcentral.nih.gov/articlerender.fcgi?artid=2064431&tool=pmcentrez&rendertype=abstract.

Mann, Matthias, Shao-En Ong, Mads Grønborg, Hanno Steen, Ole N Jensen, and Akhilesh Pandey. 2002. “Analysis of Protein Phosphorylation Using Mass Spectrometry : Deciphering the Phosphoproteome.” *Trends in Biotechnology* 20 (6): 261–268. doi:10.1016/S0167-7799(02)01944-3. http://www.sciencedirect.com/science/article/pii/S0167779902019443.

Manning, Gerard. 2005. “Genomic Overview of Protein Kinases.” *WormBook : the Online Review of C. Elegans Biology* (January): 1–19. doi:10.1895/wormbook.1.60.1. http://www.ncbi.nlm.nih.gov/pubmed/18050405.

Mansell, Ashley, Laurence Braun, Pascale Cossart, and Luke A J O Neill. 2000. “A Novel Function of InlB from Listeria Monocytogenes : Activation of NF-kB in J774 Macrophages.” *Cellular Microbiology* 2 (2): 127–136. doi:10.1046/j.1462-5822.2000.00038.x. http://onlinelibrary.wiley.com/doi/10.1046/j.1462-5822.2000.00038.x/abstract.

Marshall, Barry J, and J Robin Warren. 1984. “Unidentified Curved Bacilli in the Stomach of Patients with Gastritis and Peptic Ulceration.” *The Lancet* 323 (8390): 1311–15. doi:10.1016/S0140-6736(84)91816-6. http://www.sciencedirect.com/science/article/pii/S0140673684918166.

Mashima, Ryuichi, Kazuko Saeki, Daisuke Aki, Yasumasa Minoda, Hiromi Takaki, Takahito Sanada, Takashi Kobayashi, Hiroyuki Aburatani, Yuji Yamanashi, and Akihiko Yoshimura. 2005. “FLN29, a Novel Interferon- and LPS-inducible Gene Acting as a Negative Regulator of Toll-like Receptor Signaling.” *The Journal of Biological Chemistry* 280 (50) (December 16): 41289–97. doi:10.1074/jbc.M508221200. http://www.ncbi.nlm.nih.gov/pubmed/16221674.

Miao, Hui, Da-Qiang Li, Amitava Mukherjee, Hong Guo, Aaron Petty, Jennifer Cutter, James P Basilion, et al. 2009. “EphA2 Mediates Ligand-dependent Inhibition and Ligand-independent Promotion of Cell Migration and Invasion via a Reciprocal Regulatory Loop with Akt.” *Cancer Cell* 16 (1) (July 7): 9–20. doi:10.1016/j.ccr.2009.04.009. http://www.ncbi.nlm.nih.gov/pubmed/19573808.

Miao, Hui, and Bingcheng Wang. 2012. “EphA Receptor signaling-Complexity and Emerging Themes.” *Seminars in Cell & Developmental Biology* 23 (1) (February): 16–25. doi:10.1016/j.semcdb.2011.10.013. http://www.ncbi.nlm.nih.gov/pubmed/22040915.

Mori, Tetsiji, Akio Wanaka, Akihiko Taguchi, Kazumasa Matsumoto, and Masaya Tohyama. 1995. “Differential Expressions of the Eph Family of Receptor Tyrosine Kinase Genes (sek, Elk, Eck) in the Developing Nervous System of the Mouse.” *Brain Research. Molecular Brain Research* 29 (2) (April): 325–35. doi:10.1016/0169-328X(94)00263-E. http://www.ncbi.nlm.nih.gov/pubmed/7609620.

Mueller, Kelly L, Zeng-Quan Yang, Ramsi Haddad, Stephen P Ethier, and Julie L Boerner. 2010. “EGFR/Met Association Regulates EGFR TKI Resistance in Breast Cancer.” *Journal of Molecular Signaling* 5 (January): 8.

doi:10.1186/1750-2187-5-8.
http://www.pubmedcentral.nih.gov/articlerender.fcgi?artid=2911419&tool=pmcentrez&rendertype=abstract.

Nabetani, Takuji, Yeon-Jeong Kim, Masaki Watanabe, Yoko Ohashi, Hiroyuki Kamiguchi, and Yoshio Hirabayashi. 2009. “Improved Method of Phosphopeptides Enrichment Using Biphasic Phosphate-binding tag/C18 Tip for Versatile Analysis of Phosphorylation Dynamics.” *Proteomics* 9 (24) (December): 5525–33. doi:10.1002/pmic.200900341. http://www.ncbi.nlm.nih.gov/pubmed/19834909.

Nakamura, Takahiro, Katsuya Sakai, Toshikazu Nakamura, and Kunio Matsumoto. 2011. “Hepatocyte Growth Factor Twenty Years on: Much More Than a Growth Factor.” *Journal of Gastroenterology and Hepatology* 26 (Suppl 1) (January): 188–202. doi:10.1111/j.1440-1746.2010.06549.x. http://www.ncbi.nlm.nih.gov/pubmed/21199531.

Ndassa, Yasmine M, Chris Orsi, Jarrod A Marto, She Chen, and Mark M Ross. 2006. “Improved Immobilized Metal Affinity Chromatography for Large-Scale Phosphoproteomics Applications Research Articles.” *Journal of Proteome Research* 5 (10): 2789–2799. doi:10.1021/pr0602803. http://pubs.acs.org/doi/abs/10.1021/pr0602803.

Niemann, Hartmut. 2011. “Structural Insights into Met Receptor Activation.” *European Journal of Cell Biology* 90 (11) (January): 972–81. doi:10.1016/j.ejcb.2010.11.014. http://www.ncbi.nlm.nih.gov/pubmed/21242015.

Niemann, Hartmut, Volker Jäger, P Jonathan G Butler, Joop van den Heuvel, Sabine Schmidt, Davide Ferraris, Ermanno Gherardi, and Dirk W Heinz. 2007. “Structure of the Human Receptor Tyrosine Kinase Met in Complex with the Listeria Invasion Protein InlB.” *Cell* 130 (2) (July 27): 235–46. doi:10.1016/j.cell.2007.05.037. http://www.ncbi.nlm.nih.gov/pubmed/17662939.

Niu, Jiaxin, Jasmina Profirovic, Haiyun Pan, Rita Vaiskunaite, and Tatyana Voyno-Yasenetskaya. 2003. “G Protein Betagamma Subunits Stimulate p114RhoGEF, a Guanine Nucleotide Exchange Factor for RhoA and Rac1: Regulation of Cell Shape and Reactive Oxygen Species Production.” *Circulation Research* 93 (9) (October 31): 848–56. doi:10.1161/01.RES.0000097607.14733.0C. http://www.ncbi.nlm.nih.gov/pubmed/14512443.

Ogata, Souichi, Junji Morokuma, Tadayoshi Hayata, Gabriel Kolle, Christof Niehrs, Naoto Ueno, and Ken W Y Cho. 2007. “TGF-beta Signaling-mediated Morphogenesis : Modulation of Cell Adhesion via Cadherin Endocytosis.” *Genes & Development* 21 (14): 1817–1831. doi:10.1101/gad.1541807. http://www.ncbi.nlm.nih.gov/pmc/articles/PMC1920175/.

Olsen, Jesper V, Blagoy Blagoev, Florian Gnad, Boris Macek, Chanchal Kumar, Peter Mortensen, and Matthias Mann. 2006. “Global, in Vivo, and Site-specific

Phosphorylation Dynamics in Signaling Networks." *Cell* 127 (3) (November): 635–48. doi:10.1016/j.cell.2006.09.026. http://www.ncbi.nlm.nih.gov/pubmed/17081983.

Onishi-Haraikawa, Y, M Funaki, N Gotoh, M Shibuya, K Inukai, H Katagiri, Y Fukushima, et al. 2001. "Unique Phosphorylation Mechanism of Gab1 Using PI 3-kinase as an Adaptor Protein." *Biochemical and Biophysical Research Communications* 288 (2) (October 26): 476–82. doi:10.1006/bbrc.2001.5791. http://www.ncbi.nlm.nih.gov/pubmed/11606067.

Organ, Shawna L, Jiefei Tong, Paul Taylor, Jonathan R St-Germain, Roya Navab, Michael F Moran, and Ming-Sound Tsao. 2011. "Quantitative Phospho-Proteomic Profiling of Hepatocyte Growth Factor (HGF)-MET Signaling in Colorectal Cancer." *Journal of Proteome Research* 10 (7) (July 1): 3200–11. doi:10.1021/pr200238t. http://www.ncbi.nlm.nih.gov/pubmed/21609022.

Organ, Shawna L, and Ming-Sound Tsao. 2011. "An Overview of the c-MET Signaling Pathway." *Therapeutic Advances in Medical Oncology* 3 (1 Suppl) (November): S7–S19. doi:10.1177/1758834011422556. http://www.pubmedcentral.nih.gov/articlerender.fcgi?artid=3225017&tool=pmcentrez&rendertype=abstract.

Ozaki, Harunobu, Kenji Ishii, Hidenori Arai, Hisanori Horiuchi, Takahiro Kawamoto, Hidenori Suzuki, and Toru Kita. 2000. "Junctional Adhesion Molecule (JAM) Is Phosphorylated by Protein Kinase C Upon Platelet Activation." *Biochemical and Biophysical Research Communications* 276 (3) (October 5): 873–8. doi:10.1006/bbrc.2000.3574. http://www.ncbi.nlm.nih.gov/pubmed/11027562.

Ozen, Evin, Aysim Gozukizil, Esra Erdal, Aykut Uren, Donald P Bottaro, and Nese Atabey. 2012. "Heparin Inhibits Hepatocyte Growth Factor Induced Motility and Invasion of Hepatocellular Carcinoma Cells Through Early Growth Response Protein 1." *PloS One* 7 (8) (January): e42717. doi:10.1371/journal.pone.0042717. http://www.pubmedcentral.nih.gov/articlerender.fcgi?artid=3418296&tool=pmcentrez&rendertype=abstract.

O'Donnell, Amanda, Zaneta Odrowaz, and Andrew D Sharrocks. 2012. "Immediate-early Gene Activation by the MAPK Pathways: What Do and Don't We Know?" *Biochemical Society Transactions* 40 (1) (February): 58–66. doi:10.1042/BST20110636. http://www.ncbi.nlm.nih.gov/pubmed/22260666.

Papkoff, J, and M Aikawa. 1998. "WNT-1 and HGF Regulate GSK3 Beta Activity and Beta-catenin Signaling in Mammary Epithelial Cells." *Biochemical and Biophysical Research Communications* 247 (3) (June 29): 851–8. doi:10.1006/bbrc.1998.8888. http://www.ncbi.nlm.nih.gov/pubmed/9647782.

Pasquale, Elena B. 2008. "Eph-ephrin Bidirectional Signaling in Physiology and Disease." *Cell* 133 (1) (April 4): 38–52. doi:10.1016/j.cell.2008.03.011. http://www.ncbi.nlm.nih.gov/pubmed/18394988.

Pasquale, Elena B. 2010. “Eph Receptors and Ephrins in Cancer: Bidirectional Signalling and Beyond.” *Nature Reviews. Cancer* 10 (3) (March): 165–80. doi:10.1038/nrc2806. http://www.pubmedcentral.nih.gov/articlerender.fcgi?artid=2921274&tool=pmcentrez&rendertype=abstract.

Patel, Amanda J, and Michel Lazdunski. 2004. “The 2P-domain K+ Channels: Role in Apoptosis and Tumorigenesis.” *Pflügers Archiv : European Journal of Physiology* 448 (3) (June): 261–73. doi:10.1007/s00424-004-1255-8. http://www.ncbi.nlm.nih.gov/pubmed/15133669.

Pawson, Tony, and Piers Nash. 2000. “Protein – Protein Interactions Define Specificity in Signal Transduction.” *Genes & Development* 9 (14): 1027–1047. doi:10.1101/gad.14.9.1027. http://genesdev.cshlp.org/content/14/9/1027.long.

Peschard, Pascal, Tanya M Fournier, Louie Lamorte, Monica A Naujokas, Hamid Band, Wallace Y Langdon, and Morag Park. 2001. “Mutation of the c-Cbl TKB Domain Binding Site on the Met Receptor Tyrosine Kinase Converts It into a Transforming Protein.” *Molecular Cell* 8 (5) (November): 995–1004. doi:10.1016/S1097-2765(01)00378-1. http://www.ncbi.nlm.nih.gov/pubmed/11741535.

Peschard, Pascal, and Morag Park. 2007. “From Tpr-Met to Met, Tumorigenesis and Tubes.” *Oncogene* 26 (9) (February 26): 1276–85. doi:10.1038/sj.onc.1210201. http://www.ncbi.nlm.nih.gov/pubmed/17322912.

Ponzetto, C, a Bardelli, Z Zhen, F Maina, P dalla Zonca, S Giordano, a Graziani, G Panayotou, and P M Comoglio. 1994. “A Multifunctional Docking Site Mediates Signaling and Transformation by the Hepatocyte Growth Factor/scatter Factor Receptor Family.” *Cell* 77 (2) (April 22): 261–71. http://www.ncbi.nlm.nih.gov/pubmed/7513258.

Puthalakath, H, A Villunger, L A O’Reilly, J G Beaumont, L Coultas, R E Cheney, D C Huang, and A Strasser. 2001. “Bmf: a Proapoptotic BH3-only Protein Regulated by Interaction with the Myosin V Actin Motor Complex, Activated by Anoikis.” *Science* 293 (5536) (September 7): 1829–32. doi:10.1126/science.1062257. http://www.ncbi.nlm.nih.gov/pubmed/11546872.

Pérez-Cadahía, Beatriz, Bojan Drobic, and James R Davie. 2011. “Activation and Function of Immediate-early Genes in the Nervous System.” *Biochemistry and Cell Biology = Biochimie Et Biologie Cellulaire* 89 (1) (March): 61–73. doi:10.1139/O10-138. http://www.ncbi.nlm.nih.gov/pubmed/21326363.

Reinl, Tobias, Manfred Nimtz, Claudia Hundertmark, Thorsten Johl, György Kéri, Jürgen Wehland, Henrik Daub, and Lothar Jänsch. 2009. “Quantitative Phosphokinome Analysis of the Met Pathway Activated by the Invasin Internalin B from Listeria Monocytogenes.” *Molecular & Cellular Proteomics : MCP* 8 (12) (December): 2778–95. doi:10.1074/mcp.M800521-MCP200. http://www.pubmedcentral.nih.gov/articlerender.fcgi?artid=2816026&tool=pmcentrez&rendertype=abstract.

Ren, Y, R Li, Y Zheng, and H Busch. 1998. “Cloning and Characterization of GEF-H1, a Microtubule-associated Guanine Nucleotide Exchange Factor for Rac and Rho GTPases.” *The Journal of Biological Chemistry* 273 (52) (December 25): 34954–60. http://www.ncbi.nlm.nih.gov/pubmed/9857026.

Reyes-Turcu, Francisca E, Karen H Ventii, and Keith D Wilkinson. 2009. “Regulation and Cellular Roles of Ubiquitin-specific Deubiquitinating Enzymes.” *Annual Review of Biochemistry* 78 (January): 363–97. doi:10.1146/annurev.biochem.78.082307.091526. http://www.pubmedcentral.nih.gov/articlerender.fcgi?artid=2734102&tool=pmcentrez&rendertype=abstract.

Roig, Joan, Alexei Mikhailov, Christopher Belham, and Joseph Avruch. 2002. “Nercc1, a Mammalian NIMA-family Kinase, Binds the Ran GTPase and Regulates Mitotic Progression.” *Genes & Development* 16 (13) (July 1): 1640–58. doi:10.1101/gad.972202. http://www.pubmedcentral.nih.gov/articlerender.fcgi?artid=186374&tool=pmcentrez&rendertype=abstract.

Rosenqvist, Heidi, Juanying Ye, and Ole N Jensen. 2011. “Gel-Free Proteomics: Analytical Strategies in Mass Spectrometry-Based Phosphoproteomics.” Ed. Kris Gevaert and Joël Vandekerckhove. *Methods in Molecular Biology* 753 (Chapter 13): 183–213. doi:10.1007/978-1-61779-148-2. http://www.springerlink.com/index/10.1007/978-1-61779-148-2.

Rosário, Marta, and Walter Birchmeier. 2003. “How to Make Tubes: Signaling by the Met Receptor Tyrosine Kinase.” *Trends in Cell Biology* 13 (6) (June): 328–335. doi:10.1016/S0962-8924(03)00104-1. http://linkinghub.elsevier.com/retrieve/pii/S0962892403001041.

Ruan, Lin, Xin-Hui Li, Xun-Xun Wan, Hong Yi, Cui Li, Mao-Yu Li, Peng-Fei Zhang, et al. 2011. “Analysis of EGFR Signaling Pathway in Nasopharyngeal Carcinoma Cells by Quantitative Phosphoproteomics.” *Proteome Science* 9 (35) (January): 1–11. doi:10.1186/1477-5956-9-35. http://www.pubmedcentral.nih.gov/articlerender.fcgi?artid=3141626&tool=pmcentrez&rendertype=abstract.

Sagara, M, Y Kawasaki, SI Iemura, T Natsume, Y Takai, and Tetsu Akiyama. 2009. “Asef2 and Neurabin2 Cooperatively Regulate Actin Cytoskeletal Organization and Are Involved in HGF-induced Cell migrationRole of Asef2 and Neurabin2 in HGF-induced Cell Migration.” *Oncogene* 28 (10): 1357–65. doi:10.1038/onc.2008.478. http://www.nature.com/onc/journal/v28/n10/full/onc2008478a.html.

Sancak, Yasemin, Carson C Thoreen, Timothy R Peterson, Robert a Lindquist, Seong a Kang, Eric Spooner, Steven a Carr, and David M Sabatini. 2007. “PRAS40 Is an Insulin-regulated Inhibitor of the mTORC1 Protein Kinase.” *Molecular Cell* 25 (6) (March 23): 903–15. doi:10.1016/j.molcel.2007.03.003. http://www.ncbi.nlm.nih.gov/pubmed/17386266.

Schaller, M D. 2001. “Paxillin: a Focal Adhesion-associated Adaptor Protein.” *Oncogene* 20 (44) (October 1): 6459–72. doi:10.1038/sj.onc.1204786. http://www.ncbi.nlm.nih.gov/pubmed/11607845.

Schreiber, Thiemo B, Nina Mäusbacher, Susanne B Breitkopf, Kathrin Grundner-Culemann, and Henrik Daub. 2008. “Quantitative Phosphoproteomics--an Emerging Key Technology in Signal-transduction Research.” *Proteomics* 8 (21) (November): 4416–32. doi:10.1002/pmic.200800132. http://www.ncbi.nlm.nih.gov/pubmed/18837465.

Seet, Bruce T, Ivan Dikic, Ming-Ming Zhou, and Tony Pawson. 2006. “Reading Protein Modifications with Interaction Domains.” *Nature Reviews. Molecular Cell Biology* 7 (7) (July): 473–83. doi:10.1038/nrm1960. http://www.ncbi.nlm.nih.gov/pubmed/16829979.

Shen, B Q, J H Widdicomb, and R J Mrsny. 1999. “Hepatocyte Growth Factor Inhibits Amiloride-sensitive Na(+) Channel Function in Cystic Fibrosis Airway Epithelium in Vitro.” *Pulmonary Pharmacology & Therapeutics* 12 (3) (January): 157–64. doi:10.1006/pupt.1999.9999. http://www.ncbi.nlm.nih.gov/pubmed/10419835.

Shen, Yang, Monica Naujokas, Morag Park, and Keith Ireton. 2000. “InlB-dependent Internalization of Listeria Is Mediated by the Met Receptor Tyrosine Kinase.” *Cell* 103 (3) (October 27): 501–10. doi:10.1016/S0092-8674(00)00141-0. http://www.ncbi.nlm.nih.gov/pubmed/11081636.

Sheriff, Sulaiman, Marwan Ali, Ayesha Yahya, Khawaja H Haider, Ambikaipakan Balasubramaniam, and Hassane Amlal. 2010. “Neuropeptide Y Y5 Receptor Promotes Cell Growth Through Extracellular Signal-regulated Kinase Signaling and Cyclic AMP Inhibition in a Human Breast Cancer Cell Line.” *Molecular Cancer Research : MCR* 8 (4) (April): 604–14. doi:10.1158/1541-7786.MCR-09-0301. http://www.ncbi.nlm.nih.gov/pubmed/20332211.

Shimabukuro, Koji, Shizuko Ichinose, Ryuji Koike, Toshiro Kubota, Masahiko Yamaguchi, Masayuki Miyasaka, and Takesshi Aso. 2001. “Hepatocyte Growth Factor/scatter Factor Is Implicated in the Mode of Stromal Invasion of Uterine Squamous Cervical Cancer.” *Gynecologic Oncology* 83 (2) (November): 205–15. doi:10.1006/gyno.2001.6347. http://www.ncbi.nlm.nih.gov/pubmed/11606073.

Siltanen, Antti, Katsukiyo Kitabayashi, Päivi Lakkisto, Johanna Mäkelä, Tommi Pätilä, Masamichi Ono, Ilkka Tikkanen, Yoshiki Sawa, Esko Kankuri, and Ari Harjula. 2011. “hHGF Overexpression in Myoblast Sheets Enhances Their Angiogenic Potential in Rat Chronic Heart Failure.” *PloS One* 6 (4) (January): e19161. doi:10.1371/journal.pone.0019161. http://www.pubmedcentral.nih.gov/articlerender.fcgi?artid=3082550&tool=pmcentrez&rendertype=abstract.

Snyder, Peter M, Diane R Olson, Rajesh Kabra, Ruifeng Zhou, and Jennifer C Steines. 2004. “cAMP and Serum and Glucocorticoid-inducible Kinase (SGK) Regulate the Epithelial Na(+) Channel Through Convergent Phosphorylation

of Nedd4-2." *The Journal of Biological Chemistry* 279 (44) (October 29): 45753–8. doi:10.1074/jbc.M407858200. http://www.ncbi.nlm.nih.gov/pubmed/15328345.

Solomon, E, J Borrow, and a D Goddard. 1991. "Chromosome Aberrations and Cancer." *Science* 254 (5035) (November 22): 1153–60. doi:10.1126/science.1957167. http://www.ncbi.nlm.nih.gov/pubmed/1957167.

Sukhatme, Vikas P. 1990. "Early Transcriptional Events in Cell Growth : The Egr Family." *Journal of the American Society of Nephrology* 1 (6): 859–866. doi:1046-6673101 06-0859. http://jasn.asnjournals.org/content/1/6/859.full.pdf+html.

Takeuchi, Osamu, and Shizuo Akira. 2010. "Pattern Recognition Receptors and Inflammation." *Cell* 140 (6) (March 19): 805–20. doi:10.1016/j.cell.2010.01.022. http://www.ncbi.nlm.nih.gov/pubmed/20303872.

Tan, Bertrand Chin-Ming, and Sheng-Chung Lee. 2004. "Nek9, a Novel FACT-associated Protein, Modulates Interphase Progression." *The Journal of Biological Chemistry* 279 (10) (March): 9321–30. doi:10.1074/jbc.M311477200. http://www.ncbi.nlm.nih.gov/pubmed/14660563.

Thiery, Jean Paul. 2002. "Epithelial-mesenchymal Transitions in Tumour Progression." *Nature Reviews. Cancer* 2 (6) (June): 442–54. doi:10.1038/nrc822. http://www.ncbi.nlm.nih.gov/pubmed/12189386.

Timms, John F, and Pedro R Cutillas. 2010. "LC-MS/MS in Proteomics: Overview of Quantitative LC-MS Techniques for Proteomics and Activitomics." Ed. Pedro R. Cutillas and John F. Timms. *Methods in Molecular Biology* 658 (1): 19–45. doi:10.1007/978-1-60761-780-8. http://www.springerlink.com/index/10.1007/978-1-60761-780-8.

Tonks, Nicholas K. 2006. "Protein Tyrosine Phosphatases: From Genes, to Function, to Disease." *Nature Reviews. Molecular Cell Biology* 7 (11) (November): 833–46. doi:10.1038/nrm2039. http://www.ncbi.nlm.nih.gov/pubmed/17057753.

Trost, Matthias, Dirk Wehmhöner, Uwe Kärst, Guido Dieterich, Jürgen Wehland, and Lothar Jänsch. 2005. "Comparative Proteome Analysis of Secretory Proteins from Pathogenic and Nonpathogenic Listeria Species." *Proteomics* 5 (6) (April): 1544–57. doi:10.1002/pmic.200401024. http://www.ncbi.nlm.nih.gov/pubmed/15838904.

Trusolino, Livio, Andrea Bertotti, and Paolo M Comoglio. 2010. "MET Signalling: Principles and Functions in Development, Organ Regeneration and Cancer." *Nature Reviews. Molecular Cell Biology* 11 (12) (December): 834–48. doi:10.1038/nrm3012. http://www.ncbi.nlm.nih.gov/pubmed/21102609.

Tullai, John W, Michael E Schaffer, Steven Mullenbrock, Gabriel Sholder, Simon Kasif, and Geoffrey M Cooper. 2007. "Immediate-early and Delayed Primary

Response Genes Are Distinct in Function and Genomic Architecture." *The Journal of Biological Chemistry* 282 (33) (August 17): 23981–95. doi:10.1074/jbc.M702044200. http://www.pubmedcentral.nih.gov/articlerender.fcgi?artid=2039722&tool=pmcentrez&rendertype=abstract.

Vazquez-Boland, Jose, Michael Kuhn, Patrick Berche, Trinad Chakraborty, Gustavo Dominguez-Bernal, Werner Goebel, Bruno Gonzalez-Zorn, Jürgen Wehland, and Jürgen Kreft. 2001. "Listeria Pathogenesis and Molecular Virulence Determinants." *Clinical Microbiology Reviews* 14 (3): 584–640. doi:10.1128/CMR.14.3.584. http://www.ncbi.nlm.nih.gov/pmc/articles/PMC88991/.

Villén, Judit, and Steven P Gygi. 2008. "The SCX/IMAC Enrichment Approach for Global Phosphorylation Analysis by Mass Spectrometry." *Nature Protocols* 3 (10) (January): 1630–8. doi:10.1038/nprot.2008.150. http://www.ncbi.nlm.nih.gov/pubmed/18833199.

Vomastek, Tomás, Marcin P Iwanicki, W Richard Burack, Divya Tiwari, Devanand Kumar, J Thomas Parsons, Michael J Weber, and Vinay Kumar Nandicoori. 2008. "Extracellular Signal-regulated Kinase 2 (ERK2) Phosphorylation Sites and Docking Domain on the Nuclear Pore Complex Protein Tpr Cooperatively Regulate ERK2-Tpr Interaction." *Molecular and Cellular Biology* 28 (22) (November): 6954–66. doi:10.1128/MCB.00925-08. http://www.pubmedcentral.nih.gov/articlerender.fcgi?artid=2573295&tool=pmcentrez&rendertype=abstract.

Walker-Daniels, Jennifer, David J II Riese, and Michael S Kinch. 2002. "c-Cbl-Dependent EphA2 Protein Degradation Is Induced by Ligand Binding." *Molecular Cancer Research : MCR* 1: 79–87. http://mcr.aacrjournals.org/content/1/1/79.abstract.

Wang, Dakun, Zaibo Li, Edward M Messing, and Guan Wu. 2005. "The SPRY Domain-containing SOCS Box Protein 1 (SSB-1) Interacts with MET and Enhances the Hepatocyte Growth Factor-induced Erk-Elk-1-serum Response Element Pathway." *The Journal of Biological Chemistry* 280 (16) (April 22): 16393–401. doi:10.1074/jbc.M413897200. http://www.ncbi.nlm.nih.gov/pubmed/15713673.

Wells, C M, T Ahmed, J R W Masters, and G E Jones. 2005. "Rho Family GTPases Are Activated During HGF-stimulated Prostate Cancer-cell Scattering." *Cell Motility and the Cytoskeleton* 62 (3) (November): 180–94. doi:10.1002/cm.20095. http://www.ncbi.nlm.nih.gov/pubmed/16211585.

Wessel, D., and U.I. Flügge. 1984. "A Method for the Quantitative Recovery of Protein in Dilute Solution in the Presence of Detergents and Lipids." *Analytical Biochemistry* 138 (1): 141–143. doi:10.1016/0003-2697(84)90782-6. http://www.sciencedirect.com/science/article/pii/0003269784907826.

Van Wijk, Sjoerd J L, and H T Marc Timmers. 2010. "The Family of Ubiquitin-conjugating Enzymes (E2s): Deciding Between Life and Death of Proteins."

FASEB Journal 24 (4) (April): 981–93. doi:10.1096/fj.09-136259. http://www.ncbi.nlm.nih.gov/pubmed/19940261.

Wiley, S R, K Schooley, P J Smolak, W S Din, C P Huang, J K Nicholl, G R Sutherland, T D Smith, C Rauch, and C a Smith. 1995. “Identification and Characterization of a New Member of the TNF Family That Induces Apoptosis.” *Immunity* 3 (6) (December): 673–82. doi:10.1016/1074-7613(95)90057-8. http://www.ncbi.nlm.nih.gov/pubmed/8777713.

Wu, Yifan, Junhong Liu, Zhengping Zhang, Huang Huang, Jiayin Shen, Shuangquan Zhang, Yong Jiang, Lan Luo, and Zhimin Yin. 2009. “HSP27 Regulates IL-1 Stimulated IKK Activation Through Interacting with TRAF6 and Affecting Its Ubiquitination.” *Cellular Signalling* 21 (1) (January): 143–50. doi:10.1016/j.cellsig.2008.10.001. http://www.ncbi.nlm.nih.gov/pubmed/18950704.

Wykosky, Jill, and Waldemar Debinski. 2008. “The EphA2 Receptor and ephrinA1 Ligand in Solid Tumors: Function and Therapeutic Targeting.” *Molecular Cancer Research : MCR* 6 (12) (December): 1795–806. doi:10.1158/1541-7786.MCR-08-0244. http://www.ncbi.nlm.nih.gov/pubmed/19074825.

Yang, Jian-Ping, Mayumi Hori, Takaomi Sanda, and Takashi Okamoto. 1999. “Identification of a Novel Inhibitor of Nuclear factor-kappaB, RelA-associated Inhibitor.” *The Journal of Biological Chemistry* 274 (22) (May 28): 15662–70. doi:10.1074/jbc.274.22.15662. http://www.ncbi.nlm.nih.gov/pubmed/10336463.

Zaman, Gul, Andrew Sunters, Gabriel L Galea, Behzad Javaheri, Leanne K Saxon, Alaa Moustafa, Victoria J Armstrong, Joanna S Price, and Lance E Lanyon. 2012. “Loading-related Regulation of Transcription Factor EGR2/Krox-20 in Bone Cells Is ERK1/2 Protein-mediated and Prostaglandin, Wnt Signaling Pathway-, and Insulin-like Growth factor-I Axis-dependent.” *The Journal of Biological Chemistry* 287 (6) (February 3): 3946–62. doi:10.1074/jbc.M111.252742. http://www.pubmedcentral.nih.gov/articlerender.fcgi?artid=3281728&tool=pmcentrez&rendertype=abstract.

Zenke, Frank T, Mira Krendel, Celine DerMardirossian, Charles C King, Benjamin P Bohl, and Gary M Bokoch. 2004. “P21-activated Kinase 1 Phosphorylates and Regulates 14-3-3 Binding to GEF-H1, a Microtubule-localized Rho Exchange Factor.” *The Journal of Biological Chemistry* 279 (18) (April 30): 18392–400. doi:10.1074/jbc.M400084200. http://www.ncbi.nlm.nih.gov/pubmed/14970201.

Zhang, Yi, Manor Askenazi, Jingrui Jiang, C John Luckey, James D Griffin, and Jarrod a Marto. 2010. “A Robust Error Model for iTRAQ Quantification Reveals Divergent Signaling Between Oncogenic FLT3 Mutants in Acute Myeloid Leukemia.” *Molecular & Cellular Proteomics : MCP* 9 (5) (May): 780–90. doi:10.1074/mcp.M900452-MCP200. http://www.pubmedcentral.nih.gov/articlerender.fcgi?artid=2871413&tool=pmcentrez&rendertype=abstract.

Zhang, Yi, Alejandro Wolf-Yadlin, Phillip L Ross, Darryl J Pappin, John Rush, Douglas a Lauffenburger, and Forest M White. 2005. “Time-resolved Mass Spectrometry of Tyrosine Phosphorylation Sites in the Epidermal Growth Factor Receptor Signaling Network Reveals Dynamic Modules.” *Molecular & Cellular Proteomics : MCP* 4 (9) (September): 1240–50. doi:10.1074/mcp.M500089-MCP200. http://www.ncbi.nlm.nih.gov/pubmed/15951569.

Danksagung

Als erstes möchte ich meinem Doktorvater Prof. Dr. Lothar Jänsch für die Möglichkeit danken, dass ich diese Arbeit in seiner Gruppe anfertigen durfte. Maßgeblich haben die vielen Ideen und Diskussionen mein Thema mitgestaltet und zum Erfolg meiner Arbeit beigetragen.

Prof. Dr. Michael Steinert danke ich sehr herzlich für die Übernahme des Zweitgutachtens und seinen Rat während der Thesis Komitees. Prof. Dr. Ralf-R. Mendel danke ich für seine Bereitschaft zur Übernahme des Prüfungsvorsitzes.

Zudem danke ich Jörn Krauße aus der Molekularen Strukturbiologie, der mich regelmäßig mit rekombinant hergestellten Proteinen für die Stimulationsexperimente beliefert hat.

Anschließend danke ich meinen Kollegen in der Arbeitsgruppe Zelluläre Proteomforschung für eine angenehme Arbeitsatmosphäre. Besonderer Dank geht dabei an Dr. Uwe Kärst, der mich jederzeit mit technischem Rat und der neusten Literatur versorgte und in erstaunlicher Geschwindigkeit und Präzision das Korrekturlesen dieser Arbeit absolviert hat. Außerdem möchte ich Dr. Josef Wissing für seinen Rat bei der experimentellen Umsetzung der Versuche, und Dr. Manfred Nimtz für Hilfestellungen in der Massenspektrometrie danken. Mein Dank geht auch an Prof. Dr. Frank Klawonn und seine Bioinformatiker, die bei der statistischen Auswertung immer hilfsbereit waren. Kirsten Minkhart, Kathrin Goltz, Undine Felgenträger und Reiner Munder danke ich für die gelegentliche Unterstützung der experimentellen Arbeit. Vielen Dank an Alexander Iphöfer, Anne Kummer, Thorsten Johl und Kirstin Jurrat für schöne Stunden neben der Arbeit. Danke an meine ehemalige Doktorandenkollegin Susanne Strube, die mir über die Zeit nicht nur zu einer verlässlichen, wissenschaftlichen Diskussionspartnerin, sondern auch zu einer guten Freundin geworden ist.

Als letztes möchte ich meiner Familie und meinen Freunden für ihre Unterstützung und ihr Verständnis danken. Ganz besonderer Dank geht natürlich an meine Eltern, die mir meine akademische Ausbildung überhaupt erst ermöglicht haben

und mich zudem jederzeit mit allen zur Verfügung stehenden Mitteln motiviert haben.

Der größte Dank geht an meinen Mann Christian, der mich durch seine Liebe, sein Verständnis und seine Unterstützung die ganze Zeit über begleitet und motiviert hat. Besonders in der letzten Phase des Zusammenschreibens hast du beste Arbeit geleistet, um die Fertigstellung dieser Arbeit zu fördern und mich immer wieder aufzubauen!